Uncertain Power Flows and Transmission Planning

Final Project Report

Power Systems Engineering Research Center

A National Science Foundation
Industry/University Cooperative Research Center
since 1996

Power Systems Engineering Research Center

Uncertain Power Flows and Transmission Planning

Final Project Report

Report Authors

Jonathan Stahlhut, Student
Gerald Heydt, Professor
Arizona State University

Becky A. Westendorf, Student
Merry P. Mani, Student
Peter W. Sauer, Professor
University of Illinois at Urbana-Champaign

Gerald B. Sheblé, Project Leader
Iowa State University*

***Now employed at Portland State University**

PSERC Publication 07-07

March 2007

Information about this project

For information about this project contact:

Gerald T. Heydt
Arizona State University
Department of Electrical Engineering
Tempe, AZ 85287
Phone: 480-965-8307
Fax: 480-965-0745
Email: heydt@asu.edu

Peter W. Sauer
University of Illinois at Urbana-Champaign
Department of Electrical and Computer Engineering
1406 W. Green St.
Urbana, IL 61801
Phone: 217-333-0394
Fax: 217-333-1162
Email: sauer@ece.uiuc.edu

Power Systems Engineering Research Center

This is a project report from the Power Systems Engineering Research Center (PSERC). PSERC is a multi-university Center conducting research on challenges facing a restructuring electric power industry and educating the next generation of power engineers. More information about PSERC can be found at the Center's website: http://www.pserc.org.

For additional information, contact:

Power Systems Engineering Research Center
Arizona State University
577 Engineering Research Center
Tempe, Arizona 85287-8606
Phone: 480 965 1643
Fax: 480 965 0745

Notice Concerning Copyright Material

Acknowledgements

The work described in this report was sponsored by the Power Systems Engineering Research Center (PSERC). We express our appreciation for the support provided by PSERC's industrial members and by the National Science Foundation under grant NSF EEC-0001880 received under the Industry/University Cooperative Research Center program.

The authors thank all PSERC members for their technical advice on this project. Special thanks go to Messrs. Jerome Ryckbosch (RTE) and John Chatelain (MidAmerican) who were industry advisors for the project.

Executive Summary

Growing uncertainty in power systems, coupled with the introduction of power markets, calls for the development of new tools for planning, operations, and market-based decision-making. This project explored methods for efficiently calculating available transfer capability and quantifying transmission revenues under uncertainty. Illustrative analyses demonstrated potential uses in transmission planning.

Part I: Stochastic-Algebraic Evaluation of Available Transfer Capability for Transmission Expansion

Available transfer capability (ATC) is a measure of the "available room" in a power system to transmit power between two given points beyond already committed uses, whether for reliability or economy purposes. This makes calculation of ATC important to power market participants, system operators, and transmission planners. Power marketers trade power using a variety of tools such as the ATC calculation to make economic trade decisions and to value transmission resources. ATC is typically calculated using a deterministic model for a given system state specified by given loads, generation, line parameters and topology, system limits, etc.

Rather than what the value of the ATC was for a given state, often what is really needed for planning and operations is an estimate of what ATC will be in a future system state, such as 15 minutes ahead, a day-ahead, or farther. However, the future state of a power system is affected by a number of random (that is, uncertain or stochastic) variables. For example, if bus loads are modeled as random variables, the variables characterizing the system state (such as bus voltages and power flows) become random, too. This makes the value of ATC random, so that it can only be described using statistics such as expected value, variance, or, more broadly, a probability density function. For the case of load uncertainty, that probabilistic description of ATC can be determined once the nature of the load uncertainty is specified in an explicit statistical model. Since line power flows are an important part of the evaluation of ATC, a stochastic power flow method is needed to find the probabilistic behavior of ATC.

With load uncertainty, the stochastic ATC calculation problem could be solved using Monte Carlo analysis where a very large number of bus load cases would be used to calculate ATC between given system bus pairs. The Monte Carlo approach is computationally intensive, consuming computer resources and time. An alternative approach is to use a stochastic-algebraic method that avoids direct calculations with a large number of cases, thereby significantly reducing computational time.

In this research project, a stochastic-algebraic method was developed to calculate ATC statistics based on uncertain bus loads and transmission line availability. The system limits that were modeled included transmission line thermal rating limits, bus voltage magnitude limits, and, as a proxy for security limits, phase-angle differences across transmission lines. The stochastic-algebraic method used a linear transformation matrix, the system power flow Jacobian matrix evaluated at the system operating point. The calculation of stochastic ATC with uncertain transmission line status was performed using a modified transmission outage table.

The stochastic-algebraic method was compared to the Monte Carlo method using the WECC 179-bus system. As expected, the results showed that the stochastic-algebraic calculations were more computationally efficient than with the Monte Carlo method. A typical calculation to evaluate the ATC probability density function, mean and variance required 54,000 seconds using the Monte Carlo method versus 60 seconds using stochastic-algebraic analysis. Estimate of the mean and variance using the two methods were within 0.5 percent and 12 percent respectively for illustrative cases. Simulations also showed that if the bus load standard deviations were {5, 10, 15} percent of the expected demand, ATC had a standard deviation of {75, 150, 300} percent of the expected ATC. The addition of transmission line uncertainty changed the shape of the ATC probability distribution with more likelihood that the realized ATC would be less than the mean; however, it did not have much effect on the ATC's expected value.

How the ATC could be used in justifying and paying for transmission expansion was studied. A benefit-cost analysis example of transmission expansion was performed using the WECC 179-bus system. The analysis showed that it is possible to financially justify transmission expansion based solely on the value of increased ATC.

Directions for future work on the stochastic ATC method could include developing a stochastic ATC calculation tool, finding faster calculation methods, adding more sources of uncertainty, testing with real data, incorporating in future financial transmission rights markets, and integrating with calculation of congestion costs.

Part II: Transmission Line Revenues with Uncertainty

The regulated transmission tariff system allows transmission companies to collect revenues that allow recovery of the fixed and variable costs of transmission services, including a reasonable profit. Different forms of tariffs are in use today. One type is the postage-stamp tariff in which a price is charged per megawatt flow per mile in the system. For a particular transmission line, the revenue from a postage-stamp tariff is directly proportional to the amount of power flow through that transmission line for a given transaction times the length of the line in miles.

The primary goal of this part of the project was to evaluate and compare the Monte Carlo method with an analytical method for incorporating uncertainty in load forecasts, and to investigate the effect of line outages on transmission revenues. The theoretical basis for both the Monte Carlo method and the analytical method were explored, documented, and illustrated on the IEEE 14-bus test system. The expected value and variance of the transmission revenue were computed for the case with all lines in service and for cases when one line was outaged. The results indicate that the analytical method provides very good approximations of the exhaustive Monte Carlo method. This was observed both in the incorporation of load uncertainty and in the investigation of uncertainty in transmission line availability.

The probability distributions of hourly system revenues due to uncertainty in forecasted loads and transmission availability were also computed analytically using linear power flow methods and distribution factors. Results showed that the analytical method provided a very good approximation of the Monte Carlo simulation results, thus providing a very efficient technique to assess variation in transmission line revenue under load and transmission line uncertainties.

Part I

Stochastic-Algebraic Evaluation of Available Transfer Capability for Transmission Expansion

Authors

Jonathan Stahlhut
Gerald Heydt

Table of Contents

Table of Contents (continued)

List of Tables

List of Tables (continued)

List of Figures

List of Figures (continued)

Nomenclature

ATC	available transfer capability
$ATC^{A\text{-}B}$	available transfer capability between bus A and bus B
ATC^{+}	the ATC with respect to positive line rating limits
ATC^{-}	the ATC with respect to negative line rating limits
$ATC^{V\,max}$	the ATC with respect to voltage magnitude maximum limits
$ATC^{V\,min}$	the ATC with respect to voltage magnitude minimum limits
B_{line}	imaginary part of the transmission line admittance
c_j	jth constant in the Gram-Charlier type A series
CBM	capacity benefit margin
C_p	compounding period
C_{cong}	cost of congestion
CPF	continuation power flow
C_{te}	cost of transmission expansion
D_{ATC}	general price function of the ATC
$D_{ATC}^{(i)}$	ith exemplary general price function of the ATC
$diag(\cdots)$	a diagonal matrix of the values of the argument
$\frac{dP^{line}}{dP_{AB}}$	line flow power sensitivity factor
$\frac{d\lvert V\rvert}{dP_{AB}}$	voltage magnitude sensitivity factor
ε	average day-ahead load forecast error
$E[\cdots]$	expectation operator
$erf(x)$	error function
exp	exponential
$\Im\{\cdots\}$	Fourier transform
$f_x(x)$	probability density function
$F_x(x)$	probability distribution function
FERC	Federal Energy Regulatory Commission
FTR	financial transmission right
$G(x)$	characteristic Gaussian function
$H_j(x)$	jth Hermite polynomial
ISO	independent system operator
J	jacobian matrix
$k_x^{(n)}$	nth cumulant
L	incidence matrix
LATC	linear available transfer capability
LPM	locational pricing markets
$m_x^{(k)}$	kth raw moment of x
M_x	vector of means of variable x

$merf(x)$	error function used in MATLAB
MW	megawatts
NERC	North American Electric Reliability Counsel
N_B	number of system buses
N_L	number of system lines
OASIS	open access same-time information system
P	active power
ΔP	change in bus real power injection
$P(x)$	probability distribution function
PDF	probability density function
PF	power factor transformation matrix
pf	power factor
P^{line}	line real power flow
ΔP_{ij}^{line}	real power flow in line from bus I to bus j
$P^{load}(B)$	bus real power load at bus B
P^{Rating}	line rating
PSAT	power system analysis tool
$Pr^{(k)}(ATC)$	the kth price function of the ATC
Q	reactive power
ΔQ	change in bus reactive power injection
$Q^{load}(B)$	bus reactive power load at bus B
r	interest rate
R	resistance
S	number of transmission asset states
sgn	signum function
T_p	payback time of transmission expansion
T_{ATC}	number of hours per year that ATC is traded
TRM	transmission reliability margin
TSAT	transient security assessment tool
TTC	total transfer capability
V	voltage
$\Delta\lvert V\rvert$	change in bus voltage magnitude
$\lvert V\rvert^{max}$	bus voltage magnitude maximum
$\lvert V\rvert^{min}$	bus voltage magnitude maximum
X	reactance
x	variable
1^N	vector of ones with length N
$\mu_x^{(k)}$	kth central moment of x
μ_x	mean of random variable x
μ_{ATC}	mean of the ATC
μ_{GC}	mean used in the evaluation of the Gram-Charlier series
$\Delta\delta$	change in bus voltage angle

δ^{max}	security limit angle maximum
$\phi(\omega)$	characteristic function
$\lvert\cdots\rvert$	absolute value
Σ_{x}	covariance matrix of variable x
σ_{GC}^{2}	standard deviation of a probability density function expressed by a Gram-Charlier type A series
∞	infinity
Ξ_{ij}	submatrix of the inverse Jacobian matrix

1. Stochastic Power Flow Study Applications in Power Marketing and Power Engineering

1.1. Description of this report

This is a final report for PSERC (Power Systems Engineering Research Center) project M-10 entitled *Uncertain Power Flows and Transmission Expansion Planning*. In this report, the focus is on available transmission capability. However, portions of the entire PSERC project are also described.

The major information problem for smooth transmission expansion is the balancing of expansion costs with the cost of congestion and reliability during the operation of the energy system multiple markets over a repeated number of years. The risk of delivery failure due to transmission limitations, the risk of market power due to insufficient market reach to another supplier, and the operational risk due to maintenance schedules are known risks that must be mitigated by transmission expansion over some long-term future time horizon. This project assumes that the transmission owners are regulated entities that are compensated based on total costs each year plus a predetermined rate of return based on quality of service (performance based rates).

There are two methods that have been extended to include the role of competitive auction markets to the issues of energy system adequacy and reliability: contingency analysis including remedial action and stochastic power flow. This project will investigate the expansion of each technique to calculate price signals to justify future transmission expansion. The future transmission requirements will include adequate transmission for any seller to find an equivalent best price buyer and for any buyer to find an equivalent best price seller. This objective is to mitigate market power that an isolated seller or an isolated buyer might exercise due to congestion. Techniques to define which time periods are critical will be investigated. The future transmission requirements will include consideration for maintenance of transmission equipment to provide an adequate set of paths from each buyer (seller) to multiple sellers (buyers) in an effort to reduce periods of isolation that lead to price spikes when justified by the system expansion costs.

The contingency/remedial action approach is known to be computationally intensive over many time periods and multiple future scenarios. The original method was approved as a FERC tariff for wholesale market management in 1994. This method used costs for remedial action contracts to mitigate the changes to the loss of load probability (LOLP) and the expected unserved energy (EUE) at each distribution point in the electric transmission network. All predefined contingencies were enumerated and remedial actions selected to minimize the cost of mitigation. Monte Carlo techniques will be investigated to find the best combination of sampling and the best Linear Programming technique to reduce the computational burden. Other methods to reduce the tree size will be investigated.

The stochastic power flow algorithm will be modified to produce the same information as the contingency/remedial action method. The speed of the stochastic power flow algorithm is expected to be faster than the traditional contingency/remedial action method. The stochastic power flow work is to expand the SPF algorithms previous

developed to include the equivalent action of remedial actions to maintain the strictness of guarantee and the cost so such mitigation.

Once the future scenarios are solved, the resulting price signals will be used to justify expansion to the transmission system. It is proposed that a single year of operation be simulated in this fashion to form the basis for operation in future years. This input is then used by capital budgeting analysis based on modern portfolio theory as is typically used. Additionally, real option analysis and certain monetary equivalent may be investigated. The research focus of this proposal is the comparison of Monte Carlo combined with Linear Programming method to the stochastic power flow method. The analysis of the capital budgeting problem is only to show how the results of either program can be used to justify expansion.

Contingency/Remedial Action

One of the desired characteristics of the ideal market for electricity is that there should be several choices of electricity available for trading. Electricity is normally viewed as a homogeneous product. However, electricity contracts could be viewed as various heterogeneous products provided different contracts specify aspects of the electricity to be delivered. Previous work used strictness of guarantee to differentiate electricity contracts and these heterogeneous electricity contracts were traded in multiple auction classes. Different auction classes have different specified levels of strictness of guarantee. The specified level in each class serves as the minimum strictness of guarantee of the power that buyers bought from that class. This project will use a single auction class.

This strictness of guarantee is specified through two quantities: availability and expected energy served (EES). In brief, availability is defined in this work as the probability of the services being served to/by the particular participants for the period specified in the auction contracts. EES is defined in this work as the expected proportion of the delivered power amount to the bought power amount of a buyer in the auction period.

Remedial actions are needed so that power can be delivered from sellers to buyers promptly according to the availability and EES specified in the contracts. Remedial actions are invoked automatically or by the independent system operator in case of contingencies, which could be precontingency (invoked in expectation of a contingency), or post contingency (invoked after the occurrence of a contingency). Previous work allowed additional type of bids, contingency bids to serve as a market mechanism for the remedial actions so that there are enough remedial actions supplied to the system whenever they are needed. TPLAN and TRELSS were used as basis for the previous work for reliability assessment.

Previous work proposed market mechanisms for multiple-class auctions, which specifies the minimum strictness of guarantee of the power that buyers bought via two quantities: availability and EES. Sellers are required to specify the availability of sold power to indicate strictness of guarantee. Previous work also illustrated the procedure that the central coordinator uses for matching energy bids and contingency bids. The market illustrated in previous work provides additional price signals (availability and EES) to the traders and also provides a market mechanism for remedial actions.

By having availability and EES as additional price signals based on offered prices, traders have additional options to choose and this in turn gives more flexibility for trading. This also gives flexibility for buyers to choose electricity at a desired level of availability and EES. The buyers who need high continuity of electricity, e.g. hospitals probably select to bid in the class of high availability (which also has high EES). The proposed work may include multiple class markets.

There are several probabilistic indices that have been used in the literature for security assessment. Loss of load probability (LOLP) and expected energy not served (EENS) (or expected demand not served) are presented earlier work in this area. For example, a risk index has been used for security assessment. The indices used in this work for distinguishing each auction class from each other are availability and EES.

The market mechanism for trading power and remedial actions in auctions with a specification of availability and EES is the key component. Generation companies (GENCOs) are assumed to be sellers and energy management companies (EMCOs) are assumed to be buyers. Transmission companies (TRANSCOs) are assumed regulated. An independent contract administrator (ICA) is the central coordinator, which provides the combined services of the independent system operator (ISO) and the regional transmission organization (RTO) as a seamless organization.

Availability

The availability level used in this work is defined as the probability of the services being served to/by the particular participants for the period specified in the auction contracts. In each auction class, there are two quantities specified: availability and EES. The availability level specified in each auction class is subject to the EMCOs, which are assumed to buy energy for customers. In each class, the availability level specified indicates the minimum availability guaranteed to the EMCOs that buy power from that auction class.

In the process of matching bids, the loss of load probability (LOLP) is calculated for each auction class and the availability level is calculated as one minus the LOLP. The LOLP in each class can be calculated from the summation of the probabilities of contingencies that cause curtailing of the bought power of EMCO(s) in that class. The method used for calculating the LOLP is probabilistic and based on contingency enumeration. The calculation is aimed for operation and steady-state scenarios.

EES

In each auction class, an EES is specified in addition to the availability. The EES specified in each auction class is subject to the EMCOs, which are assumed to buy the power. In each class, the EES level specified indicates the minimum EES guaranteed to all the EMCOs that buy power from that auction class.

The EES used in this work is defined as the expected *proportion* of the delivered power amount to the bought power amount of an EMCO in the auction period. EES is calculated from one minus EENS. The EENS used in this work is defined as the expected *proportion* of the non-delivered (i.e., curtailed) power amount to the bought power amount of an EMCO in the auction period.

Energy Bids

Previous work assumed that there are two types of bids, energy bids and contingency bids. Energy bid by an EMCO is composed of bid price, bid amount, and the desired auction class for the bid to be matched. Power bid of a GENCO is the same as power bid of a buyer but with an additional bid specification. The additional bid specification that the GENCO needs to submit is the guaranteed availability of supplied power. This project will use this assumption.

Contingency Bids

Apart from power bids, players (GENCOs and EMCOs) can submit contingency bids, which are defined as bids for each remedial action. A contingency bid is composed of bid price, bid amount, an offered remedial action, and an auction class for the contingency bid to be matched. Penalties are imposed for the undelivered remedial actions. Such bids are sometimes called contingency contracts.

Remedial Actions

In the deregulated market, some remedial actions that were classified in different categories in the past should be classified into the same category in the deregulated market. For example, generation redispatch and load shedding should no longer be separated because double-sided auctions are used and both GENCOs and EMCOs can submit bids for the market. This work assumes that the remedial actions are paid regardless

Previous work used an LP-based formulation for optimizing the remedial actions when the contingency causes line overloading. The only remedial actions considered were reserves by GENCOs and shed-load by EMCOs. Other remedial actions to cure other problems resulting from contingencies can be incorporated similarly into the formulation but are not in the scope of this work. The LP-based optimal remedial action formulations are well presented in the literature which include other remedial actions not considered in the formulation shown below. The only minor modification for applying those formulations to the auction problem is to change the objective function to be minimizing the cost of contingency bids submitted by GENCOs and EMCOs and the remedial action costs of TRANSCOs. The cost of each contingency bid can be constructed similarly to which are presented.

Note that if the remedial actions are infeasible (i.e., cannot cure the violated operational limits); the contracts of GENCOs will be allowed to be partly or fully taken away.

The above data is the basis for evaluation of the transmission expansion plan using classical financial techniques similar to Black Scholes (Real Options). These tools require a probabilistic or stochastic model to evaluate the future cash flows. The cash flows for a transmission line are based on the use of the line and the payment method in place. This project assumes that the use of transmission equipment is based on the postage stamp method. The dollar per megawatt mile method data requirements will be investigated if time permits.

1.2. Project overview

For power engineering and power marketing tasks, a number of computational tools have been developed. Among those tools is the utilization of a power system transmission effectiveness index known as the Available Transfer Capability (ATC). The ATC is the amount of power that can be transmitted between two given buses in a power system. Under deregulation, transmission paths are heavily used to buy and sell (i.e., 'trade') electric power. Numerical values for the ATC in megawatts are commonly used to determine the amount of money that is generated for a trade. In addition to the use of ATC in evaluating market trading scenarios in an operating environment, ATC could also be used to evaluate alternative sources of electric power in a planning environment. Transmission expansion might be used to improve ATC, and cost/benefit analysis could be used to evaluate given expansion scenarios.

The stochastic nature of power systems show that load demands have a probabilistic behavior. The probabilistic behavior of the loads suggest that the ATC is also probabilistic. Evaluating the stochastic ATC is important for:

- Aid in operating decisions
- Project revenue from transmission services sales
- Identify the type and location of transmission expansion.

1.3. Statement of the stochastic ATC evaluation problem

Power systems in general are random in nature. If bus loads are considered to be random, all of the variables (e.g. bus load voltages and line power flows) resulting from a power flow study become random. Since the ATC is based on these variables, the ATC can be considered as random. The stochastic ATC evaluation problem is the evaluation of the statistical model of the ATC given a statistical model of the system loads. Traditionally, ATC calculation is considered to be deterministic. For most cases, a stochastic ATC calculation problem can be solved using a Monte Carlo analysis. That is, a very large number of system load cases could be used in calculating ATC between given pairs of system buses. Because of the degrees of freedom of the load randomness, in order to obtain the best results from a Monte Carlo analysis, a large number of trials have to be solved. This results in a long computational time. Stochastic-algebraic methods of ATC calculation that avoid direct simulation and calculation of a large number of trials can have a significant decrease in the computational time. Such an "stochastic-algebraic method" is an analysis based on algebraic properties of transformations and probability density functions and probability theory.

1.4. Available transfer capability

The Federal Energy Regulatory Commission (FERC), in response to the development of the Federal Power Act in 1992, issued a series of proposed rules that provided hints to the direction that FERC was headed and sought industry comment. After gathering the wide number of industrial comments, FERC issued the Orders No. 888 [1] and 889 [2] in 1996. These orders established certain guidelines that energy

markets have to follow which played key roles in opening the US energy market to competition.

FERC Order 888 further opens access to existing electric power transmission networks and allows for a better customer choice. Order 888 mandated the separation of electrical services and marketing functions which required utilities to provide open access to their tariffs, and gave existing utilities the right to recover stranded costs from energy customers from investments based on the older regulations.

FERC Order 889 mandated the information of energy market indicators such as Available Transfer Capability (ATC) and Total Transfer Capability (TTC) available to potential competitors, and posting of the energy market indicators on the Open Access Same-time Information System (OASIS) [2]. ATC is defined by the FERC as the measure of transfer capability remaining in the physical transmission network over committed uses. Also, the TTC is defined as the total amount of power that can be sent in a reliable manner. The purpose of calculation and posting of market indicators such as ATC and TTC to OASIS is to further the open access of the bulk transmission system by providing a market signal of the capability of a transmission system to deliver energy, which would spur competitive bidding in the energy market.

The NERC formed the official definition and proposed a numerical approximation of the ATC in 1995 and 1996 [3,4]. The documents by NERC defined ATC as a measure of transfer capability. This capability is the remaining available transfer in the physical transmission network above already committed uses. The NERC further defines ATC as a function of increases in power transfers between different systems where as the transfers increase, the flows in transmission lines increase. The TTC is the largest flow in the selected transmission system for which there are no reliability concerns such as thermal overloads, voltage limit violations, voltage collapse, system stability and any other system reliability problems. The TTC minus the base case flow and appropriate transmission margin is the ATC for the selected transmission system. Figure 1.1 shows an NERC depiction of ATC. The top line of Figure 1.1 is the TTC. The changes in TTC depict changing reliability concerns, temperature and other factors that would cause change in the maximum amount of power that can be transferred [3,4]. Recallability is defined as "the right of a transmission provider to interrupt all or part of a transmission service for any reason, including economic, that is consistent with FERC policy and the transmission provider's transmission service tariffs or contract provisions". Non–recallability is defined as transmission service that can only be interrupted in cases where system reliability is threatened or an emergency exists. The recallable and non-recallable ATC scheduled are based on the base case load flows which already exist in the system. The Independent System Operator (ISO) has an option to disconnect loads that are a part of the recallable scheduled loads that affect the ATC transfer. The Transmission Reliability Margin (TRM) is a small amount of reserved available power that insures a margin of stability in the system if faults or interruptions occur.

Ejebe [5] implemented a program for ATC calculations based on a full AC power flow solution. The features of the program determine the reactive power flows, voltage limits and voltage collapse, as well as thermal loading effects. A continuation power flow (CPF) is used that is based on the Newton power flow algorithm with adaptive localization. Due to the large number of contingencies that are needed to determine ATC for each transfer, a large computation time results.

Gravener [6] observed, from a test case of the Pennsylvania-Jersey-Maryland Interconnection, that ATC needed to account for the uncertainties that exist in the physical structure of the power system. An ATC calculator was developed which included both linear and nonlinear analysis. Results showed that when the transfer step sizes in the ATC search pattern were varied, ATC values varied as much as 8%. The variation of ATC values in the calculator has an enormous impact on the energy market and improvement on the search algorithms to decrease the variation needs to be implemented.

Ejebe [7] implemented a linear ATC (LATC) calculator based on the linear incremental power flow approximation. The LATC calculator provides a reasonable accurate approximation of the ATC much faster than exact methods. The thermal limits of the line flows and calculation of time independent generating and line outage contingencies before LATC make the calculation of the ATC faster. LATC tests were done on two large practical systems that provided a close approximation to the exact value of ATC with a faster speed than the continuation power flow method.

Sauer [8] presented some initial concepts on including reactive power in linear methods for computing ATC. The reactive power flows are first determined. The ATC is then attained using active power distribution factors. Results show that inclusion of reactive power in linear ATC can reduce errors in the estimation of the maximum transaction over a transmission system. The computation method can be efficiently implemented in linear ATC programs, without considerable increase in computer requirements. Sauer's consideration of reactive power in the ATC calculation is only applied to small systems and needs to be tested and evaluated for practicality in large systems.

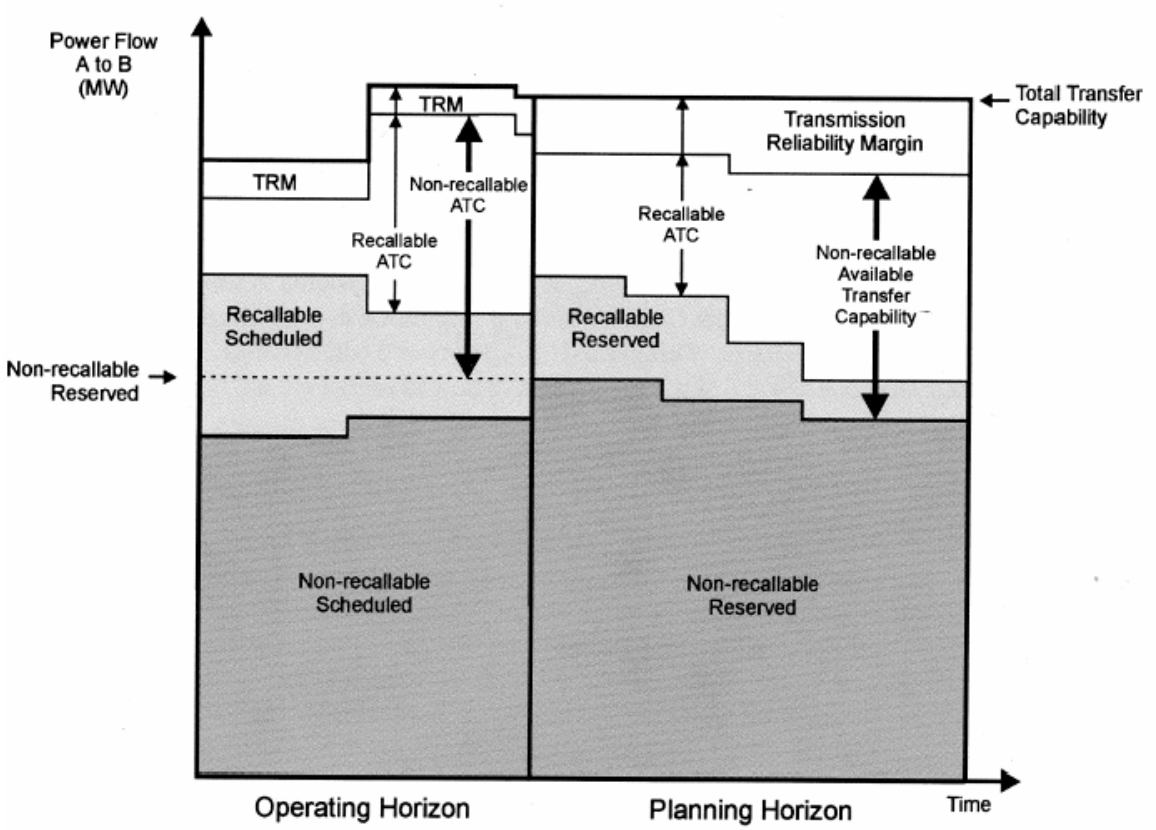

Figure 1.1. TTC, ATC, and related terms in a transmission service reservation system

(Taken directly from [9])

Gaino and Padilha-Feltrin [9] also include reactive power in a liner method of computing the ATC. The reactive power flows computation is approximated by exact circle equations for the transmission line complex flow and the ATC is calculated using power flow distribution factors. They went on to show that the ATC can be increased by finding the best group of busses which can have their injected reactive power modified in order to alleviate overloads in the transmission lines. Results from their method show that adding reactive power flows in the ATC computation to a traditional linear distribution factor approach results in more accurate estimates for the ATC.

Othman, Mohamed, and Hussain [10] illustrate a computationally fast and accurate method of finding the ATC. They implement a cubic-spline interpolation curve fitting technique which reduces the computation time of the power flow computations. The ATC is limited by voltage and power flow limits. The voltage and power flow limits are used in a plot and the ATC is determined at the point where an increase of real power transfer intersects the curves. Their results show that their method is accurate and faster than an iterative AC power flow computation which is demonstrated on a realistic 241 bus system.

Xia and Chan [11] developed an ATC calculation which considers transient stability constraints. The method is solved by using a direct nonlinear primal-dual interior point method [91]. The transient stability constraints are first converted into equivalents

and then incorporated into an optimal power flow study. Their consideration of transient stability constraints is only applied to small systems and needs to be tested in large systems.

Cui, Bie and Wang [12] propose a method of forming a probabilistic ATC study based on a Monte Carlo simulation [16-24] with a sensitivity analysis. The Monte Carlo simulation analyzes the power system uncertainties and the ATC is then calculated using a sensitivity analysis. Their method develops a new load model which considers the impact of load uncertainties which includes the system load level and bus fluctuations on the ATC. Their results show an efficient ATC calculation on a small system and should be retested on a larger system. The probabilistic ATC calculation provides a good compromise between the computing time versus precision for a 23 bus system.

Kumar, Reddy and Venkaih [13] propose a real time ATC calculation using three different techniques:

- Back propagation algorithm
- Radial basis function neural network
- Adaptive neuro fuzzy inference system.

Each of these intelligent techniques trace all the paths between the transfer busses of the ATC. The path with the least impedance is chosen as a basis of pattern generation in the intelligent programs. The calculation methods are tested on a 24 bus system considering only line thermal ratings and a few selected line outages. Each of the three intelligent techniques resulted in similar values of the ATC, but further comparison should be preformed with a more accepted ATC calculation method.

Su [14] proposes a computation of ATC which accounts for the uncertainty effects in the computation. The method uses a point estimate method to calculate the ATC. The statistical moments of the ATC are found with respect to the uncertainty in system parameters. The bus load injections are assumed to be normal. The proposed method is tested against a Monte Carlo method using a 24 bus system. Results show that the method has an execution time considerably shorter than a Monte Carlo method, and the expected value is accurate to within 5% of the Monte Carlo method.

1.5. Stochastic load flow studies

Power flow studies have been a major part of the analysis and design of power systems. Throughout the history of load flow techniques, the data that are provided in order to calculate the load flow variables are generally considered to be constant and deterministic. The inputs to a load flow analysis are, in most cases, a snapshot value of a wide range of operating point data. This technique gives a picture on what happens in the system, but engineers often need to know the effect of a range of operational load values. Since the 1970s, researchers have been studying data ranging in the power flow study context. Probabilistic or stochastic load flow methods are an approach to accommodate and model the random nature of the operational load and generation data.

Throughout the 1970s and 1980s a number of papers addressed different techniques involved to analyze various formulations of the stochastic load flow problem. Vorsic, Muzek, and Skerbinek [15] summarized the different stochastic load flow techniques in three basic methods:

- Monte Carlo
- convolution
- method of statistical moments.

The Monte Carlo method is a known method to obtain the solution of the stochastic load flow problem. This method utilizes repeated trials of the deterministic load flow technique to determine the probability distributions of the nodal powers, line flows and losses. Since the accuracy of the probability distribution of line flows, voltages and losses is presumed to be better when modeling all stochastic inputs over a large number of trials, the Monte Carlo method is often characterized by a large computation time. Nonetheless, the Monte Carlo method has been used in many general engineering applications [16-24]. This method has an appeal that a wide range of stochastic phenomena can be modeled, thus suggesting "accuracy" in the results. The Monte Carlo approach does not rely on any required system characteristics: e.g., nonlinear systems are just as readily studied as linear systems. But computational burden is a clear disadvantage of the Monte Carlo approach and researchers have sought faster methods to calculate the probability distributions. The Monte Carlo method can be used to verify and validate these faster methods. Also, no matter how large the number of trials in a Monte Carlo simulation, there is always an issue with not studying a particularly problematic condition. As an example, how many coin tosses are needed to find the probability that a coin lands on edge?

Returning to the stochastic power flow studies, the convolution method was perhaps first researched by Borkowska [25]. Prior to her paper, there was little research done in determining the effect of the uncertainty of load data to the uncertainty of bus voltage and line power flow. Borkowska's work concentrated on how probability density functions of the input bus variables calculated through load flow equations yield density functions of branch power flows. She assumed that active and reactive power flows are independent of each other. The random processes associated with the input bus variables are assumed independent and have a general statistical distribution which is calculated though linear load flow analysis using a convolution technique. The resulting density function gives a practical view of the probability of exceeding the capacity limit in branch flows and the practical and probable range of branch load values. Some problems in her assumptions are the nonlinear relation between node loads and branch flows, and proper balance of generation and loads.

Dopazo, Klitin, and Sasson [26] addressed the stochastic load flow problem approximately at the same time as Borkowska. Their objective was similar to Borkowska's convolution method but with a different approach. Employing a method that assumed normally distributed variables of load bus P and Q and normally distributed generator bus variables P and V, Dopazo, Klitin, and Sasson calculated load flows using classical methods. A covariance matrix of the load flow data is formed. Using the variances assumed for the input data, another covariance matrix is formed. The two covariance matrices are then used to obtain confidence limits, or ranges of which the true value has a given probability of existence (e.g., a 99% confidence interval). Note that normally distributed complex random variables have their difficulties as described in [27-33].

The method of statistical moments, used by Sauer and Heydt [27], relates to the processing of the statistical moments of univariate and multivariate random variables. For the univariate case, the *k*th central statistical moments ($k > 1$) of random variable x are

$$\mu_x = E(x^k)$$

$$\mu_x^{(k)} = E((x - m_x^{(1)})^k)$$

where *E(...)* denotes expectation. In order to use rather simple properties of statistical moments, of *Y* given $Y = AX$, and given the moments of a multivariate random variable *X*, the electric power flow problem is linearized. Following linearization of the system equations, the statistical moments of voltages and load flows are used to determine the distribution of voltages and load flows. Although the foregoing discussion mentions the univariate case, the method of moments is readily applicable in the multivariate case. The method works well solving the stochastic load flow equations with errors in the output data being smaller than other methods [25, 26]. Note that the probability density function of a random variable is not determined by its statistical moments in general, but in practical engineering applications one may assume that the density and distribution are uniquely determined by the statistical moments. [28-34].

A simpler solution of the Sauer and Heydt's approach was done by Patra and Misera [35]. A proposed method of cumulants by Sanabria and Dhillon [36] is the basis of the work done by Patra and Misra. The method, like [27], uses the method of statistical moments to analyze the complex random variables while using the Gram-Charlier expansion [29] to approximate the probability density functions of the output bus voltages and line flows. Simply stated, the Gram-Charlier expansion is a technique used to obtain a probability density of a random variable given its statistical moments. The Gram-Charlier series has been used in recent applications such as a stochastic-algebraic available transfer capability calculation [95] and in optical communications systems [96]. The method is usually formulated in terms of cumulants. The cumulants k_n of a random variable can be found from the statistical moments of the distribution. In terms of the first four raw moments of random variable x, the first four cumulants of *x* are,

$$k_x^{(1)} = \mu_x$$

$$k_x^{(2)} = m_x^{(2)} - (m_x^{(1)})^2$$

$$k_x^{(3)} = m_x^{(3)} - 3m_x^{(2)}m_x^{(1)} + 2(m_x^{(1)})^3$$

$$k_x^{(4)} = m_x^{(4)} - 4m_x^{(3)}m_x^{(1)} - 3(m_x^{(2)})^2 + 12m_x^{(2)}(m_x^{(1)})^2 - 6(m_x^{(1)})^4$$

where $m_x^{(n)}$ with is the nth raw moment of the random variable *x*. The cumulants are used in the Gram-Charlier expansion where the bus voltages and line flows are obtained from both the statistical moments and cumulants. Conclusions of Patra and Misera's work show that their technique has better computational advantages compared to existing methods using complex random variables for the load flow. However, Patra and Misera's method seems to give higher errors than in [27].

Zhang and Lee [37] proposed a method of computing a probabilistic load flow study in large power systems. The method is proposed to be a quick screening tool to analyze major investments on improving transmission system inadequacy. Zhang and Lee's scheme combines the determination of line flow cumulants and the Gram-Charlier expansion to obtain probabilistic distribution functions of the transmission line flows. Their conclusions show that their method is able to accurately approximate the cumulative distribution function of transmission line flows for small systems. They state that future research will consider applying their method to larger size systems.

In private communication with some researchers in the area of stochastic power flow studies, it appears that despite the intellectual appeal of the stochastic power flow algorithm, and despite the valid claims of potential value of the method, this stochastic-algebraic tool has not been in widespread use at any stage of power engineering.

1.6. Probability density fitting

An important step in a stochastic load flow problem is the representation of the line loading data (i.e., *P,Q*), or line load statistical moments into a probability density function. Sauer [37] implemented the Gram-Charlier type A [29,38] series in the stochastic load flow problem. The general concept of construction of a probability density function has occupied considerable attention in the classical probability literature. Alternatives are illustrated here with the implication that the probability density function of ATC might be better constructed using one of these alternatives. Three different fitting theories based on the works of Karl Pearson, H. L. Gram, C. V. Charlier, and F. Y. Edgeworth are well documented [38-41] and have many distinguishing qualities. Perhaps the largest number of applications of the orthogonal series expansions of probability density functions is relegated to the pre-digital era.

Pearson's distributions [29] provide a systematic approach to fit statistical moments to one of twelve specific closed form density functions. Three are well known normal, beta, and gamma density functions. The criteria for determining which of the twelve densities to use are given in [29], and the process is quite lengthy. The process for determining the distribution as well as the criteria has a significant disadvantage of the required data due to the large size as well as the lengthy computation time needed to run in a computer program [29,38-41].

The Gram-Charlier and Edgeworth series [29,38-40] are independently derived representations of a density function as an infinite series of a sum of orthogonal functions involving statistical moments and cumulants. The methods generally stem from the uniqueness of the characteristic function

$$\phi_x(t) = E[\,e^{jtx}\,] = \int_{-\infty}^{\infty} e^{-jtx} f(x)dx\,.$$

Note that there is an ambiguity of sign in the –jtx term of the characteristic equation. In electrical engineering, the sign is negative, and in mathematics the sign is positive.

Three of the Gram-Charlier series have been proposed based on an infinite series of functions of Hermite polynomials and statistical moments. The type A series is the most commonly used type and is based on derivatives of the characteristic function of the

normal distribution. The characteristic function of a probability density function is its Fourier transform,

$$\Im\{f_x(x)\} = \phi_x(t).$$

The Gram-Charlier series type A has been widely applied and can accurately represent many density functions, but in some cases, can produce negative frequencies. The type B and C series [29,38] are based on derivatives of the Poisson density and the gamma and beta densities. All of these kernel functions are orthogonal functions. The type B series has certain mathematical advantages and this series has been used to accommodate discontinuous variation resembling the Poisson distribution. The type B series is rarely used. The type C series, based on derivatives of the gamma and beta densities, was proposed by Charlier to avoid negative frequencies but never has had the appeal of the type A series.

The Edgeworth series [39-41], which resembles the Gram-Charlier series, utilizes cumulants, instead of statistical moments in an infinite series based on the derivates of the same normal, Poisson, gamma and beta densities. References [28-34,38-40] are general references on the subject of random variables, stochastic processes and non-deterministic systems.

1.7. Organization of this report

Chapter 1 describes the overview of the report and provides a literature summary of stochastic load flow, ATC, and probability density function fitting. In Chapter 2, a method of analytically calculating the stochastic ATC with bus load uncertainty is presented. Chapter 3 illustrates the stochastic ATC calculation. Chapter 4 extends the stochastic ATC calculation developed in Chapter 2. Transmission element outage uncertainty is added to the calculation. Chapter 5 provides illustrations of the stochastic ATC calculation with bus load and transmission element uncertainties. Conclusions drawn from the examples in Chapters 3 and 5 are provided in Chapter 6. Transmission expansion is addressed in Chapter 7 with a cost to benefit analysis. Conclusions of the report and possible future work ideas are shown in Chapter 8. Appendices A-H provides the following additional information:

- Appendix A – information on the calculation of statistical moments and other statistical properties used in the report.
- Appendix B – a subroutine in MATLAB written to calculate the probability density function by using statistical moments. The resulting PDF is called the Gram-Charlier series.
- Appendix C – a derivation of the PDF of the minimum of several random variables is developed. This derivation is important in the final steps of the stochastic ATC calculation shown in Chapter 2.
- Appendix D - useful information on the NERC E-tag process is presented. E-tag is widely used in deregulated power systems for the trade of power.
- Appendix E – WECC system data used in all the WECC 179 bus examples is shown.

- Appendix F – stochastic ATC calculations are provided using the IEEE 14 bus system. These examples provide some different cases of stochastic ATC not shown with the WECC system.
- Appendix G – the limitations used in the WECC examples is presented in this appendix.
- Appendix H- provides a list of examples used in the report

2. Probabilistic Available Transfer Capability

2.1. Available transfer capability and open access of transmission systems

In order to provide open access to electric power transmission networks and promote generation competition and customer choice, the Federal Energy Regulatory Commission requires that available transfer capability be made available on a publicly accessible OASIS. ATC is defined as a measure of the transfer capability, or available "room" in the physical transmission network for transfers of power for further commercial activity, over and above already committed uses. That is, ATC is the megawatt capability of the system for tag schedules. Appendix D illustrates the method of E-tagging developed by the NERC.

As an illustration, consider Figure 2.1 in which 1000 MW is transmitted from bus A1 to bus B1. If the path rating is 1500 MW and if no parallel paths exist from A to B, the ATC from A1 to B1 is 500 MW.

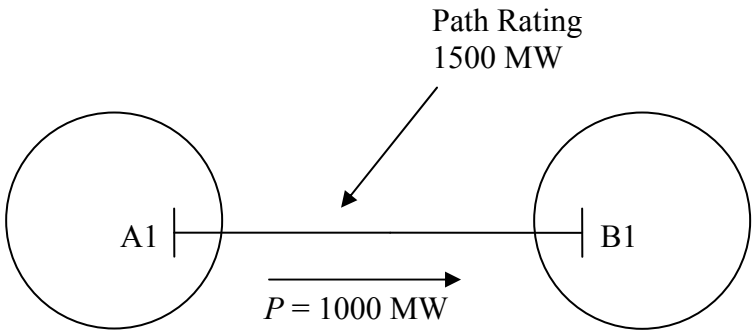

Figure 2.1. Illustration of ATC

Due to uncertainty in bus loading, the power flows within a power network also become uncertain. By applying the theory of functions of several random variables, the statistical moments of line power flows within a system can be found. Information on statistical moments is shown in Appendix A. Although difficult to find analytically, the statistical moments of the line power flows can be estimated by:

- applying a stochastic load flow algorithm to the existing system
- assuming bus loads to be normally distributed.

The uncertainty of the future loads implies that the power flow is probabilistic. Thus, a stochastic load flow study should be used. The stochastic load flow study yields the statistical moments describing the behavior of the line power flows. This uncertain behavior of line power flows affects ATC and causes ATC to be probabilistic. The proposed algorithm described in this chapter is for the utilization of stochastic methods for ATC calculation and power marketing. Figure 2.2 shows the general concept. In order to develop a model that captures the stochastic aspects of ATC, it is necessary to use a statistical model. The Gram-Charlier series is proposed as a statistical model of the ATC.

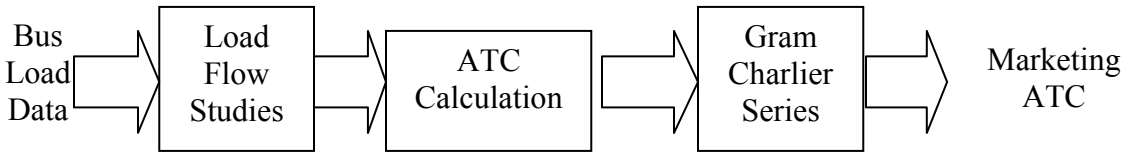

Figure 2.2. The general concept of the proposed algorithm

2.2. Statistical moments of line flows and bus voltage magnitudes

The stochastic power flow algorithm utilizes a direct transformation of statistics to obtain selected statistical results. In this section, the statistical moments of line active power flows and bus voltage magnitudes in a power system are considered. Consider Figure 2.3 as an example of the stochastic load flow method of finding the line flows and voltage magnitudes and the statistical moments of those flows and magnitudes.

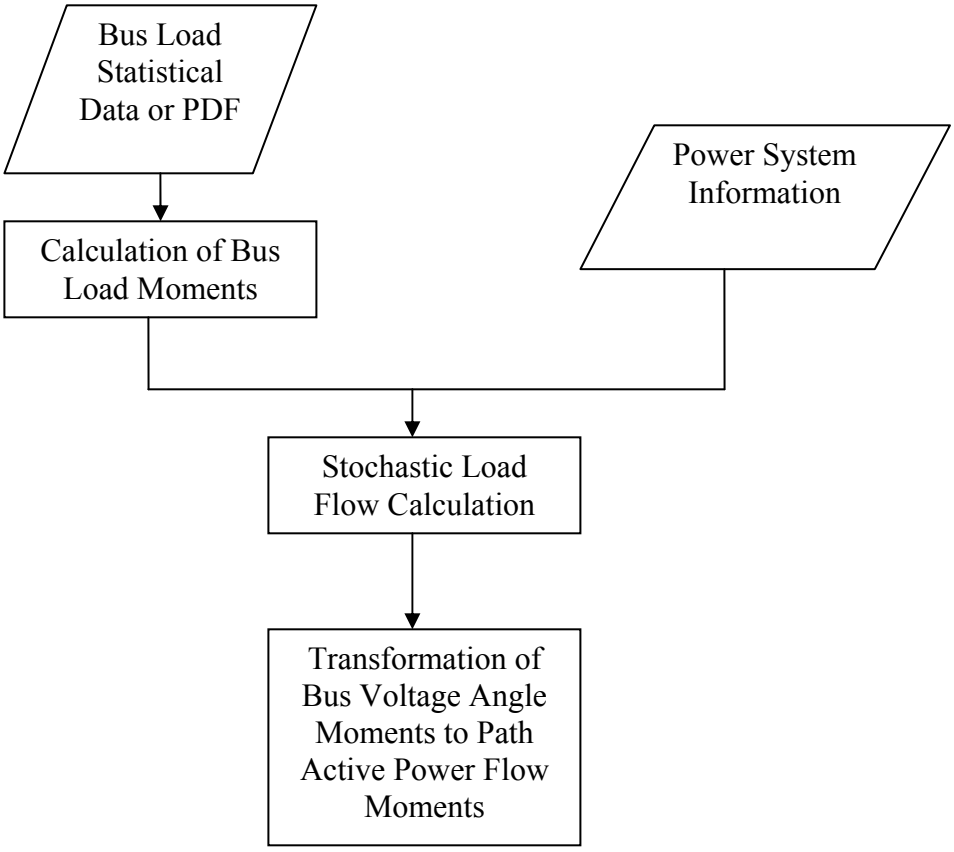

Figure 2.3. Stochastic load flow study process

The concept of a stochastic power flow study is that if bus load moments are known, then those moments can be transformed into moments of active line flows and bus voltage magnitudes. Assuming that bus load statistics are Gaussian, a direct

transformation of moments can be performed using a linear transformation [15,25-27,35-36]

$$Y = AX. \tag{2.1}$$

Let X be a multivariate Gaussian distributed vector with mean vector M_x and covariance matrix Σ_x. The resulting mean and covariance of Y are

$$M_Y = AM_X \tag{2.2}$$

$$\Sigma_Y = A\Sigma_X A^t. \tag{2.3}$$

The approximation of statistical independence is made to estimate the higher order moments.

The stochastic load flow uses information from the inverse power flow study Jacobian matrix to find an approximation of the change in bus voltage magnitude and transmission line flows,

$$\begin{bmatrix} \Delta\delta \\ \Delta|V| \end{bmatrix} = [J]^{-1} \begin{bmatrix} \Delta P \\ \Delta Q \end{bmatrix}. \tag{2.4}$$

This yields an approximation of the change in bus voltage magnitude and bus voltage angle. Equation (2.4) can be decoupled into two parts

$$[J]^{-1} = \begin{bmatrix} \Xi_{11} & \Xi_{12} \\ \Xi_{21} & \Xi_{22} \end{bmatrix} \tag{2.5}$$

$$\Delta\delta = \Xi_{11}\Delta P + \Xi_{12}\Delta Q \tag{2.6}$$

$$\Delta|V| = \Xi_{21}\Delta P + \Xi_{22}\Delta Q \tag{2.7}$$

in which Ξ_{ij} is the submatrix of the inverse Jacobian matrix from the solution point of a power flow. From (2.7), the change in voltage magnitude is found, and (2.6) can be used to find the change in transmission line flows.

The change in transmission line flows within a system can be approximated by

$$\Delta P_{ij}^{line} = (\Delta\delta_i - \Delta\delta_j) B_{line} \tag{2.8}$$

where i and j represent sending and receiving buses, ΔP_{ij}^{line} is the change in line real power flow from bus i to bus j, and B_{line} is the imaginary part of the transmission line admittance. In order to convert this single line approximation into an approximation which includes all transmission lines (and transformers) in the system, an incidence matrix needs to be formed.

The incidence matrix L is of size (number of branches) x (number of busses) and includes only 0, 1 and -1 for its elements [42]. Each row of the incidence matrix represents each transmission line of the system corresponds to a +1 in the sending end bus column and -1 in the receiving end column. For example, if a representation of a

transmission line from bus 2 to bus 4 of a 5 bus system needs to be represented in an incidence matrix, the corresponding row for that transmission line in the incidence matrix would be

$$[\,0\ 1\ 0\ -1\ 0\,]. \tag{2.9}$$

Then,

$$\Delta\delta' = L\Delta\delta \tag{2.10}$$

where $\Delta\delta'$ is the vector form of all the $(\Delta\delta_i - \Delta\delta_j)$ in the system, L is the incidence matrix, and $\Delta\delta$ is the result of (2.6). A matrix representation of B_{line} is $diag(B_{line})$, where $diag(B_{line})$ represents a (number of branches) x (number of branches) diagonal matrix whose elements are B_{line} (for each transmission line of the system). Then,

$$\Delta P^{line} = diag(B_{line})L(\Xi_{11}\Delta P + \Xi_{12}\Delta Q) \tag{2.11}$$

$$\Delta|V| = \Xi_{21}\Delta P + \Xi_{22}\Delta Q\,. \tag{2.12}$$

In order to proceed with the transformation shown in (2.1), Equations (2.11-12) need to be reconfigured into functions of one variable, namely ΔP. It is assumed that the individual power factors (*pf*) of each load are constant, i.e. statistically there is a 100% correlation between the active power load P and reactive power load Q. If load power factors are known, let

$$PF=diag(tan(acos(pf))) \tag{2.13}$$

where *PF* is the transformation matrix, and *pf* is the power factor of each load. In (2.13), the popular MATLAB syntax is used with the elements pf arranged as a diagonal matrix, *acos(...)*giving a diagonal matrix of arccosines of the *pf* terms, and *tan(...)* giving a diagonal matrix of tangents of the above mentioned angles. Equations (2.11-12) can be reconfigured,

$$\Delta P^{line} = diag(B_{line})L(\Xi_{11} + \Xi_{12}PF)\Delta P \tag{2.14}$$

$$\Delta|V| = (\Xi_{21} + \Xi_{22}PF)\Delta P\,. \tag{2.15}$$

Using the linear transformation in (2.2-3), the mean and variance for ΔP^{line} and $\Delta|V|$ can be found,

$$\mu_{\Delta P^{line}} = diag(B_{line})L(\Xi_{11} + \Xi_{12}PF)\mu_{\Delta P} \tag{2.16}$$

$$\mu^{(2)}_{\Delta P^{line}} = diag(B_{line})L(\Xi_{11} + \Xi_{12}PF)\mu^{(2)}_{\Delta P}(diag(B_{line})L(\Xi_{11} + \Xi_{12}PF))^t \tag{2.17}$$

$$\mu_{\Delta|V|} = (\Xi_{21} + \Xi_{22}PF)\mu_{\Delta P} \tag{2.18}$$

$$\mu^{(2)}_{\Delta|V|} = (\Xi_{21} + \Xi_{22}PF)\mu^{(2)}_{\Delta P}(\Xi_{21} + \Xi_{22}PF)^t, \tag{2.19}$$

where $\mu_{\Delta P}^{(k)}$ is the *k*th central moment of the random variable ΔP.

In order to find the statistical moments of line power flows in a stochastic load flow problem, the bus loads have to be represented by probabilistic models. If data for the bus loads are known, raw statistical moments are generated from the sample data using (2.20),

$$m_x^{(k)} = \frac{\sum_{i=1}^{n} x_i^k}{n}, \tag{2.20}$$

where *k* is the moment order, and *n* is the number of samples and x_i is the datum sample *i*.

If bus data are not known, statistical moment generating functions available in [29] can generate statistical moments for a given probability density. If bus load moments are in a form of a probability density function, a moment generating function can be used to find the moments of the bus loads. Given a random variable *x* and a probability distribution function *f(x)* then the characteristic function $\phi_x(t)$ can also be called the moment-generating function. For a continuous distribution,

$$\phi_x(t) = \int_{-\infty}^{\infty} e^{-jtx} f(x)dx = 1 - jtm_x^{(1)} - \frac{1}{2!}t^2 m_x^{(2)} + \ldots. \tag{2.21}$$

Raw moments of *x* are found from the derivates of $\phi_x(t)$. The raw moments can are calculated by

$$m_x^{(1)} = \frac{d\phi_x(t)}{dt}$$
$$m_x^{(2)} = \frac{d^2\phi_x(t)}{dt^2}$$
$$m_x^{(3)} = \frac{d^3\phi_x(t)}{dt^3}.$$

- In most cases the probability density function of the bus loads are:
- Non stationary (statistical moments vary with time)
- Correlated among themselves
- Complex
- Not any recognized distribution.

However, the normal uncorrelated density is commonly used as a "first cut" approximation [15,25-27,35-36].

Many different stochastic power flow algorithms exist as documented by [15,25-27,35-36,42]. The computational time of algebraic based stochastic power flow methods compared to a Monte Carlo approach may be significantly less, but at the potential cost of lots of accuracy. That is, Monte Carlo methods generally do not require linear systems or simple mathematical formulations, but many purely analytical methods do have these

limitations. From an operational point of view, complex mathematical structure is of little consequence because once an algorithm is programmed and rendered as a software tool, only accuracy and execution time are important. Figure 2.3 illustrates the stochastic load flow study process. Inputs into the stochastic load flow study calculation are the bus load statistical moments and power system information (e.g., line impedances, PV bus information, transformer impedances, and shunt capacitor admittances). Stochastic power flow formulations usually do not consider complexities such as P-V buses, Q-limits, and tap changer limits.

2.3. Deterministic approximation of available transfer capability

Before considering a probabilistic method of finding the stochastic ATC, a deterministic method is developed. The deterministic method limits the ATC transfer in a system due to two different fundamental limitations: bus voltage magnitude and transmission line / transformer thermal rating. Both long term and short term thermal ratings can be accommodated. Both contingencies have been widely used in the literature [10,43] and are the basis for a good approximation of the ATC. The subject of security limits for transmission paths will be briefly discussed below.

The deterministic ATC calculation method uses information from the inverse Jacobian matrix at the solution point of a load flow to find an approximation of the change in bus voltage magnitude and transmission line flows. Equations (2.11-12) from the stochastic load flow study form the basis (with a slight modification) of a linear approximation for ΔP^{line} and $\Delta|V|$. The modification to 2.11-12) is the use of the variable ΔP. If A represents the sending end bus, and B represents the receiving end bus, ΔP becomes a vector with 1 in the Ath row and -1 in the Bth row. This changes the representation of ΔP^{line} and $\Delta|V|$, therefore $\frac{dP^{line}}{dP_{AB}}$ and $\frac{d|V|}{dP_{AB}}$ are used to represent the $\frac{dP^{line}}{dP_{AB}}$ and $\frac{d|V|}{dP_{AB}}$ for a given ATC transfer. Inequalities for $\frac{dP^{line}}{dP_{AB}}$ and $\frac{d|V|}{dP_{AB}}$ are set up using transmission thermal line ratings and the maximum and minimum $|V|$ limits. Using P^{line} from a base case load flow study and the transmission thermal line ratings, P^{Rating}, two inequalities are written. These inequalities account for the two directions that power can flow in a transmission line,

$$ATC^{A-B}\left(\frac{dP^{line}}{dP_{AB}}\right) + P^{line} \le P^{Rating} \tag{2.22}$$

$$-P^{Rating} \le ATC^{A-B}\left(\frac{dP^{line}}{dP_{AB}}\right) + P^{line}. \tag{2.23}$$

Two more inequalities are written to model $|V|$ upper and lower limits

$$ATC^{A-B}\left(\frac{d|V|}{dP_{AB}}\right) + |V| \le |V|^{max} \tag{2.24}$$

$$|V|^{min} \le ATC^{A-B}\left(\frac{d|V|}{dP_{AB}}\right) + |V| \tag{2.25}$$

where ATC^{A-B} is the available transfer capability from bus *A* to bus *B*. Note that (2.24-25) assume the worst case scenario of voltages V_A and V_B being in phase. Using all four inequalities, (2.22-25), a linear optimization program maximizes the scalar value of the constrained ATC^{A-B}.

In addition to the P^{line} and $|V|$ limits, security limits often determine ATC, especially for long lines. The static security limits could be interpreted as phase angle limits,

$$-\delta^{max} \le \delta_i - \delta_j \le \delta^{max}. \tag{2.26}$$

The $\delta_i - \delta_j$ term can be approximated by a linear function of ATC similar to (2.6). The extra two inequalities so formed would need to be included with the inequalities in (2.12-13).

Due to the nonlinear behavior of power systems, linearly approximating $\frac{dP^{line}}{dP_{AB}}$ and $\frac{d|V|}{dP_{AB}}$ as constants can yield errors in evaluating ATC. In order to get a more precise ATC, an iterative approach can be used. The iterative approach, shown in Figure 2.4, updates the load at bus *B* of the system with the ATC calculated. This is repeated until the change in ATC is smaller than a specified tolerance (*tol*). Since initial estimates of the ATC can be overestimated based on the $|V|$ contingency, an acceleration factor greater than 1.00 can be used with $\frac{d|V|}{dP_{AB}}$ in order to underestimate the ATC. The need for an "acceleration factor" was found in actual implementation of this concept. When the iterate gets close to the ATC, the acceleration factor is made equal to 1.00 and the calculation is iterated until the tolerance is met.

2.4. Stochastic evaluation of available transfer capability

The method of finding the stochastic ATC is more complex than the deterministic case. The method, illustrated in Figure 2.5, utilizes a stochastic load flow formulation, the deterministic ATC calculation, a Gram-Charlier series approximation of a probability density function, and a method of manipulating probability density functions of several random variables. The stochastic load flow and deterministic ATC calculations are used to calculate statistical moments of the ATC in the probabilistic formulation. The moments of the ATC are calculated in four separate groups, one for each of the constraints in (2.22-25). Each of these groups represents a random variable. The Gram-Charlier series is used to find the probability density function for each group. Statistical properties of functions of several random variables [44] are used to find the resulting in a probability density function of the ATC.

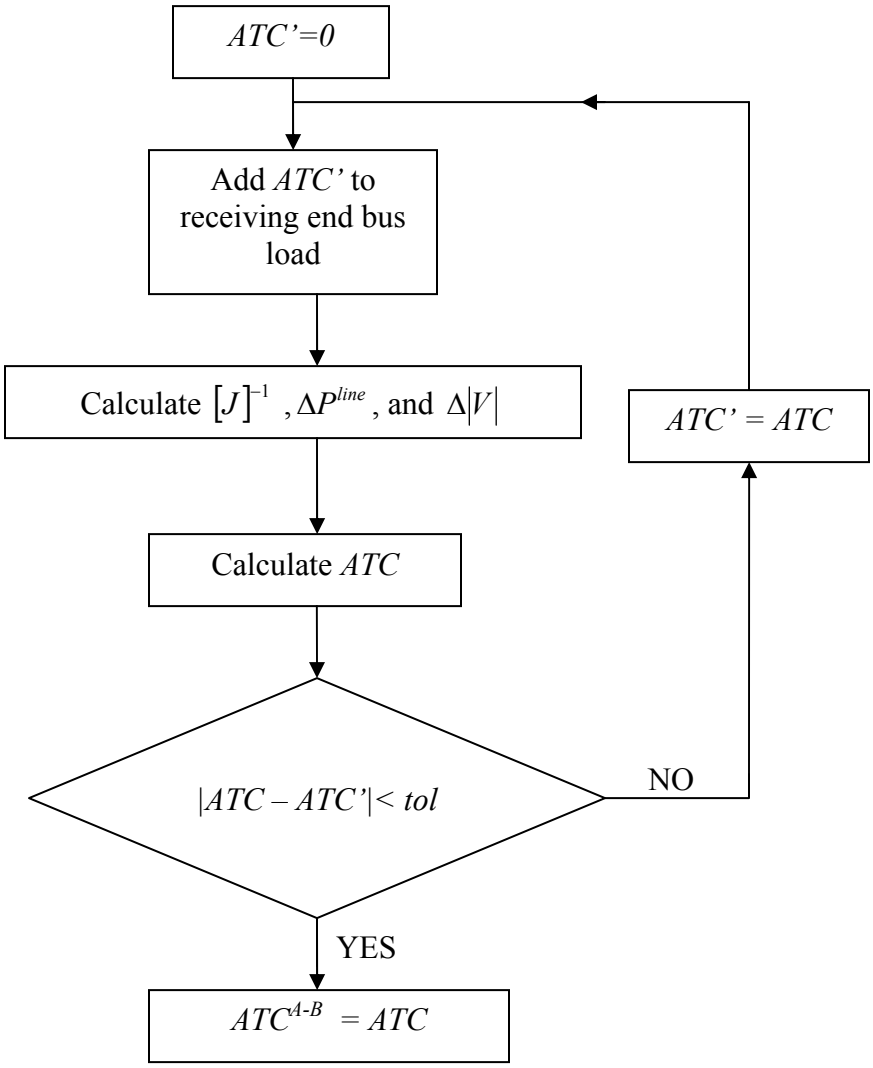

Figure 2.4. Deterministic ATC algorithm calculated using an iterative method

The deterministic evaluation of ATC is used in conjunction with a stochastic load flow study as a first step in finding the stochastic ATC. A stochastic load flow algorithm is used as shown in Section 2.2 to find the statistical moments of the system line flows and bus voltage magnitudes. The system line flows and bus voltage magnitudes are then linearly transformed using the results of the deterministic ATC evaluation in Section 2.3. The result from the deterministic ATC study used is the system Jacobian matrix at the ATC solution point. The assumption made is that of the linearized power flow formulation. For the convenience of the reader, Table 2.1 lists the dimensions of all the various terms in 2.31-2.48.

Equations (2.22-25) ultimately serve as the limitations that constrain the ATC. Reordering those equations yields

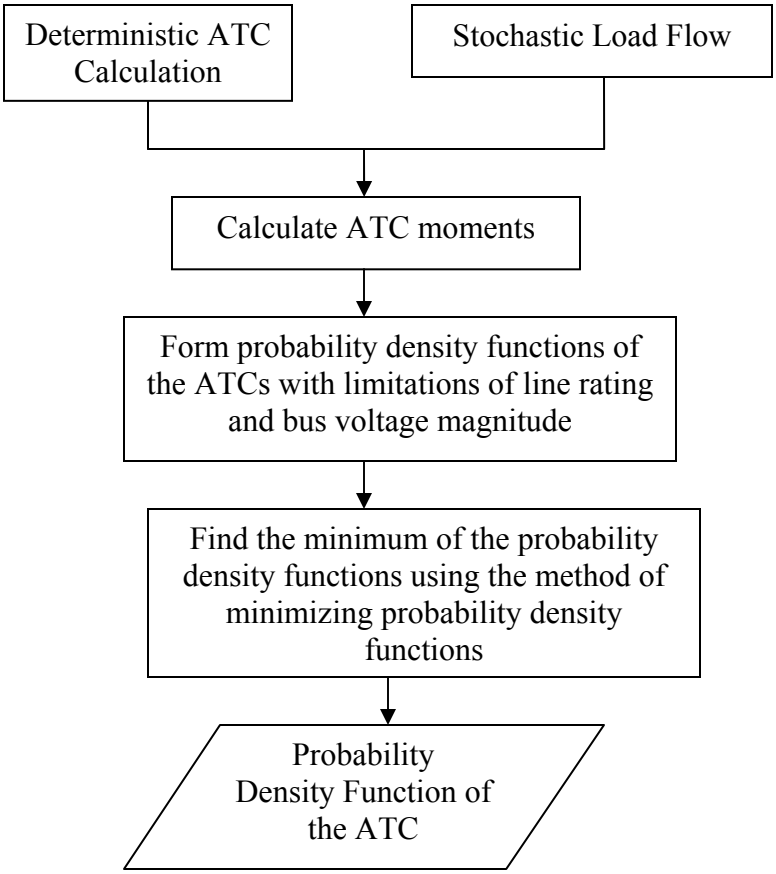

Figure 2.5. Sample stochastic ATC calculation algorithm

Table 2.1 Dimensions of terms in (2.31-2.48)

Symbol	Description	Rows	Columns
ATC^{A-B}	ATC from bus A o bus B	1	1
B_{line}	Imaginary part of the transmission line admittance matrix	N_L	N_L
$diag(B_{line})$	Diagonal elements of transmission line admittance matrix	N_L	1
$\frac{dP^{line}}{dP_{AB}}$	Line flow sensitivity factor	N_L	1
$\frac{d\lvert V\rvert}{dP_{AB}}$	Bus voltage sensitivity factor	N_B	1
L	Incidence matrix	N_L	N_B
$\mu_{P^{Rating}-P^{line}}$	Mean of $P^{Rating} - P^{line}$	N_L	1
$\mu_{\lvert V\rvert^{max}-\lvert V\rvert}$	Mean of the vector whose entries are ($k=1,\ldots, N_B$) $\lvert V_k^{max}\rvert - \lvert V_k\rvert$	N_B	1
$\mu_{\lvert V\rvert^{min}-\lvert V\rvert}$	Mean of the vector whose entries are ($k=1,\ldots, N_B$) $\lvert V_k^{min}\rvert - \lvert V_k\rvert$	N_B	1
$\mu_{-P^{Rating}-P^{line}}$	Mean of $-P^{Rating} - P^{line}$	N_L	1
1^{N_L}	Vector of ones	N_L	1
1^{N_B}	Vector of ones	N_B	1
P_{line}^{Base}	Real power flows at system base case	N_L	1
P^{Rating}	Line thermal ratings	N_L	1
PF	Power factor matrix	N_B	N_B
pf	Load power factor	1	1
$\mu_{\Delta P}^{(1)}$	Mean of bus real power injection	N_B	1
$\mu_{P^{Rating}-P^{line}}^{(2)}$	Central 2nd moment of $P^{Rating} - P^{line}$	N_L	1
$\mu_{-P^{Rating}-P^{line}}^{(2)}$	Central 2nd moment of $-P^{Rating} - P^{line}$	N_L	1
$\mu_{\lvert V\rvert^{max}-\lvert V\rvert}^{(2)}$	Central 2nd moment of $\lvert V^{max}\rvert - \lvert V\rvert$	N_B	1
$\mu_{\lvert V\rvert^{min}-\lvert V\rvert}^{(2)}$	Central 2nd moment of $\lvert V^{min}\rvert - \lvert V\rvert$	N_B	1
$\lvert V\rvert^{max}$	Vector of bus voltage maxima	N_B	1
$\lvert V\rvert^{Base}$	Vector of base case bus voltages	N_B	1
$\lvert V\rvert^{min}$	Vector of bus voltage minima	N_B	1
Ξ_{ij}	Submatrix of the inverse Jacobian matrix	N_B	N_B

N_B = number of buses. N_L = number of lines

$$ATC^{A-B}\left(\frac{dP^{line}}{dP_{AB}}\right) \le P^{Rating} - P^{line} \tag{2.27}$$

$$-P^{Rating} - P^{line} \le ATC^{A-B}\left(\frac{dP^{line}}{dP_{AB}}\right) \tag{2.28}$$

$$ATC^{A-B}\left(\frac{d|V|}{dP_{AB}}\right) \le |V|^{max} - |V| \tag{2.29}$$

$$|V|^{min} - |V| \le ATC^{A-B}\left(\frac{d|V|}{dP_{AB}}\right). \tag{2.30}$$

Information from a stochastic load flow solution is used to find the statistics for $P^{Rating} - P^{line}$ in (2.27), $-P^{Rating} - P^{line}$ in (2.28), $|V|^{max} - |V|$ in (2.29), and $|V|^{min} - |V|$ in (2.30). A stochastic load flow study results in statistics for P^{line} and $|V|$. If P^{Rating}, $|V|^{max}$, and $|V|^{min}$ are assumed to be statistically constant, then the statistics for $P^{Rating} - P^{line}$, $-P^{Rating} - P^{line}$, $|V|^{max} - |V|$, and $|V|^{min} - |V|$ can be calculated:

- Statistics for $P^{Rating} - P^{line}$

Mean: $\mu_{P^{Rating}-P^{line}} = P^{Rating} - P_{line}^{Base} - diag(B_{line})L(\Xi_{11} + \Xi_{12}PF)\mu_{\Delta P}$ (2.31)

Central 2nd moment:

$$\mu^{(2)}_{P^{Rating}-P^{line}} = diag(B_{line})L(\Xi_{11} + \Xi_{12}PF)\mu^{(2)}_{\Delta P}(diag(B_{line})L(\Xi_{11} + \Xi_{12}PF))^t \tag{2.32}$$

- Statistics for $-P^{Rating} - P^{line}$

Mean:

$$\mu_{-P^{Rating}-P^{line}} = -P^{Rating} - P_{line}^{Base} - diag(B_{line})L(\Xi_{11} + \Xi_{12}PF)\mu_{\Delta P} \tag{2.33}$$

Central 2nd moment:

$$\mu^{(2)}_{-P^{Rating}-P^{line}} = diag(B_{line})L(\Xi_{11} + \Xi_{12}PF)\mu^{(2)}_{\Delta P}(diag(B_{line})L(\Xi_{11} + \Xi_{12}PF))^t \tag{2.34}$$

- Statistics for $|V|^{max} - |V|$

Mean: $\mu_{|V|^{max}-|V|} = |V|^{max} - |V|^{Base} - (\Xi_{21} + \Xi_{22} PF)\mu_{\Delta P}$ (2.35)

Central 2nd moment:

$$\mu^{(2)}_{|V|^{max}-|V|} = (\Xi_{21} + \Xi_{22} PF)\mu^{(2)}_{\Delta P}(\Xi_{21} + \Xi_{22} PF)^t \quad (2.36)$$

- Statistics for $|V|^{min} - |V|$

Mean: $\mu_{|V|^{min}-|V|} = |V|^{min} - |V|^{Base} - (\Xi_{21} + \Xi_{22} PF)\mu_{\Delta P}$ (2.37)

Central 2nd moment: $\mu^{(2)}_{|V|^{min}-|V|} = (\Xi_{21} + \Xi_{22} PF)\mu^{(2)}_{\Delta P}(\Xi_{21} + \Xi_{22} PF)^t$ (2.38)

where P^{Base}_{line} is the system real line flows using the mean of each load and $|V|^{Base}$ is the system bus voltage magnitudes found by using the mean of each load. Note: formulating probability density functions becomes less complex if central moments are used.

The vectors $\frac{dP^{line}}{dP_{AB}}$ and $\frac{d|V|}{dP_{AB}}$ are formed from using the deterministic ATC evaluation discussed in Section 2.3. The $\frac{dP^{line}}{dP_{AB}}$ and $\frac{d|V|}{dP_{AB}}$ terms found from the deterministic approximation result in vectors. Equations (2.27-30) are rewritten using the form of (2.31-38)

$$ATC^{A-B}\left(\frac{dP^{line}}{dP_{AB}}\right) \le P^{+} \quad (2.39)$$

$$P^{-} \le ATC^{A-B}\left(\frac{dP^{line}}{dP_{AB}}\right). \quad (2.40)$$

$$ATC^{A-B}\left(\frac{d|V|}{dP_{AB}}\right) \le V^{max} \quad (2.41)$$

$$V^{min} \le ATC^{A-B}\left(\frac{d|V|}{dP_{AB}}\right). \quad (2.42)$$

where

$$P^{+} = P^{Rating} - P^{line} \qquad P^{-} = -P^{Rating} - P^{line}$$

$$V^{max} = |V|^{max} - |V| \qquad V^{min} = |V|^{min} - |V|$$

In order to implement linear transformation for (2.39-42), the vectors $ATC^{A-B}(\frac{d|V|}{dP_{AB}})$ and $ATC^{A-B}(\frac{dP^{line}}{dP_{AB}})$ are first reformulated. Note: as discussed in Section 2.3, the variable ATC^{A-B} is a scalar. Vectors $\frac{dP^{line}}{dP_{AB}}$ and $\frac{d|V|}{dP_{AB}}$ are rewritten as diagonal matrices, $diag(\frac{dP^{line}}{dP_{AB}})$ and $diag(\frac{d|V|}{dP_{AB}})$ where $diag(\cdots)$ is the construction of a matrix of diagonal elements consistent with the dimension of X, (e.g. if. X^T =[3,4,5], $diag(X) = \begin{pmatrix} 3 & 0 & 0 \\ 0 & 4 & 0 \\ 0 & 0 & 5 \end{pmatrix}$). The ATC^{A-B} is multiplied by a vector with one column and a number of rows to be conformable as indicated by,

$$diag(\frac{dP^{line}}{dP_{AB}})(ATC^{A-B})(1^{N_L}) = ATC^{A-B}(\frac{dP^{line}}{dP_{AB}}) \tag{2.43}$$

$$diag(\frac{d|V|}{dP_{AB}})(ATC^{A-B})(1^{N_B}) = ATC^{A-B}(\frac{d|V|}{dP_{AB}}), \tag{2.44}$$

where 1^a represents a vector of ones with one column and a number of rows. Refer to Table 2.1 for a listing of all dimensions.

Equations (2.43-44) are substituted into (2.39-42) and reordered,

$$(ATC^{A-B})(1^{N_L}) \le \left[diag(\frac{dP^{line}}{dP_{AB}}) \right]^{-1} P^{+} \tag{2.45}$$

$$\left[diag(\frac{dP^{line}}{dP_{AB}}) \right]^{-1} P^{-} \le (ATC^{A-B})(1^{N_L}) \tag{2.46}$$

$$(ATC^{A-B})(1^{N_B}) \le \left[diag(\frac{d|V|}{dP_{AB}}) \right]^{-1} V^{max} \tag{2.47}$$

$$\left[diag(\frac{d|V|}{dP_{AB}}) \right]^{-1} V^{min} \le (ATC^{A-B})(1^{N_B}). \tag{2.48}$$

In order to distinguish between each of the ATC^{A-B} values due to their respective limitations from (2.45-48), each ATC^{A-B} is renamed:

- ATC^{+} represents ATC^{A-B} in (2.45)
- ATC^{-} represents ATC^{A-B} in (2.46)

- $ATC^{V\,max}$ represents ATC^{A-B} in (2.47)
- $ATC^{V\,min}$ represents ATC^{A-B} in (2.48).

Equations (2.45-48) are now in a form in which the statistics for each of the following can be found: $ATC^{+}(1^{N_L})$, $ATC^{-}(1^{N_L})$, $ATC^{Vmax}(1^{N_B})$, $ATC^{Vmin}(1^{N_B})$. For each row of (2.45-48), a probability density function can be formed using a Gram-Charlier type A series approximation illustrated in Section 2.5. For example, if there are four buses and six lines in a system where the stochastic ATC is to be calculated, (2.45-46) have six probability density functions each and (2.47-48) have four probability density functions each. The Gram-Charlier type A series is a series approximation of the probability density function in terms of statistical moments. Therefore if the statistics of $ATC^{+}(1^{N_L})$, $ATC^{-}(1^{N_L})$, $ATC^{Vmax}(1^{N_B})$, $ATC^{Vmin}(1^{N_B})$ are found, then a probability density function for each can be found. In order to find the probability density functions of only ATC^{+}, ATC^{-}, $ATC^{V\,max}$, and $ATC^{V\,min}$ a method of manipulating probability distribution functions needs to be discussed. The evolution of (2.39-42) to the probability density function of the ATC is illustrated in Figure 2.6.

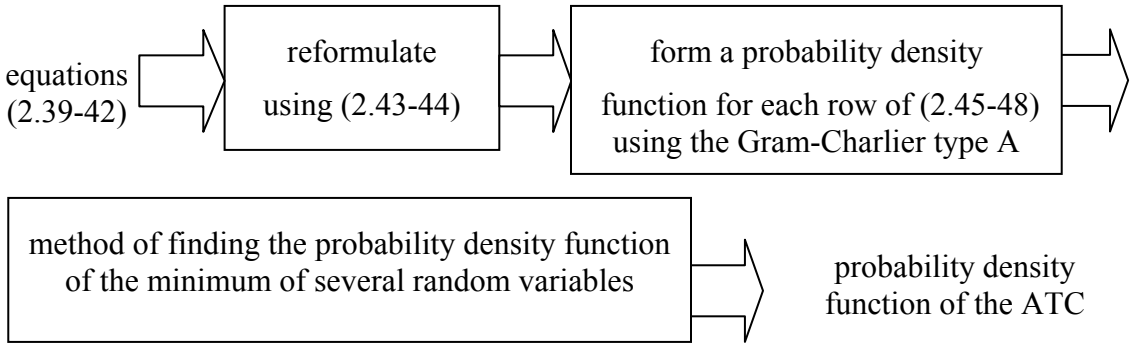

Figure 2.6. The evolution of (2.39-48) to the probability density function of the ATC

The probability density function of ATC^{+}, ATC^{-}, $ATC^{V\,max}$, and $ATC^{V\,min}$ is found from the probability density function of each set of $ATC^{+}(1^{N_L})$, $ATC^{-}(1^{N_L})$, $ATC^{Vmax}(1^{N_B})$, $ATC^{Vmin}(1^{N_B})$. Since many of the probability density functions for each set of $ATC^{+}(1^{N_L})$, $ATC^{-}(1^{N_L})$, $ATC^{Vmax}(1^{N_B})$, $ATC^{Vmin}(1^{N_B})$ can lie close to each other, finding the probability density function of each is not simply finding the minimum of the mean. Papoulis [44] illustrates a scheme to find probability density function of the minimum of several random variables. A derivation of the probability density function of the minimum of several random variables by Papoulis is shown in Appendix C. The result is that if any number n of independent random variables form a function

$$min(x_1 \ldots x_n) = z, \tag{2.49}$$

the probability density function $f_z(z)$ becomes

$$f_z(z) = \sum_{i=1}^{n} f_{x_i}(z) \sum_{j=1, j\neq i}^{n} [1 - F_{x_j}(z)] . \tag{2.50}$$

Since (2.50) has been established and that the probability density functions for each set of $ATC^{+}(1^{N_L})$, $ATC^{-}(1^{N_L})$, $ATC^{Vmax}(1^{N_B})$, $ATC^{Vmin}(1^{N_B})$ are known, and that the probability distribution functions can be found by integration, the probability density functions for ATC^{+}, ATC^{-}, $ATC^{V\,max}$, and $ATC^{V\,min}$ can be found using (2.50). Using the probability density functions for ATC^{+}, ATC^{-}, $ATC^{V\,max}$, and $ATC^{V\,min}$, (2.50) can be used once again to find the probability density function of the ATC,

$$f_{ATC}(ATC^{A-B}) = \sum_{\substack{i=ATC^{+},ATC^{-},\\ ATC^{V\,max},ATC^{V\,min}}} f_i(ATC^{A-B}) \sum_{\substack{j=ATC^{+},ATC^{-},\\ ATC^{V\,max},ATC^{V\,min},j\neq i}} [1 - F_j(ATC^{A-B})] . \tag{2.51}$$

2.5. Calculating the Gram-Charlier series

The mean, variance, and other raw moments of an ATC transfer can be used to obtain an approximation of the probability density function. If higher order statistical moments of the ATC are known, the Gram-Charlier type A series for this purpose yields an approximate probability density function of the ATC. The script written in MATLAB is shown in Appendix A.

The Gram-Charlier type A series is a standard measure frequency function, denoted as *f(x),* with the mean $\mu_{GC} = 0$ and variance $\sigma_{GC}^2 = 1$ expanded in a series of derivatives of the standard measure normal (Gaussian) function

$$G(x) = \frac{1}{\sqrt{2\pi}} e^{-\frac{x^2}{2}} . \tag{2.52}$$

The derivatives of (2.52) result in a Taylor series representation, as shown in [29]. This Taylor series is the Gram-Charlier type A series

$$f(x) = \sum_{j=0}^{\infty} c_j H_j(x) G(x), \tag{2.53}$$

where c_j are constants based on a function of standardized moments, $H_j(x)$ are Hermite polynomials, and *G(x)* is the characteristic Gaussian function. The first five Hermite polynomials are

$$H_0(x) = 1$$
$$H_1(x) = x$$
$$H_2(x) = x^2 - 1$$
$$H_3(x) = x^3 - 3x$$
$$H_4(x) = x^4 - 6x^2 + 3$$
$$H_5(x) = x^5 - 10x^3 + 15,$$

where x is a scalar. For i greater than 1 the Hermite polynomials are,

$$H_i(x) = x^i + \sum_{k=2}^{t} (-1)^{k-1} x^{i-2(k-1)} \binom{i}{2(k-1)} \prod_{r=1,3,5}^{2k-3} r, \tag{2.54}$$

where

$$\binom{a}{b} = \frac{a!}{b!(a-b)!}, \; t = \frac{i+1}{2} \text{ for odd } i \text{ and } t = \frac{i+2}{2} \text{ for even } i.$$

The constant c_j in the Gram-Charlier type A series is found using standard measure,

$$c_n = \frac{1}{n!} \left[\frac{m_{ATC}^{(n)}}{(m_{ATC}^{(2)})^{n/2}} + \sum_{k=2}^{t} (-1)^{k-1} \frac{m_{ATC}^{(n-2(k-1))}}{(m_{ATC}^{(2)})^{\frac{n-2(k-1)}{2}}} \binom{i}{2(k-1)} \prod_{v=1,3,5}^{2k-3} v \right]. \tag{2.55}$$

For central moments, the first five values for c_n become

$$\begin{aligned}
c_0 &= 1 \\
c_1 &= 0 \\
c_2 &= \frac{1}{2}\left(\frac{m_{ATC}^{(2)}}{m_{ATC}^{(2)}} - 1\right) \\
c_3 &= \frac{1}{6}\frac{m_{ATC}^{(3)}}{m_{ATC}^{(2)}} \\
c_4 &= \frac{1}{24}\left(\frac{m_{ATC}^{(4)}}{(m_{ATC}^{(2)})^{3/2}} - 6\frac{m_{ATC}^{(2)}}{m_{ATC}^{(2)}} + 3\right) \\
c_5 &= \frac{1}{120}\left(\frac{m_{ATC}^{(5)}}{(m_{ATC}^{(2)})^{5/2}} - 10\frac{m_{ATC}^{(3)}}{(m_{ATC}^{(2)})^{3/2}}\right).
\end{aligned}$$

Using the Hermite polynomials, $H_j(x)$, and Gram-Charlier constants, c_j, a formal expression of *f(x)* is

$$f(x) = G(x)\left[1 + \frac{1}{2}\left(\frac{m_{ATC}^{(2)}}{\sigma^2} - 1\right)H_2 + \frac{1}{6}\frac{m_{ATC}^{(3)}}{\sigma^3}H_3 + \frac{1}{24}\left(\frac{m_{ATC}^{(4)}}{\sigma^4} - 6\frac{m_{ATC}^{(2)}}{\sigma^2} + 3\right)H_4 + \ldots\right]. \tag{2.56}$$

Since *f(x)* is found using a standard measure random variable $\mu_{GC} = 0$ and $\sigma_{GC}^2 = 1$, f(x) needs to be transformed into a function *f(y)* so that the probability density function of ATC has mean $\mu_{GC} = \mu_{ATC}$ and variance $\sigma_{GC}^2 = \sigma_{ATC}^2$. The standard measure transformation used for the Gram-Charlier type A series is

$$x = \frac{y - \mu_{ATC}}{\sigma_{ATC}},$$

where x are the standard measure variables of the ATC, y are the real variables of the ATC, μ_{ATC} is the mean of the ATC, and σ_{ATC} is the standard deviation of the ATC. The new Gaussian function now becomes,

$$G(y) = \frac{1}{\sqrt{2\pi}} e^{-\frac{1}{2}(\frac{y-\mu_{ATC}}{\sigma_{ATC}})^2}. \tag{2.57}$$

The resulting probability density function *f(y)* is the actual distribution of ATC

$$f(y) = \frac{1}{\sigma_{ATC}} \sum_{j=0}^{\infty} c_j H_j(y) G(y). \tag{2.58}$$

2.6. Summary of the proposed algorithm

Figure 2.7 illustrates the entire stochastic ATC algorithm. The deterministic ATC calculation algorithm (Section 2.3) and a stochastic load flow algorithm (Section 2.2) are first performed. The outputs used from the deterministic ATC algorithm are the system Jacobian, bus voltage magnitudes, and transmission line flows. The stochastic load flow algorithm outputs the statistical moments of the transmission line flows and bus voltage magnitudes, which are used with the Jacobian at point X in Figure 2.7 and relevant system parameters to form the moments of $ATC^{+}(1^{N_L})$, $ATC^{-}(1^{N_L})$, $ATC^{Vmax}(1^{N_B})$, $ATC^{Vmin}(1^{N_B})$ using (2.45-48). The moments are then used to form sets of probability density functions using the Gram-Charlier type A series. For each set of probability density functions associated with $ATC^{+}(1^{N_L})$, $ATC^{-}(1^{N_L})$, $ATC^{Vmax}(1^{N_B})$, $ATC^{Vmin}(1^{N_B})$, the probability density function is found, resulting in the four probability density functions f_{ATC+}, f_{ATC^-}, $f_{ATC^{V\,max}}$, and $f_{ATC^{V\,min}}$. The resulting four probability density functions are then used with (2.51) to find the probability density function of the minimum of the four intermediate ATCs calculated. The resulting probability density function is $f_{ATC}(ATC^{A-B})$ and can be used to find the mean and variance of the ATC. The quantity $f_{ATC}(ATC^{A-B})$ can also be used, in conjunction with a price function, to find the expected price of the transfer.

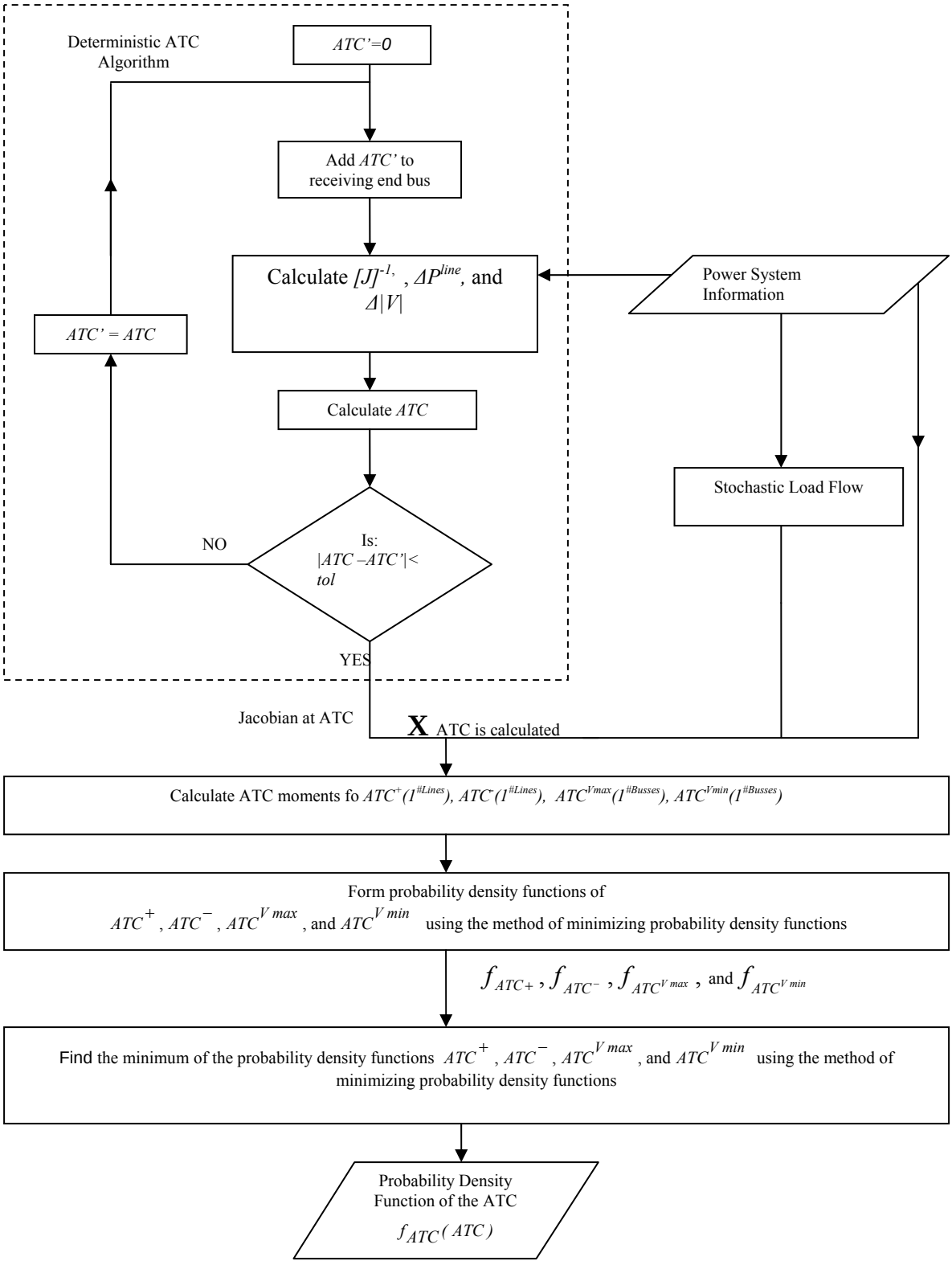

Figure 2.7 Stochastic ATC algorithm

3. Stochastic Available Transfer Capability Applications

3.1. Introduction

In this chapter, illustrations of stochastic ATC calculations are given. For this purpose the WECC 179 bus test bed [52] is used. This test bed was inspired by the actual WECC system in 2000. The data used in the examples here are representative of the real system at some point in time, but do not represent WECC system or load data at present. The WECC 179 bus test bed is intended to give an understanding of how the stochastic ATC problem is formed and determined. There are five different examples shown in this chapter, one for the deterministic ATC calculation, and two different examples for the stochastic ATC calculation using two methods. The two methods used are the algebraic method discussed in Chapter 2, and the iterative Monte Carlo method discussed in Section 3.5.

For purposes of terminology, the term "stochastic-algebraic method" refers to the method in Chapter 2 in which mathematical properties of functions of multivariate variables is used as opposed to Monte Carlo – repeated trials. Of course, both the Monte Carlo and "stochastic-algebraic method" are analytical in the sense that results are used to analyze alternative scenarios. Nonetheless, the term "stochastic-algebraic method" is reserved here for the mathematical, non-repeated trial approach. All examples are listed in Appendix H. The bus loads for the stochastic ATC are modeled using information from a day ahead-load forecast. The method utilized for bus load modeling is shown in Section 3.3.

3.2. WECC 179 test bed and examples

The WECC 179 bus test bed is a power system which contains 263 lines as shown in Figure 3.1. The system data are shown in Appendix E. Limitations of line thermal rating and voltage magnitude are shown in Appendix G. As commonly used in stochastic load flow examples, the active power loads are represented by normally distributed pseudorandom variables, with reactive powers found by using constant power factors of the loads. A detailed modeling scheme for the statistics of the bus loads is shown in Section 3.4.

The examples shown in this chapter are divided into five parts. The first part is the deterministic ATC shown in Section 3.3 and this example is called WECC-D. The second and third parts are a stochastic ATC example in which all bus loads are considered to be random. Two techniques will be illustrated as examples of the calculation of the stochastic ATC with all bus loads considered random. Example WECC-MCC is a Monte Carlo based example. Example WECC-S uses stochastic analysis. Both WECC-S and WECC-MC methods are compared and are shown in Section 3.6. The fourth and fifth examples are a stochastic ATC example but with large bus loads considered to be random. All these examples are performed using Monte Carlo and stochastic analysis methods. The examples are denoted as WECC-MCLx and WECC-SLx and are shown in Section 3.7, where L represents the examples with large bus loads larger than x considered to be random. There are four sets of these examples which are denoted as WECC-MCL100, WECC-SL100, WECC-MCL500, WECC-SL500, WECC-MCL1000,

WECC-SL1000, WECC-MCL1500, and WECC-SL1500. The listing of all examples in Appendix H should help identify the example conditions.

3.3. Deterministic ATC

The deterministic ATC calculation is a major part of the stochastic ATC calculation process. The Jacobian matrix taken from the deterministic ATC calculation is used as a linear transformation matrix in the stochastic ATC algorithm. Therefore, it is important that the deterministic ATC formulation is accurate.

The deterministic ATC formulation is shown in Section 2.3 and is used with the WECC system to find the deterministic ATC. For the WECC system, there are 31862 different ATC transfers but only ten different cases are illustrated. Table 3.1 lists only 10 representative ATC values. These cases were compared to a computationally intensive iterative approach illustrated in Figure 3.2. The deterministic ATC affectively finds the approximate ATC of the system. The approach shown in Figure 3.2 is initialized at the base case and there is zero $ATC^{A\text{-}B}$ added to the system. $ATC^{A\text{-}B}$ is added to the bus load generator at bus A and as a constant power factor load at bus B. Since $ATC^{A\text{-}B}$ is in units of MW, the active and reactive power added at bus B are,

$$P^{load}(B) = P^{load}(B) + ATC^{A\text{-}B},$$

$$Q^{load}(B) = Q^{load}(B) + sgn(Q^{load}(B))sin(acos(pf(B)))ATC^{A\text{-}B}.$$

where *sgn* which is the signum function which represents the sign of a real number.

Since there are a few loads in the WECC system which are leading power factor, term $sgn\,(Q^{load}(B))$ is used to preserve the negative sign of the load in such a case.

Once the bus load at bus B is updated, a load flow study is preformed where $|V|$ and line flows are found and compared to their respective limits. If all the limits are not violated, the quantity $\Delta ATC^{A\text{-}B}$ is added to the $ATC^{A\text{-}B}$ and the study is reiterated. When the $ATC^{A\text{-}B}$ reaches the point where there is a limit violation, the $ATC^{A\text{-B}}$ is achieved, and becomes the $ATC^{A\text{-}B}$ of the previous iteration.

The deterministic ATC algorithm from Section 2.3 is compared to the approximate real deterministic ATC and is shown in Table 3.1. Because there are 179 busses in the WECC test bed, there are 15931 possible $ATC^{A\text{-B}}$ values corresponding to the pairs A,B.

Table 3.1 Deterministic ATC results for Example WECC-D

From Bus	To Bus	Actual ATC (MW)	Deterministic ATC (MW)
3	8	1141	1146
8	112	965.1	965.2
44	160	483.3	483.7
3	155	498.1	498.3
5	141	739.4	739.7
39	57	876.1	876.3
64	9	257.9	258.1
12	60	1015	1015.1
78	103	618	619.3
34	64	181	181.4

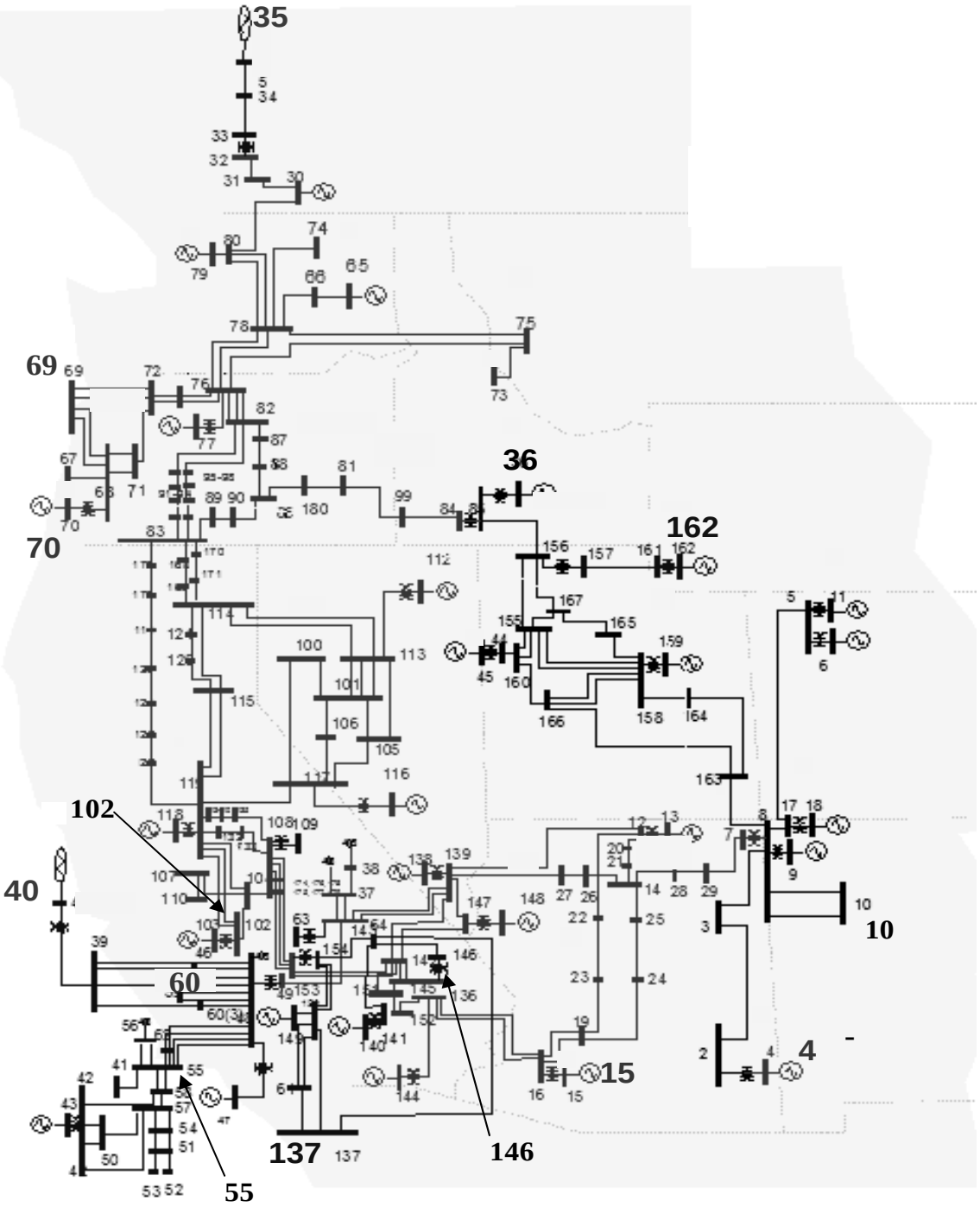

Figure 3.1. The WECC 179 bus test bed used in examples WECC-x

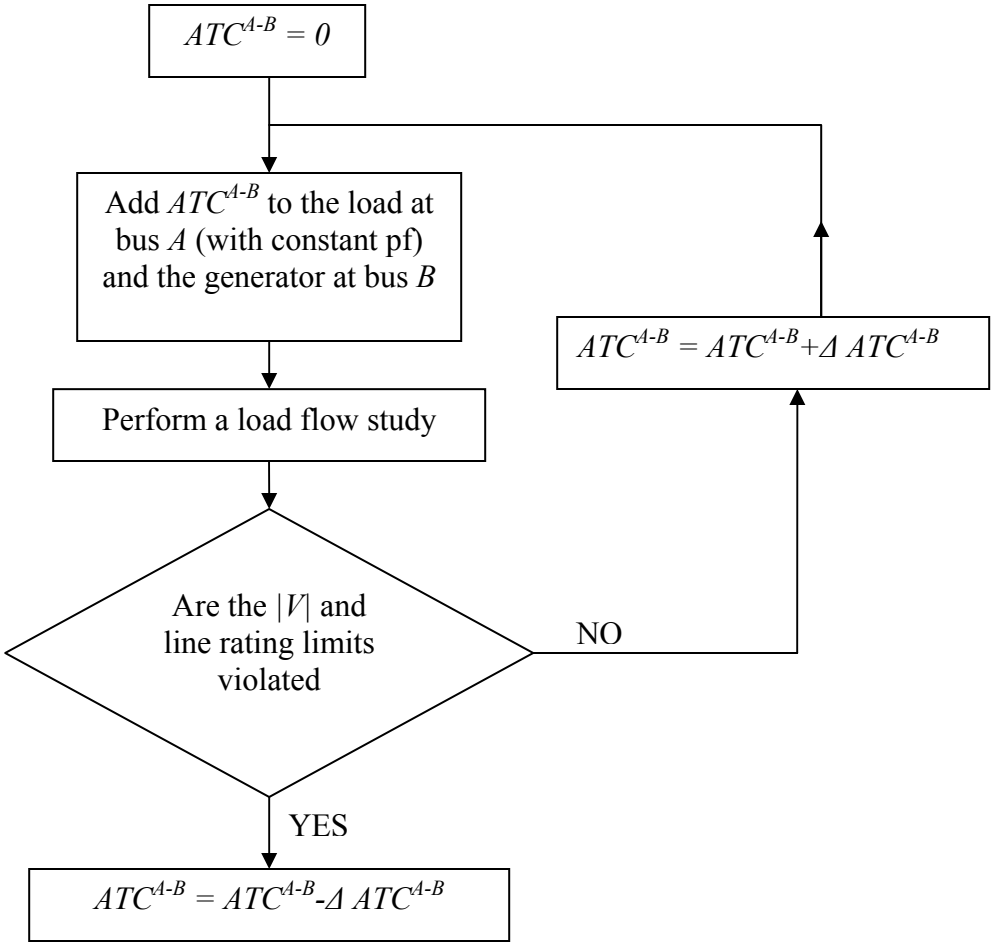

Figure 3.2. Deterministic ATC iterative approach used in example WECC-D

3.4. Modeling of bus load statistics

In a majority of the stochastic load flow studies, bus loads are often assumed to be Gaussian [15,25-27,35-36]. The process of the stochastic load flow study and stochastic ATC calculation in this report also assumes the bus loads to be Gaussian. A linear transformation of statistical moments of bus loads is preformed to obtain the statistical moments of the ATC. If the mean of each bus load of the WECC 179 bus system is assumed to be base case bus loads, where do the other statistical moments come from? It is assumed that the statistical moments for all the bus loads are the result of errors in a day-ahead load forecast.

There are a number of day-ahead load forecast algorithms in the literature [46-51]. Each forecast technique results in an error which can be used to estimate a probability density function of the bus load. Table 3.2 shows the different load

forecasting errors that different programs have when estimating the load forecast. Note that [46] is a seven day ahead forecast.

The error function can be used to find the standard deviation of the load forecast error,

$$erf(x) = \frac{2}{\sigma\sqrt{2\pi}} \int_0^x e^{-\frac{y^2}{2\sigma^2}} dy . \tag{3.1}$$

If a band of $\pm\varepsilon$ is known and assumed to be Gaussian distributed, the error function for this band is assumed to be equal to (±0.9). Neglecting the load forecast errors in references [46,49], an average day ahead load forecast error can be found,

$$\varepsilon = 1.04\%. \tag{3.1}$$

The parameter ε is used to estimate the standard deviation of the bus loads. It is assumed that 90% of the time, the bus load error lies in the band +/- 1.04%, from (3.1), in a Gaussian distribution. Therefore a method is developed to find the standard deviation of the error using this information.

Table 3.2 Load forecast errors for different forecast methods

Reference	Minimum Load Forecast Error (%)	Maximum Load Forecast Error (%)	Time Horizon	Method
[46]	3.39	9.97	7 Days	ARIMA model and transfer function model
[47]	1.06	1.19	1 Day	time series forecasting
[48]	1.79	5.53	Day Ahead Holiday	fuzzy linear regression
[49]	0.55	1.07	1 Day	hybrid fuzzy neural network
[50]	0.9	1.49	1 Day	hybrid fuzzy neural network

Therefore σ in (3.1) can be found using simple statistical analysis, e.g. using MATLAB. In MATLAB, the error function is defined as follows

$$merf(x) = \frac{2}{\sqrt{\pi}} \int_0^x e^{-u^2} du . \tag{3.3}$$

By performing a transformation of variables, *erf* can be found in terms of *merf*.

$$u = \frac{y}{\sqrt{2}\sigma} \qquad du = \frac{dy}{\sqrt{2}\sigma} \tag{3.4}$$

$$erf = \frac{2}{\sigma\sqrt{2\pi}} \int_0^x e^{-\frac{y^2}{2\sigma^2}} dy$$

$$erf = \frac{2\sqrt{2}\sigma}{\sigma\sqrt{2\pi}} \int_0^{x/\sqrt{2}\sigma} e^{-u^2} du \qquad (3.5)$$

$$erf = \frac{2}{\sqrt{\pi}} \int_0^{x/\sqrt{2}\sigma} e^{-u^2} du$$

$$erf = merf\left(\frac{x}{\sqrt{2}\sigma}\right).$$

If erf = 0.9 and x = 1.04, σ can be found numerically,

$$\sigma_p = 0.8596 \qquad (3.6)$$

The bus load variance can be modeled using the standard deviation in (3.6) and the mean of the bus loads

$$\sum_i^{Load} = \left(\sigma_p P_i^{load}\right)^2 \qquad (3.7)$$

where $\sum_i^{Load}$ is the variance of the real power load at bus i, and P_i^{load} is the mean of the load at bus i. In (3.7) all parameters are scalar. The notation $\sum$ for variance is usually used for the covariance matrix, but hopefully this will not be confused with summation.

Long term load forecasting can be used in conjunction with to stochastic ATC in transmission expansion scenarios. Applications of neural networks and expert systems for long term load forecasts from 1 year to 10 years are widely used [79-82]. Calculation errors for the long term load forecasting range from 10% to 20%. A calculation error of 20% is assumed and is substituted for ε in the analysis of finding the standard deviation of the bus loads from (3.3-3.6). From the analysis, it can be shown that a typical standard deviation of the bus loads for a long term load forecast (with erf =0.9 and ε = 20.0) is σ_p = 12.0%. The value σ_p can once again be used in conjunction with (3.7) to find the bus load variances, instead with long term load forecasts considered.

3.5. Monte Carlo simulation

A Monte Carlo study is used to compare and verify the results of the algebraic stochastic ATC calculation method to approximate actual values of the stochastic ATC. A Monte Carlo study is performed which compares the results of the stochastic-algebraic method to an approximate actual value of the stochastic ATC. The Monte Carlo study is similar to the deterministic study in Section 3.3 and is shown in Figure 3.3. A Monte Carlo study is repeated many times to get the statistics of the ATC. Initially, the bus loads are pseudorandomly generated and applied to the approximate deterministic ATC calculation. When the sample ATC is found, it is saved and the process is repeated many times.

3.6. Examples WECC-MC and WECC-S

Using the WECC-179 bus test bed, a stochastic-algebraic and Monte Carlo simulated ATC analysis of the system using MATLAB will illustrate the degree of agreement of both methods. Even though the Monte Carlo method is an "exact" process of finding the ATC given a sample operating condition and other given simplifying assumptions, the computation time for the method is quite large while the stochastic determination of ATC reduces the computation time significantly. In the WECC system, the average bus load mean is 225.688 MW and the standard deviation for that bus load mean can be found from the previous section and is 194.001 MW. From [93] the number of trials needed to represent the normal distribution for the mean and standard deviation given can be found. For simplicity, a Monte Carlo study is preformed to see how many trials are needed to have bus load mean and standard deviation agree within 5 percent of the values of 225.688 MW for the mean and 194.001 MW for the standard deviation. As a result about 800 trials are needed to represent the bus load mean and standard deviation statistics to within 5 percent. The WECC system has 104 bus loads. In order to keep the same resolution of 800 trials for 104 random variables, the Monte Carlo study performed should include at least 800^{104} or $8.34e^{301}$ trials. Note that $8.34e^{301}$ is nearly impossible to perform on a desktop PC, therefore when Monte Carlo trials are used as a comparison with the stochastic-algebraic method, the reduced number of trials used for comparison will introduce some error in the resulting statistics.

For the WECC system 10000 trials are ran and the computation time is about 24 hours. The Gram-Charlier type A series for $p_{ATC}(ATC)$ appears to be accurately represented using the first 40 statistical moments for each transfer and resulting in a probability of 1.000 when the series is integrated from $ATC = -\infty$ to ∞. Figs. 3.4-3.8 show plots of the probability density functions for the transfer between each bus pair of the system.

This section shows results of the stochastic ATC analysis in the WECC-179 bus test bed. Since the test bed has 263 different power lines and devices, only 5 exemplary transfers are analyzed as shown in Table 3.3

Data from Table 3.4 show the difference between the Monte Carlo and stochastic statistical moments which are calculated from the probability density $f(x)$ is obtained from the Gram-Charlier series using

$$u_{ATC}^{(k)} = \int_{-\infty}^{\infty} (x - m_x^{(1)})^k f(x) dx, \quad k > 1 \tag{3.8}$$

where k is the moment order, $m_x^{(1)}$ is the mean of the datum x and $f(x)$ is the probability density function represented by the Gram-Charlier type A series.

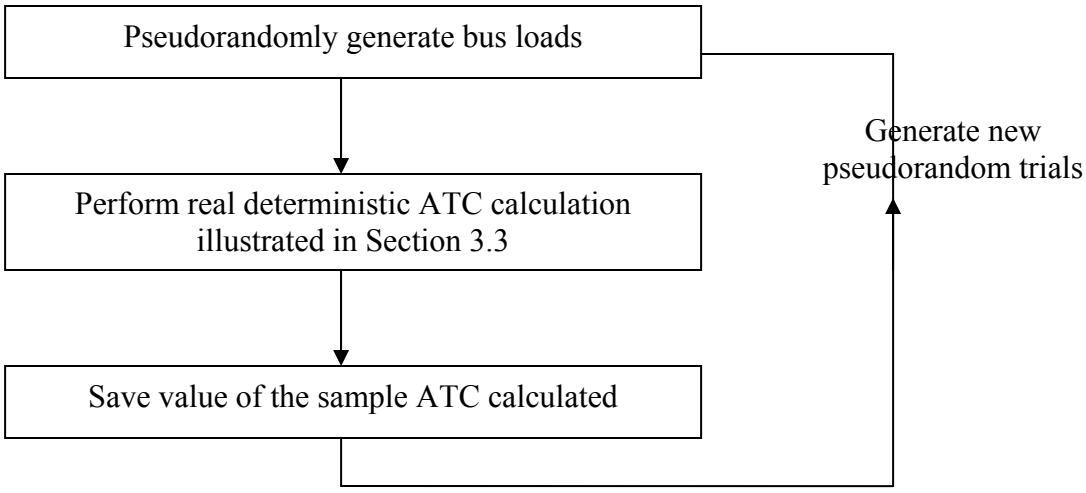

Figure 3.3. Monte Carlo stochastic ATC

Table 3.3 Five selected transfers used for examples WECC-S and WECC-MC

Sending Bus	Receiving Bus
78	103
3	155
3	8
44	160
34	64

As shown in Table 3.4, the differences in the mean between the Monte Carlo and stochastic-algebraic method moments have small error (~1%). The small error in the mean should warrant agreement between the stochastic-algebraic and Monte Carlo methods. Figures 3.4 – 3.8 show the agreement graphically using probability density functions.

3.7. Stochastic ATC considering large bus loads to be random

In large systems, one way to decrease the computational burden of a stochastic ATC study can be done by only considering large bus loads to be random. The examples illustrated in this section are results from the stochastic ATC considering bus loads larger than 100, 500, 1000, and 1500 MW. For each of the four cases the stochastic-algebraic and Monte Carlo studies are performed and compared. Tables 3.5-8 show the results.

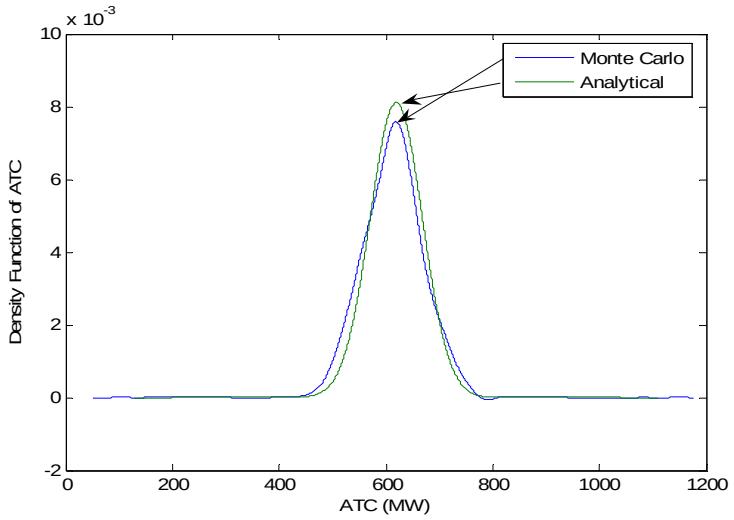

Figure 3.4. PDF of the ATC transfer from 78 to 103 for examples WECC-S and WECC-MC

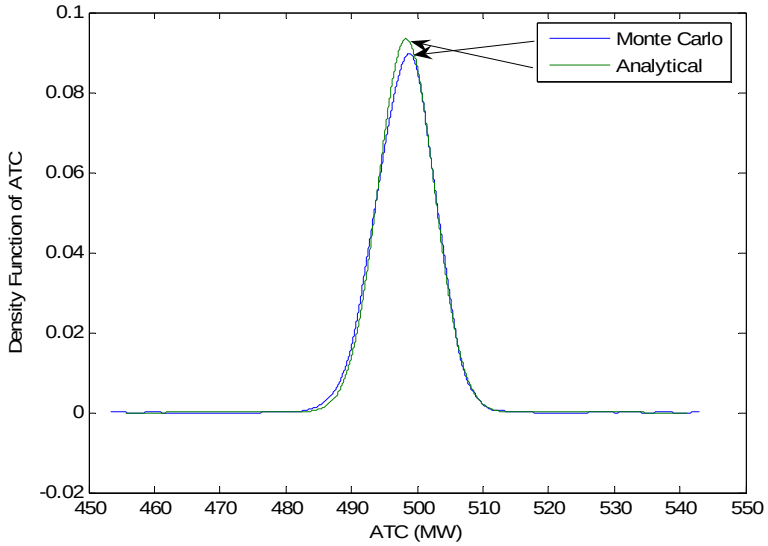

Figure 3.5. PDF of the ATC transfer from 3 to 155 for examples WECC-S and WECC-MC

Table 3.4 The mean and standard deviation selected transfers at the ATC limit for examples WECC-MC and WECC-S

		Stochastic-Algebraic Method WECC-S		Monte Carlo Method WECC-MC	
Sending Bus	Receiving Bus	Mean *(MW)*	Sending Bus	Receiving Bus	Mean *(MW)*
78	103	619.38	78	103	619.38
3	155	498.34	3	155	498.34
3	8	1145.3	3	8	1145.3
44	160	483.69	44	160	483.69
34	64	181.37	34	64	181.37

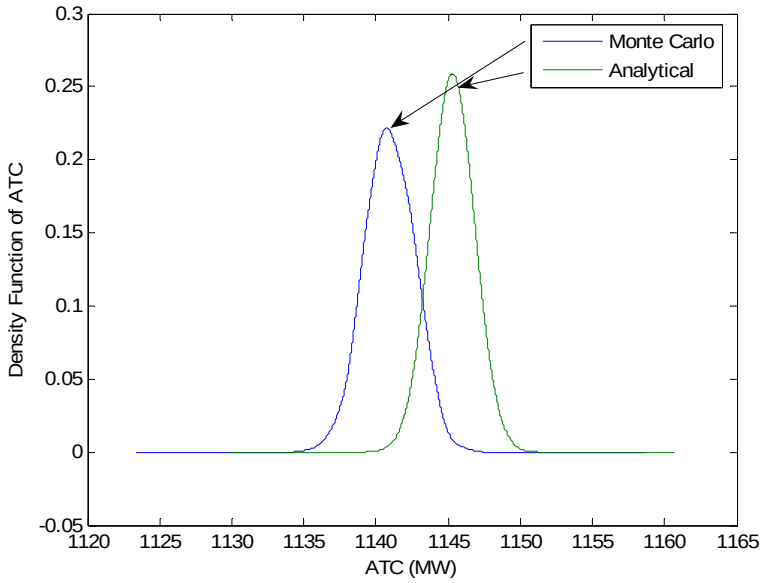

Figure 3.6. PDF of the ATC transfer from 3 to 8 for examples WECC-S and WECC-MC

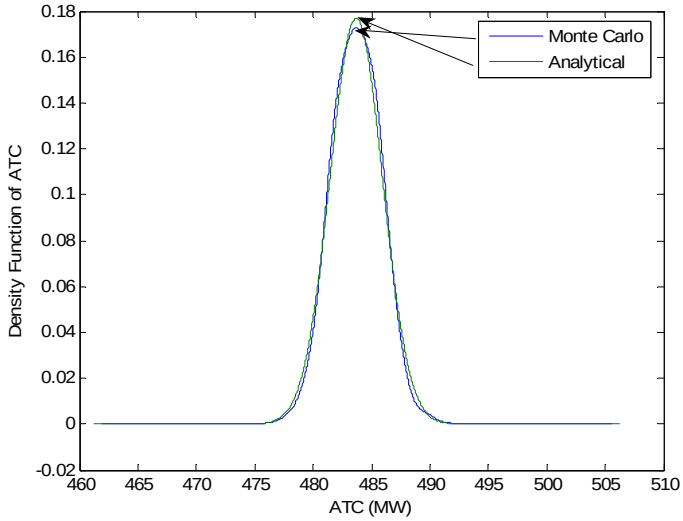

Figure 3.7. PDF of the ATC transfer from 44 to 160 for examples WECC-S and WECC-MC

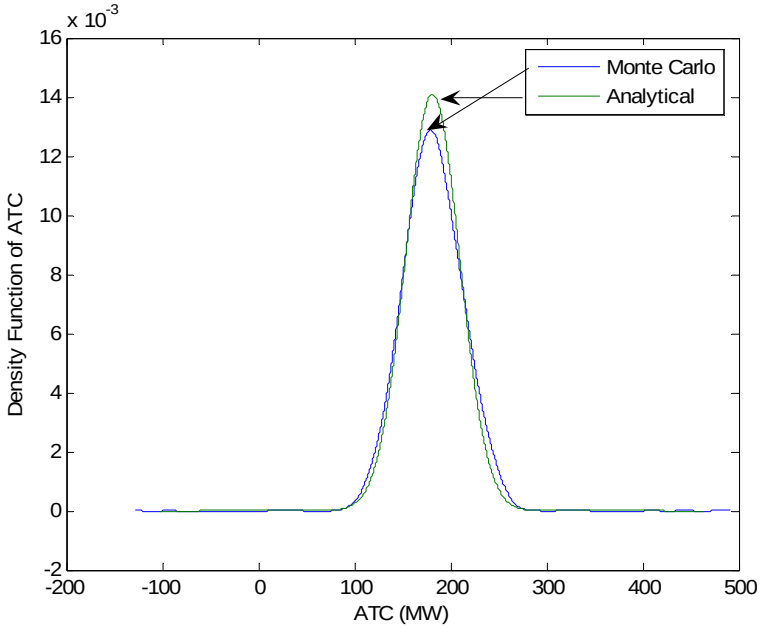

Figure 3.8. PDF of the ATC transfer from 34 to 64 for examples WECC-S and WECC-MC

Table 3.5 The mean and standard deviation selected transfers at the ATC limit for examples WECC-MCL100 and WECC-SL100

		Stochastic-Algebraic Method WECC-S		Monte Carlo Method WECC-MC	
Sending Bus	Receiving Bus	Mean *(MW)*	Standard Deviation *(MW)*	Mean *(MW)*	Standard Deviation *(MW)*
78	103	619.38	34.676	612.64	56.725
3	155	498.34	4.2724	497.81	4.4449
3	8	1141	1.0798	1141	1.5667
44	160	483.69	2.07	483.74	2.1914
34	64	181.37	28.313	182.01	29.985

Table 3.6 The mean and standard deviation selected transfers at the ATC limit for examples WECC-MCL500 and WECC-SL500

		Stochastic-Algebraic Method WECC-S		Monte Carlo Method WECC-MC	
Sending Bus	Receiving Bus	Mean *(MW)*	Standard Deviation *(MW)*	Mean *(MW)*	Standard Deviation *(MW)*
78	103	619.38	36.673	614.3	57.173
3	155	498.34	2.5738	497.89	3.9884
3	8	1141	0.92141	1140.9	1.5425
44	160	483.69	0.17359	483.66	0.28073
34	64	181.37	24.309	181.68	31.496

Table 3.7 The mean and standard deviation selected transfers at the ATC limit for examples WECC-MCL1000 and WECC-SL1000

		Stochastic-Algebraic Method WECC-S		Monte Carlo Method WECC-MC	
Sending Bus	Receiving Bus	Mean *(MW)*	Standard Deviation *(MW)*	Mean *(MW)*	Standard Deviation *(MW)*
78	103	619.38	36.442	614.94	54.965
3	155	498.34	3.5581	498.03	3.9581
3	8	1141	0	1140.9	1.5824
44	160	483.69	0.22238	483.64	0.27863
34	64	181.37	24.309	179.48	31.327

Table 3.8 The mean and standard deviation selected transfers at the ATC limit for examples WECC-MCL1500 and WECC-SL1500

		Stochastic-Algebraic Method WECC-S		Monte Carlo Method WECC-MC	
Sending Bus	Receiving Bus	Mean *(MW)*	Standard Deviation *(MW)*	Mean *(MW)*	Standard Deviation *(MW)*
78	103	619.38	50.636	614.25	53.969
3	155	498.34	3.5578	498.27	4.1115
3	8	1141	0	1141	1.4891
44	160	483.69	0.2217	483.66	0.27283
34	64	181.37	24.309	181.36	30.446

3.8. Expected price of transfer

ATC is one of the major tools used for the trading of power in an energy market. Therefore a power marketer would want to know a dollar amount of how much the ATC is worth. The value of ATC can be expressed as the maximum amount of money generated from a particular transfer, or the ATC could be used for transmission usage costs and reliability charges [94]. For each of the transfers shown in Examples WECC-S and WECC-SL, 3 different price functions denominated $D_{ATC}^{(1)}$, $D_{ATC}^{(2)}$, $D_{ATC}^{(3)}$ from (3.9-11) are used to illustrate the price of the transfer. The Gram-Charlier Series type A representation of the probability density for each transfer from the stochastic method,

f_{ATC}, is used in the determination the expected value of the price. The expected price is found by (3.12).

$$D_{ATC}^{(1)}(ATC) = 100(ATC^{A-B})^3 + 300(ATC^{A-B})^2 + 300(ATC^{A-B}) + 100 \quad (\$/Wh) \tag{3.9}$$

$$D_{ATC}^{(2)}(ATC) = 100(ATC^{A-B})^2 + 400(ATC^{A-B}) + 400 \quad (\$/Wh) \tag{3.10}$$

$$D_{ATC}^{(3)}(ATC) = 10(ATC^{A-B}) + 40 \quad (\$/MWh) \tag{3.11}$$

$$E[D_{ATC}^{(X)}] = \int_{-\infty}^{\infty} D_{ATC}^{(X)}(x) f_{ATC}(x) dx . \tag{3.12}$$

In Table 3.9, the data for the expected prices for all the cases in Example WECC-S are shown which are possible amounts of money that can be generated for each transfer. The three columns at the right in Table 3.9 correspond to the three ATC prices given in (3.9-11).

Conclusions from this chapter are discussed in Chapter 6.

Table 3.9 Expected price of ATC in example WECC-S for three price equations (3.9-11)

Transfer		$E[D_{ATC}^{(1)}]$	$E[D_{ATC}^{(2)}]$	$E[D_{ATC}^{(3)}]$
Sending	Receiving	*($/h)*	*($/h)*	*($/h)*
78	103	24211.00	38.85	6233.80
3	155	12379.00	25.04	5023.40
3	8	150230.00	131.63	11493.00
44	160	11317.00	23.59	4876.90
34	64	640.31	3.44	1853.70

4. Stochastic-Algebraic ATC Evaluation with the Integration of Transmission Asset Uncertainty

4.1. Introduction

The purpose of this chapter is to extend the stochastic-algebraic ATC calculation described in Chapter 2 to include a model of the uncertainty of the status of transmission asset. Inclusion of transmission element status is of high importance in the stochastic ATC calculation because the status of transmission paths has the possibility to drastically change the statistics of the ATC.

4.2. Incorporation of transmission element uncertainty

Equation (2.61) results in a representative density function of the ATC based on the randomness of the bus loads and considering limitations of bus voltage magnitude and transmission path thermal ratings. It may be of further use to incorporate the statistics of the status of the transmission circuits in the system.

Transmission lines and transformers (i.e., transmission assets) can be statistically modeled by considering the status of the device as ON or OFF. Equipment forced outage data may be available or assumed in broad categories (e.g., by voltage rating [55]). The forced outage rates [66] that capture transmission path uncertainty can be integrated with the stochastic ATC calculation to obtain a figure that better characterizes transmission system operation. Transmission line forced outages have been heavily studied, and values of the forced outage rates [66] can be calculated from [58-61]. Other uses of transmission line outages in power system studies are shown in [58-65].

Integration of transmission line uncertainty into stochastic ATC calculation is performed by constructing a table similar to Table 4.1. Table 4.1 bears some resemblance to a generation capacity outage table [66], but Table 4.1 is related to transmission equipment rather than generating unit status. The first N_L columns show all the possible states of transmission availability (as ON or OFF or simply 0, 1). For each system state, the stochastic ATC calculation from Chapter 2 is performed resulting in a probability density function for each calculation. The probability density functions are tabulated in the transmission outage table. The column labeled “Probability” shows the probability of being in that transmission system state. The calculation of the probabilities in this column is performed using the forced outage rates of each transmission line and the assumption of independent events. As a result, the “Probability” column depicted in Table 4.1 sums to one. Once all the probability density functions of the ATC and the probabilities of transmission availability are calculated, a new probability density function of the stochastic ATC is calculated. The new probability density function of the ATC is calculated by multiplying the stochastic ATC probability density function of the system state by the probability of occurrence; the results are added together to form a new stochastic ATC probability density function. The assumption made is that of independent events.

4.3. Reduction of the transmission outage table

The number of system outage states is 2^N, where N represents the number of lines. Using a widely accepted industry practice of considering only single line outages, the transmission outage table has one row for all lines in service plus N rows for each single line outage ("N-1") case. Thus the reduced transmission outage table has N+1 rows. If it is desired to proceed to the N-2 analysis, for example, a large transmission outage table is needed and some assumption of statistical dependence of outage events must be made. For the case of assumed independence of outage events, probabilities listed in the transmission outage table become very small for N-2 case and beyond (N-k case, $k > 2$) while the number of rows in the table increases to $(½)N^2 + (½)N$. This analysis does not include the effect of coalescence of rows. Coalescence of rows occurs in the transmission outage table when two or more rows have identical PDFs. In this case, for independent events, it is possible to represent that row once representing the probability of occurrence as the simple sum of the original row probabilities. Coalescence frequently occurs for the case that busses A and B are joined by multiple transmission circuits on a common right of way. A decrease of the number of rows in the transmission outage table can be realized by contingency ranking considering only the most severe contingencies.

In power marketing, the ATC has a commercial value and is termed here as "the value of energy as limited by ATC and time". The commercial value is based on the value of a non zero power transfer which is limited by the ATC for some specific time period. If power is traded at the ATC level, the money generated for a specific transfer is maximized. Therefore, calculations of money generated from a specific transfer based on the results of a stochastic ATC calculation are optimistic.

If the probability density function $f_{ATC}(ATC^{A-B})$ is known, the expected price of the transfer can be evaluated using $f_{ATC}(ATC^{A-B})$ and a price function D_{ATC}. The quantity D_{ATC} represents the price of the power in *$/MW* for current market conditions. The quantity $ATC^{A\text{-}B}$ is assumed to be in place for a given time interval (e.g., 15 minutes). Therefore D_{ATC} is also specified for that time interval. It could be argued that D_{ATC} is given in *$/MWh*; however, the assumption of a fixed 15 minute time interval is made in the discussion below. The quantity D_{ATC} is a random variable in this probabilistic formulation. An engineer may want to know the expected price for a future transfer traded at the ATC level and this price is determined by

$$E[D_{ATC}] = \int_{-\infty}^{\infty} D_{ATC}(x) f_{D_{ATC}}(D_{ATC}) dD_{ATC} \,. \tag{4.1}$$

Again, $E[D_{ATC}]$ is for a 15 minute time interval expressed in dollars.

4.4. Transmission outage table discussion

The purpose of this section is to provide a brief illustration on how the transmission outage table is used in the stochastic ATC study. The use of the transmission outage table is limited to the number of system transmission outage states considered. For most cases the N and N-1 cases are only considered. This limits the number of entries in the transmission outage table to N+1. The probability of a particular system state can be found using the forced outage rate

Table 4.1 Pictorial of a "transmission outage table"

Line Status				PDF of the ATC	Probability
1	2	…	N_L		
1	1	…	1		
1	1	…	0		
…	…	…	…		
0	0	…	0		

of each of the transmission lines. For most cases, the forced outage rate is small, and the *N* and *N*-1 cases represent at least 95% of the "Probability" column in the transmission outage table. For states beyond the *N*-1 case, values in the "Probability" column tend to become very small. To illustrate this, Table 4.2 shows the probability of occurrence of a system outage state for the WECC system of 179 busses and 263 lines. The forced outage rate is taken from Appendix G which presumably represents real data. From Table 4.2, about 98.7% of the probability is accounted for in the "Probability" column of a transmission forced outage table when the *N* and *N*-1 transmission system outage states are considered. The probability of occurrence of the *N*-2 and *N*-*k, k* > 2 states are small. Therefore the contributions to the outcome of a stochastic ATC study are considered to be negligible. Note that the number of transmission system outage states *S*, is related to the number of system lines N_L and number of lines on outage that are considered, *k*, by

$$S = \frac{N_L!}{(N_L - k)!\,k!}. \tag{4.2}$$

For the WECC 179 bus system, if the *N* and *N*-1 transmission system states are considered in the analysis of stochastic ATC, the stochastic ATC algorithm from Chapter 2 is performed a total of 264 times. Each run of the stochastic ATC algorithm represents the stochastic ATC for each of the 264 transmission system outage states. The results for each stochastic ATC calculation is a probability density function, therefore a total of 264 probability density functions are found. Each probability density function fits into the corresponding row in Table 4.1.

Table 4.2 Probability of the transmission system states for the WECC 179 bus system

State	Number of transmission system states	Probability of one element in the state	Total probability
N	1	0.8424	0.8424
N-1	263	$5.49*10^{-4}$	0.144387
N-2	34453	$3.58*10^{-7}$	0.0134
…	…	…	…
No lines in service	1	$3.05*10^{-832}$	$3.05*10^{-832}$

To illustrate the calculation method of finding the stochastic ATC with transmission element uncertainty included, a small system with three transmission lines is considered. Table 4.3 shows a transmission outage table for the system with three transmission lines. It is assumed that only the *N* and *N*-1 cases are to be considered in the stochastic ATC calculation. Therefore the total number of system transmission outage states is four. It is assumed that the forced outage rate of one transmission line is 0.01. The final result of the calculation of the stochastic ATC from Table 4.3 is

$$f_{atc} = (0.9703)f_1(x) + (0.0098)f_2(x) + (0.0098)f_3(x) + (0.0098)f_4(x).$$

This simple illustration should clarify how the stochastic ATC is calculated by including transmission line uncertainty.

Conclusions and observations from this chapter are discussed in Chapter 6.

Table 4.3 Transmission outage table of a three line power system

Line Status			PDF of the ATC	Forced outage rate
1	2	3		
1	1	1	$f_1(x)$	0.9703
1	1	0	$f_2(x)$	0.0098
1	0	1	$f_3(x)$	0.0098
0	1	1	$f_4(x)$	0.0098

5. Applications of Stochastic ATC Calculations with Transmission Element Uncertainty

5.1. Introduction

In this chapter, illustrations of the stochastic ATC calculation considering both bus loading and transmission element status uncertainty are given. For this purpose the WECC 179 bus test bed [52] is used. This test bed was inspired by the actual WECC in 2000. The data used in the examples here are representative of the real system at some point in time, but do not represent WECC data at present. The WECC 179 bus test bed is intended to give an understanding of how the stochastic ATC problem is formed and solved. Eight different ATC transfers are considered and compared to results from the stochastic ATC method of only considering bus loading to be uncertain. The two methods used are as described in Chapters 2 and 4. All examples are listed in Appendix H. The bus loads for the stochastic ATC are modeled using information from a day ahead-load forecast. The method for bus load modeling is shown in Section 3.3. The transmission line uncertainty is modeled considering the top twenty most severe line outage contingencies. Severity of a line outage is based on a transient stability index using commercial software PSAT and TSAT.

5.2. Line outage contingency ranking of the WECC 179 bus system

In calculating the stochastic ATC, the number of considered system states can be initially decreased to the *N* and *N*-1 cases. It might be more beneficial to further decrease the system states to speed up the calculation process. Further decrease of the number of transmission asset forced outage states can be accomplished by considering the most severe line outage contingencies. A line outage contingency ranking study is performed on the WECC 179 bus system. The contingency ranking is performed on the following software packages:

- power systems analysis tool (PSAT)
- transient security assessment tool (TSAT).

The contingency ranking is performed by taking a single line out of the system and running a stability study. A transient stability index is calculated and stored for each contingency. The transient stability index gives a measure of how severe a contingency is. The transient stability index [67,68] used for this purpose is a number between -100 and 100. Negative values represent unstable cases, and positive values represent stable cases. The smaller the transient stability index, the more severe the contingency. This process is repeated until each single line outage case is studied individually.

Results from the contingency ranking show that the WECC 179 bus system has a large number of single line outage contingencies that are unstable. These contingencies are shown in Table 5.1. Comparing Table 5.1 to the system topology, it is initially seen that most of the insecure contingencies are radial lines connected to generators. Other contingencies in Table 5.1 are not radial elements, but networked elements. These network elements are shown in Figure 5.1. These two groups of lines are important to

system stability and are also not considered as part of the top twenty most severe ranked contingencies. The twenty worst ranked contingencies considered in the stochastic ATC are shown in Table 5.2.

Table 5.1 Unstable contingencies of the WECC 179 bus system

From	To	Transient Stability Index	Status
39	40	-93.6	Insecure
157	161	-93.57	Insecure
31	32	-93.52	Insecure
32	33	-93.52	Insecure
33	34	-93.52	Insecure
78	66	-93.43	Insecure
138	139	-93.42	Insecure
31	30	-93.42	Insecure
42	43	-93.4	Insecure
76	77	-93.4	Insecure
102	103	-93.32	Insecure
140	141	-93.29	Insecure
116	117	-93.28	Insecure
12	13	-93.28	Insecure
118	119	-93.28	Insecure
161	162	-93.26	Insecure
17	18	-93.21	Insecure
144	145	-93.15	Insecure
112	113	-93.09	Insecure
16	15	-93.09	Insecure
80	79	-93.08	Insecure
5	6	-93.05	Insecure
8	9	-93.04	Insecure
34	35	-93.03	Insecure
158	159	-93.03	Insecure
147	148	-92.98	Insecure
66	65	-92.98	Insecure
2	4	-92.97	Insecure
149	150	-92.97	Insecure
5	1	-92.92	Insecure
44	45	-92.86	Insecure
68	70	-92.76	Insecure
85	36	-89.86	Insecure
156	157	-85.98	Insecure
48	47	-84.01	Insecure

Table 5.1 (continued) Unstable contingencies of the WECC 179 bus system

From	To	Transient Stability Index	Status
3	8	-84.01	Insecure
2	3	-54.46	Insecure
141	143	-54.46	Insecure

Table 5.2 Twenty most severe contingencies for the WECC 179 bus system

From	To	Transient Stability Index	Status
17	5	48.92	Secure
5	160	49.93	Secure
75	7	50.52	Secure
8	17	50.81	Secure
31	80	54.92	Secure
156	85	55.07	Secure
117	119	57.28	Secure
60	61	58.1	Secure
26	27	58.72	Secure
14	26	58.96	Secure
113	114	59.02	Secure
136	152	59.07	Secure
142	64	59.13	Secure
27	139	59.23	Secure
134	104	59.32	Secure
119	134	59.36	Secure
80	78	59.59	Secure
133	108	59.82	Secure
139	142	59.83	Secure
88	86	59.84	Secure

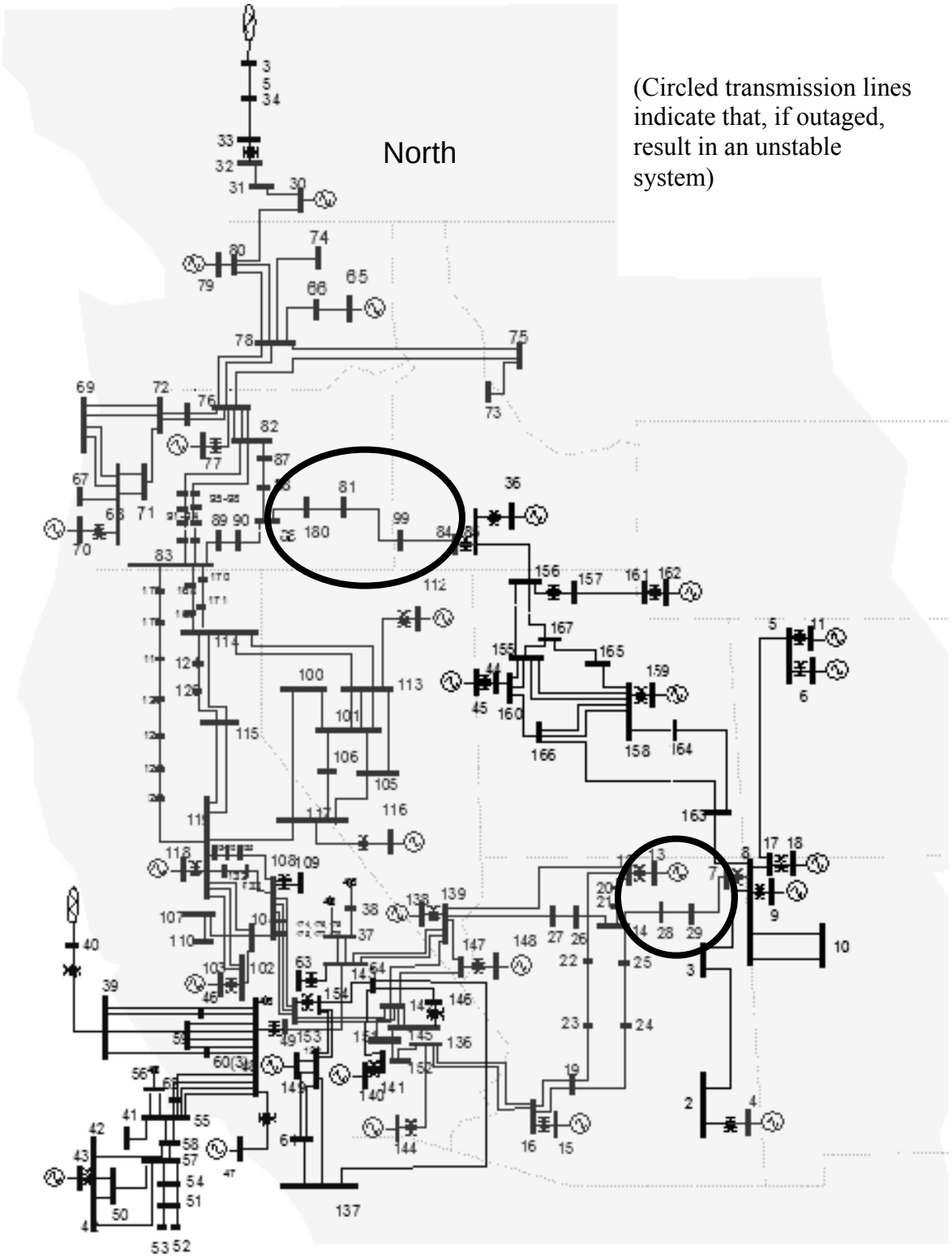

Figure 5.1. Insecure transmission lines in the WECC 179 bus system

5.3. Example WECC-STLU

Using the WECC-179 bus test bed, the stochastic-algebraic ATC calculation with transmission element uncertainty is considered. Since the test bed has 263 different power lines and devices, only 7 exemplary transfers are illustrated as shown in Table 5.3

The system element outages considered are shown in Table 5.2. The outages of the elements in Table 5.2 represent the most severe 20 stable contingences of the system. The results considering transmission element uncertainty are compared to the stochastic ATC calculation without considering transmission element uncertainty. Monte Carlo trials are not preformed due to the required of time to get a good estimate of the ATC statistics. Based on results from Chapter 3, the number of Monte Carlo trials needed to keep the same resolution of 1000 trials for this case is 1000^{20}. This represents about 10^{57} days needed to model one transfer at the same resolution. Table 5.4 shows the mean, variance, skew, and kurtosis statistics for the transfers considered. Calculation methods for these statistics are shown in Appendix A. Table 5.5 shows various cumulative probabilities for each of the transfers. Figs. 5.2-5.8 show plots of the probability density functions for the transfer between each bus pair of the system considering the uncertainty of transmission element status. Figs 5.9-5.15 show cumulative probability density function plots for the transfer between each bus pair considering the uncertainty of transmission element status.

Conclusions and observations from this chapter are discussed in Chapter 6.

Table 5.3 Selected power transfers used for examples WECC-STLU

Sending Bus	Receiving Bus
35	102
40	10
70	10
36	137
4	137
162	69
15	55

Table 5.4 The statistical measures for selected transfers*

Transfer		Mean (*MW*)	Variance (MW^2)	Skew	Kurtosis
35-102	no lines out	613.85	4496.70	-0.01	3.02
	N-1 case	614.06	4583.20	0.10	3.77
40-10	no lines out	1760.50	26.98	-25.88	8947
	N-1 case	1760.50	57.58	-8.21	3190.50
70-10	no lines out	1004.60	670990	0.20	1.11
	N-1 case	995.47	665340	0.23	1.13
36-137	no lines out	1427.50	8086.20	0.01	3.23
	N-1 case	1427.30	8195.00	0.01	3.44
4-137	no lines out	1273.20	2.64	-483.1	417170
	N-1 case	1277.00	621.80	16.52	382.78
162-69	no lines out	767.83	23.74	4.48	1350.2
	N-1 case	767.96	63.52	12.53	1461.8
15-55	no lines out	2127.60	200.24	-3.10	333.56
	N-1 case	2121.50	3170.80	17.16	422.90

* The *N*-1 case refers to a single transmission component outage taken from a contingency raking (20 worst cases considered)

Table 5.5 Probabilities of ATC*

Transfer		Pr(ATC <0MW)	Pr(ATC <500MW)	Pr(ATC <1000MW)	Pr(ATC <1500MW)
35-102	no lines out	1.21E-06	0.046217	0.99995	1
	N-1 case	1.33E-06	0.046263	0.99973	0.99992
40-10	no lines out	2.73E-07	5.59E-07	8.59E-07	1.17E-06
	N-1 case	4.32E-07	8.79E-07	1.34E-06	1.85E-06
70-10	no lines out	0.013158	0.55313	0.55955	0.55955
	N-1 case	0.013549	0.54785	0.55462	0.55463
36-137	no lines out	9.05E-07	2.07E-06	4.59E-06	0.79348
	N-1 case	1.53E-06	3.34E-06	2.94E-05	0.79348
4-137	no lines out	4.13E-07	8.59E-07	1.34E-06	0.99999
	N-1 case	7.85E-07	1.63E-06	2.56E-06	0.99953
162-69	no lines out	4.07E-07	8.42E-07	1	1
	N-1 case	2.74E-06	6.51E-06	0.99955	0.99998
15-55	no lines out	1.57E-09	7.68E-07	1.49E-06	2.29E-06
	N-1 case	1.72E-09	8.38E-07	1.62E-06	2.49E-06

* The N-1 case refers to a single transmission component outage taken from a contingency raking (20 most severe cases considered)

Table 5.5 continued Probabilities of ATC*

Transfer		Pr(ATC <1750MW)	Pr(ATC <2000MW)	Pr(ATC <3500MW)	Pr(ATC <4000MW)
35-102	no lines out	1	1	1	1
	N-1 case	1	1	1	1
40-10	no lines out	0.028149	1	1	1
	N-1 case	0.028401	0.99966	1	1
70-10	no lines out	0.55955	0.99998	1	1
	N-1 case	0.55464	0.99112	1	1
36-137	no lines out	0.99975	1	1	1
	N-1 case	0.99951	0.99996	1	1
4-137	no lines out	1	1	1	1
	N-1 case	1	1	1	1
162-69	no lines out	1	1	1	1
	N-1 case	1	1	1	1
15-55	no lines out	2.73E-06	3.21E-06	1	1
	N-1 case	2.97E-06	3.48E-06	0.9946	0.9951

* The N-1 case refers to a single transmission component outage taken from a contingency raking (20 most severe cases considered)

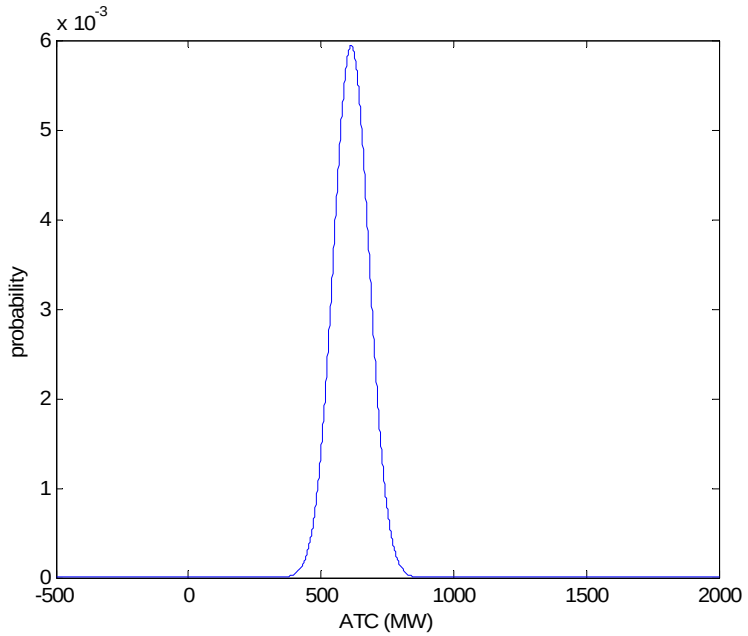

Figure 5.2. PDF of the transfer at the ATC limit from 35 to 102 for example WECC-STLU

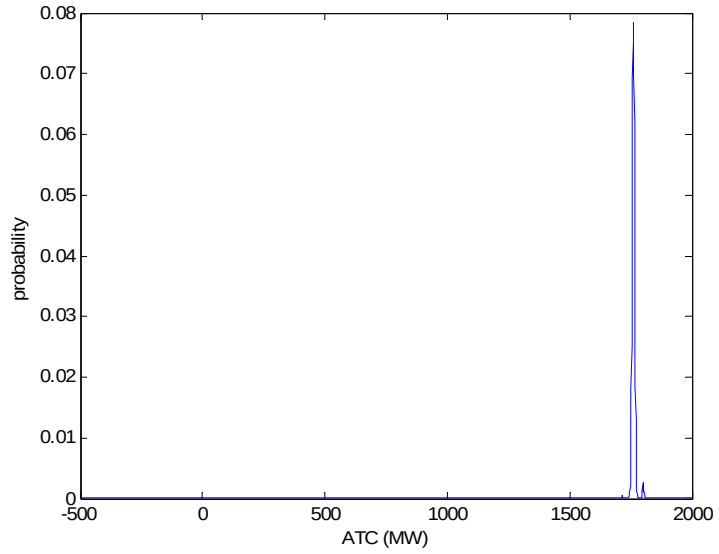

Figure 5.3. PDF of the transfer at the ATC limit from 40 to 10 for example WECC-STLU

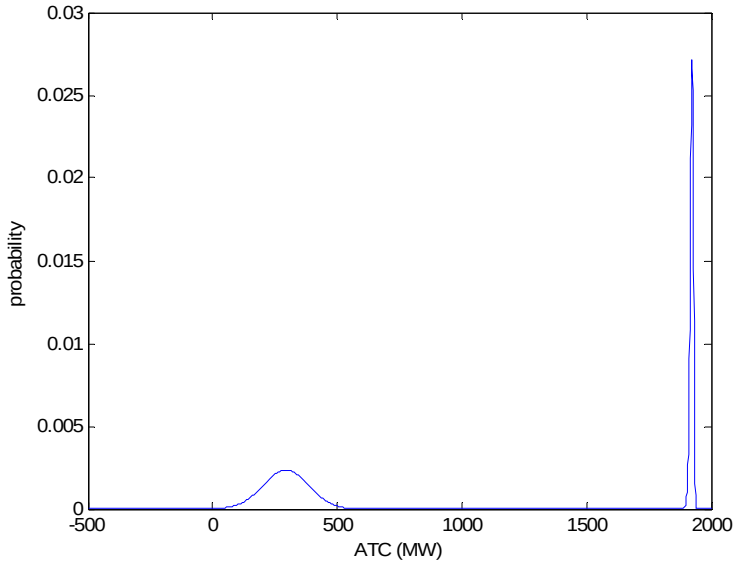

Figure 5.4. PDF of the transfer at the ATC limit from 70 to 10 for example WECC-STLU. Bimodal PDF occurs due to inclusion of transmission outages.

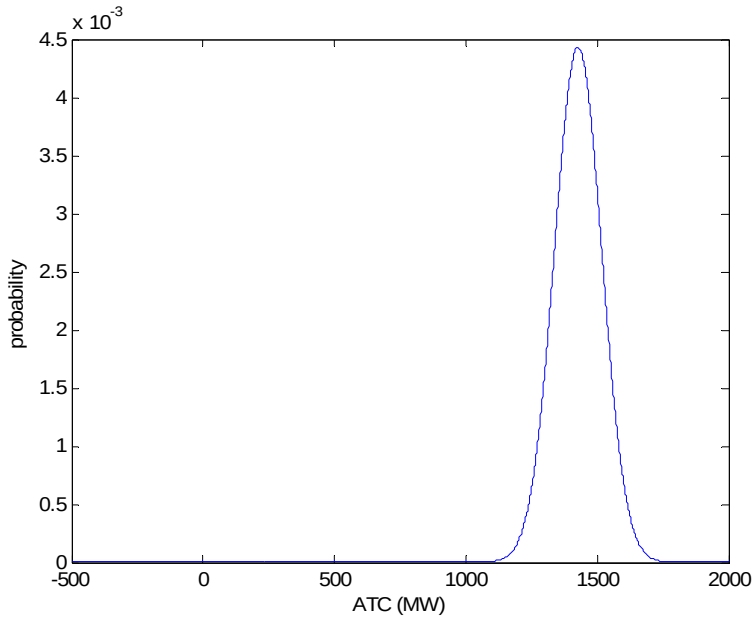

Figure 5.5. PDF of the transfer at the ATC limit from 36 to 137 for example WECC-STLU

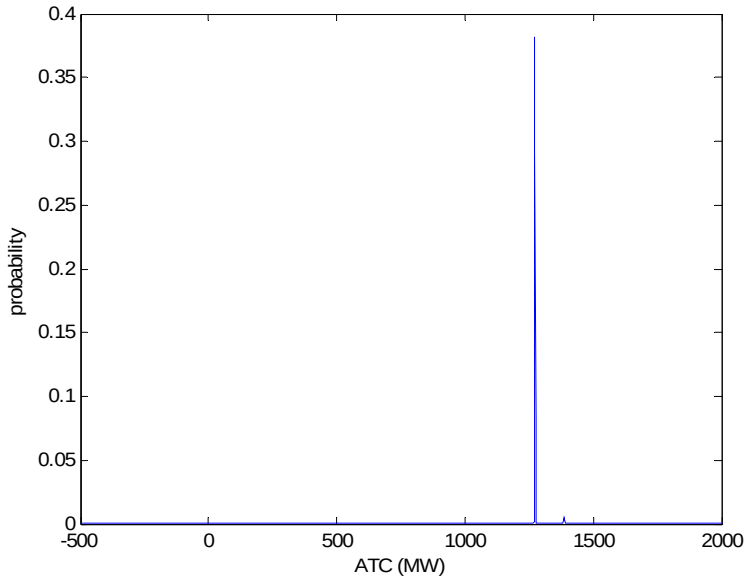

Figure 5.6. PDF of the transfer at the ATC limit from 4 to 137 for example WECC-STLU

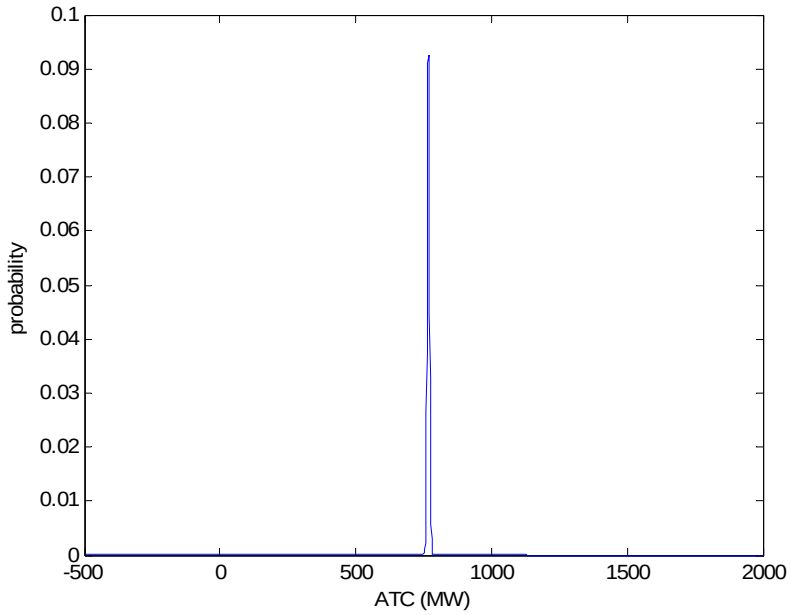

Figure 5.7. PDF of the transfer at the ATC limit from 162 to 69 for example WECC-STLU

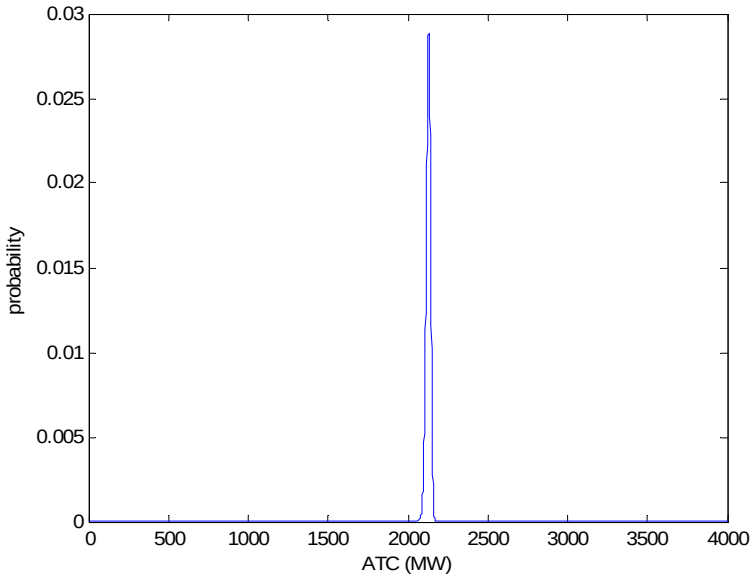

Figure 5.8. PDF of the transfer at the ATC limit from 15 to 55 for example WECC-STLU

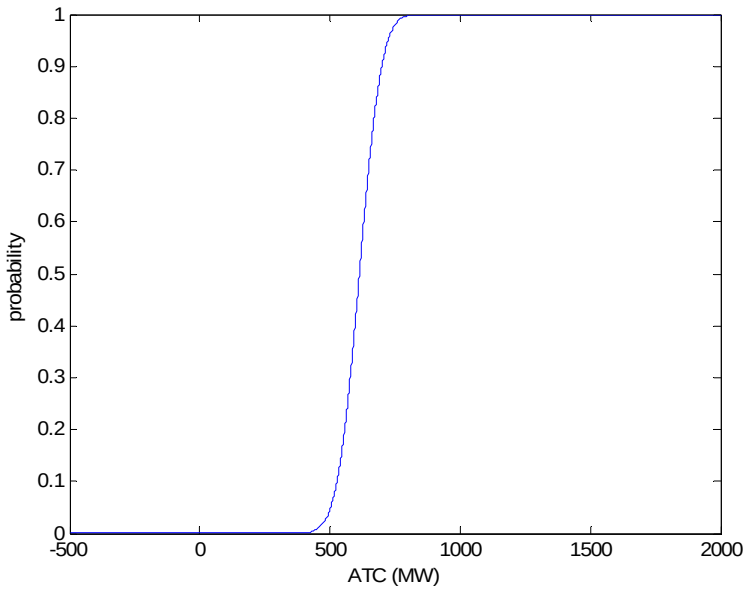

Figure 5.9. CDF of the transfer at the ATC limit from 35 to 102 for example WECC-STLU

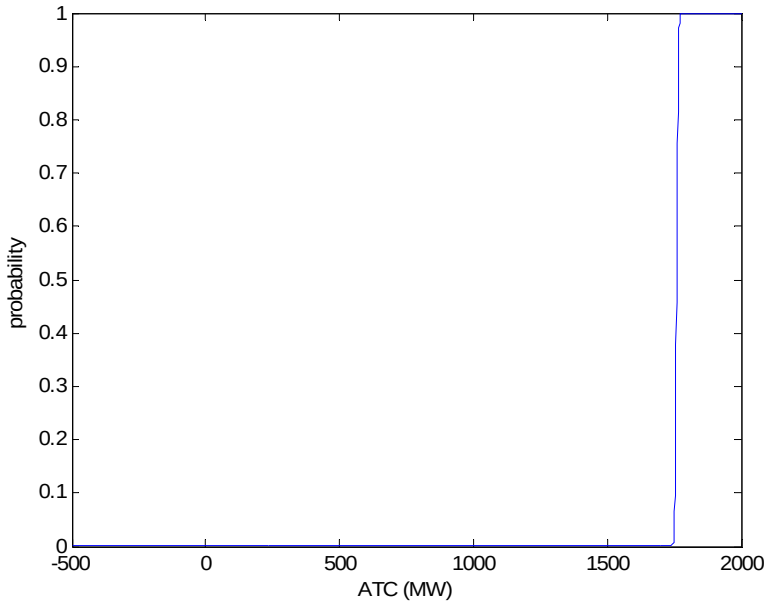

Figure 5.10. CDF of the transfer at the ATC limit from 40 to 10 for example WECC-STLU

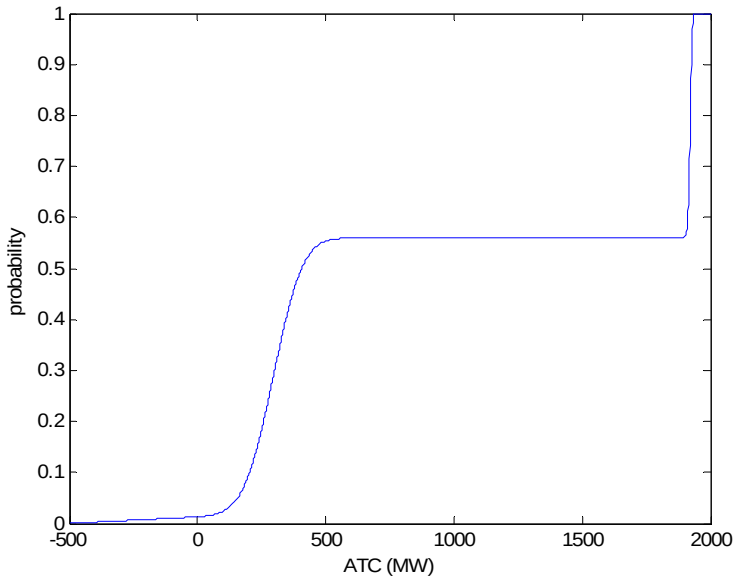

Figure 5.11. CDF of the transfer at the ATC limit from 70 to 10 for example WECC-STLU

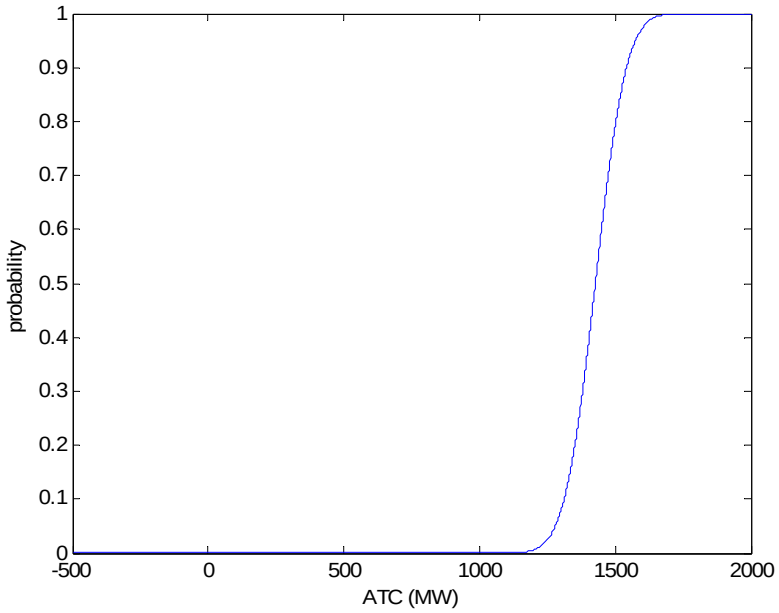

Figure 5.12. CDF of the transfer at the ATC limit from 36 to 137 for example WECC-STLU

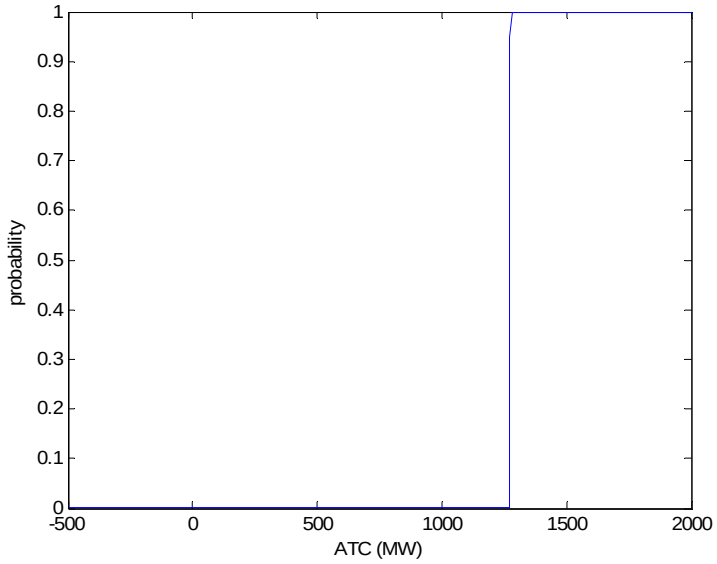

Figure 5.13. CDF of the transfer at the ATC limit from 4 to 137 for example WECC-STLU

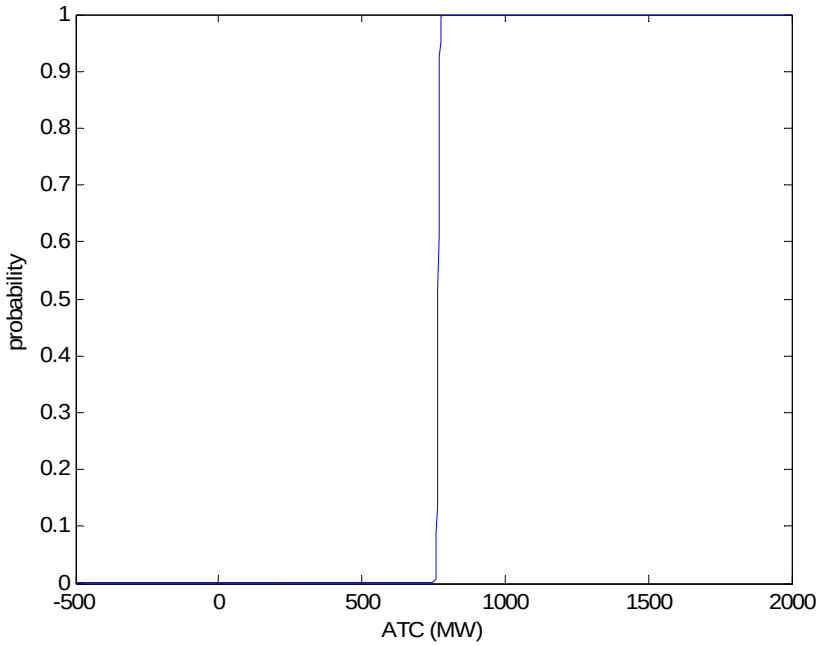

Figure 5.14. CDF of the transfer at the ATC limit from 162 to 69 for example WECC-STLU

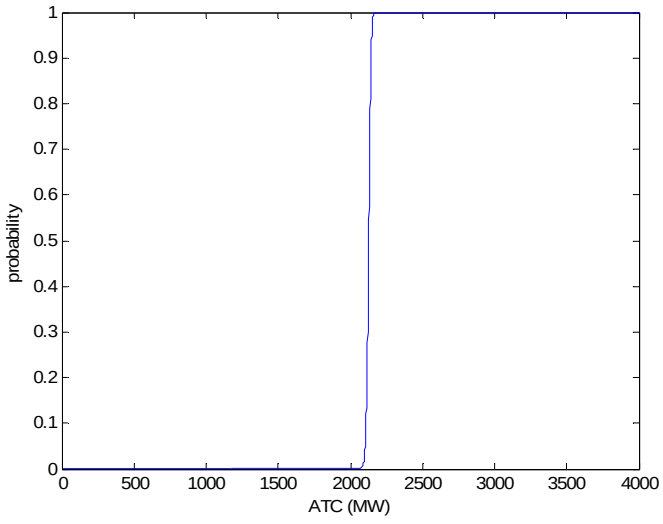

Figure 5.15. CDF of the transfer at the ATC limit from 15 to 55 for example WECC-STLU

6. Conclusions Drawn from the Example

6.1. Conclusions drawn from example WECC-D

Example WECC-D is shown in Section 3.3. In this example, a deterministic ATC study is performed (using a full analysis) and is compared to an approximate deterministic ATC study (using the incremental technique shown in Chapter 3). Note that all examples in this study are simulations using system data inspired by the WECC. None of the examples use historical real data. The deterministic ATC study is an important part of the stochastic ATC study. The major information from the deterministic ATC study is the system Jacobian matrix at the solution. At this point, the limitations for the ATC are linearized using the information from the Jacobian matrix at the solution of the deterministic ATC. If the deterministic ATC study is properly performed, then the confidence of the mapping functions used in the stochastic-algebraic ATC study is high.

Table 6.1 shows errors in the results of Table 3.1 in the deterministic ATC study. The error tabulated in Table 6.1 is the difference between the ATC calculated from a full analysis and that calculated using the approximate incremental technique described in Chapter 3. The errors shown in Table 6.1 suggest that the deterministic ATC calculation algorithm derived in Section 2.3 is a good approximation of the deterministic ATC calculation. Therefore, there is confidence that the resulting Jacobian matrix at the solution point of the deterministic ATC algorithm is a good linear approximation for the ATC. This resulting Jacobian matrix is used as a mapping matrix for the constraints of the stochastic ATC.

6.2. Conclusions drawn from example WECC-S and WECC-MC

Examples WECC-S and WECC-MC show an agreement between the Monte Carlo and stochastic analysis methods for evaluating the stochastic ATC for a fairly realistic power system. Table 6.2 shows errors in the mean and standard deviation between the Monte Carlo and stochastic analysis methods. The mean of the ATC as calculated using the Monte Carlo method versus the stochastic-algebraic method have small differences (e.g., much less than 1%). Errors for the standard deviation between the two methods are between 3 and 13 %. Errors of the standard deviation between the two methods can be the result of a combination of several factors.

In Example WECC-MC:

More trials are needed in the Monte Carlo study. In Chapter 3, an approximation of 800^{104} trials are needed to represent the statistics of the system. 10000 trials are used for each stochastic ATC study. If more trials are used, the standard deviations in the Monte Carlo analysis of the ATC is expected to be closer to the standard deviations of the stochastic-algebraic ATC calculation.

The Monte Carlo analysis is terminated when the difference between the ATC of the previous iteration and the ATC of the in progress iteration is within a certain difference error. This error for the WECC-MC example is 10^{-2} MW. If the difference in

ATC from iteration to iteration is small (e.g., << 10^{-2}), then the ATC from busses [3, 3, 44] to busses [155, 8, 160] has enhanced accuracy.

Table 6.1 Error* of the deterministic ATC results from example WECC-D

From Bus	To Bus	ATC Error (%)
3	8	0.43821
8	112	0.01036
44	160	0.08276
3	155	0.04015
5	141	0.04057
39	57	0.02283
64	9	0.07755
12	60	0.00985
78	103	0.21036
34	64	0.22099

* Error = (Deterministic ATC – Actual ATC) / Actual ATC

Table 6.2 Errors* of the mean and standard deviation from examples WECC-S and WECC-MC

From Bus	To Bus	Error in the mean (%)	Error in the standard deviation (%)
78	103	0.70716	12.9126
3	155	0.02809	4.64255
3	8	0.37545	12.5269
44	160	0.00413	3.31439
34	64	0.22606	8.58527

* Error in the mean = (mean(WECC-S) – mean(WECC-MC)) /mean(WECC-S)
Error in the std = (std(WECC-S) – std(WECC-MC)) /std(WECC-S)

In Example WECC-S:

Errors can also be introduced by using the Gram-Charlier type A series approximation. The number of statistical moments used in the stochastic-algebraic ATC problem is 10. The Gram-Charlier type A series is an infinite serious approximation and is better represented when moments beyond the mean and variance are used in the formulation. Also, this series appears quite frequently in the algorithm of the stochastic-algebraic ATC calculation. The series is used to approximate the probability density function of all the ATC limitations considered in the study. The number of Gram-Charlier type A series approximations used in the stochastic-algebraic study is shown in Table 6.3. This large number of series used in the stochastic-algebraic ATC calculation can

therefore be a contribution of the error in the standard deviations between examples WECC-MC and WECC-S

Table 6.3 The number of Gram-Charlier type A series approximations used in example WECC-S

Limitation	Number of Gram-Charlier type A Series
Voltage Magnitude High	178
Voltage Magnitude Low	178
Line Power Flow	263
Total	619

The reduction of computation time is the main motivation behind developing a stochastic-algebraic ATC calculation. A 1000 trial Monte Carlo study of the stochastic ATC calculation for this system has an execution time of about 15 hours per each trial using a 2.5 GHz personal computer. Since the bus loads are modeled based on the day ahead load forecast error, the time needed to solve a Monte Carlo ATC study is unacceptable. Table 6.4 shows the computation time for each of the five transfers used in example WECC-S. These computation times are about 1 minute and would be acceptable to a power marketer who is attempting to buy/sell power in the day ahead time frame.

Table 6.4 Computation times of the ATC transfers in example WECC-S

From Bus	To Bus	Computation Time* (seconds)
78	103	67.36
3	155	49.94
3	8	57.53
44	160	46.57
34	64	47.22

A 2.5 GHz personal computer was used

6.3. Conclusions drawn from examples WECC-S100, WECC-S500, WECC-S1000, WECC-S1500, WECC-MC100, WECC-MC500, WECC-MC1000 and WECC-MC1500

The examples shown in Section 3.7 illustrate the stochastic ATC for the WECC system considering only the large bus loads to be random. The examples are split into four different categories:

- Bus loads over 100 MW considered to be random
- Bus loads over 500 MW considered to be random
- Bus loads over 1000 MW considered to be random
- Bus loads over 1500 MW considered to be random.

The purpose of these examples is to show how the stochastic ATC changes by decreasing the amount of random bus loads. The bus loads that are considered to be random have the same mean and variance as the bus loads used in example WECC-S. The results show that the difference in standard deviation between the Monte Carlo and stochastic-algebraic solutions has similar results to examples WECC-MC and WECC-S.

One important outcome from the examples discussed in this section is the behavior of the statistics of the ATC. This behavior is evident considering a relatively small number of bus loads to be random. Large bus loads are selected because it is assumed that their statistics have the most impact on the statistics of the ATC. Results show that when considering a smaller number of random bus loads for the system, the stochastic ATC of the system become more deterministic (i.e. standard deviation is small). Table 6.5 shows this evolution of the stochastic ATC to deterministic ATC for the transfer from bus 3 to bus 8. The standard deviation when all bus loads of the system from Table 6.5 is 1.5418 MW. This standard deviation becomes zero when only bus loads greater than 1000 MW are considered. Since a zero standard deviation is a characteristic of a deterministic ATC study, these results show that considering a smaller number of bus loads has a negative impact on the accuracy of the stochastic ATC. Therefore, in order to properly model the stochastic ATC, the system should include models of the maximum possible number of random bus loads.

Table 6.5 Results from the stochastic-algebraic method for the transfer from bus 3 to 8 for the WECC System

Smallest random bus load		Stochastic-Algebraic Method	
Loads below this level not modeled stochastically	Example	Mean (MW)	Standard Deviation (MW)
0 MW	WECC-S	1145.3	1.5418
100 MW	WECC-S100	1141	1.0798
500 MW	WECC-S500	1141	0.92141
1000 MW	WECC-S1000	1141	0
1500 MW	WECC-S1500	1141	0

6.4. Conclusions drawn from example WECC-STLU

The purpose of example WECC-STLU (shown in section 5.3) is to illustrate the concepts of Chapter 4. Chapter 4 discusses the addition of transmission uncertainty to the stochastic ATC calculation. Example WECC-STLU uses the same stochastic ATC calculation method as discussed in Chapter 2 along with a transmission outage table. The transmission outage table includes only the top twenty *N*-1 highest ranked contingencies from a contingency ranking program (TSAT). The results of the stochastic ATC calculation (including transmission element status uncertainty) are compared to the stochastic ATC calculation with only bus loads considered uncertain.

The results between the two calculation methods are shown in Table 6.6. Table 6.6 shows the percent difference between the two calculation methods. Incorporating

transmission line uncertainty does not drastically affect the mean of the ATC. The resulting percent changes in the mean are less than 1%. Since the probability of occurrence of the N-1 states are 0.0006518 for each of the transmission lines and 0.00292304 for each of the transformers, addition of the means of each transmission line outage status will result in a small change in the overall calculated mean. Although the value of the mean of the ATC is significant in the use of the ATC for operations and planning, the changes in the variance, skew, and kurtosis can possibly change how the ATC is used in the trade of power.

Unlike the percent difference in the mean, the changes in the variance, skew, and kurtosis are quite significant when integrating transmission asset status uncertainty in the stochastic ATC calculation. Information on the properties of skew and kurtosis can be found in Appendix A. Changes in these statistical measures represent changes in the shape of the density function that represents the ATC. For most of the cases, the skew of the ATC decreases (from the no line out case to the 20 *N*-1 cases). For a majority of cases, when a transmission system element is taken out of the system, the mean of the ATC decreases. The decrease of skew is expected due to the addition of the 20 *N*-1 stochastic ATC random variables with means less than the stochastic ATC with all lines. The more negative the skew is the denser is the left side of the distribution is. Therefore, the addition of the transmission uncertainty to the stochastic ATC adds more weight to the left side of the density curve of the ATC. The shift of weight to the left side is important in the calculation probabilities of the ATC.

The probabilities of the ATC are important in the trade of power if ATC is used. Prices of the power can be negotiated by the probability of the ATC. Different pricing levels of the transfer of power can be based on the probability of the ATC. For example, a transfer for 200 MW is to be traded. The probability of ATC is found from the probability density function:

- probability($ATC \leq 150\ MW$) = 0.7
- probability($ATC \leq 200\ MW$) = 0.8
- probability($ATC \leq 300\ MW$) = 1.0

the price of the transfer can be split into two different categories based on these probabilities. The first category is contracted power that is to not be interrupted. This category can be based on the probability $P \leq ATC$. For this case, the probability of the *ATC* greater than 200 MW is 0.2. If the probability of the *ATC* greater than the necessary transfer is within a certain range, then a contracted price can be negotiated with transfer of power at the full ATC "level". If the probability of the *ATC* greater than the necessary transfer is 0.2, then the contract of the example will be a full uninterrupted energy transfer at the ATC level. If the probability of the *ATC* greater than the necessary transfer is less than 0.2, then the second category of contracted power can be used. This second category can be based on a different ATC price along with the possibility of interrupted service. For example, if the probability of the A*TC* greater than the necessary transfer is 0.3, and the 200 *MW* of transfer is being negotiated, then 150 *MW* can be contracted out using the first category with uninterrupted service and the additional 50 *MW* is contracted using the second category with possible interrupted service. Therefore, the use of the probabilities of the ATC could be of some use in the trade of power across the network.

Table 6.6 Comparison of the ATC statistics when the transmission asset uncertainty is considered vs. when transmission asset uncertainty is not considered in example WECC-STLU

Transfer	Difference in the mean (*MW*)	Difference in the variance (MW^2)	Difference in the skew	Difference in the kurtosis
35-102	-0.0341	-1.887	-110	-19.893
40-10	0	53.143	215.225	-180.426
70-10	0.917	0.849	-13.043	-1.769
36-137	0.014	-1.327	0	-6.104
4-137	-0.297	-99.575	-3024.334	108884
162-69	-0.0169	-62.625	-64.245	-7.634
15-55	0.287	-93.684	-118.061	-21.125

7. Stochastic-Algebraic ATC Calculation and Transmission Expansion

7.1. Introduction

Transmission expansion of a power system enhances the ability of the system to transport power. With transmission expansion, new paths can be installed or existing paths can be upgraded to allow for the system to have increased power transfers and concomitant increased power market participation, and potentially enhanced operating environment. Since transmission expansion of a system can cost power companies significant investment in money, a cost to benefit analysis is commonly preformed as part of the extensive considerations to justify the transmission expansion. There are a wide range of issues that are also associated with potential transmission expansion including:

- financial
- systems engineering
- environmental impact
- public acceptance
- expected load growth
- contractual agreement
- political
- reliability
- right of way availability.

The stochastic ATC is suggested to be used as a tool in the addition of transmission assets.

7.2. Cost to benefit analysis of transmission expansion using stochastic ATC

Stochastic ATC can be integrated into the array of tools for the analysis of transmission expansion of a system. In the planning stage of transmission expansion, engineers typically perform a cost to benefit analysis to justify in part the transmission expansion of the system. A new analytical procedure in the cost to benefit analysis of transmission expansion could include the stochastic ATC calculation. Cost to benefit analysis usually entails the manipulation and analysis of data including present values and trends in load and available generation. If stochastic ATC calculation is used in the cost to benefit analysis, various data will need to augment the traditional data. For example, the statistics of loads will be needed; generation levels and base case power flows will need to be modeled probabilistically; future market prices will be needed; typical time intervals that the ATC is traded will be needed.

Equation (7.1) shows the time it takes to payback the costs of transmission expansion of the system on the basis of elementary considerations,

$$T_p = \frac{C_{te}}{\Delta\mu_{ATC} T_{ATC} D_{ATC}} \tag{7.1}$$

where:

- Tp is the payback time of transmission expansion
- C_{te} is the cost of transmission expansion
- $\Delta\mu_{ATC}$ is the change of the mean of ATC
- T_{ATC} is the number of hours per year that power is traded at the ATC level
- $D_{ATC}(P)$ is the value of the traded power and is dependent on the power level.

The calculation of (7.1) can be calculated in sections based on low-medium-and high power. The calculation of (7.1) in these sections allows for the changes of $D_{ATC}(P)$, T_{ATC}, $\Delta\mu_{ATC}$, C_{te} to be properly reflected in Tp. This equation is used as the basis of the cost to benefit analysis of transmission expansion. The equation can be used to evaluate payback time vs. hours that the transfer is limited by the ATC. The concept of (7.1) is illustrated in Section 7.3.

It can be assumed that real options analysis [70-71] is used to find the future values of ATC. Therefore the future value of money needs to be used to evaluate D_{ATC}. It is also important to note that the cost of transmission expansion C_{te} should be modified to include interest [72-73]. The calculation of the cost of transmission expansion with interest rates can be preformed using one of two different functions:

Simple interest: $1 + rt$

Compound interest: $\left(1 + \frac{r}{C_p}\right)^{C_p t}$

where r is the interest rate, t is the time elapsed from the start of the interest rate calculation, and C_p is the number of compounding intervals per time t. Incorporating simple interest (with t equal to payback) into (7.1) yields

$$T_p = \frac{C_{te}(1+r)T_p}{\Delta\mu_{ATC} T_{ATC} D_{ATC}}. \tag{7.2}$$

Reformulation of (7.2) yields the payback for transmission expansion with simple interest included,

$$T_p = \frac{C_{te}}{\Delta\mu_{ATC} T_{ATC} D_{ATC}(1-r)}. \tag{7.3}$$

Incorporating compound interest (with t equal to T_p) into (7.1) yields

$$T_p = \frac{C_{te}\left(1 + \frac{r}{C_p}\right)^{C_p T_p}}{\Delta\mu_{ATC} T_{ATC} D_{ATC}}. \tag{7.4}$$

A Taylor series expansion of $\left(1+\frac{r}{C_p}\right)^{C_pT_P}$ is used to reformulate (7.4) from which the payback can be estimated. The Taylor series expansion about point a is truncated at the second term and is,

$$\left(1+\frac{r}{C_p}\right)^{(cp)T_p} \cong \left(1+\frac{r}{C_p}\right)^{(cp)a}\left[1+C_p\left(T_p-a\right)ln\left(1+\frac{r}{C_p}\right)\right]. \tag{7.5}$$

If point a is taken to be zero (i.e., (7.5) turns into a Maclaurin series), (7.5) can be substituted into (7.4) to yield a payback function considering compound interest

$$T_p = \frac{C_{te}}{\Delta\mu_{ATC}T_{ATC}D_{ATC}\left(1-C_p\,ln\left(1+\frac{r}{C_p}\right)\right)}. \tag{7.6}$$

Observation of (7.6) indicates:

If $r = 0$, (7.1) results

If $\frac{C_{te}}{\Delta m_{ATC}^{(1)}T_{ATC}D_{ATC}}$ is viewed as a simple unitless constant, the impact of interest rate r on T_p is

$$T_p \approx \frac{1}{1-C_p\,ln\left(1+\frac{r}{C_p}\right)}. \tag{7.7}$$

Equation (7.7), for small r, becomes

$$T_p \approx 1+r$$

which is consistent with the simple interest model in (7.3).

7.3. Transmission congestion and cost of congestion

The cost of congestion is important in considering the sale of power across the network. A financial cost to benefit analysis of transmission expansion would be impacted by the cost of congestion. The cost of congestion typically is used in two different ways: nodal pricing and buy-back pricing. Nodal pricing considers congestion at nodes in a power system. The cost of congestion is paid for by the consumers and GENCOs are compensated for the congestion. These consumer payments are typically higher than the payments to GENCOs. Buy-back pricing shares the costs of congestion on a pro-rata basis by the consumers and is added to the unconstrained market clearing price and does not consider the effects on the transmission network caused by different consumers. Further information on the cost of congestion can be found in [74-78,97-99].

Inclusion of the costs of congestion to the calculation of the value of ATC could impact the payback time of transmission expansion. If a particular ATC transfer causes congestion at certain nodes in the power system, the cost of congestion could cause the

value of the ATC to significantly decrease. This phenomenon is dependent on the power levels of market sales: if the sales are at power levels close to the ATC, and if the power levels cause congestion and other costs, the dollar value (or price) of ATC will be impacted. The costs of congestion would add (subtract) some to (from) the price (value) of the transaction. This would change the way payback time of transmission expansion is calculated in (7.1). An additional function would have to be added to D_{ATC} in order to account for the cost of congestion,

$$T_p = \frac{C_{te}}{\Delta\mu_{ATC} T_{ATC} D_{ATC} \left(1 - C_{cong}(P)\right)} \tag{7.8}$$

where $C_{cong}(P)$ is a function of the cost of congestion at the power level P of the transfer.

Research has been performed on the calculation of congestion costs associated with the ATC [78]. The method uses a DC optimal power flow, Monte-Carlo simulations of uncertainty of forecasted system conditions, and concepts of locational marginal pricing to calculate the cost of congestion in real time. Possible integration of the ideas in [78] to the stochastic ATC calculation are proposed as future work and is listed in Section 8.2.

7.4. Illustration of the cost to benefit analysis of transmission expansion

The WECC test bed is used to illustrate the cost to benefit analysis of transmission expansion of the system using stochastic ATC. This example is denominated ATC example WECC-TE. The system data are shown in Appendix E. The path ratings used for this case are not the values shown Appendix E, but instead are 200% of the base case system flows. The change in path ratings is used to simulate a system based on ATC transfers limited by the transmission path ratings. Again, the number of possible ATC transfers in this system are 69432, four different ATC transfers are presented here as illustrations. All illustrations in this chapter assume that the interest rate of the money borrowed to complete transmission expansion is zero. That is, the payback function used for these examples is taken from (7.1). These illustrations are shown in Table 7.1.

In the illustration, the interest rate r is assumed to be zero and the cost of congestion is not included.

A stochastic ATC study is first preformed without transmission expansion. The mean and variance of the ATC for this study for each of the transfers in Table 7.1 is shown in Table 7.2. For this case, it is assumed that there are no new transmission rights of way going to be built. That is, existing paths are going to be upgraded. For each of the ATC analyses shown in Table 7.2, the path which limits the ATC is considered as possible transmission expansion. The limiting system paths which limits each of the ATC transfers is shown in Table 7.3

Table 7.1 Transfers used for the cost to benefit analysis of Example WECC-TE

From Bus	To Bus
4	10
112	137
35	107
43	39

Table 7.2 Mean and variance of the ATC without transmission expansion in example WECC-TE

From Bus	To Bus	Mean *MW*	Variance MW^2
4	10	200.29	40188.0
112	137	670.64	173140.0
35	107	643.11	171340.0
43	39	462.69	2415.7

Table 7.3 Paths which limit the transfer of ATC in example WECC-TE

Original transfer		Transmission added to path	
From Bus	To Bus	From Bus	To Bus
4	10	8	10
112	137	150	154
35	107	150	154
43	39	39	60

A new stochastic ATC study is preformed with the transmission expansion component added to the system. The results from the new stochastic ATC study are shown in Table 7.4. Results from Tables 7.2 and 7.4 are used with (7.1) to find the payback of transmission expansion of the system. The value of the profit for the transfers are assumed to be 20 $/MWh. The cost of adding extra transmission is found based on the cost of $550,000 per mile of new transmission added in 1995. This figure comes from [56] and is based on a 230 kV circuit in 1995. Using the US consumer price index, the cost of new transmission is recalculated for June 2006,

Cost of new transmission =

$$\frac{CPI_{June,2006}}{CPI_{June,1995}}(550000) = \frac{202.9}{152.5}(550000) = \$731770 . \tag{7.9}$$

The line lengths for the transmission paths added need to be calculated. The WECC test bed used for these tests did not include line lengths. It is possible, for illustrative purposes, to approximate and typify line length based on the given value of the line resistance and a typical value of resistance for a high voltage conductor (e.g.,

0.10 ohms/mile [59]). The calculated line lengths are shown in Table 7.5. Figs. 7.1-7.4 show the pay back time vs. the hours that the transfer is limited by the ATC per year.

Table 7.4 Mean and variance of the ATC with transmission expansion in example WECC-TE

From Bus	To Bus	Mean *MW*	Variance MW^2
4	10	600.88	361130
112	137	823.60	175350
35	107	793.95	173040
43	39	1045.70	10999

Table 7.5 Lengths of the new transmission lines added in example WECC-TE

From Bus	To Bus	Line Length (miles)
8	10	7
150	154	71.25
39	60	50.6

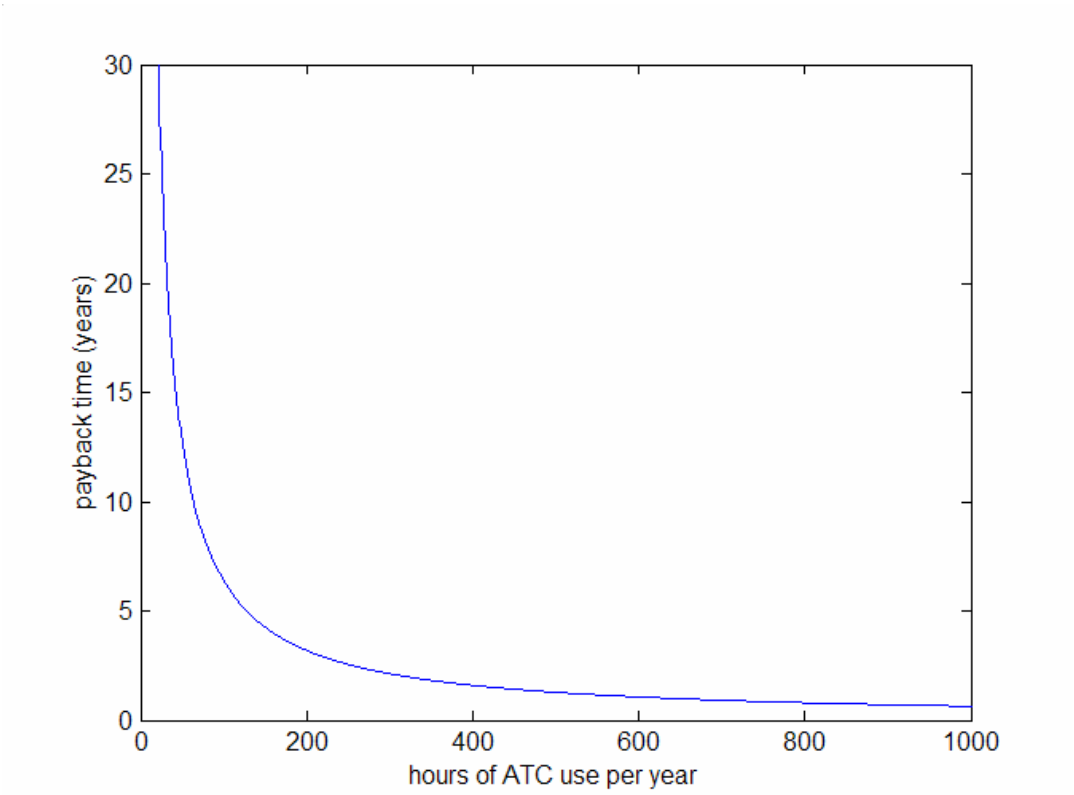

Figure 7.1 Payback time for adding one additional line to (8-10) vs. the annual hours that the transfer is limited by the ATC (4-10) use in example WECC-TE

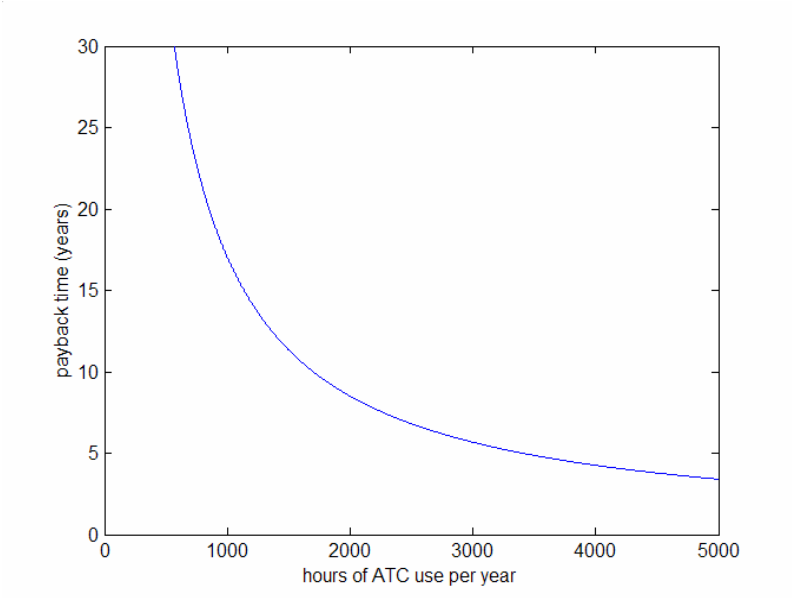

Figure 7.2 Payback time for adding one additional line to (8-10) vs. the annual hours that the transfer is limited by the ATC (50-154) use in example WECC-TE

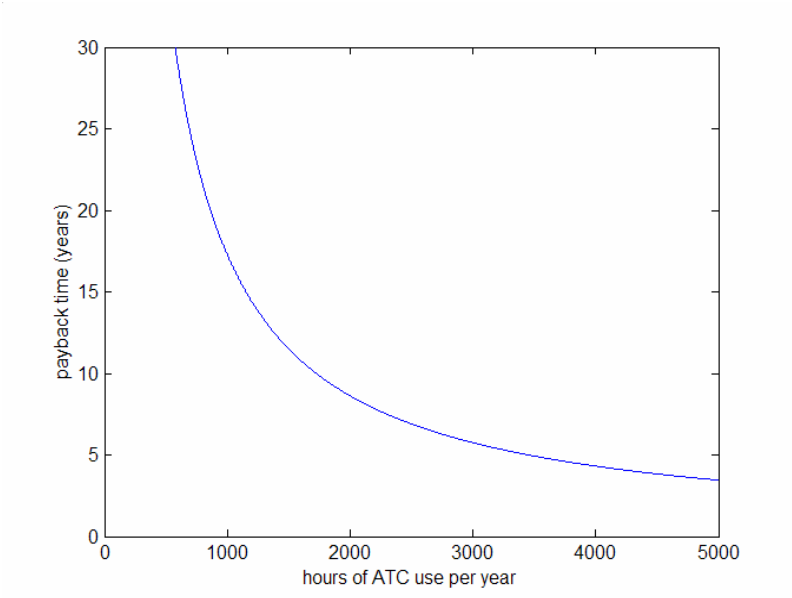

Figure 7.3 Payback time for adding one additional line to (112-137) vs. the annual hours that the transfer is limited by the ATC (50-154) use in example WECC-TE

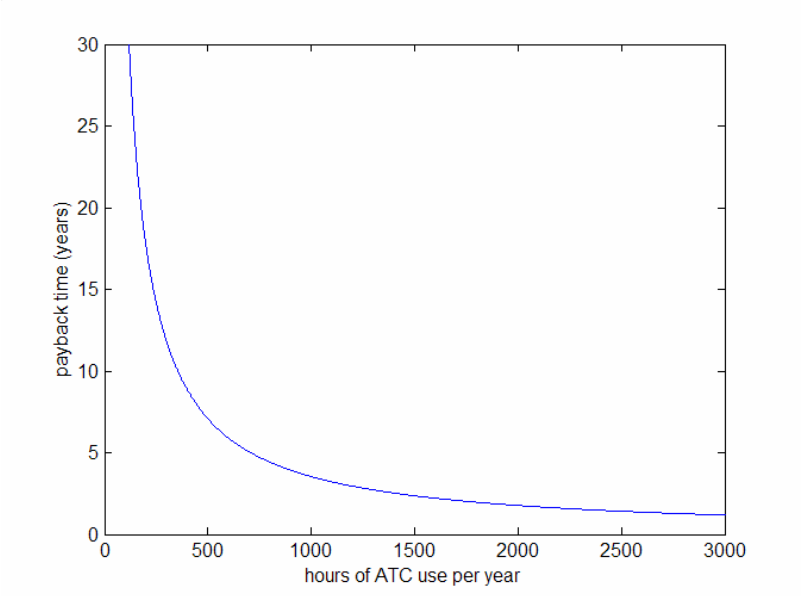

Figure 7.4 Payback time for adding one additional line to (43-39) vs. the annual hours that the transfer is limited by the ATC (39-60) use in example WECC-TE

7.5. Conclusions based on transmission expansion experiments

In Section 7.3 a transmission expansion cost to benefit analysis is shown using the ATC. Four different cases are shown in which result in graphs of payback times based on the ATC. These graphs can be used to assist in the justification of transmission expansion. For example, if the payback time for the addition of the transmission lines to the system is to be less than ten years, then the amount of time that ATC has to be traded per year (based on 20 $/MWh sale) can be calculated. The amount of time that ATC has to be traded based on a 10 year payback for all four examples is shown in Table 7.6. Results from Table 7.6 can be used to justify transmission expansion. Small number of hours that ATC traded per year can be used to justify transmission expansion based on the sale of power at ATC levels.

On the basis of limited experiments using the WECC test bed, simple formulations of the cost to benefit problem, and using assumed ATC dollar values, it is conjectured that some transmission corridor capacity expansion could realize a payback period of less than 5 years even for limited amount of time that power is traded near ATC levels (e.g., 200 hours that the transfer is limited by the ATC use per year). This statement is based on the analysis of line 4-10 as shown in Figure 7.1.

The analysis shown in this chapter does not include a number of issues that should be included in transmission expansion. These issues include, but are not limited to:

- Interest rate is not included in example WECC-TE
- Limited examples studied
- The number of hours that the sale of power is limited by the ATC is not really included
- Load forecasts are not very accurate in a 2 year and beyond ahead time horizon.

- Environmental impact and other issued not modeled in the analysis
- Volatile spot market is not modeled [92].

Table 7.6 Amount of time that ATC has to be traded based on a 10 year pay back in example WECC-TE

From Bus	To Bus	Hours at which power sales at or near ATC limit
4	10	64
112	137	1688
35	107	1712
43	39	352

8. Conclusions and Future Work

8.1. Conclusions

Power marketers have the option to trade power using a variety of tools including measures and indices. Among those tools is the ATC calculation. Power systems are probabilistic in nature, and the probabilistic calculation of ATC is recommended. Since line power flows are an important part of the evaluation of ATC, a stochastic power flow problem can be used to find the probabilistic behavior of ATC. If bus load models can be statistically approximated using existing data, line flows can be modeled probabilistically resulting in multiple statistical moments for each line flow as well as a probability density function for each line. The observation that ATC is a stochastic quantity and the means of calculating the stochastic ATC are the main contributions of this report.

Evaluating a stochastic ATC problem using a stochastic analysis method, as opposed to a Monte Carlo method, decreases the computational time. The decrease in computational time can result in a more efficient method of evaluating the stochastic ATC as well as offering power marketers fast determination of the expected price of ATC for any given transfer. In tests on a 179 bus system, a typical calculation time to evaluate the probability density function, mean and variance of ATC requires 54,000 seconds using the Monte Carlo method versus 60 seconds using a stochastic-algebraic analysis. The two cited calculation methods generally agree within 0.5 percent in the mean, and 12 percent in the variance for the illustrative cases studied.

The results shown in Chapter 3 suggest that the stochastic-algebraic method provides a good approximation of the stochastic ATC based on a day-ahead load forecast. If a small percentage of the total load is to be considered random (e.g., 20% of the total number of busses), the stochastic-algebraic ATC calculation solution reduces to a deterministic ATC approximation. Therefore, if the objective is to capture the stochastic behavior of ATC, it is necessary to model as much of the total system load as possible when performing the stochastic-algebraic stochastic ATC calculation.

The results shown in Chapter 5 suggest that the addition of transmission element uncertainty to the stochastic ATC changes the shape of the probability density of the ATC. The shape of the probability density of the ATC affects the probabilities of certain values of ATC. For a majority of the cases, inclusion of transmission element uncertainty causes the probability distributions of the ATC to have a small (e.g., <1%) change in the mean. Further, inclusion of transmission uncertainty generally results in the appearance of higher tail weight at the left (i.e., ATC < mean). Also, as discussed in Chapter 6, the distribution of the ATC can be used to classify different levels of prices and/or services for a specified power transfer.

Chapter 7 illustrates how the ATC can be used in transmission expansion. Basic cost to benefit analysis shows that it is possible to financially justify transmission expansion of the system solely based on the ATC. The increase of the ATC for a given transfer after transmission expansion can, in some cases, justify the cost of adding new transmission assets to the system. A “typical” payback for certain transmission expansion considering 1000 hours per year of power exchanges at the ATC limit, ranges from 5 to 20 years for the WECC tests. The “payback” for transmission expansion is based on the

market price of the energy and the amount of time (per year) that power is sold within the ATC limit.

The importance of using a stochastic calculation method to evaluate ATC lies in the fact that load uncertainty is modeled. If the standard deviation of the load is {5, 10, 15} percent of the average demand, in a typical calculation, the ATC has a standard deviation of {75, 150, 300} percent of the expected ATC. The cited load variation was selected to illustrate 15 minute ahead calculation of ATC. If the probabilistic variation of the load is ignored, the standard deviation of the ATC is zero (i.e., the deterministic case).

Table 8.1 summarizes the primary contributions of this report. Table 8.2 summarizes the secondary contributions of this report.

8.2. Future work

With the deregulation of the power system, ATC is calculated daily and is used in the trading of power. A stochastic ATC calculation could benefit the E-tag approval process. Research in the use of stochastic ATC calculations as an operations tool is recommended. Faster methods of calculating the stochastic ATC based on uncertainty of bus load and transmission element status would need to be found.

There are a variety of other uncertainties that are in power systems. Generation availability, transmission line parameters, transformer taps and shunt capacitor status have potential uncertainty. Integration of these uncertainties to the stochastic model could provide a more accurate measure of the ATC statistics for operations and transmission expansion.

Testing with real data can be used to verify the stochastic ATC calculation in real life scenarios. The real data can be taken from power market histories. These histories would need to provide information (for a specific time interval) of

- bus loads
- existing power transfers
- known ATC values for various transfers in the network
- transmission element status
- generator status
- network topology.
- Testing using real data can validate the stochastic ATC calculation.

Research has been performed on the calculation of congestion costs associated with the ATC [78]. The method uses a DC optimal power flow, Monte-Carlo simulations of uncertainty of forecasted system conditions, and concepts of locational marginal pricing to calculate the cost of congestion in real time. The system uncertainties included are load forecast errors and transmission element status. The method does not consider reactive power flows and transfers. It is possible to replace the Monte-Carlo simulations with a stochastic ATC calculation. The integration of the stochastic ATC calculation could provide a faster calculation of the real time congestion costs.

Open transmission access has implemented locational pricing markets (LPM). The LPM allow for the price of the transmission of power to vary in different transmission paths in the system. Before the implementations of LPM, the transmission rights were physical flowgates (e.g., the connecting transmission paths between existing

systems). Since open transmission access has resulted in the use of LPM, transmission rights changed from physical flowgate rights to point to point financial transmission rights (FTR). Since power can now be traded, FTR have an important role in the pricing of electrical energy trading [83-90]. The FTR have an economic value and take a role in the pricing of electrical energy. For various instances in [83-90], the ATC is proposed to be used as part of the auction of FTR. In power markets, future FTR markets are becoming important. Since the ATC is used as part of the auction of short term FTR, it is proposed that the stochastic ATC calculation can be used in part of the long term FTR markets.

Table 8.3 summarizes suggestions for future work.

Table 8.1 Primary contributions of the report

Contribution	Basis		
	System theory	Probability theory	Illustrations
ATC is a stochastic quantity that can be modeled probabilistically		X	
Calculation of the statistics of the ATC is possible using a stochastic-algebraic method based on linear power flows, stochastic power flow, linear transformation of moments, and the Gram-Charlier type A series approximation.	X	X	
Inclusion of transmission element uncertainty in stochastic ATC calculation is possible using a tabular approach (transmission outage table)	X	X	
Use of power marketing with stochastic ATC has been illustrated using a simplified WECC test bed			X
Tests on the simplified WECC test bed imply that short (e.g., > 5 years) payback may be possible for selected transmission expansion based on the modest assumptions of ATC use.			X

Table 8.2 Secondary contributions of the report

Contribution	Basis		
	System theory	Probability theory	Illustrations
Examples of stochastic ATC are shown using the WECC and IEEE 14 bus test beds			X
Comparison of the stochastic-algebraic ATC calculation to a Monte Carlo calculation		X	X
Use of the Gram-Charlier type A series as an approximation of probability density functions of the ATC		X	
An innovative use of stochastic power flow in the stochastic-algebraic ATC calculation	X	X	
The use of a contingency ranking and transmission outage study on the simplified WECC test bed to decrease the number of system transmission states in the transmission outage table	X		

Table 8.3 Summary of future work suggestions

Future Work	Potential solution approach		
	System theory	Probability theory	Experimentation
Stochastic ATC as an operations tool	X		
Faster calculation methods	X	X	
Addition of other uncertainties		X	
Testing with real data			X
Integration of the stochastic ATC with future FTR markets	X		
Integration of the stochastic ATC calculation to the costs of congestion in [83]	X		

REFERENCES

[1] Federal Energy Regulatory Commission, "Promoting utility competition through open access, non-discriminatory transmission service by public utilities: recovery of stranded costs by public utilities and transmitting utilities," Order No. 888, Final Rule, FERC, April 24, 1996.

[2] Federal Energy Regulatory Commission, "Open access same-time information system and standards of conduct," Order No. 889, Final Rule, FERC, April 24, 1996.

[3] North American Electric Reliability Council, "Available transfer capability definitions and determination," June 1996.

[4] North American Electric Reliability Council, "Transmission transfer capability," May 1995.

[5] G. Ejebe, J. Waight, M. Santos-Nieto, W. Tinney, "Fast calculation of linear available transfer capability," IEEE Transactions on Power Systems, Vol. 15, No. 3, Aug. 2000, pp. 1112-1116.

[6] M. Gravener, C. Nwankpa, T. Yeoh, "ATC computational issues," Proceedings of the 32nd Hawaii International Conference on System Sciences, Jan. 5-8, 1999. pp. 1-6.

[7] G. Ejebe, J. Tong, J. Waight, J. Frame, X. Wang, W. Tinney, "Available transfer capability calculations," IEEE Transactions on Power Systems, Vol. 13, No. 4, November 1998, pp. 1521-1527.

[8] S. Grijalva, P. Sauer, "Reactive power considerations in linear ATC computation," Proceedings of the 32nd Hawaii International Conference on System Sciences, Jan. 5-8, 1999, pp. 1-11.

[9] F. C. Gaino, A. Padilha-Feltrin, "Influence of the supply of reactive power in the calculation of the transfer capability," Proceedings of the 2004 IEEE/PES Transmission and Distribution Conference & Exposition: Latin America, November 2004, pp. 190-195.

[10] M. M. Othman, A. Mohamed, A. Hussain, "Fast evaluation of available transfer capability considering the cubic-spline interpolation technique," Proceedings of the National Power and Energy Conference, November 2004, pp. 253-256.

[11] Y. Xia, K. W. Chan, M. Liu, J. Wu, "Calculation of available transfer capability with transient stability constraints," Proceedings of the 2004 IEEE International Conference on Electric Utility Deregulation, November 2004, pp. 128-132.

[12] Y. Cui, Z. Bie, X. Wang, "Study on calculation of probabilistic available transfer capability," Proceedings of the IEEE International Conference on Power System Technology, Vol. 4, October 13-17, 2002, pp. 2052-2056.

[13] D. M. V. Kumar, G. N. Reddy, C. Venkaiah, "Available transfer capability (ATC) determination using intelligent techniques," Proceedings of the IEEE Power India Conference, April 10-12, 2006.

[14] C. Su, "Transfer capability uncertainty computation," Proceedings of the 2004 International Conference on Power System Technology, November 2004, pp. 586-591.

[15] J. Vorsic, V. Muzek, G. Skerbinek, "Stochastic load flow analysis," Proceedings of the Electrotechnical Conference, Vol. 2, May 22-24, 1991, pp. 1445 – 1448.

[16] P. Jorgensen, J. S. Christensen, J. O. Tande, "Probabilistic load flow calculation using Monte Carlo techniques for distribution network with wind turbines," Proceedings on 8th International Conference on Harmonics And Quality of Power, Vol. 2 , 14-16 Oct. 1998, pp.1146–1151.

[17] A.B. Owen, " Monte Carlo extension of quasi-Monte Carlo," Winter Simulation Conference Proceedings, Vol. 1 , 13-16 Dec. 1998, pp. 571–577.

[18] C. Bensk, E. Cabau, "New benchmark for unreplicated experimental-design analysis," Proceedings on Reliability and Maintainability Symposium, pp. 242–245.

[19] I. Beich, F. Sullivan, "The importance of importance sampling," Computing in Science & Engineering, Vol. 1, March-April 1999, pp. 71–73.

[20] J.T Saraiva, V. Miranda, M.A.C.C Matos," Generation and load uncertainties incorporated in load flow studies," Proceeding on the 6th Mediterranean Electrotechnical Conference, 22-24 May 1991, pp. 1339-1342.

[21] A. Dimitrovski, K. Tomsovic," Boundary load flow solutions," IEEE Transactions on Power Systems, Vol. 19 , Feb. 2004, pp. 348–355.

[22] J. Choi, S. Moon, H. Kim, B. Lee, R. Billinton," Development of the ELDC and reliability evaluation of composite power system using Monte Carlo method," Power Engineering Society Summer Meeting, 2000, Vol. 4 , 16-20 July 2000, pp. 2063–2068.

[23] R. Billinton, L. Gan," A Monte Carlo simulation model for adequacy assessment of multi-area generating systems," Third International Conference on Probabilistic Methods Applied to Electric Power Systems, 3-5 Jul 1991, pp. 317–322.

[24] G.M. Huang, P. Yan, "Composite system adequacy evaluation using sequential Monte Carlo simulation for deregulated power systems," 2002 IEEE Power Engineering Society Summer Meeting, Vol. 2 , 21-25 July 2002, pp. 856–861.

[25] B. Borkowska, "Probabilistic load flow," IEEE Trans. on Power Apparatus and Systems, PAS -93, No. 3, 1974, pp. 752-759.

[26] J. Dopazo, O. Klitin, A. Sasson, "Stochastic load flows," IEEE Trans. on Power Apparatus and Systems, PAS-94, No. 2, 1975, pp. 299 -309.

[27] P. Sauer, "A generalized stochastic power flow algorithm," Ph. D. Thesis, Purdue University, W. LaFayette, IN, 1977.

[28] H. Cramer, Mathematical Methods of Statistics, Princeton University Press, Princeton, New Jersey, 1954.

[29] M. G. Kendall and A. Stuart, The Advanced Theory of Statistics, Vol. 1, Second Edition, Hafner Publishing Company, New York, N. Y., 1963.

[30] N. R. Goodman, "Statistical analysis based on a certain multivariate complex gaussian distribution (An Introduction)," Annals of Mathematical Statistics, Vol. 34, 1963, p. 152.

[31] W. Feller, An Introduction to Probability Theory and Its Applications, Vol. II, Second Edition, John Wiley and Sons, Inc. New York, NY, 1971.

[32] A. Papoulis, Probability, Random Variables, and Stochastic Processes, McGraw Hill, New York, NY, 1965.

[33] K. S. Miller, Multidimensional Gaussian Distributions, Wiley and Sons, New York, NY, 1964.

[34] R. V. Hogg, A. T. Cragin, Introduction to Mathematical Statistics, Third Edition, Macmillan Publishing Company, Inc., New York, New York, 1970.

[35] S. Patra, R. B. Misera, "Probabilistic load flow solution using method of moments," IEEE 2nd International on Advances in Power Systems Control, Operation and Management, Dec. 1993, pp. 922-934.

[36] L. Sanabria, T. Dhillion, "Stochastic power flow using cumulants and Von Mises functions," International Journal of Electric Power and Energy Systems, Vol. 8, 1986, pp. 47-60.

[37] P. Zhang, S. T. Lee, "Probabilistic load flow computation using the method of combined cumulants and Gram-Charlier expansion," IEEE Transactions on Power Systems, Vol. 19, No. 1, February 2004, pp. 676-682.

[38] C. U. L., Charlier, "Application de la theorie des probabilities a l'astronomie," Vol. II, Part IV of the Traite edited by Borel, Paris, France, 1931.

[39] F. Y. Edgeworth, "The law of error," Transactions Cambridge Philosophical Society, Vol. 20, 1905-1908, p. 45.

[40] A. L. Bowley, "F. Y. Edgeworth's Contributions to mathematical statistics," Reprint by Augustus M. Kelly Publishers, Clifton, New Jersey, 1972.

[41] P. J. Bickel, "Edgeworth expansions in nonparametric statistics," The Annal of Statistics, Vol. 2, No. 1, 1974, pp. 1-20.

[42] G. T. Heydt, Computer Analysis Methods for Power Systems, Macmillan, New York, 1996.

[43] B. Mozafari, A. M. Ranjbar, A. R. Shirani, A. Barkeseh, "A comprehensive method for available transfer capability calculation in a deregulated power system," 2004 IEEE International Conference on Electric Utility Deregulation, April 2004, pp. 680-685.

[44] A. Papoulis, S. Pillai, Probability, Random Variables, and Stochastic Processes, 4th ed., McGraw Hill, 2002.

[45] R. Christie, "Power system test archive," 1999, available at, http://www.ee.washington.edu/research/pstca/pf14/pg_tca14bus.htm

[46] M.Y. Cho, J.C. Hwang, C.S. Chen, "Customer short term load forecasting by using ARIMA transfer function model," Proceedings of Energy Management and Power Delivery, Vol. 1, Nov 21-23, 1995, pp. 317-322.

[47] G. Mu, Y.H. Chen, Z. F. Liu, W. D. Fan, "Studies on the forecasting errors of the short term load forecast," Proceedings on Power System Technology, Vol. 1, Oct. 13-17, 2002, pp. 636-640.

[48] K. B. Song, Y. S. Baek. D. H. Hong, G. Jang, "Short-term load forecasting for the holidays using fuzzy linear regression method," IEEE Transactions on Power Systems, Vol. 20, Feb. 2005, pp. 96-101.

[49] D. Srinivasan, A.C. Liew, C.S. Chang, "Forecasting daily load curves using a hybrid fuzzy-neural approach," IEE Proceedings on Generation, Transmission and Distribution, Vol. 141, Nov. 1994, pp. 561-567.

[50] D. Srinivasan, A.C. Liew, C.S. Chang, E. K. Chan, "Practical implementation of a hybrid fuzzy neural network for one-day-ahead load forecasting," IEE Proceedings on Generation, Transmission and Distribution, Vol. 145, Nov. 1998, pp. 687-692.

[51] E.A. Feinberg, D. Genethliou, J.T. Hajagos, B.G. Irrgang, R.J. Rossin, "Load pocket forecasting software," IEEE PES Power Systems Conference and Exposition, Oct. 10-13 2004, Vol. 3, pp. 1386-1390.

[52] Iowa State University, "Power system test archive," 1999, available at, http://design-2.ee.iastate.edu/timedomain/wecc.iee

[53] J.W. Stahlhut, G. T. Heydt, G.B. Sheble, "A stochastic evaluation of available transfer capability," IEEE PES General Meeting, June 12-16, 2005, San Francisco, CA, pp. 2393 – 2399.

[55] A. Phelps, J. Hudson, A. Rodriquez, "NERC E-Tag 1.7 Training Workshops," 2005, available at, http://reg.tsin.com/Tagging/e-tag/etag1_7Training_FINAL4.ppt

[55] D. O. Koval, "Frequency of transmission line outages in Canada," Industry Application Society Annual Meeting, Oct. 1994, vol. 3, pp. 2201-2208.

[56] University of Missouri Rolla, "Upgrading transmission capacity for wholesale electric power trade," 2006, available at, http://www.ece.umr.edu/links/power/Energy_Course/energy/Deregulation/table2.html

[57] Rhode Island Department of Labor and Training, "US consumer price index," 2006. http://www.dlt.ri.gov/lmi/business/cpi.htm

[58] S. Bin, D. Koval Xu Wilsun, J. Salmon, S. Shen, "An analysis of extreme-weather-related transmission line outages," Proceedings of the IEEE Canadian Conference on Electrical and Computer Engineering, Vol. 2, May 1998, pp. 697-700.

[59] S. Bin, D. Koval, S. Shen, "Modeling extreme-weather-related transmission line outages," Proceedings of the IEEE Canadian Conference on Electrical and Computer Engineering, Vol. 3, May 1998, pp. 1271-1276.

[60] D. Koval, A. Chowdhury, "An investigation into extreme-weather-caused transmission line unavailability," Proceedings of the IEEE Power Engineering Society General Meeting, Vol. 3,June 2005, pp. 2425-2428.

[61] D. Koval, "Frequency of transmission line outages in Canada," Proceedings of the 1994 IEEE Industry Applications Society Annual Meeting, Vol. 3, Oct 1994, pp. 2201-2208.

[62] C. Lee, N. Chen, "Distribution factors of reactive power flow in transmission line and transformer outage studies," IEEE Transactions on Power Systems, Vol. 7 , Feb. 1992, pp. 194-200.

[63] N. Sohtaoglu, "Evaluation of transmission losses in power system contingency analysis," Proceedings of the Mediterranean Electrotechnical Conference, Vol. 2, May 1998, pp. 936-940.

[64] Q. Chen, C. Jaing, W. Qiu, J. Mccalley, "Probability models for estimating the probabilities of cascading outages in high voltage transmission network," IEEE Transactions on Power Systems, Vol. 21, Aug 2006, pp. 1423-1431.

[65] E. Preston, M. Baughman, W. Grady, "A new model for outaging transmission lines in large electric networks," IEEE Transactions on Power Systems, Vol. 14, May 1999, pp. 412-418.

[66] R. Billinton, R. Ringlee, Power System Reliability Calculations, MIT Press, Boston, 1973.

[67] M. Haque, "Hybrid method of determining the transient stability margin of a power system," IEE Proceedings of Generation, Transmission and Distribution, Vol. 143. Jan. 1996, pp. 27-32.

[68] A. Padilha, E. Denis, "Transient stability indices from a hybrid approach," IEEE Porto Power Tech Proceedings, Vol. 2, Sept. 2001.

[69] P. M. Anderson, Analysis of Faulted Power Systems, Wiley and Sons, New York, 1995.

[70] J. Stahlhut, F. Gao, K. Hedman, B. Westendorf, G. Sheble, G. Heydt, P. Sauer, "Uncertain power flows and transmission expansion planning," 34th North American Power Symposium (NAPS), Ames, IA, Oct. 2005, pp. 489-496.

[71] K. Hedman, F. Gao, G. Sheble, "Overview of transmission expansion planning using real options analysis," 34th North American Power Symposium (NAPS), Ames, IA, Oct. 2005, pp. 497-502.

[72] J. Riggs, Essentials of Engineering Economics, McGraw-Hill, New York, 1982.

[73] M. Kurtz, Handbook of Engineering Economics, McGraw-Hill, New York, 1984.

[74] X. Hongfei, L. Weidong, W. Liming, "Congestion assessment for transmission planning in competitive electricity markets," Asia and Pacific IEEE Transmission and Distribution Conference and Exhibition, Aug. 2005, pp. 1-6.

[75] H. Jiang, Y. Zhou, J. Peng, "A new user oriented method for congestion cost allocation," Proceedings of the International Conference on Power System Technology, vol. 2, Oct. 2002, pp. 949 – 952.

[76] Z. Wu, Y. Wang, H. Qing, Y. Yang, "Continuous integration congestion cost allocation based on sensitivity," IEE Proceedings on Generation, Transmission and Distribution, Vol. 151, July 2004, pp. 421-426.

[77] A. Shirani, H. Siahkali, "Traceable flow method in determination of congestion cost assignment in open access power system network," IEEE Transmission and Distribution Conference and Exhibition, vol. 2, Oct. 2002, pp. 734-738.

[78] B. Corniere, L. martin, S. Vitet, N. Hadjsaid, A. Phadke, "Assessment of the congestion cost and risk of curtailment associated with available transfer capability," IEEE Power Engineering Society Winter Meeting, vol. 2, Jan 2000, pp. 891 – 896.

[79] A. Parlos, E. Oufi, J. Muthusami, A. Patton, A. Atiya, "Development of an intelligent long-term electric load forecasting system," International Conference on Intelligent Systems Applications to Power Systems, Feb 1996, pp. 288-292.

[80] T. Khoa, L. Phuong, P. Binh, N. Lien, "Application of wavelet and neural network to long-term load forecasting," International Conference on Power System Technology, Vol.1 Nov. 2004, pp. 840-844.

[81] M. Kandill, S. El-Debeiky, N. Hasanien, "Long-term load forecasting for fast developing utility using a knowledge-based expert system," IEEE Transactions on Power Systems, Vol. 17, May 2002, pp. 491-496.

[82] M. Farahat, "Long-term industrial load forecasting and planning using neural networks technique and fuzzy inference method," International Universities Power Engineering Conference, Vol.1, Sept. 2004, pp. 368-372.

[83] L. Tao, M. Shahindepour, "Risk-constrained FTR bidding strategy in transmission markets," IEEE Transactions on Power Systems, vol. 20, May 2005, pp. 1014-1021.

[84] X. Ma, D. Sun, G. Rosenwald, A. Ott, "Advanced financial transmission rights in the PJM market," IEEE Power Engineering Society General Meeting, vol. 2, July 2003.

[85] H. Yan, "A power marketer's perspective of financial transmission right," IEEE Power Engineering Society Winter Meeting, vol. 1, Feb 2001, pp. 383-385.

[86] T. Li, M. Shanidehpour, Z. Li, "Bidding strategy for FTR obligations in transmission markets," IEE Proceedings on Generation, Transmission, and Distribution, vol. 152, May 2005, pp. 422-428.

[87] T. Kristiansen, "Merchant transmission expansion based on financial transmission rights," Proceeding of the Annual Hawaii International Conference on System Sciences, Jan. 2005.

[88] A. Bykhovsky, D. James, C. Hanson, "Introduction of option financial transmission rights into the New England market," IEEE Power Engineering Society General Meeting, vol.1, June 2005, pp. 237-242.

[89] P. Gribik, D. Shirmohammadi, J. Graves, J. Kritikson, "Transmission rights and transmission expansions," IEEE Transactions on Power Systems, vol. 20, Nov. 2005, pp. 1728-1737.

[90] B. Lesieutre, I. Hiskens, "Convexity of the set of feasible injections and revenue adequacy in FTR markets," IEEE Transactions on Power Systems, vol. 20, Nov. 2005, pp. 1790-1798.

[91] J. Benjamin, Interior Point Techniques in Optimization, Kluwer Academic Publishers, 1997.

[92] R. Baldick, U. Helman, B. Hobbs, R. O'Neill, "Design of efficient generation markets," IEEE Proceedings, Vol. 93, Issue 11, Nov 2005, pp. 1998-2012.

[93] R. Johnson, Miller and Freund's Probability and Statistics for Engineers, Prentice Hall, New Jersey, 1994.

[94] J. Yu, A. Patton, "Transmission use charges including reliability costs," Power Engineering Society Winter Meeting, Vol. 2, Jan. 2000, pp. 866-871.

[95] J. Stahlhut, G. T. Heydt "Stochastic calculation of available transfer capability," IEEE Trans. Power Systems, submitted July 2006.

[96] M. Naarathy, "Accurate evaluation of bit-error rates of optical communication systems using the Gram-Charlier series," IEEE Transactions on Communications, Vol. 54, No. 2, Feb. 2006, pp. 295-301.

[97] F. Jian, J. Lamont, "A combined framework for service identification and congestion management," IEEE Transactions on Power Systems, Vol. 16, No. 1, Feb 2001, pp. 56-61.

[98] M. Baran, V. Banunarayanan, K. Garren, "Equitable allocation of congestion relief to transactions," IEEE Transactions on Power Systems, Vol. 15, No. 2, May 2000, pp. 579-585.

[99] N. Rau, "Transmission loss and congestion cost allocation-an approach based on responsibility," IEEE Transactions on Power Systems, Vol 15, No. 4, May 2000, pp. 1401-1409.

APPENDIX A: Useful Information on Statistical Moments

A.1 Basics of statistical moments

Statistical moments are used to provide some sort of "measure" that a probability distribution has. The most important and useful moment is the center of a distribution of X. This center is called the mean, and is usually denoted as the E[X], or the expectation of X,

$$E[X] = \int_{-\infty}^{\infty} xf(x)dx. \tag{A.1}$$

The mean is just one measure that a probability distribution has. The variance is another popular statistical measure of a probability distribution. The variance is a measure of the spread of the distribution. The variance is typically symbolized as σ^2 or Var[X]. The variance is calculated as the second central moment.

Moments are calculated in two different ways. Raw moments, are moments calculated about the origin, or zero. The kth raw moment can be calculated as

$$u_k = E[X^k] = \int_{-\infty}^{\infty} x^k f(x)dx. \tag{A.2}$$

Central moments are often more useful in practical applications. The central moment is the moment calculated about the mean,

$$u_k' = E[(X-u)^k] = \int_{-\infty}^{\infty} (x-u)^k f(x)dx. \tag{A.3}$$

A.2 Useful properties of moments

The following are some useful properties of the expectation operator and moments

Linear Property

$$E[aX+b] = aE[X]+b. \tag{A.4}$$

Variance of Linear Combination

$$Var[aX+b] = a^2 Var[X]. \tag{A.5}$$

Properties of Several random variables

$$E[X+Y] = E[X]+E[Y]. \tag{A.6}$$

$$E[XY] = E[X]E[Y]. \tag{A.7}$$

$$Var[X+Y] = Var[X]+Var[Y]-2*E[(X-u_x)(Y-u_y)]. \tag{A.8}$$

Also two additional unitless measures are used with the mean and variance to help describe a probability distribution. These additional measures are the skewness and kurtosis. The skewness is defined as

$$skew = \frac{\mu_x^{(3)}}{\sigma^3}. \tag{A.9}$$

The measure of skew is often useful to determine if a distribution of not symmetric. If the tail of the distribution is longer on the right, the skewness is a positive number. The skewness of a normal distribution is zero. The kurtosis is defined as

$$kurtosis = \frac{\mu_x^{(4)}}{\sigma^4}. \tag{A.10}$$

The kurtosis is a measure of peakedness of a distribution. A distribution that has a high kurtosis has a sharp peak while a low kurtosis has a more rounded peak. The kurtosis can range from -2 to $+\infty$. The kurtosis of a normal distribution is 3.

A.3 Moment conversions

This section shows some useful conversions between several raw and central moments as shown in [29]. Conversions of the first four raw moments (beyond the first) to central moments are

$$\mu_x^{(2)} = m_x^{(2)} - \mu_x{}^2 \tag{A.11}$$

$$\mu_x^{(3)} = m_x^{(3)} - 3m_x^{(1)}m_x^{(2)} + 2\mu_x{}^3 \tag{A.12}$$

$$\mu_x^{(4)} = m_x^{(4)} - 4m_x^{(1)}m_x^{(3)} + 6m_x^{(1)2}m_x^{(2)} - 3\mu_x{}^4. \tag{A.13}$$

Conversions of the first four central moments to raw moments are

$$m_x^{(2)} = \mu_x^{(2)} + \mu_x{}^2 \tag{A.14}$$

$$m_x^{(3)} = \mu_x^{(3)} + 3m_x^{(1)}\mu_x^{(2)} + \mu_x{}^3 \tag{A.15}$$

$$m_x^{(4)} = \mu_x^{(4)} + 4m_x^{(1)}\mu_x^{(3)} + 6m_x^{(1)2}\mu_x^{(2)} + \mu_x{}^4. \tag{A.16}$$

9. APPENDIX B: The Gram-Charlier Series Subroutine

```
%%%%%%%%%%%%%%%%%%%%%%
% The Gram-Charlier Series Subroutine   %
%       Jonathan W. Stahlhut                  %
%%%%%%%%%%%%%%%%%%%%%%
function [f,y] = GCS(Moments_ATC)

x = -10:.1:10; %initial range of x for the standard Gram-Charlier Series(GCS)
n = size(Moments_ATC,2); %how many moments of the ATC are used to approximate
the GCS, for all examples will equal 5

% Subroutine to find the first n Hermite Polynomials
b = 1;
for a = 1:n
   if b == 1
      t = (a+1)/2;
      b = 0;
   else
      t = (a+2)/2;
      b = 1;
   end
   H(a,:) = X.^a;
   kk = 1;
   for k = 2:t
      kk = kk*(2*k-3);
      H(a,:) = H(a,:) + (-1)^(k-1)*(X.^(a-2*(k-1)))*(factorial(a)/(factorial(2*(k-
1))*(factorial(a-2*(k-1)))))*kk;
   end
end

% the first five GCS constants cj
c = [ 0
Moments_ATC(2)/Moments(ATC(2))-1
Moments_ATC(3)/Moments_ATC(2)^(3/2)
Moments_ATC(4)/Moments_ATC(2)^(4/2)-6*Moments_ATC(2)/Moments_ATC(2)+3
Moments_ATC(5)/Moments_ATC(2)^(5/2)-
10*Moments_ATC(3)/Moments_ATC(2)^(3/2)
];

%Gaussian Function
G = (1/(sqrt(2*pi)))*exp((-X.^2)/2);
```

```
%iterative procedue to find the standard GCS with the Hermite Polynomials and the GCS
constants
GCS_CH = 1;
for g = 1:5
GCS_CH = GCS_CH + (1/factorial(g))*c(g)*H(g,:);
end

% the standard Gram-Charlier Series
GCS = G.*(GCS_CH);

% the GCS using the real values for the ATC
f = GCS./sqrt(Moments_ATC(2));
y = sqrt(Moments_ATC(2)).*X + Moments_ATC(1);
```

APPENDIX C: Derivation of the PDF of the Minimum of Several Random Variables

If x and y are random variables, and a random variable z is defined as

$$min(x, y) \le z \tag{C.1}$$

and the probability density functions f_x and f_y are known as well as the probability distribution functions F_x and F_y, the probability distribution of z can be found. For a given z, the region Dz of the xy plane such that

$$min(x, y) \le z \Rightarrow \quad x \le z, \quad y \le z \tag{C.2}$$

is shown in Figure C.1.

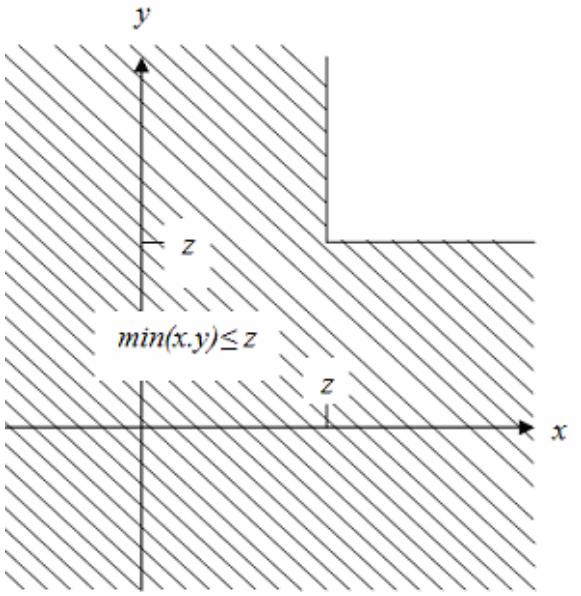

Figure C.1. Pictorial of min(x,y) ≤z

To find $F_z(z)$, the mass in D_z needs to be determined. This mass equals the mass in $F_x(z)$ in the half plane $x \le z$ plus the mass $F_y(z)$ in the half plane $y \le z$ minus the mass $F_{xy}(z,z)$ in the region $x \le z$, $y \le z$

$$F_z(z) = F_x(z) + F_y(z) - F_{xy}(z). \tag{C.3}$$

If the random variables x and y are independent, then the above yields

$$F_z(z) = F_x(z) + F_y(z) - F_x(z)F_y(z). \tag{C.4}$$

The probability density function $f_z(z)$ is found by differentiating (2.55),

$$f_z(z) = f_x(z) + f_y(z) - f_x(z)F_y(z) - f_y(z)F_x(z). \tag{C.5}$$

Reordering (2.56) yields

$$f_z(z) = f_x(z)[1 - F_y(z)] + f_y(z)[1 - F_x(z)] . \tag{C.6}$$

If a third random variable w is introduced, with probability density function f_w and probability distribution function F_w,

$$min(x, y, w) \le z , \tag{C.7}$$

it can be shown that

$$\begin{aligned} f_z(z) = {} & f_x(z)[1 - F_y(z)][1 - F_w(z)] + f_y(z)[1 - F_x(z)][1 - F_w(z)] \\ & + f_w(z)[1 - F_x(z)][1 - F_y(z)] . \end{aligned} \tag{C.8}$$

Therefore the result is that if any number n of independent random variables form a function

$$min(x_1 ... x_n) \le z , \tag{C.9}$$

the probability density function $f_z(z)$ becomes

$$f_z(z) = \sum_{i=1}^{n} f_{x_i}(z) \sum_{j=1, j\neq i}^{n} [1 - F_{x_j}(z)] . \tag{C.10}$$

APPENDIX D: NERC E-Tag

According to the NERC Policy 3, "full-time E-Tag monitoring" is required of all control areas, transmission providers, and purchasing-selling entities [54]. The purpose of E-Tags is to enable power marketing in a coordinated way. Par of the E-Tag process is to help decrease the amount of transmission system congestion and to help security coordinators and control areas assess reliability impacts and curtail transactions when necessary.

Purchase selling entities submit tags to a tag authority service. The authority performs contingency analysis and assessment and dynamic security assessment. The authority approves or rejects the E-Tag request as appropriate. Once the tags are approved, power can be traded in the network. The tags are usually submitted in the day-ahead time frame.

One important component of an E-Tag is transmission stacking. Each physical segment of the power system (e.g., transmission line or transformer) must support the energy flowing through the segment during the tagged schedule. The power flow through each segment is stacked either horizontally or vertically, or a combination of both. Figs. D.1 and D.2 show horizontal and vertical stacking respectively. A tag authority service assembles all of the submitted tags for a specified time frame, and stacks the tags. If a tag is stacked and violates the maximum energy flow through the physical segment, the tag would be denied. Figure D.3 illustrates an example of transmission stacking which incorporates both horizontal and vertical stacking.

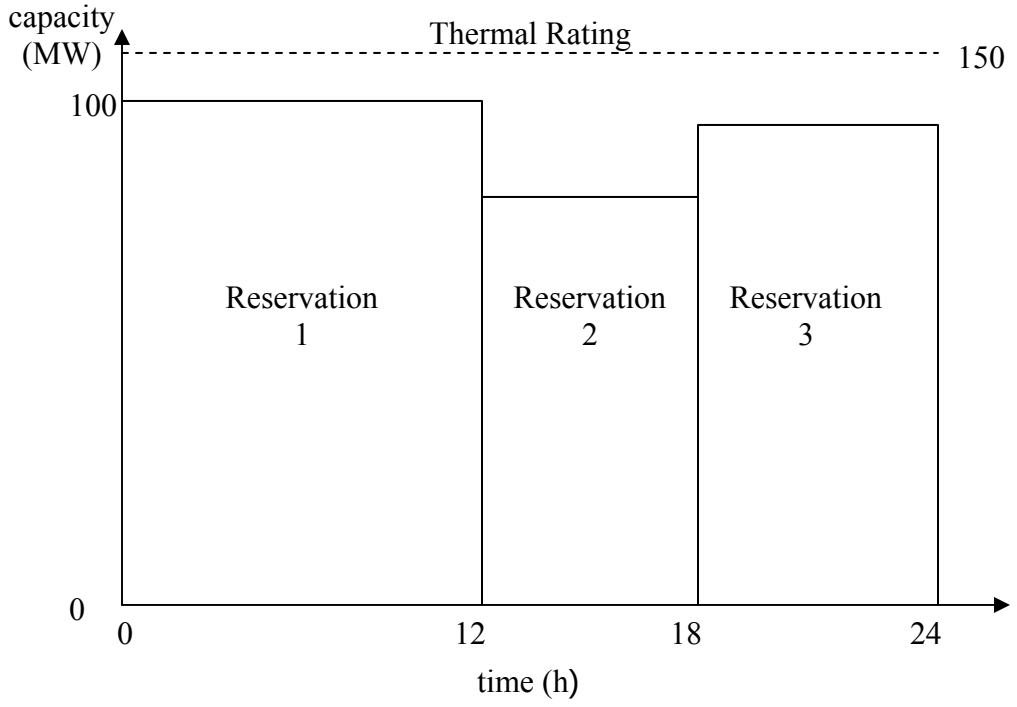

Figure D.1 Horizontal stacking of three E-Tags

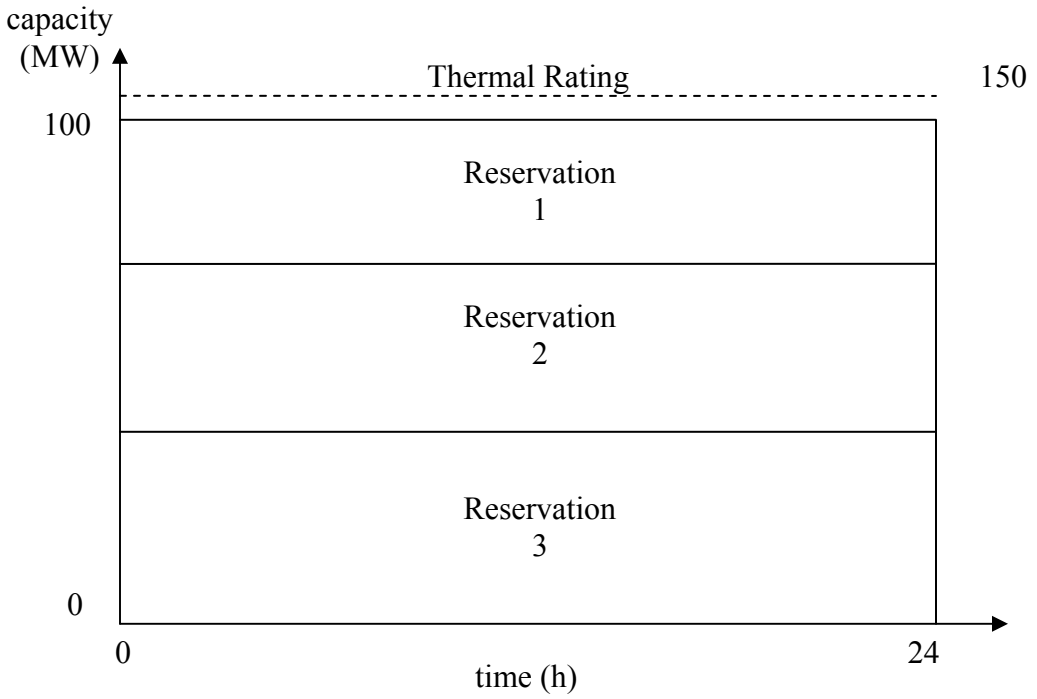

Figure D.2. Vertical stacking of three E-Tags

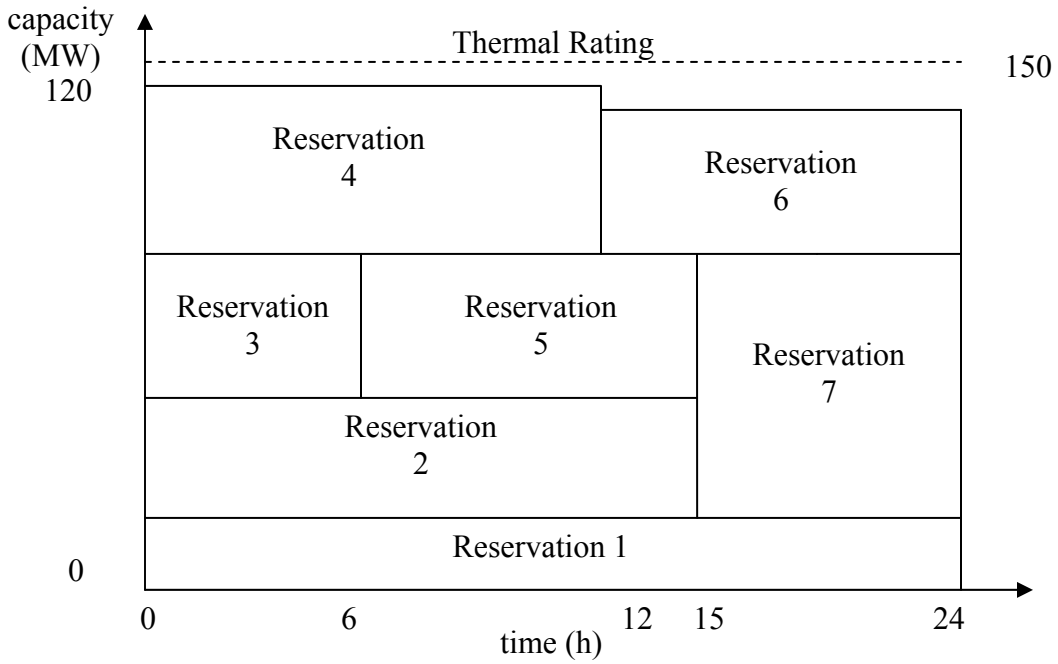

Figure D.3. Transmission stacking of several E-Tags

APPENDIX E:WECC System Data

Table E.1 The WECC test bed system data*

Line No.	Between buses		*R* (p.u.)	*X* (p.u.)	Line charging susceptance (p.u.)	Tap setting	Rating (MW)
1	4	159	0.00811	0.1369	2.4348	1	730.46
2	2	7	0.00179	0.01988	2.576	1	5030.2
3	7	16	0.0005	0.0053	0.0882	1	18868
4	16	4	0.00977	0.11	2	1	909.09
5	11	19	0	-0.00634	0	1	15773
6	19	20	0.00077	0.01804	1.3984	1	5543.2
7	20	13	0	-0.00634	0	1	15773
8	11	21	0	-0.01188	0	1	8417.5
9	21	22	0.00241	0.05865	4.8656	1	1705
10	22	18	0	-0.01188	0	1	8417.5
11	13	23	0	-0.00826	0	1	12107
12	23	24	0.00179	0.04244	3.3922	1	2356.3
13	24	18	0	-0.00826	0	1	12107
14	13	25	0	-0.01795	0	1	5571
15	25	26	0.00207	0.04959	3.9516	1	2016.5
16	26	138	0	-0.01795	0	1	5571
17	15	18	0.0004	0.0096	0.9038	1	10417
18	15	18	0.0004	0.0096	0.9038	1	10417
19	6	27	0	-0.00408	0	1	24510
20	27	28	0.00177	0.04189	3.3446	1	2387.2
21	28	13	0	-0.00612	0	1	16340
22	30	31	0.0035	0.07	4.606	1	1428.6
23	32	33	0.002	0.02	0.8	1	5000
24	51	62	0.0107	0.07905	0.3667	1	1265
25	52	62	0.0107	0.07905	0.3667	1	1265
26	54	40	0.00047	0.00723	0.01624	1	13831
27	54	57	0.00119	0.01244	0.02798	1	8038.6
28	54	57	0.00119	0.01244	0.02798	1	8038.6
29	56	41	0.00201	0.03074	0.06886	1	3253.1
30	56	53	0.00073	0.01025	0.02558	1	9756.1
31	56	53	0.00073	0.01025	0.02558	1	9756.1

*On a 100 MVA Base

Table E.1 continued The WECC test bed system data*

Line No.	Between buses		R (p.u.)	X (p.u.)	Line charging susceptance (p.u.)	Tap setting	Rating (MW)
32	56	57	0.0011	0.01189	0.02514	1	8410.4
33	61	54	0.00128	0.00979	0.0212	1	10215
34	63	48	0.00083	0.01884	1.6667	1	5307.9
35	40	57	0.00035	0.00536	0.01204	1	18657
36	36	37	0.00074	0.01861	1.4026	1	5373.5
37	36	55	0.00082	0.01668	1.188	1	5995.2
38	36	63	0	0.00159	0.12002	1	62893
39	36	63	0	0.00159	0.12002	1	62893
40	41	57	0.00281	0.04296	0.09648	1	2327.7
41	47	61	0.00138	0.01116	0.0247	1	8960.6
42	47	61	0.00138	0.01116	0.0247	1	8960.6
43	49	41	0.0022	0.03422	0.07716	1	2922.3
44	49	41	0.00238	0.03669	0.08284	1	2725.5
45	49	56	0.00037	0.00366	0.0083	1	27322
46	49	57	0.00055	0.00586	0.01246	1	17065
47	47	54	0.00229	0.01583	0.0306	1	6317.1
48	47	54	0.00229	0.01583	0.0306	1	6317.1
49	38	45	0.00221	0.03346	0.07338	1	2988.6
50	38	47	0.0029	0.038	0.0824	1	2631.6
51	38	58	0.00309	0.04677	0.1008	1	2138.1
52	38	59	0.00226	0.03422	0.07506	1	2922.3
53	47	45	0.00029	0.00434	0.0095	1	23041
54	47	58	0.00141	0.00967	0.0194	1	10341
55	47	58	0.00141	0.00967	0.0194	1	10341
56	47	58	0.00161	0.00971	0.01928	1	10299
57	47	58	0.00161	0.00971	0.01928	1	10299
58	47	59	0.00027	0.00393	0.00918	1	25445
59	47	59	0.00027	0.00393	0.00918	1	25445
60	47	59	0.00027	0.00393	0.00918	1	25445
61	74	77	0.00142	0.02258	1.88	1	4428.7
62	74	75	0.00196	0.03304	1.88	1	3026.6

*On a 100 MVA Base

Table E.1 continued The WECC test bed system data*

Line No.	Between buses		*R* (p.u.)	*X* (p.u.)	Line charging susceptance (p.u.)	Tap setting	Rating (MW)
63	74	72	0.00179	0.01405	3.68	1	7117.4
64	77	73	0.00113	0.02069	1.8553	1	4833.3
65	77	75	0.0012	0.02316	1.7152	1	4317.8
66	77	75	0.0003	0.02	3.6	1	5000
67	79	77	0.0002	0.0082	1.3	1	12195
68	79	77	0.0002	0.0082	1.3	1	12195
69	67	70	6.00E-05	0.00131	0.00378	1	76336
70	67	70	6.00E-05	0.00116	0.00332	1	86207
71	68	71	1.00E-05	0.0003	0.01434	1	3.33E+05
72	68	71	1.00E-05	0.0003	0.01844	1	3.33E+05
73	68	75	0.00023	0.00451	0.3332	1	22173
74	68	75	0.0002	0.00446	0.305	1	22422
75	81	75	0.00063	0.01412	1.0976	1	7082.2
76	81	75	0.00109	0.02408	1.5554	1	4152.8
77	81	75	0.00108	0.02409	1.5535	1	4151.1
78	81	86	0.00041	0.00737	0.72694	1	13569
79	86	87	0	-0.01263	0	1	7917.7
80	87	85	0.0006	0.01036	1.0146	1	9652.5
81	82	88	0.00072	0.01382	1.2757	1	7235.9
82	88	89	0	-0.00858	0	1	11655
83	89	85	0.00012	0.00238	0.21926	1	42017
84	81	90	0.00066	0.01266	0.95976	1	7898.9
85	90	91	0	-0.01263	0	1	7917.7
86	91	92	0.00074	0.01428	1.0822	1	7002.8
87	92	93	0	-0.01263	0	1	7917.7
88	93	82	0.00078	0.01502	1.1381	1	6657.8
89	81	94	0.00066	0.01266	0.95976	1	7898.9
90	94	95	0	-0.01263	0	1	7917.7
91	95	96	0.00074	0.01428	1.0822	1	7002.8
92	96	97	0	-0.01263	0	1	7917.7
93	97	82	0.00074	0.01413	1.0663	1	7077.1

*On a 100 MVA Base

Table E.1 continued The WECC test bed system data*

Line No.	Between buses		*R* (p.u.)	*X* (p.u.)	Line charging susceptance (p.u.)	Tap setting	Rating (MW)
94	80	98	0.00264	0.05356	5.2907	1	1867.1
95	98	83	0	-0.02667	0	1	3749.5
96	110	119	0	-0.01	0	1	10000
97	119	120	0.00076	0.01952	1.8245	1	5123
98	120	121	0	-0.01	0	1	10000
99	121	122	0.00082	0.02119	1.9842	1	4719.2
100	122	118	0	-0.01	0	1	10000
101	106	103	0.00083	0.01985	0	1	5037.8
102	106	107	0.00153	0.0147	0	1	6802.7
103	109	106	0.00053	0.01297	0	1	7710.1
104	113	123	2.00E-05	-0.00998	0	1	10020
105	123	124	0.0014	0.02338	1.475	1	4277.2
106	124	114	1.00E-05	-0.00666	0	1	15015
107	113	125	2.00E-05	-0.00998	0	1	10020
108	125	126	0.0014	0.02338	1.475	1	4277.2
109	126	114	1.00E-05	-0.00666	0	1	15015
110	114	127	1.00E-05	-0.0112	0	1	8928.6
111	127	128	0.00154	0.03409	2.3114	1	2933.4
112	128	118	1.00E-05	-0.0112	0	1	8928.6
113	114	129	1.00E-05	-0.0072	0	1	13889
114	129	130	0.00095	0.02102	1.4252	1	4757.4
115	130	118	1.00E-05	-0.0036	0	1	27778
116	100	112	0.01113	0.06678	0.07286	1	1497.5
117	100	112	0.0105	0.0654	0.0686	1	1529.1
118	100	112	0.01105	0.06642	0.0716	1	1505.6
119	100	116	0.03903	0.27403	0.31072	1	364.92
120	100	99	0.02482	0.16938	0.20232	1	590.39
121	99	116	0.0148	0.10101	0.12066	1	990
122	100	104	0.01382	0.09268	0.1106	1	1079
123	104	116	0.03058	0.2046	0.24472	1	488.76
124	100	105	0.01668	0.11381	0.13608	1	878.66

*On a 100 MVA Base

Table E.1 continued The WECC test bed system data*

Line No.	Between buses		*R* (p.u.)	*X* (p.u.)	Line charging susceptance (p.u.)	Tap setting	Rating (MW)
125	105	116	0.02235	0.16106	0.18342	1	620.89
126	118	131	1.00E-05	-0.00755	0	1	13245
127	131	132	0.00165	0.05719	2.4774	1	1748.6
128	132	107	2.00E-05	-0.01331	0	1	7513.1
129	118	133	1.00E-05	-0.01098	0	1	9107.5
130	133	103	0.00093	0.03644	1.3895	1	2744.2
131	103	134	0.00072	0.016	1.0879	1	6250
132	134	107	2.00E-05	-0.00998	0	1	10020
133	103	101	0.00079	0.01937	1.3285	1	5162.6
134	101	107	0.00087	0.02087	1.4571	1	4791.6
135	101	107	0.00087	0.02087	1.4571	1	4791.6
136	141	152	0.00044	0.01125	0.8292	1	8888.9
137	141	152	0.00044	0.01125	0.8292	1	8888.9
138	141	146	0.0019	0.031	4.1402	1	3225.8
139	138	141	0.00193	0.02779	4.6712	1	3598.4
140	146	138	0.00056	0.01415	1.0429	1	7067.1
141	135	151	0.00042	0.00905	0.66794	1	11050
142	141	150	0.0006	0.0128	0.9462	1	7812.5
143	144	150	0.00021	0.00457	0.32336	1	21882
144	150	151	0.0004	0.0093	0.6856	1	10753
145	141	144	0.00028	0.00753	0.51736	1	13280
146	141	144	0.00035	0.0075	0.5536	1	13333
147	149	153	0.00285	0.03649	0.12656	1	2740.5
148	149	153	0.00138	0.03399	0.11252	1	2942
149	136	142	0.0019	0.0258	0.0984	1	3876
150	136	149	0.00845	0.07034	0.15954	1	1421.7
151	140	142	0.0011	0.0127	0.048	1	7874
152	153	142	0.0032	0.0395	0.144	1	2531.6
153	145	142	0.00138	0.05399	0.15252	1	1852.2
154	155	166	0.0016	0.0226	0.381	1	4424.8
155	154	166	0.0008	0.0106	0.2039	1	9434

*On a 100 MVA Base

Table E.1 continued The WECC test bed system data*

Line No.	Between buses		*R* (p.u.)	*X* (p.u.)	Line charging susceptance (p.u.)	Tap setting	Rating (MW)
156	155	154	0.0024	0.0332	0.5849	1	3012
157	154	159	0.0017	0.0225	0.3992	1	4444.4
158	154	159	0.0021	0.0238	0.3845	1	4201.7
159	157	163	0.0096	0.0878	1.4265	1	1139
160	154	157	0.0052	0.0602	1.01	1	1661.1
161	154	157	0.0049	0.0537	0.8843	1	1862.2
162	154	164	0.0012	0.0172	0.2987	1	5814
163	157	165	0.0034	0.0374	0.6208	1	2673.8
164	157	165	0.0034	0.0372	0.6182	1	2688.2
165	159	165	0.0038	0.034	0.5824	1	2941.2
166	159	165	0.0032	0.0349	0.5722	1	2865.3
167	156	160	0.0108	0.0965	0.3296	1	1036.3
168	157	164	0.0034	0.0392	0.6524	1	2551
169	30	79	0.00083	0.0239	3.3	1	4184.1
170	77	65	0.0007	0.074	4.87	1	1351.4
171	82	167	0	-0.0072	0	1	13889
172	167	168	0.00103	0.02338	1.5804	1	4277.2
173	168	113	0	-0.0072	0	1	13889
174	82	169	0	-0.00864	0	1	11574
175	169	170	0.00107	0.0247	1.527	1	4048.6
176	170	113	0	-0.0072	0	1	13889
177	82	171	0	-0.01	0	1	10000
178	171	172	0.00103	0.0323	2.796	1	3096
179	172	110	0	-0.01	0	1	10000
180	107	173	0	-0.00935	0	1	10695
181	173	174	0.00123	0.02659	1.987	1	3760.8
182	174	152	0	-0.00935	0	1	10695
183	107	175	0	-0.00944	0	1	10593
184	175	176	0.00123	0.02662	1.9888	1	3756.6
185	176	152	0	-0.00935	0	1	10695
186	107	177	0	-0.00935	0	1	10695

*On a 100 MVA Base

Table E.1 continued The WECC test bed system data*

Line No.	Between buses		*R* (p.u.)	*X* (p.u.)	Line charging susceptance (p.u.)	Tap setting	Rating (MW)
187	177	178	0.00112	0.02517	1.8359	1	3973
188	178	152	0	-0.0084	0	1	11905
189	141	63	0.0002	0.0041	0.2962	1	24390
190	138	63	0.00179	0.02524	0.53546	1	3962
191	138	63	0.00179	0.02524	0.53546	1	3962
192	149	60	0.00065	0.01187	0.04672	1	8424.6
193	149	60	0.00065	0.01187	0.04672	1	8424.6
194	136	60	0.0014	0.0264	0.102	1	3787.9
195	11	138	0.0028	0.0211	1.0194	1	4739.3
196	15	135	0.00259	0.02967	2.153	1	3370.4
197	15	135	0.00259	0.02967	2.153	1	3370.4
198	80	179	0	-0.02667	0	1	3749.5
199	179	85	0.00122	0.02373	2.2071	1	4214.1
200	155	84	0.0062	0.0673	1.1156	1	1485.9
201	43	159	0.0018	0.0245	0.4392	1	4081.6
202	43	159	0.0018	0.0245	0.4392	1	4081.6
203	162	7	0.0048	0.0436	0.7078	1	2293.6
204	4	10	0	0.015	0	1	6666.7
205	1	2	0	0.0146	0	1	6849.3
206	15	14	5.50E-05	0.00495	0	0.90408	20202
207	1	3	0	0.017303	0	1.0477	5779.3
208	16	17	0	0.006	0	0.95831	16667
209	6	7	0	0.011	0	0.94073	9090.9
210	6	7	0	0.011	0	0.94073	9090.9
211	7	8	0	0.0059	0	1	16949
212	7	9	0.00028	0.0138	0	1	7246.4
213	7	9	0.00029	0.0139	0	1	7194.2
214	11	12	0	0.00666	0	0.92593	15015
215	31	32	0	0.01	0	0.90909	10000
216	30	29	0	0.0015	0	0.95238	66667
217	33	34	0	0.002	0	1	50000

*On a 100 MVA Base

Table E.1 continued The WECC test bed system data*

Line No.	Between buses		*R* (p.u.)	*X* (p.u.)	Line charging susceptance (p.u.)	Tap setting	Rating (MW)
218	63	62	0.000201	0.023381	0	1.0216	4277
219	43	44	0	0.0052	0	0.97561	19231
220	65	64	0	0.005	0	0.91743	20000
221	83	84	0	0.0072	0	0.95238	13889
222	79	78	0	0.0025	0	0.93809	40000
223	71	70	0	0.002205	0	0.97714	45351
224	67	66	0.000893	0.029903	0	1.0129	3344.1
225	68	67	0.000198	0.011808	0	0.97675	8468.8
226	68	67	8.80E-05	0.007354	0	0.97675	13598
227	75	76	0	0.003751	0	0.911	26660
228	67	69	0	0.010339	0	0.95648	9672.1
229	111	112	0	0.022812	0	1.09	4383.7
230	112	113	9.90E-05	0.017397	0	0.89366	5748.1
231	117	118	0	0.004477	0	1.058	22336
232	115	116	0	0.01815	0	1.1	5509.6
233	116	118	0.000198	0.012502	0	0.89366	7998.7
234	108	107	0.000298	0.017397	0	0.89366	5748.1
235	108	107	0.000198	0.011896	0	0.89366	8406.2
236	101	102	0	0.0098	0	0.95238	10204
237	152	153	0	0.01149	0	0.94065	8703.2
238	152	153	0	0.01149	0	0.94065	8703.2
239	152	153	0	0.01149	0	0.94065	8703.2
240	137	138	0	0.01512	0	1.004	6613.8
241	146	147	0	0.0098	0	0.95238	10204
242	139	140	0	0.003654	0	1.0218	27367
243	143	144	0	0.005161	0	1.016	19376
244	144	145	0	0.005	0	1	20000
245	51	50	0.00059	0.01491	0	0.9983	6706.9
246	52	50	0.00059	0.01491	0	0.9983	6706.9
247	53	50	0.0003	0.0133	0	1	7518.8
248	53	50	0.0003	0.0134	0	1	7462.7

*On a 100 MVA Base

Table E.1 continued The WECC test bed system data*

Line No.	Between buses		*R* (p.u.)	*X* (p.u.)	Line charging susceptance (p.u.)	Tap setting	Rating (MW)
249	55	54	0.00013	0.01386	0	0.98951	7215
250	55	54	0.00013	0.01386	0	0.98951	7215
251	37	47	0.00013	0.00693	0	0.95238	14430
252	41	42	0.00058	0.02535	0	0.9532	3944.8
253	48	47	0.00026	0.01386	0	0.95238	7215
254	47	46	0.00499	0.11473	0	0.95438	871.61
255	38	39	0.0005	0.0238	0	1	4201.7
256	59	60	0	0.001148	0	0.98687	87108
257	148	149	0	0.010263	0	1.0131	9743.7
258	4	5	0	0.01238	0	1	8077.5
259	157	158	0.0002	0.0058	0	1.0147	17241
260	163	162	0	0.0195	0	1	5128.2
261	155	156	0.0003	0.0181	0	1	5524.9
262	160	161	0.0005	0.0141	0	0.94447	7092.2
263	84	35	0	0.0046	0	1	21739

*On a 100 MVA Base

The values in Table E.2 are 30% reduced from the original file found in [52]. The 30% reduction was chosen so that a contingency analysis would not include certain lines in the analysis. All the negative loadings (which are representation of dc transmission lines in the system) in the system were not reduced.

Table E.2 The WECC test bed bus data

Bus	Active Power(MW)	Reactive Power (MW)	Generation (MW)	Generation (MVAR)
1	1225	-56	0	0
2	0	0	0	0
3	70	0	560	86.128
4	1645	-127	0	0
5	70	0	733.6	-93.037
6	0	0	0	0
7	167.3	-56	0	0
8	70	0	1512	-21.371
9	97.79	16.66	0	0
10	70	0	1435	325.374
11	63	49	0	0
12	70	0	1183	136.703
13	0	0	0	0
14	70	0	1848	265.132
15	555.38	144.9	0	0
16	588	3.5	0	0
17	70	0	673.4	104.125
18	431.9	-69	0	0
19	0	0	0	0
20	0	0	0	0
21	0	0	0	0
22	0	0	0	0
23	0	0	0	0
24	0	0	0	0
25	0	0	0	0
26	0	0	0	0
27	0	0	0	0
28	0	0	0	0
29	70	0	3115	707.63
30	3080	700	0	0
31	0	0	0	0
32	0	0	0	0
33	2520	490	0	0
34	70	0	3136	805.07

Table E.2 continued The WECC test bed bus data

Bus	Active Power(MW)	Reactive Power (MW)	Generation (MW)	Generation (MVAR)
35	70	0	1148	199.86
36	-1862	679.7	0	0
37	0	0	0	0
38	0	0	0	0
39	70	0	140	-36.519
40	94.5	18.9	0	0
41	0	0	0	0
42	70	0	227.5	47.775
43	1437.1	634.97	0	0
44	70	0	1246	374.21
45	-72.8	-17	0	0
46	70	0	77	20.356
47	84.7	17.5	0	0
48	0	0	0	0
49	224	45.5	0	0
50	166.04	-63.2	0	0
51	0	0	0	0
52	0	0	0	0
53	96.6	19.6	0	0
54	565.46	92.47	0	0
55	0	0	0	0
56	81.9	16.8	0	0
57	84.7	17.5	0	0
58	621.39	-6.2	0	0
59	-2771	1157.8	0	0
60	280.7	56.42	0	0
61	143.64	12.32	0	0
62	-129	22.54	0	0
63	0	0	0	0
64	70	0	2037	666.91
65	1190	210	0	0
66	112	21.875	0	0
67	-67.5	112	0	0
68	-44.2	15.4	0	0

Table E.2 continued The WECC test bed bus data

Bus	Active Power(MW)	Reactive Power (MW)	Generation (MW)	Generation (MVAR)
69	70	0	910.7	301.48
70	2195.9	1176.7	0	0
71	0	0	0	0
72	-1525	-50	0	0
73	0	0	0	0
74	1808.8	275.8	0	0
75	2240	770	0	0
76	70	0	3621.5	597.42
77	2450	350	0	0
78	70	0	6965	1296.8
79	3500	280	0	0
80	0	0	0	0
81	-66.6	-97	0	0
82	-339	-119	0	0
83	0	0	0	0
84	427	-414	0	0
85	0	0	0	0
86	0	0	0	0
87	0	0	0	0
88	0	0	0	0
89	0	0	0	0
90	0	0	0	0
91	0	0	0	0
92	0	0	0	0
93	0	0	0	0
94	0	0	0	0
95	0	0	0	0
96	0	0	0	0
97	0	0	0	0
98	0	0	0	0
99	-43.3	14	0	0
100	147.28	-77	0	0

Table E.2 continued The WECC test bed bus data

Bus	Active Power(MW)	Reactive Power (MW)	Generation (MW)	Generation (MVAR)
101	35	17.5	0	0
102	70	0	535.5	-144.49
103	213.5	-7.6	0	0
104	19.25	-0.1	0	0
105	5.607	0	0	0
106	185.5	9.8	0	0
107	38.92	-329	0	0
108	544.32	22.82	0	0
109	28	15.05	0	0
110	-189	43.05	0	0
111	70	0	739.9	17.815
112	103.6	0	0	0
113	0	0	0	0
114	-0.7	82.95	0	0
115	70	0	415.8	134.44
116	618.8	38.36	0	0
117	70	0	2426.9	1157.5
118	3962.7	2443.7	0	0
119	0	0	0	0
120	0	0	0	0
121	0	0	0	0
122	0	0	0	0
123	0	0	0	0
124	0	0	0	0
125	0	0	0	0
126	0	0	0	0
127	0	0	0	0
128	0	0	0	0
129	0	0	0	0
130	0	0	0	0
131	0	0	0	0
132	0	0	0	0

Table E.2 continued The WECC test bed bus data

Bus	Active Power(MW)	Reactive Power (MW)	Generation (MW)	Generation (MVAR)
133	0	0	0	0
134	0	0	0	0
135	599.2	13.72	0	0
136	122.5	12.6	0	0
137	70	0	687.89	-90.188
138	631.61	-11.4	0	0
139	70	0	2236.5	722.89
140	2233.7	441	0	0
141	142.94	-28.2	0	0
142	264.18	45.15	0	0
143	70	0	1183	415.48
144	2168.6	832.3	0	0
145	0	0	0	0
146	0	0	0	0
147	70	0	1176	312.59
148	70	0	1540	275.6
149	2182.6	54.6	0	0
150	861	50.96	0	0
151	284.2	28.7	0	0
152	0	0	0	0
153	746.2	-10.8	0	0
154	320.39	57.19	0	0
155	23.73	8.33	0	0
156	103.6	-7.9	0	0
157	81.27	26.88	0	0
158	70	0	1165.5	-21.952
159	-62	8.96	0	0
160	178.5	70	0	0
161	70	0	311.5	64.211
162	0	0	0	0
163	22.12	8.05	0	0
164	98.84	49.98	0	0

Table E.2 continued The WECC test bed bus data

Bus	Active Power(MW)	Reactive Power (MW)	Generation (MW)	Generation (MVAR)
165	265.3	-43	0	0
166	129.5	54.95	0	0
167	0	0	0	0
168	0	0	0	0
169	0	0	0	0
170	0	0	0	0
171	0	0	0	0
172	0	0	0	0
173	0	0	0	0
174	0	0	0	0
175	0	0	0	0
176	0	0	0	0
177	0	0	0	0
178	0	0	0	0
179	0	0	0	0

APPENDIX F: Stochastic ATC Calculation of the 14 BUS SYSTEM

F.1 The 14 bus test bed and examples

The 14 bus test bed [54] consists of 20 lines as shown in Figure F.1. The system data are shown in Table F.1. This system is a representation consisting of transformers, synchronous condensers and complex power loads. All bus loads are once again represented by normally distributed pseudorandom variables with means and variances given in Table F.2. The ATC calculation for this system is illustrated by comparing the stochastic-algebraic method to the Monte Carlo method. The examples offered are denominated as 14-S and 14-MC.

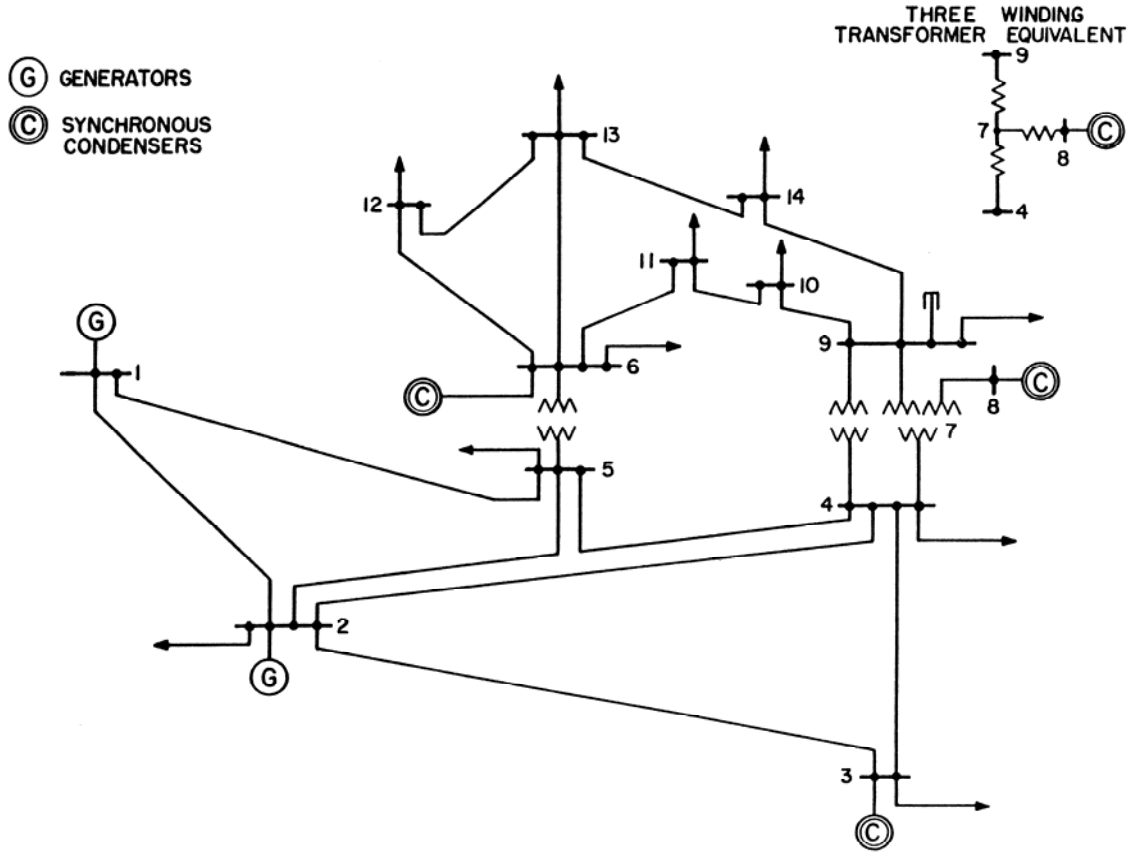

Figure F.1 The 14 bus test bed
(taken directly from [54])

Table F.1 The 14 bus test bed system data *

Line No.	Between buses		*R* (p.u.)	*X* (p.u.)	Line charging susceptance in per unit	Tap setting	Rating (MW)
1	1	2	0.01938	0.05917	0.0528	0	200
2	1	5	0.05403	0.22304	0.0492	0	110
3	2	3	0.04699	0.19797	0.0438	0	110
4	2	4	0.05811	0.17632	0.034	0	80
5	2	5	0.05695	0.17388	0.0346	0	70
6	3	4	0.06701	0.17103	0.0128	0	50
7	4	5	0.01335	0.04211	0	0	100
8	4	7	0	0.20912	0	0.978	50
9	4	9	0	0.55618	0	0.969	50
10	5	6	0	0.25202	0	0.932	70
11	6	11	0.09498	0.1989	0	0	30
12	6	12	0.12291	0.25581	0	0	30
13	6	13	0.06615	0.13027	0	0	50
14	7	8	0	0.17615	0	0	60
15	7	9	0	0.11001	0	0	60
16	9	10	0.03181	0.0845	0	0	50
17	9	14	0.12711	0.27038	0	0	50
18	10	11	0.08205	0.19207	0	0	50
19	12	13	0.22092	0.19988	0	0	50
20	13	14	0.17093	0.34802	0	0	50

* On a 100 MVA base

Table F.2 The14 bus test bed bus data

Bus	Active Power (MW)	Reactive Power (MVAR)	Generation (MW)
1	22	0	-
2	94	12.7	40
3	48	19	0
4	8	-3.9	0
5	12	1.6	0
6	30	7.5	0
7	0	0	0
8	0	0	0
9	9	16.6	0
10	0	5.8	0
11	3.5	1.8	0
12	6	1.6	0
13	14	5.8	0
14	15	5	0

F.2 Example 14-S

Using the IEEE-14 bus test bed, a stochastic-algebraic and Monte Carlo simulated ATC analysis of the system using MATLAB will illustrate the agreement of both methods. The value of the bus load standard deviation is 0.1 % of the actual bus load. Even though the Monte Carlo method is an "exact" process of finding the ATC given a sample operating condition, the computation time for the method is quite large while the stochastic determination of ATC reduces the computation time significantly. The Gram-Charlier type A series appears to be accurately represented using the first 40 statistical moments for each transfer resulting in a probability of 1.000 when the series is integrated from $-\infty$ to ∞. 5 exemplary transfers are listed Table F.3

Table F.3 Transfers used for Examples 14-S and 14-MC

Sending	Receiving
1	13
2	14
1	6
3	9
2	11

Data from Table F.4 show the difference between the Monte Carlo and stochastic statistical moments which are calculated from the Gram-Charlier series using

$$m_{(ATC)}^{(k)} = \int_{-\infty}^{\infty} (x - u_x)^k f(x) dx \tag{F.1}$$

where k is the moment order, u_x is the mean of the datum x and $f(x)$ is the probability density function represented by the Gram-Charlier type A series.

As shown in Table F.4, the differences between the Monte Carlo and stochastic moments have small error. These small errors should warrant agreement between the stochastic and Monte Carlo methods.

F.3 Additional Examples

The IEEE 14 Bus test bed is used as an illustration of several different special examples of the stochastic ATC from bus 1 to bus 6 considering all ATC limitations as well as transmission line outage contingences. The five different examples are:

- Normal Stochastic ATC calculation (example 14-N)
- Normal Stochastic ATC calculation without transmission line outage contingencies (example 14-NTLO)
- Stochastic ATC considering tight line rating limits (example 14-LR)
- Stochastic ATC considering tight voltage rating limits (example 14-VR)
- Special case of the Stochastic ATC were the distribution of the ATC is not normally distributed (example 14-SP). The transfer for this example is changed to 2-13.

Table F.4 The mean and standard deviation selected ATC transfers for examples 14-MC and 14-S

		Stochastic-Algebraic Method 14-S		Monte Carlo Method 14-MC	
Sending Bus	Receiving Bus	Mean *(MW)*	Standard Deviation *(MW)*	Mean *(MW)*	Standard Deviation *(MW)*
1	13	106.3226	.2926	106.3231	0.1367
2	14	54.894	0.483	51.6605	0.1527
1	6	213.3323	0.0252	213.3355	0.6638
3	9	102.69	0.65568	99.7869	0.2702
2	11	77.299	1.1446	74.3582	0.0934

The standard deviation of the bus load in these examples is 30% of the bus load value. Note this is much larger than the standard deviation of the bus loads in Example 14-S. Example 14-N illustrates the normal calculation of the stochastic ATC. Bus voltage and thermal line rating limits as well as the *N*-1 transmission line outage contingencies are modeled. The limitations for upper and lower bus voltage magnitude

limits are 13% and 5% of the base case voltages. These limitations are chosen based on the Class B service. Each line of the system at the base case is assumed to be 10% loaded. Therefore line ratings are calculated based on the 10% loading. The loaded line 10% is chosen such that when each *N*-1 contingency is preformed, all load flows are within line ratings. Example 14-NTLO illustrates the stochastic ATC with no line outage contingencies. Example 14-LR illustrates the stochastic ATC with only the line rating limits and transmission line outage contingences. The line ratings are the same as Example 14-N and all *N*-1 contingencies are considered. Example 14-VR illustrates the stochastic ATC with only the bus voltage magnitude limits and transmission line outage contingences. The bus voltage magnitude limits are the same as Example 14-N and all *N*-1 contingencies are considered. All IEE 14 bus examples result in Gaussian distributions at the solution of the stochastic ATC calculation. Example 14-SP illustrates the stochastic ATC in which the resulting probability distribution does not graphically appear to be Gaussian. The transfer for this example has changed to 2-13.

F.4 Results for example 14-N

Figures F.2-F.3 illustrate the probability density and cumulative density functions for Example 14-N. The resulting statistical measures from Example 14-N are shown in Table F.5.

Table F.5 The mean, variance, skew and kurtosis of the ATC transfer from 1 to 6 for example 14-N

Mean (*MW*)	209.8855
Variance (MW^2)	111.1645
Skew	-13.0317
Kurtosis	204.8191

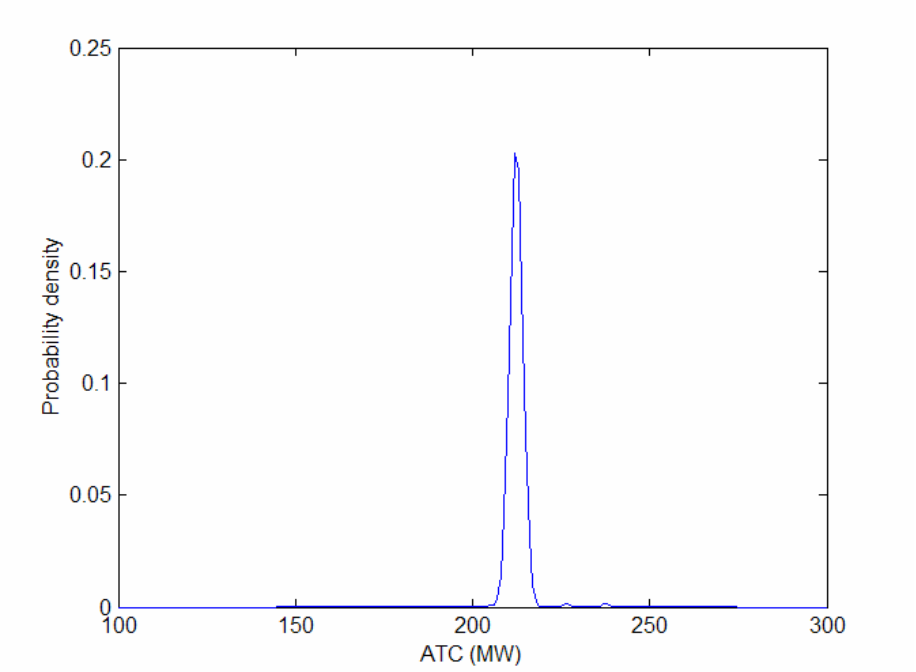

Figure F.2 PDF of the ATC transfer from 1 to 6 for example 14-N

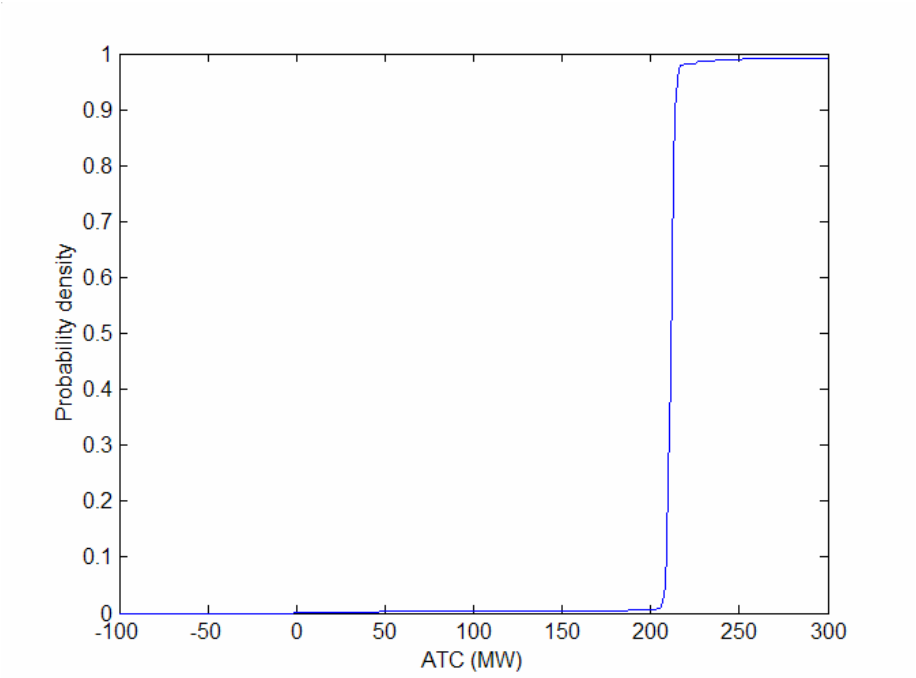

Figure F.3 CDF of the ATC transfer from 1 to 6 for example 14-N

F.5 Results for example 14-NTLO

Figures F.4-F.5 illustrate the probability density and cumulative density functions for Example 14-NTLO. The resulting statistical measures from Example 14-NTLO are shown in Table F.6.

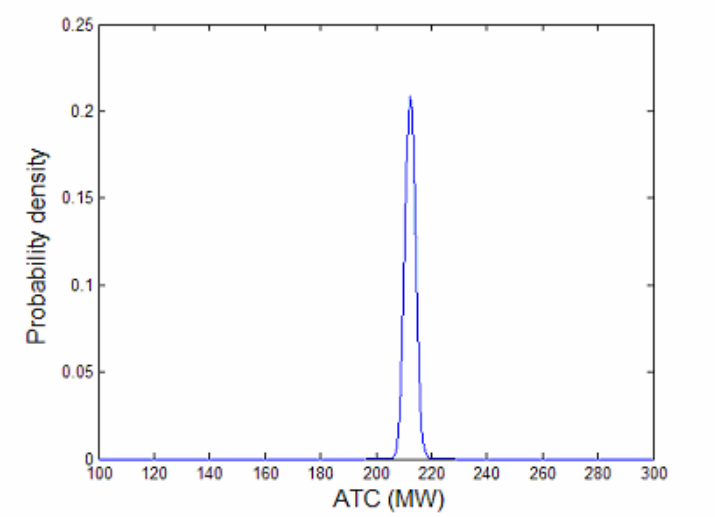

Figure F.4 PDF of the ATC transfer from 1 to 6 for example 14-NTLO

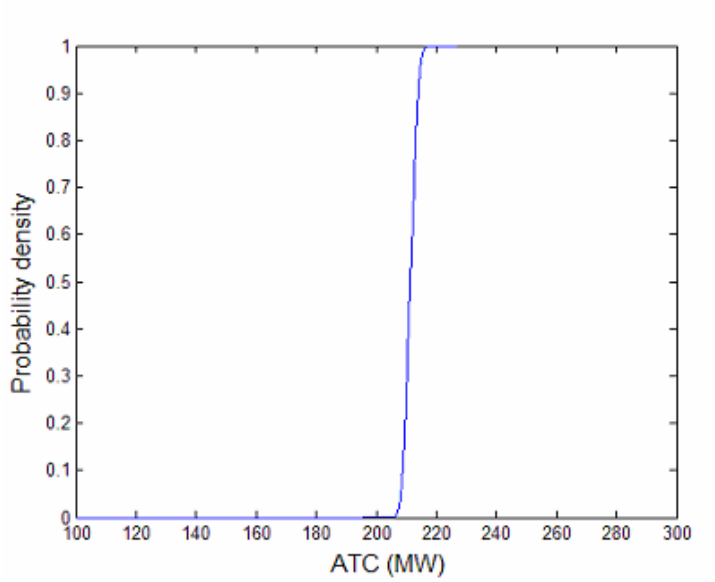

Figure F.5 CDF of the ATC transfer from 1 to 6 for example 14-NTLO

Table F.6 The mean, variance, skew and kurtosis of the ATC transfer from 1 to 6 for example 14-NTLO

Mean (*MW*)	212.3635
Variance (MW^2)	3.5188
Skew	0
Kurtosis	3

F.6 Results for example 14-LR

Figures F.6-F.7 illustrate the probability density and cumulative density functions for Example 14-LR. The resulting statistical measures from Example 14-LR are shown in Table F.7.

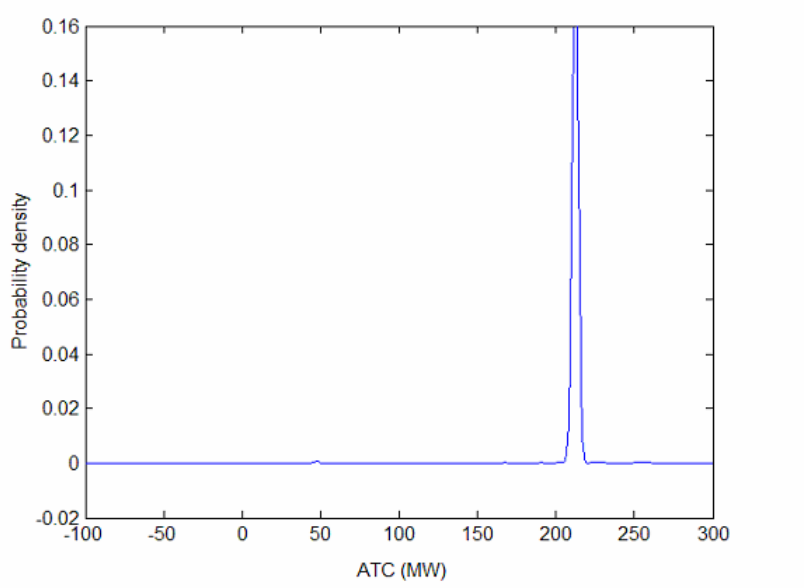

Figure F.6 PDF of the ATC transfer from 1 to 6 for example 14-LR

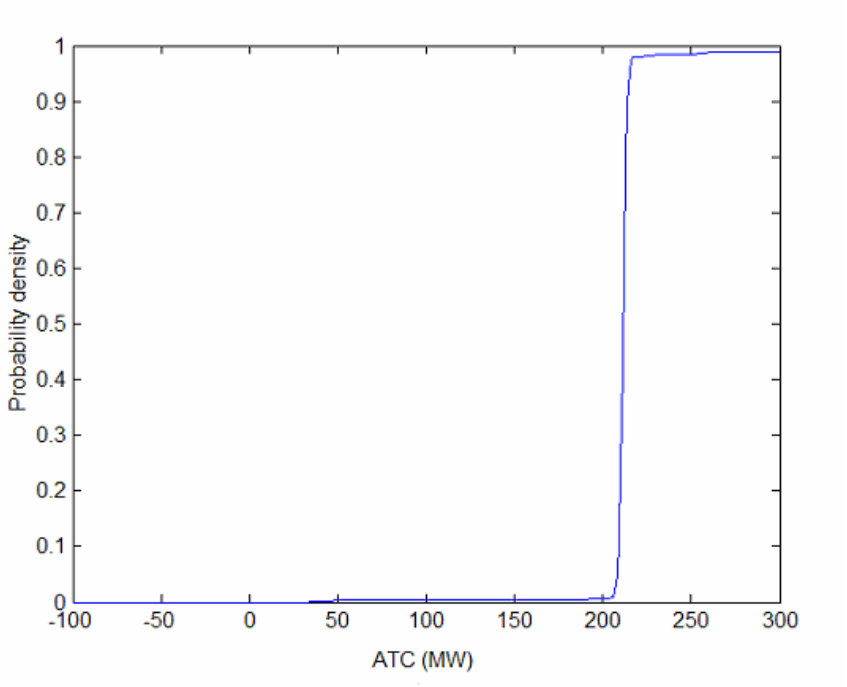

Figure F.7 PDF of the ATC transfer from 1 to 6 for example 14-LR

Table F.7 The mean, variance, skew and kurtosis of the ATC transfer from 1 to 6 for example 14-LR

Mean (*MW*)	209.4899
Variance (MW^2)	99.3333
Skew	-11.9458
Kurtosis	203.4154

F.7 Results for example 14-VR

Figures F.8-F.9 illustrate the probability density and cumulative density functions for Example 14-VR. The resulting statistical measures from Example 14-VR are shown in Table F.8.

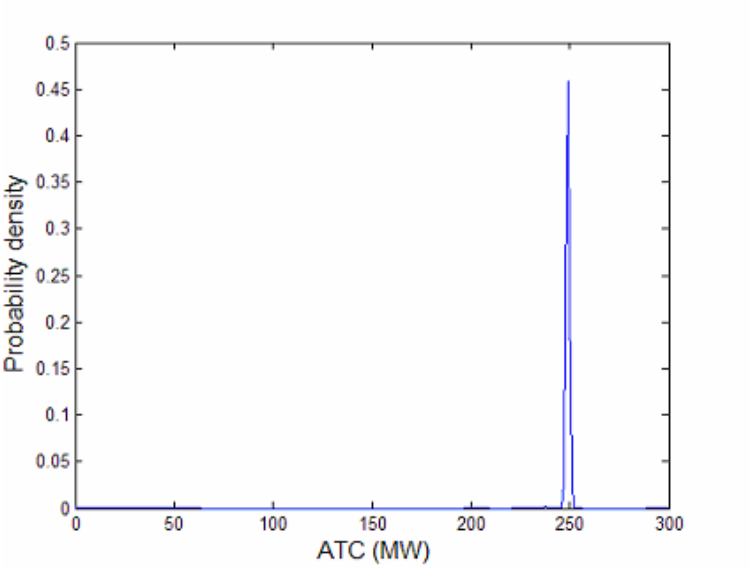

Figure F.8 PDF of the ATC transfer from 1 to 6 for example 14-VR

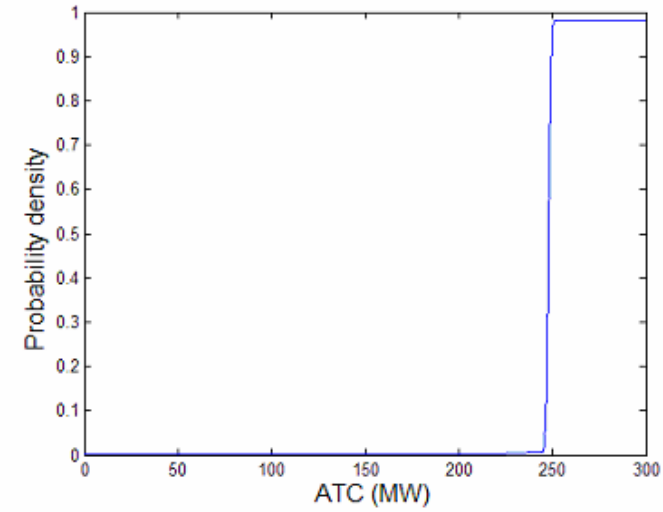

Figure F.9 PDF of the ATC transfer from 1 to 6 for example 14-VR

Table F.8 The mean, variance, skew and kurtosis of the ATC transfer from 1 to 6 for example 14-VR

Mean (*MW*)	243.8290
Variance (MW^2)	56.0070
Skew	-12.5428
Kurtosis	345.1316

F.8 Results for example 14-SP

Figures F.10-F.11 illustrate the probability density and cumulative density functions for Example 14-SP. The resulting statistical measures from Example 14-SP are shown in Table F.9.

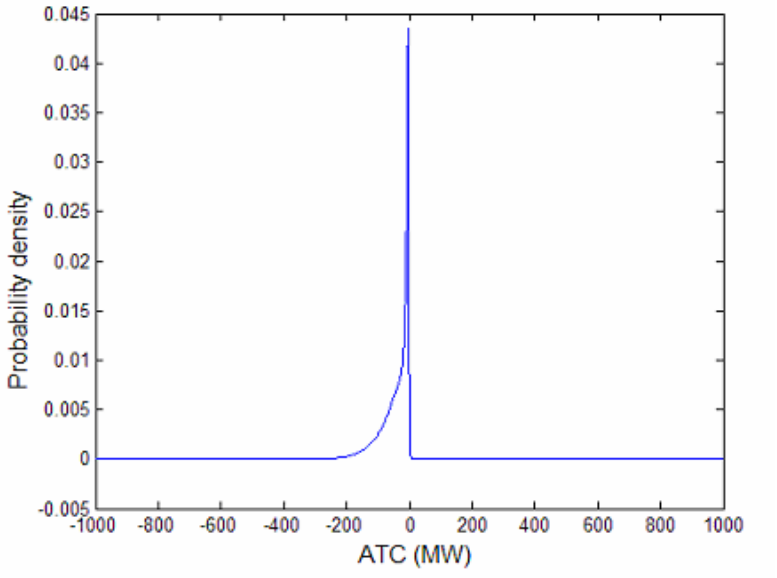

Figure F.10 PDF of the ATC transfer from 2 to 13 for example 14-SP

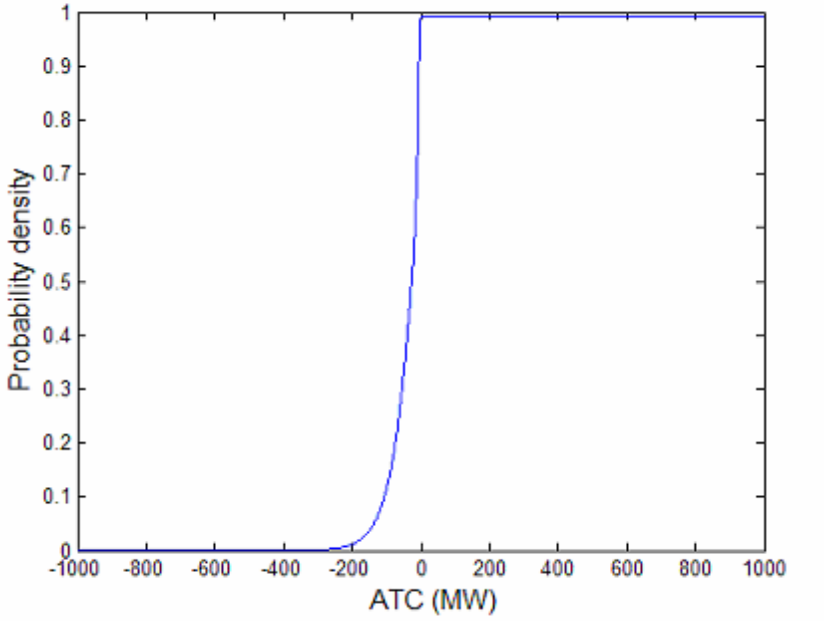

Figure F.11 CDF of the ATC transfer from 2 to 13 for example 14-SP

Table F.9 The mean, variance, skew and kurtosis of the ATC transfer from 2 to 13 for example 14-SP

Mean (*MW*)	-42.8421
Variance (MW^2)	2.6315e+003
Skew	-4.4155
Kurtosis	52.3342

APPENDIX G: Limitations Used in the WECC Examples

This appendix shows the values of the thermal line ratings, voltage magnitude limits, and the values of the forced outage rates used in the numerical examples in Chapters 3 and 5.

The voltage magnitude limits are 0.87 p.u. for the lower limit and 1.10 p.u. for the upper limit. Table D.1 shows the values of the thermal line ratings for each line of the system. The values of the forced outage rates for the system elements used in Example WECC-STLU are

- 0.0006518 for each of the transmission lines
- 0.00292304 for each of the transformers.

These values of forced outage rates are taken from a study of the frequency of transmission line and transformer outages in Canada from 1988-1992 [61].

APPENDIX H: List of the Examples

This appendix shows a list and explanation for all examples in this report. Tables H.1 and H.2 show the list of examples and their conditions. In Table H.1, for each example, an "x" in the corresponding box shows which analysis and test beds are used. In Table H.2, for each example, an "x' in the corresponding box are the ATC transfers shown using the WECC test bed. In Table H.3, for each example, an "x' in the corresponding box are the ATC transfers shown using the 14 bus test bed. For each example, the corresponding mean and variance are shown. In examples WECC-MC, WECC-S, 14-S, and 14-D, probability density function plots are shown.

Example WECC-D illustrates the deterministic ATC analysis on the WECC test bed. The conditions for Example WECC-D are

- all system elements in service
- all bus loads are modeled by their mean value only
- the ATC transfers illustrated in Table H.2.

Example WECC-MC illustrates the Monte Carlo analysis method of finding the stochastic ATC. The conditions for Example WECC-MC are

- all system elements in service
- bus loads are modeled using method of Section 3.4
- the ATC transfers illustrated in Table H.2.

Example WECC-S illustrates the stochastic analysis method of finding the stochastic ATC. The conditions for Example WECC-S are

- all system elements in service
- bus loads are modeled using method of Section 3.4

Table H.1 The analysis, test bed, and line outage case possibility for all examples

Example	Deterministic analysis	Stochastic analysis	Monte Carlo analysis	WECC Test Bed	14 Bus Test Bed	Transmission outage rates modeled
WECC-D	x			x		
WECC-MC			x	x		
WECC-S		x		x		
WECC-MCL100			x	x		
WECC-SL100		x		x		
WECC-MCL500			x	x		
WECC-SL500		x		x		
WECC-MCL1000			x	x		
WECC-SL1000		x		x		
WECC-MCL1500			x	x		
WECC-SL1500		x		x		
WECC-STLU		x		x		x
14-S		x			x	
14-MC			x		x	
14-N		x			x	
14-NTLO		x			x	
14-LR		x			x	
14-VR		x			x	
14-SP		x			x	

Table H.2 Transfers that are shown for examples using the WECC test bed

Example	78-103	3-155	3-8	44-160	34-64	8-112	5-141	39-57	64-9	12-60
WECC-D	x	x	x	x	x	x	x	x	x	x
WECC-MC	x	x	x	x	x					
WECC-S	x	x	x	x	x					
WECC-MCL100	x	x	x	x	x					
WECC-SL100	x	x	x	x	x					
WECC-MCL500	x	x	x	x	x					
WECC-SL500	x	x	x	x	x					
WECC-MCL1000	x	x	x	x	x					
WECC-SL1000	x	x	x	x	x					
ECC-MCL1500	x	x	x	x	x					
WECC-SL1500	x	x	x	x	x					

Table H.2 continued Transfers that are shown for examples using the WECC test bed

Example	35-102	40-10	70-10	36-137	4-137	162-69	15-55
WECC-STLU	x	x	x	x	x	x	x

Table H.3 Transfers that are shown for examples using the 14 bus test bed

Example	1-13	2-14	1-6	3-9	2-11	2-13
14-S	x	x	x	x	x	
14-MC	x	x	x	x	x	
14_N			x			
14-NTLO			x			
14-LR			x			
14-VR			x			
14-SP						x

the ATC transfers illustrated in Table H.2.

Example WECC-MC is used in comparison with Example WECC-S to validate the stochastic analysis method to find the stochastic ATC.

Example WECC-MC100 illustrates the Monte Carlo analysis method of finding the stochastic ATC. The conditions for Example WECC-MC100 are

- all system elements in service
- bus loads over 100 MW are modeled using method of Section 3.4
- bus loads under 100 MW are modeled by their mean only
- the ATC transfers illustrated in Table H.2.

Example WECC-S100 illustrates the stochastic analysis method of finding the stochastic ATC. The conditions for Example WECC-S100 are

- all system elements in service
- bus loads over 100 MW are modeled using method of Section 3.4
- bus loads under 100 MW are modeled by their mean only
- the ATC transfers illustrated in Table H.2.

Example WECC-MC500 illustrates the Monte Carlo analysis method of finding the stochastic ATC. The conditions for Example WECC-MC500 are

- all system elements in service
- bus loads over 500 MW are modeled using method of Section 3.4

- bus loads under 500 MW are modeled by their mean only
- the ATC transfers illustrated in Table H.2.

Example WECC-S500 illustrates the stochastic analysis method of finding the stochastic ATC. The conditions for Example WECC-S500 are

- all system elements in service
- bus loads over 500 MW are modeled using method of Section 3.4
- bus loads under 500 MW are modeled by their mean only
- the ATC transfers illustrated in Table H.2.

Example WECC-MC1000 illustrates the Monte Carlo analysis method of finding the stochastic ATC. The conditions for Example WECC-MC1000 are

- all system elements in service
- bus loads over 1000 MW are modeled using method of Section 3.4
- bus loads under 1000 MW are modeled by their mean only
- the ATC transfers illustrated in Table H.2.

Example WECC-S1000 illustrates the stochastic analysis method of finding the stochastic ATC. The conditions for Example WECC-S1000 are

- all system elements in service
- bus loads over 1000 MW are modeled using method of Section 3.4
- bus loads under 1000 MW are modeled by their mean only
- the ATC transfers illustrated in Table H.2.

Example WECC-MC1500 illustrates the Monte Carlo analysis method of finding the stochastic ATC. The conditions for Example WECC-MC1500 are

- all system elements in service
- bus loads over 1500 MW are modeled using method of Section 3.4
- bus loads under 1500 MW are modeled by their mean only
- the ATC transfers illustrated in Table H.2.

Example WECC-S1500 illustrates the stochastic analysis method of finding the stochastic ATC. The conditions for Example WECC-S1500 are

- all system elements in service
- bus loads over 1500 MW are modeled using method of Section 3.4
- bus loads under 1500 MW are modeled by their mean only
- the ATC transfers illustrated in Table H.2.

Example WECC-STLU illustrates the stochastic analysis method of finding the stochastic ATC with transmission element uncertainty considered. The conditions for Example WECC-STLU are

- Twenty worst ranked contingencies modeled
- all system elements in service
- bus loads are modeled using method of Section 3.4
- the ATC transfers illustrated in Table H.2.

Example 14-MC illustrates the Monte Carlo analysis method of finding the stochastic ATC. The conditions for Example 14-MC are

- all system elements in service
- bus loads are modeled using method of Section 3.4
- the ATC transfers illustrated in Table H.3.

Example 14-S illustrates the stochastic analysis method of finding the stochastic ATC. The conditions for Example 14-S are

- all system elements in service
- bus loads are modeled using method of Section 3.4
- the ATC transfers illustrated in Table H.3.

Example 14-MC is used in comparison with Example 14-S to validate the stochastic analysis method to find the stochastic ATC.

Example 14-N illustrates the stochastic analysis method of finding the stochastic ATC. The conditions for Example 14-N are

- N-1 contingencies considered
- bus loads are modeled using method of Section 3.4 with larger variance
- the ATC transfers illustrated in Table H.3.

Example 14-NTLO illustrates the stochastic analysis method of finding the stochastic ATC. The conditions for Example 14-NTLO are

- all system elements in service
- bus loads are modeled using method of Section 3.4 with larger variance
- the ATC transfers illustrated in Table H.3.

Example 14-LR illustrates the stochastic analysis method of finding the stochastic ATC without considering bus voltage magnitude limits. The conditions for Example 14-LR are

- N-1 contingencies considered

- bus loads are modeled using method of Section 3.4 with larger variance
- the ATC transfers illustrated in Table H.3
- bus voltage magnitude limits are not considered.

Example 14-VR illustrates the stochastic analysis method of finding the stochastic ATC without considering line ratings limits. The conditions for Example 14-VR are

- N-1 contingencies considered
- bus loads are modeled using method of Section 3.4 with larger variance
- the ATC transfers illustrated in Table H.3
- line rating limits are not considered.

Example 14-SP illustrates the stochastic analysis method of finding the stochastic ATC. The purpose of this example is to show a result that does not have a Gaussian distribution for the ATC. The conditions for Example 14-SP are

- N-1 contingencies considered
- bus loads are modeled using method of Section 3.4 with larger variance
- the ATC transfers illustrated in Table H.3.

Example WECC-TE illustrates how values of power traded near ATC levels can be integrated into the cost to benefit analysis of transmission expansion of a power system. The conditions for Example WECC-TE are

- bus loads are modeled using method of Section 3.4.
- the ATC transfers illustrated are (4-10), (112-137), (35-107), and (43-39).

Part II

Transmission Line Revenues with Uncertainty

Authors

Becky A. Westendorf
Merry P. Mani
Peter W. Sauer

Table of Contents

List of Tables

List of Figures

1. Introduction

1.1 Background

With the restructuring of the electric power system, the role of transmission companies is to provide reliable electric service to customers [1]. The "unbundling" of vertically integrated utilities has introduced a competitive market where customers may select their supplier based on competitive pricing and reliability. As a result, the transmission companies are required to allow "open access" of the transmission lines by allowing third parties to complete transactions to customers within the limits of the system using the transmission lines owned by a transmission company. In 1994, the Federal Energy Regulatory Commission (FERC) first announced a new standard which defined the provisions that needed to be made for "open access" transmission services. This standard called for an open-access transmission tariff to be established on the transmission lines such that it is not anticompetitive or discriminatory to third parties. In other words, under the same or comparable conditions, a transmission company may not assign different tariffs to distinct third parties for access of the transmission lines to gain a competitive edge [2]. The regulated tariff system allows transmission companies to collect an "Authorized Income" which helps the companies recover the fixed and variable costs of the transmission lines and to also make a reasonable profit [3]. Different forms of tariffs are in use today. One particular type is the postage-stamp tariff. This particular type of tariff assigns a value per megawatt flow for the system and is directly proportional to the amount of power flow through a transmission line for a transaction. As a result, the revenue generated from transmission tariffs for the system's ability to serve load can be used to determine the economic value of a transmission system.

However, the ability of a transmission system to serve loads is an important factor that weighs heavily on the reliability of the system. The economic value of the transmission system generated from tariffs is affected by the ability to serve load, which depends on certain characteristics of the system, such as thermal, voltage, and stability limits. These characteristics, in turn, limit the ability of the transmission system to transfer power among elements in the system and to deliver power from the generation source to the customers or customer demand centers. As a result, the criteria used for the planning and expansion of the system must ensure that the system is able to deliver and transfer power to meet the total customer demand in the event of disturbances or contingencies by operating reliably within the limits of the system [1].

The concept of system reliability can be separated into two aspects, system adequacy and system security. System adequacy is defined in [1], [4] using the NERC definition as "the ability of the electric system to supply aggregate electrical demand and energy requirements of customers at all times taking into account scheduled and reasonably expected unscheduled outages of system elements." System security is also defined in [1], [4] as "the ability of the electric system to withstand sudden disturbances such as electric short circuits or unanticipated loss of system facilities." System security can be divided into two more areas referring to the ability of the system to withstand internal failures and sudden natural disturbances such as network overloads and instability problems, and the ability of the system to avoid external interference or attacks [4]. To ensure that the system performs adequately and securely, resource and transmission adequacy criteria are currently in use today. Resource adequacy criteria are usually determined by multiple factors specific to a particular region. Therefore, NERC currently depends on the regions or regional members of NERC to determine their resource adequacy

criteria [1]. Presently, regions have begun to shift to a probabilistic planning criteria approach while some still maintain a deterministic planning approach.

1.2 Probabilistic Planning

Probabilistic planning has been incorporated into most regional planning criteria. Probabilistic planning criteria use performance characteristics of the electric system components and other factors to predict the likelihood that the customer peak demand and energy requirements are served over a period of time. These criteria can also incorporate the possibility of uncertainties such as forced outages of generating units, variations in weather, and variations in customer demand [1].

Two reliability indices that are used in probabilistic planning criteria are the Loss of Load Expectation (LOLE) and the Expect Unserved Energy (EUE). The LOLE is defined in [1] as the "number of expected days per year that available generation capacity is insufficient to serve daily peak demand" (load). The LOLE can be measured in days or hours per year. Usually, if the LOLE is measured in days per year, the index compares the peak daily load with the available generation. However, if the LOLE is measured in hours per year, the index compares the hourly load with available generation. The LOLE is also expressed as the loss of load probability (LOLP). The LOLP is the probability or proportion of the number of days per year, hours per year, or events per season, that the available generation capacity does not serve the daily or hourly peak load demand. A typical standard using this reliability index is the "1 day in 10 year" standard. This standard sets a value for the LOLP of 0.1 days/year stating that the generation capacity must be adequate to maintain an LOLP of 0.1 days/year. The EUE measures the expected amount of energy that is not supplied per year due to generation capacity deficiencies or shortages in basic energy supplies. This reliability index is predominantly used by systems with large amounts of hydro generation and may also be measured deterministically [1].

By incorporating probabilistic planning, system operators can analyze factors affecting system performance and assess risk using the probabilistic reliability indices. The ability to consider the probability of large contingencies actually occurring allows for more efficient system operation. In contrast, the deterministic criteria consider the loss of a single element regardless of the probability of that loss actually occurring. Probabilistic tools also may incorporate the planning and operating uncertainties by illustrating the effects uncertainties in the system have on the reliability indices [4]. Such methods may take into account the possible forced outages of generating units, weather, or changes in customer demand [1]. However, computation time may increase since calculations of the reliability indices and probabilities rely on computer simulations and involved calculations due to the complexity of the system to model [1], [4].

Uncertainties in the system are important in considering the system reliability. The uncertainty in the demand or load stems from the fact that the load is a constantly varying parameter that is largely uncertain [5]. The load forecast is based on historical data [4]. Therefore, this data can illustrate that the demand is affected by demographic and economic factors such as economic growth, environmental factors such as temperature and precipitation, electronically controlled loads, and variations in load power factors [4] – [6]. Uncertainties in the load forecast can exist as short-term and long-term uncertainties. Long-term uncertainties in the load forecast theoretically could increase due to the restructuring of the electric system and the introduction of competition and customer choice. Customers may be more willing to shop around for the best value as opposed to remaining in a long-term contract [4]. Short-term uncertainties in

load exist mainly due to time and weather factors. The load may vary due to the seasonal, daily, weekly, or even holiday cycles [5].

Load uncertainty can be modeled by a number of different methods. Many methods use a stochastic process to incorporate load uncertainty. As defined in [4], a stochastic process refers to a "set of random variables ordered in a given sequence often with time as an indexing parameter." In [7], the load was modeled at each bus as a normal distribution of the peak forecasted load. Then, random samples from the normal distribution were obtained to determine the load at each bus. The variations and uncertainties in the load were also represented using a normal distribution in the symmetrical case in [5]. This model divided the load variation into a weekday or weekend, according to the particular season, and then divided the load for the day in to two separate categories, dividing the high load during the day and the low load for the load during the evening hours. The Task Force on Bulk Power System Reliability of the IEEE-PES Application of Probability Methods Subcommittee notes that most load models include a "correlated" load model in which the loads at all load buses increase and decrease simultaneously and in the same proportion. The committee states that this assumption yields pessimistic results, whereas models incorporating loads that are randomly varied independently of each other yield optimistic results [8].

Li Wenyuan and R. Billinton observe in [9] the effect of bus load uncertainty on the reliability indices used to evaluate the composite system adequacy. In this investigation, the total system load uncertainty is modeled using a tabulating technique of a normal distribution. The bus loads are then determined using a covariance matrix in which the loads at the buses are neither dependent nor independent. Therefore, the bus loads are correlated by using the covariance matrix. The tabulating technique of the normal distribution was compared to a discrete enumeration model of a normal distribution. According to the results, Wenyuan and Billinton conclude that the enumeration model of normal distribution requires a large number of discrete intervals to provide accurate results for large load standard deviations. Also, load uncertainty increased the system inadequacy or reliability indices. Increases in the standard deviation of the load at the buses increased the reliability indices.

Further consideration of load uncertainty examined the effects of load uncertainty on the probabilistic planning reliability indices in determining production costs. As previously mentioned, in [7] the uncertainty in the load was modeled using random samples from a normal distribution. A computer procedure to develop the production costing used Monte Carlo simulations in considering the load uncertainty and the system component availability. Research and surveys were performed to estimate the cost to the customer of electrical service interruptions. The reliability indices were calculated with the consideration of load uncertainty .

Michael Emmerton and Don Somatilake both review the probabilistic transmission planning methods that are currently available and are in practice. These planning methods consist of the Markov State method, the Frequency-Duration method, and the Monte Carlo method. Software packages are available that include models of sources of uncertainty, such as those that exist in the load, may include tradeoffs in representation of details in the generation and transmission systems [6].

The deviation in the amount of revenue from the tariffs due to the load uncertainty is a measure of the risk due to load uncertainty. The investigation can be divided into three steps. First, the income from transmission tariffs based on $/MW-mile for an entire year using hourly conditions was computed using historical hourly load data for one year scaled to match the load schedule of the IEEE 14-bus system. This process produced the hourly incomes using an

assumed tariff of $0.04 per MW-mile for each transmission line. An annual income was also computed by summing the hourly incomes for the year. In the second step, the hourly incomes calculated in step 1 were computed by randomly sampling from a known distribution. The random sample at each hour was considered to be an error in the forecast for that hour. For each hour, the hourly incomes were calculated by sampling from the known distribution 100 times to provide 100 revenue values for that same hour. These revenue values for each hour provided the statistical distribution (based on 100 samples) of the transmission line income for each hour of the day throughout the year. In the final step, analytical methods incorporating linear power flows and sensitivity factors were used to estimate the distribution of the hourly and total income.

Planning also involves studying system performance with various options in transmission line construction and utilization. This study examined the sensitivity of the expected transmission line revenue to the actual transmission line configuration. That is, a base case was studied with a certain transmission line topology, resulting in a base case expected revenue. This expected revenue was then repeated for the various contingency cases where lines were removed one at a time. Collectively the results indicate how the expected revenue might vary with transmission topology.

1.3 Report Organization

This report is essentially divided into five parts. Chapter 2 describes the test system that was used for the analysis. Chapter 3 presents the results of uncertainty in loading using a Monte Carlo techniques. Chapter 4 presents the results of uncertainty in loading using an analytical technique. Chapter 5 compares these two techniques. Chapter 6 provides the results of analysis using various system line topologies. Chapter 7 provides conclusions and recommendations.

2. The Test System

Upon agreement with all of the other investigators on this project, the IEEE 14-bus test system was chosen for the test system. This test system contains 14 buses, 20 transmission lines, 2 generators, 3 synchronous condensers, and 3 transformers. Buses 1-5 have a nominal voltage of 69 kV, while buses 6-14 have a nominal voltage of 138 kV. Figure 2.1 displays the one-line diagram of the system using the PowerWorld Simulator 10.0 software.

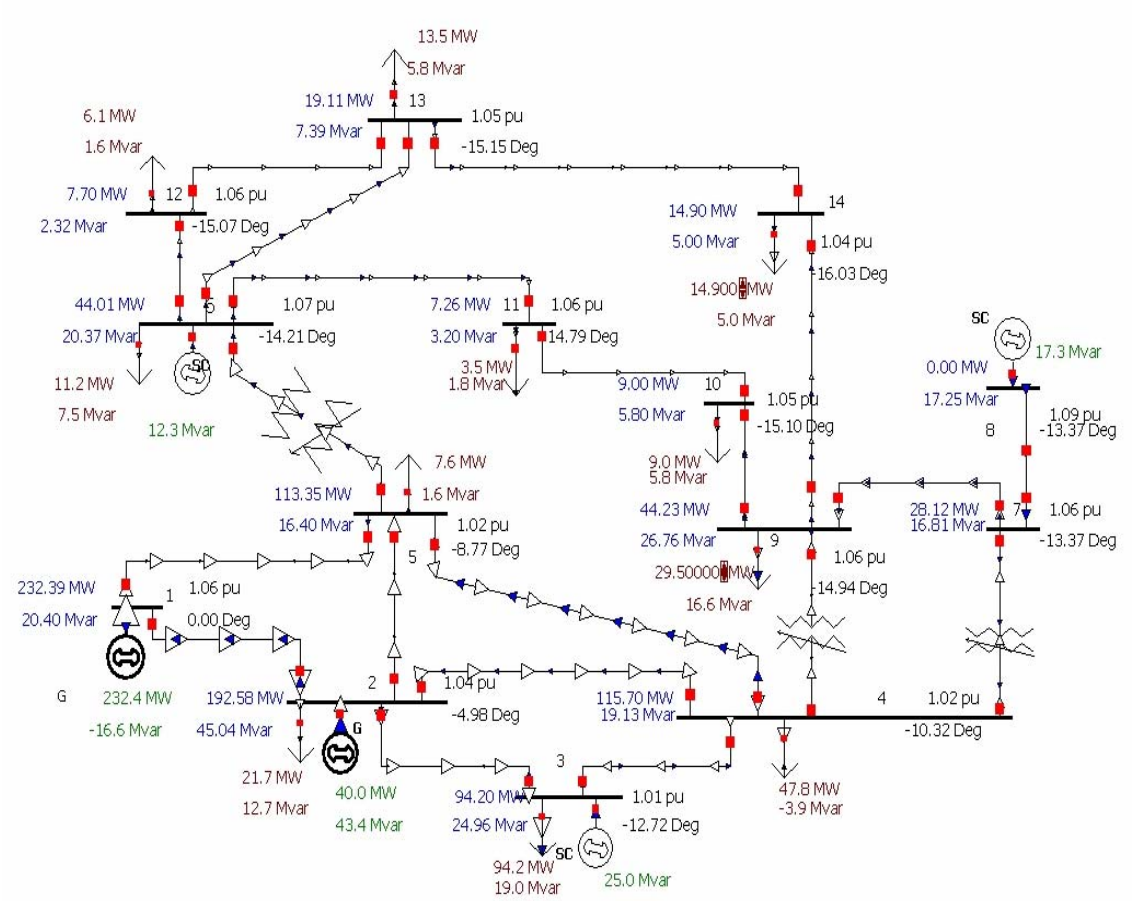

Figure 2.1 IEEE 14-bus test system one-line diagram

2.1 Test System Parameters

The test system is defined by the set of parameters for the generation, transmission lines, and load schedules at each bus. The transmission line parameters that are used to generate the test system base case are taken from [10] and are listed in Table 2.1.

Table 2.1 IEEE 14-Bus System Line Parameters

Line	Between Buses		Nominal Voltage	Resistance, r_{ij}	Reactance, x_{ij}	Line Charging Susceptance	Tap Setting
L	*i*	*J*	kV	p.u.	p.u.	p.u.	
1	1	2	69	0.01938	0.05917	0.0528	0
2	1	5	69	0.05403	0.22304	0.0492	0
3	2	3	69	0.04699	0.19797	0.0438	0
4	2	4	69	0.05811	0.17632	0.0374	0
5	2	5	69	0.05695	0.17388	0.034	0
6	3	4	69	0.06701	0.17103	0.0346	0
7	4	5	69	0.01335	0.04211	0.0128	0
8	4	7	69/138*	0	0.20912	0	0.978
9	4	9	69/138*	0	0.55618	0	0.969
10	5	6	69/138*	0	0.25202	0	0.932
11	6	11	138	0.09498	0.1989	0	0
12	6	12	138	0.12291	0.25581	0	0
13	6	13	138	0.06615	0.13027	0	0
14	7	8	138	0	0.17615	0	0
15	7	9	138	0	0.11001	0	0
16	9	10	138	0.03181	0.0845	0	0
17	9	14	138	0.12711	0.27038	0	0
18	10	11	138	0.08205	0.19207	0	0
19	12	13	138	0.22092	0.19988	0	0
20	13	14	138	0.17093	0.34802	0	0

*Represents the nominal voltage of the low/high sides of the transformer branches

Further information is necessary for the calculation of the total system revenue for each hour for this investigation. Because the transmission tariff is a function of the length of each transmission line, an estimate of the transmission line lengths is necessary. Since this information is not normally given for test systems such as this one, it was necessary to develop a method to estimate the length of the lines in the test system. The total impedance of a transmission line is dependent on the length of the line. For example, a transmission line that is 2.0 miles in length will have a greater impedance than if the transmission line was only 1.0 mile in length. As a result, a method for estimating the lengths of the transmission lines in the IEEE

14-bus test system based on the total line impedance of each line listed in Table 2.1 was developed as follows. A power base for the system was assumed to be S_{base}= 100 MVA. Using the nominal voltages, V_{base}, of the transmission lines and the power base of the system, each transmission line reactance value in Table 2.1, $x_{l_{p.u.}}$, can be converted to the reactance value in ohms, $x_{l_{ohms}}$, as shown in Equation (2.1).

$$x_{l_{ohms}} = x_{l_{p.u.}} * \frac{V_{base}^2}{S_{base}} \tag{2.1}$$

The length of the line was then calculated assuming that for a standard transmission line, the reactance is determined to by a conversion factor of 0.7 Ω/mile. Secondly, lines containing transformers (i.e., lines 8-10) were considered to be zero-length lines. The length of the transmission line was therefore calculated using Equation (2.2).

$$l_l = \frac{x_{l_{ohms}}}{0.7\ \Omega / \text{mile}} \tag{2.2}$$

Equation (2.2) thus calculates the length of the transmission line *l* from the corresponding line reactance. For example, using Table 2.1 and Equations (2.1) and (2.2), the reactance in ohms and the length of line 5 connecting bus 2 to bus 5 in the system can be calculated as shown in Equations (2.3) and (2.4), respectively.

$$x_{5_{ohms}} = 0.17388 * \frac{(69\ \text{kV})^2}{100\ \text{MVA}} = 8.2784\ \Omega \tag{2.3}$$

$$l_5 = \frac{8.2784\Omega}{0.7\ \Omega / \text{mile}} = 11.826\ \text{miles} \tag{2.4}$$

In this way, the remaining lengths of the transmission lines listed in Table 2.1 were calculated and are displayed in Table 2.2. The line lengths listed in Table 2.2 illustrate the relationship between the reactance of the line and the length of the transmission line. Lines 11-20 of the system are over twice as long as lines 1-7 of the system. This property is due to the reactance of the lines. Lines 11-20 are 138-kV lines and therefore have larger reactances than lines 1-6 of the system.

Table 2.2 Transmission Line Lengths

Line Number	"To" and "From" Buses		Reactance $x_{l_{p.u.}}$ (p.u.)	Reactance $x_{l_{ohms}}$ (Ohms)	Line Length l_l (miles)
	I	*j*			
1	1	2	0.05917	2.8171	4.02
2	1	5	0.22304	10.6189	15.17
3	2	3	0.19797	9.4254	13.46
4	2	4	0.17632	8.3946	11.99
5	2	5	0.17388	8.2784	11.83
6	3	4	0.17103	8.1427	11.63
7	4	5	0.04211	2.0049	2.86
8	4	7	0.20912	0	0
9	4	9	0.55618	0	0
10	5	6	0.25202	0	0
11	6	11	0.1989	37.8785	54.11
12	6	12	0.25581	48.7165	69.59
13	6	13	0.13027	24.8086	35.44
14	7	8	0.17615	33.5460	47.92
15	7	9	0.11001	20.9503	29.93
16	9	10	0.0845	16.0922	22.99
17	9	14	0.27038	51.4912	73.56
18	10	11	0.19207	36.5778	52.25
19	12	13	0.19988	38.0651	54.38
20	13	14	0.34802	66.2769	94.68

2.2 Base Case Solution

After all of the parameters and line lengths were established for the IEEE 14-bus test system in Figure 2.1, bus 1 was chosen as the system swing bus. As a result, the voltage angle at bus 1 is set at 0˚ with a voltage magnitude of $|V_1| = 1.06$ p.u. Applying these definitions, a power flow was performed on the test system to determine the base case parameters for the generation and load at each bus. Table 2.3 displays the base case parameter values. Summing all of the real power loads at the load buses in Table 2.3, the total system base case load is 259 MW. The angle

and voltage magnitude at bus 1, the system swing bus, remains constant at 0˚ and 1.06 p.u., respectively. Real power generation is supplied by both bus 1 and bus 2.

Table 2.3 Base Case Power Flow Solution

Name	Nom kV	Voltage p.u.	Voltage kV	Angle Deg	Load		Generation		Act G Shunt MW	Act B Shunt Mvar
					MW	MVar	MW	MVar		
Bus 1	69	1.06	73.14	0	0	0	232.4	-16.9	0	0
Bus 2	69	1.045	72.1	-4.98	21.7	12.7	40	42.2	0	0
Bus 3	69	1.01	69.69	-12.72	94.2	19	0	23.3	0	0
Bus 4	69	1.019	70.3	-10.33	47.8	-3.9	0	0	0	0
Bus 5	69	1.02	70.41	-8.78	7.6	1.6	0	0	0	0
Bus 6	138	1.07	147.66	-14.21	11.2	7.5	0	11.8	0	0
Bus 7	138	1.063	146.63	-13.37	0	0	0	0	0	0
Bus 8	138	1.09	150.42	-13.37	0	0	0	17	0	0
Bus 9	138	1.058	145.94	-14.95	29.5	16.6	0	0	0	22.4
Bus 10	138	1.052	145.22	-15.1	9.0	5.8	0	0	0	0
Bus 11	138	1.058	145.95	-14.79	3.5	1.8	0	0	0	0
Bus 12	138	1.055	145.63	-15.07	6.1	1.6	0	0	0	0
Bus 13	138	1.05	144.99	-15.15	13.5	5.8	0	0	0	0
Bus 14	138	1.037	143.05	-16.04	14.9	5	0	0	0	0

The power flow result shows that the system generates a total of 272.4 MW of real power for serving a total load of 259 MW and, while doing so, suffers a loss of 13.4 MW (about 5%).

2.3 Defining the Load Forecast

The load forecast for power systems follows a typical variation according to the hour of a particular day. Variations in the load exist between each hour throughout the course of one day. Additionally, variations in the system load exist between each day, holiday, and season (i.e., Winter, Spring, Summer, and Fall). These variations in the system load complicate the analysis of power system states and stability. However, the randomness of typical system loads can be characterized by making assumptions as stated in [11]. The system loads are time-variant, but the variations at each minute are almost negligible such that the load is almost constant from minute to minute. Thus, the variations in loads can be predicted at each hour by using a typical curve from [11] shown in Figure 2.2.

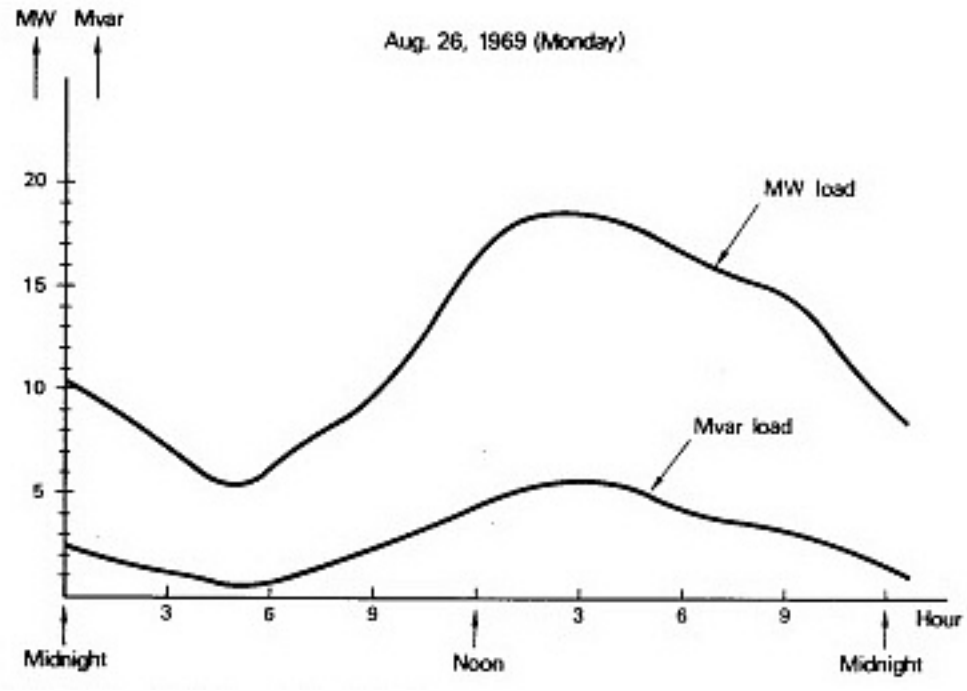

Figure 2.2 Typical load variation as taken from [11]

Figure 2.2 illustrates the change in load demand throughout the course of a day. There is an increase in the real power demand throughout the course of the morning. The peak load for the day is reached around 3:00 p.m. The load then decreases for the remainder of the day.

A load forecast taking into account these hourly variations was developed for this investigation by using publicly accessible approximate historical load data for each hour of every day for the year 2004 from the PJM website [12]. PJM is a regional transmission organization (RTO) that manages the wholesale electricity transactions in all or portions of Delaware, Illinois, Indiana, Kentucky, Maryland, Michigan, New Jersey, Ohio, Pennsylvania, Tennessee, Virginia, West Virginia, and the District of Columbia. The PJM Interconnection is divided into regions as designated in the load data file for the year. In the year 2004, the historical load data lists five regions. However, three of the five regions were added to the PJM Interconnection in 2004. As of the end of 2004, the addition of the three regions increased the PJM peak load to 106 000 MW as stated in [12]. The areas that were introduced into the PJM Interconnection in 2004 include Northern Illinois (Commonwealth Edison) (NI), Dayton Power and Light (DAY), and American Electric Power (AEP). Because these three areas were added during 2004, a complete annual listing of the integrated hourly loads for the entire year does not exist. Therefore, for the purpose of this study, the load data for one year was necessary, which resulted in using the PJM load data for the PJM-E area.

The hourly load data for PJM-E area on January 14, 2004, was scaled to match the system load of 259 MW of the IEEE 14-bus test system. The value, 27 077 MW is taken as the base load for conversion of all the loads to the IEEE 14-bus system. Thus, 31 887 MW on the PJM network for 1:00 a.m. on January 14, 2004, scaled down to 259*31 887/27 077 = 305 MW on the IEEE 14-bus system. The loads for the remaining hours are scaled down in a similar way and are tabulated in Table 2.4.

Table 2.4 Test System Hourly Load Schedule for January 14, 2004

Date	Time	PJM Load	New scaled down Load
1/14/2004	100	31 887	305
1/14/2004	200	31 255	299
1/14/2004	300	31 110	298
1/14/2004	400	31 343	300
1/14/2004	500	32 098	307
1/14/2004	600	34 662	332
1/14/2004	700	38 820	371
1/14/2004	800	41 334	395
1/14/2004	900	40 991	392
1/14/2004	1000	40 634	389
1/14/2004	1100	40 207	385
1/14/2004	1200	39 803	381
1/14/2004	1300	39 749	380
1/14/2004	1400	39 574	379
1/14/2004	1500	39 207	375
1/14/2004	1600	39 276	376
1/14/2004	1700	40 829	391
1/14/2004	1800	43 497	416
1/14/2004	1900	44 020	421
1/14/2004	2000	43 473	416
1/14/2004	2100	42 635	408
1/14/2004	2200	40 692	389
1/14/2004	2300	37 800	362
1/14/2004	2400	34 992	335

The IEEE 14-bus system was loaded according to the new load schedule for each hour of the day. Therefore, for hour 1, the total load served by the IEEE 14-bus system is 305 MW; for hour 2, the total load served by the system is 299 MW and so on. With new loads assigned, a

power flow was performed for each hour and the megawatt flowing over each line was calculated.

Note that the total system load at each hour was divided among the load buses in the same ratio as the original IEEE 14-bus load. For example, the total load on the original IEEE 14-bus system was 259 MW. Out of the total 259 MW, bus two served a load of 21.7 MW, i.e., 21.7/259*100 = 8.38% of the total load. Therefore, also under the newly assigned load schedule, bus two will serve 8.38% of the total load. Thus, for hour 1, out of the total load of 305 MW, bus 2 will serve 305*8.38/100 = 25.55 MW. Other buses also share the total load in the manner discussed above. The distribution of loads among the load buses for hour one is tabulated in Table 2.5.

Table 2.5 Load Scheduling for 1:00 a.m. on January 14, 2004.

Load Bus	Old Load Corresponding To 259 MW(hour # 1)	Original ratio of load Sharing among the buses	New Load Corresponding To 305 MW (hour #1)
Bus 1	0	0	0
Bus 2	21.7	8.38%	25.5539
Bus 3	94.2	36.37%	110.93
Bus 4	47.8	18.46%	56.2893
Bus 5	7.6	2.93%	8.9498
Bus 6	11.2	4.32%	13.1891
Bus 7	0	0	0
Bus 8	0	0	0
Bus 9	29.5	11.39%	34.7392
Bus 10	9	3.47%	10.5984
Bus 11	3.5	1.35%	4.1216

In the same manner, the load distribution among the load buses for all 24 hours was calculated. With this hourly system load, the revenue generated from transmission tariffs can be computed. Power flow was done and the megawatt flowing through each line for each hour was determined. The megawatt flowing over each line is the megawatt flow after the transmission losses are deducted. Table 2.6 shows the line megawatt flows for 1:00 a.m. on January 14, 2004, and the line lengths.

Table 2.6 Megawatt Flows for 1:00 a.m. on January 14, 2004.

Line Number	From Bus	To Bus	Line MW	Line length
1	1	2	186.9152	4.02
2	1	5	86.9395	15.17
3	2	3	83.7163	13.46
4	2	4	63.5775	11.99
5	2	5	47.2278	11.83
6	3	4	27.2077	11.63
7	4	5	72.4193	2.86
8	4	7	33.0398	0
9	4	9	18.9023	0
10	5	6	52.0646	0
11	6	11	8.6411	54.11
12	6	12	9.0803	69.59
13	6	13	20.6982	35.44
14	7	8	0.0021	47.92
15	7	9	33.0419	29.93
16	9	10	6.0975	22.99
17	9	14	10.9348	73.56
18	10	11	4.5016	52.25
19	12	13	1.8882	54.38
20	13	14	6.6125	94.68

An hourly transmission tariff was assumed to be $0.04/MW-mile. Then, revenue for hour 1 is 0.04 * linelength * LineMW = $ 390.96, where the “LineMW’’ and “linelength” are vectors storing the values of column 4 and 5, respectively, of Table 2.6. The revenue for the remaining hours was calculated in this manner and is given in Table 2.7. This result forms the base case revenue for the remaining study.

Table 2.7 Base Case Loading and Revenue.

Time	Date	Base Case System Load, Ptot (MW)	Base Case Total Revenue ($)
100	1/14/04	305	390.96
200	1/14/04	299	382.95
300	1/14/04	298	381.11
400	1/14/04	300	384.06
500	1/14/04	307	393.56
600	1/14/04	332	426.22
700	1/14/04	371	479.04
800	1/14/04	395	510.85
900	1/14/04	392	506.51
1000	1/14/04	389	501.86
1100	1/14/04	385	496.49
1200	1/14/04	381	491.41
1300	1/14/04	380	490.73
1400	1/14/04	379	488.53
1500	1/14/04	375	483.91
1600	1/14/04	376	484.78
1700	1/14/04	391	504.46
1800	1/14/04	416	538.33
1900	1/14/04	421	544.99
2000	1/14/04	416	538.02
2100	1/14/04	408	527.33
2200	1/14/04	389	502.73
2300	1/14/04	362	466.21
2400	1/14/04	305	430.47

A Matlab code was created to establish the load forecast for the IEEE 14-bus test system using the text file from [13] required to sort and scale the PJM-E load data. The base case parameters in Table 2.3 from the power flow are considered to be the system load at the first hour associated with 1:00 a.m. on January 1, 2004. Because the year 2004 was a leap year, the

load forecast for the year was assigned in 8784 hourly increments. Figure 2.3 illustrates the annual variation in system load using the load data scaled to match the IEEE 14-bus test system.

By establishing the hourly system load, the revenue generated from transmission tariffs can be calculated. The hourly transmission tariff was assumed to be \$0.04/MW-mile. With this value as the transmission tariff, the revenue generated for one transmission line in a 24-hour day would be approximately \$0.96/MW-mile. Therefore, this would generate an annual income of \$350.40/MW-mile. Over a span of 5 years, an income of \$1,752/MW-mile would be generated.

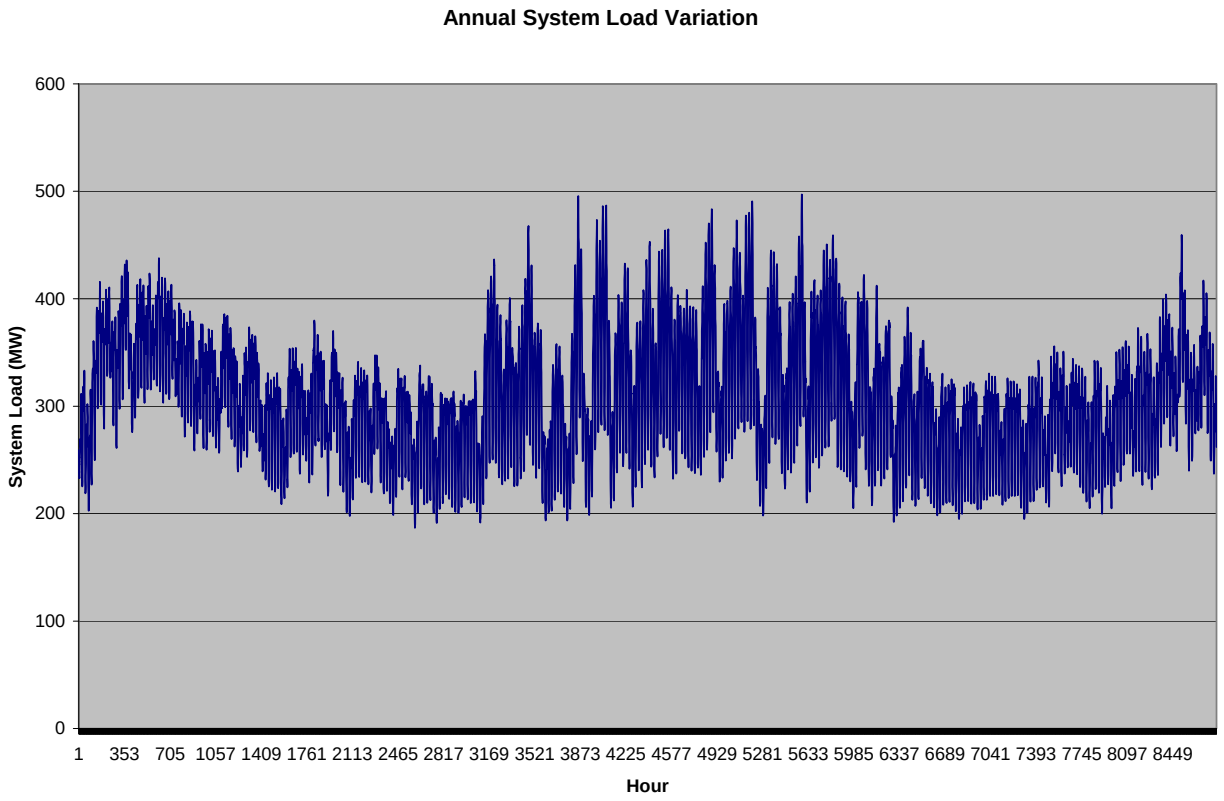

Figure 2.3 System load for each hour of the year

The revenue generated from the transmission tariffs, I_l, is directly related to the transmission tariff t = \$0.04/MW-mile, the transmission line lengths l_l, as given in Table 2.2, and the megawatt flows on the transmission lines f_l, by Equation (2.5).

$$I_l = tl_l f_l \tag{2.5}$$

Using load forecast determined from the historical PJM load data, power flows were conducted to determine the megawatt flows on the transmission lines allowing the calculation of each line revenue for the hour using Equation (2.5). The total revenue generated for each hour is calculated by summing all of the line revenues calculated from the power flows. Figure 2.4 displays the total system revenue for every 8784-hour increment in the year.

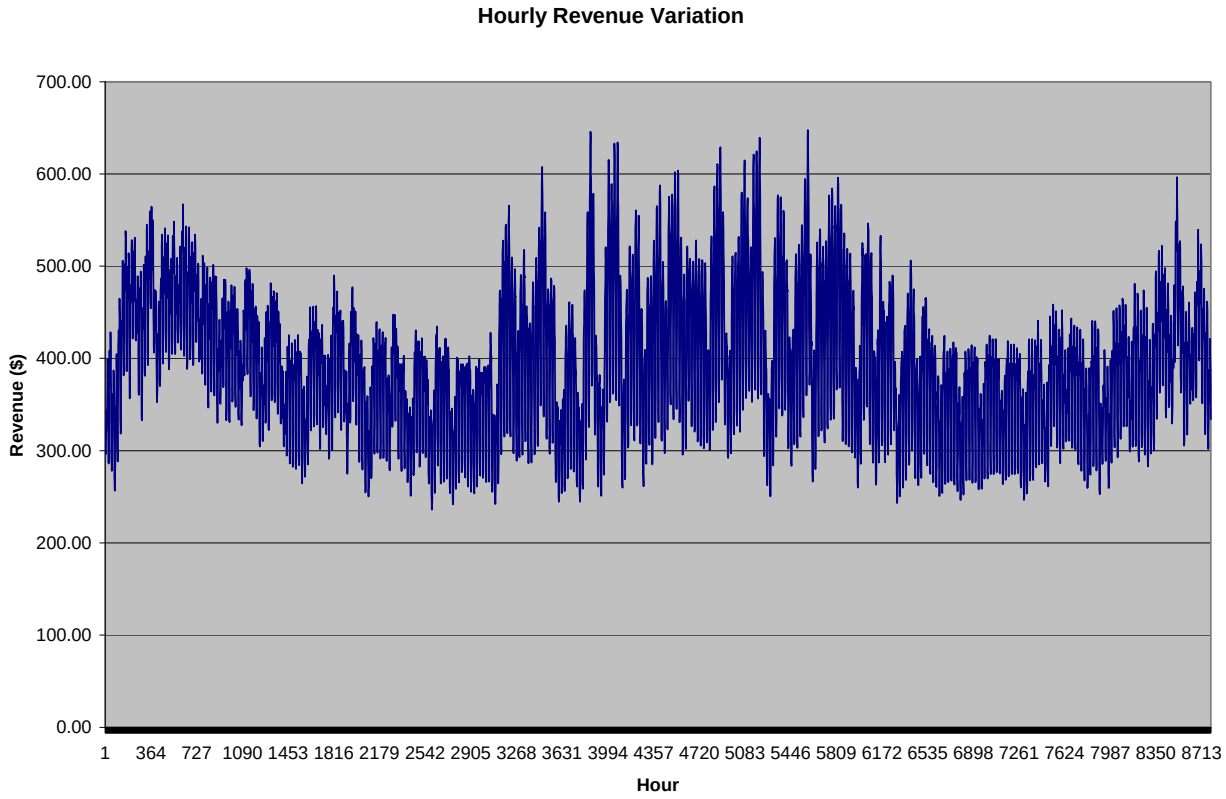

Figure 2.4 Total revenue for each hour throughout the year

The total hourly revenue generated using the load forecast is considered to be the base case revenue. A value for the annual revenue is calculated by summing the 8784 hourly revenues for the year. The annual revenue for the base case is about $3.5M. The system load assigned by the load forecast for each hour is considered to be the base case system load for each hour. For clarity, this report gives results only for one day – January 14, 2004.

Table 2.4 Base Case System Load and Total Revenue Values (Jan 14, 2004)

Hour of the year	Time	Date	Base Case Load, P_{tot}^{0} (MW)	Base Case Revenue, I^{0} ($)
313	100	1/14/04	305	390.96
314	200	1/14/04	299	382.95
315	300	1/14/04	298	381.11
316	400	1/14/04	300	384.06
317	500	1/14/04	307	393.56
318	600	1/14/04	332	426.22
319	700	1/14/04	371	479.04
320	800	1/14/04	395	510.85
321	900	1/14/04	392	506.51
322	1000	1/14/04	389	501.86
323	1100	1/14/04	385	496.49
324	1200	1/14/04	381	491.41
325	1300	1/14/04	380	490.73
326	1400	1/14/04	379	488.53
327	1500	1/14/04	375	483.91
328	1600	1/14/04	376	484.78
329	1700	1/14/04	391	504.46
330	1800	1/14/04	416	538.33
331	1900	1/14/04	421	544.99
332	2000	1/14/04	416	538.02
333	2100	1/14/04	408	527.33
334	2200	1/14/04	389	502.73
335	2300	1/14/04	362	466.21
336	2400	1/13/04	305	430.47

3. Monte Carlo Simulations

Uncertainty in the load forecast was introduced using a random variable sampled from a normal distribution. The uncertainty in the load was then applied to the IEEE 14-bus test system to calculate the power flows and total revenue generated using the transmission tariff specified in Chapter 2. The importance of each step in the simulation is identified in the following sections.

3.1 Normal Random Number Generator

The selection of a random number generator is important to the accuracy of the Monte Carlo simulations. The normal random number generator supplied by the Matlab software is built from a uniform random number generator. According to [14], the normal random number generator uses a table lookup algorithm. Uniform random numbers are generated in the same plane and are accepted if each falls under the area of the probability density function for a normal distribution. If the uniform random number generated does not fall under the area of the probability density function, then the number is rejected. The area under the probability density function is divided into 128 sections with equal areas. Figure 3.1 from [14] illustrates an estimation of the probability density function area using eight sections of equal area.

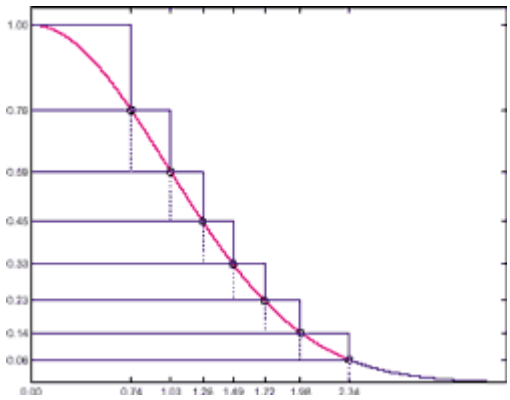

Figure 3.1 Area estimation by step functions for the probability density function of a normal distribution as shown in [14]

The period of the normal random number generator used is 2^{64} [14]. The state of the normal random number generator is set to the clock to initialize the random number generator to a different state for every sample. Figure 3.2 displays a histogram of 100 random variables using the normal random number generator with the mean μ set at zero and the standard deviation σ set at 0.03.

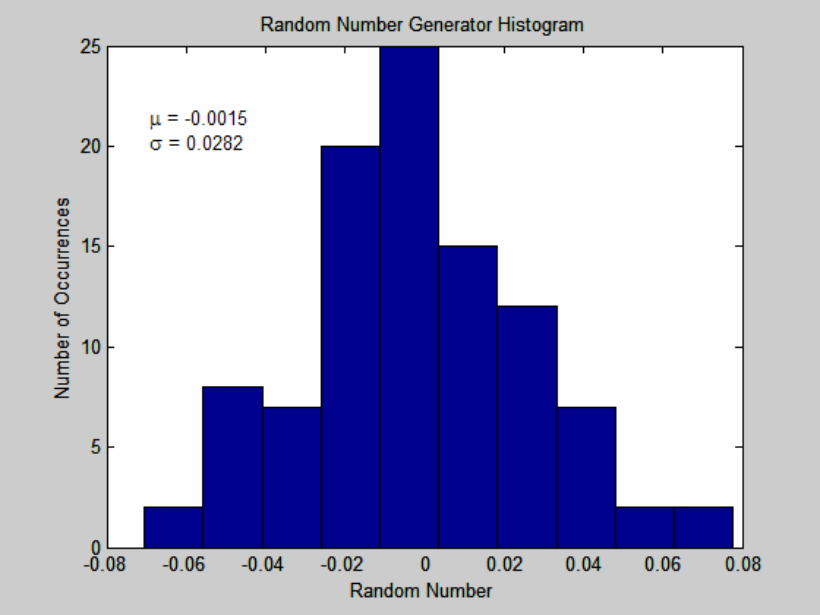

Figure 3.2 Histogram displaying the distribution of the random numbers generated by the random number generator using 100 samples

Figure 3.2 also displays the mean of the random number generator as $\mu = -0.0015$. The random number generator was set to produce a mean of zero. The standard deviation of the 100 samples was $\sigma = 0.0282$. With a standard deviation originally set as $\sigma = 0.03$, the distribution of 100 samples produced approximately a 6.38% error. After multiple samples were drawn using the normal random number generator, the percent deviation from the theoretical values of the mean and standard deviation proved adequate for this investigation.

3.2 Power Flow Simulation

Using the random number generator discussed in the previous section, the Monte Carlo simulations were performed using Matlab software in conjunction with SimAuto 10.0 and PowerWorld Simulator 10.0. The random number generator was used to draw 100 samples for each hour to represent the error in the load forecast for the respective hour. The random variable was multiplied with the total base case system load for the hour by obtaining the base case system parameters as computed in Chapter 2. The resulting value was represented as the amount of megawatt error in the system load forecast for the hour. The error was then distributed to the loads at the buses according to the percentage of contribution of each bus to the total system load in the base case. Therefore, the percentage of total system load at each load bus remained the same for every hour.

With the change in the load, a power flow was performed to determine the new power flows on all of the transmission lines. The power flow solution provided the power at the "to" bus and power at the "from" bus of each transmission line. For purposes of this analysis, the power flow on the transmission lines used to calculate the transmission revenue generated from the transmission tariff was computed using the smallest absolute value of the two power flows. Therefore, the revenue generated for each line is calculated using Equation (2.5), where the power flows on the transmission lines are the power flows after transmission line losses are

subtracted. The total system revenue was generated by summing the revenues generated from all of the lines for the hour. For each of the 100 samples in a one-hour increment, the simulation provided a value for the total transmission revenue. Figure 3.3 displays the algorithm used for the stochastic simulations.

Once all 100 samples were computed, the mean and standard deviation of the system revenue for each hour was calculated. For the statistical samples, the mean and the standard deviation were calculated using the following definitions in [15]. Suppose that the sample size consists of n observations where each random sample is identified as η_i for samples $i = 1, 2, \ldots, n$. All η_i are independent observations from the same parent distribution and are random to the point that if 100 new samples were collected for the hour, these samples would be different from the original samples obtained. Because samples for this experiment are obtained from a normal distribution, the parent distribution, which describes how the values of η_i are distributed, should be a normal distribution. Thus, the sample mean of the 100 samples for each hour was calculated according to Equation (3.1).

$$\mu = \frac{\sum_{i=1}^{n} \eta_i}{n} \tag{3.1}$$

Therefore, for this investigation, there were $n = 100$ samples for each hour with a normal distribution. The sample standard deviation σ was calculated according to Equation (3.2).

$$\sigma = \sqrt{\frac{\sum_{i=1}^{n} (\eta_i - \mu)^2}{n-1}} \tag{3.2}$$

Using Equations (3.1) and (3.2), the unbiased sample standard deviation and sample mean were then calculated for the 100 samples for each hour.

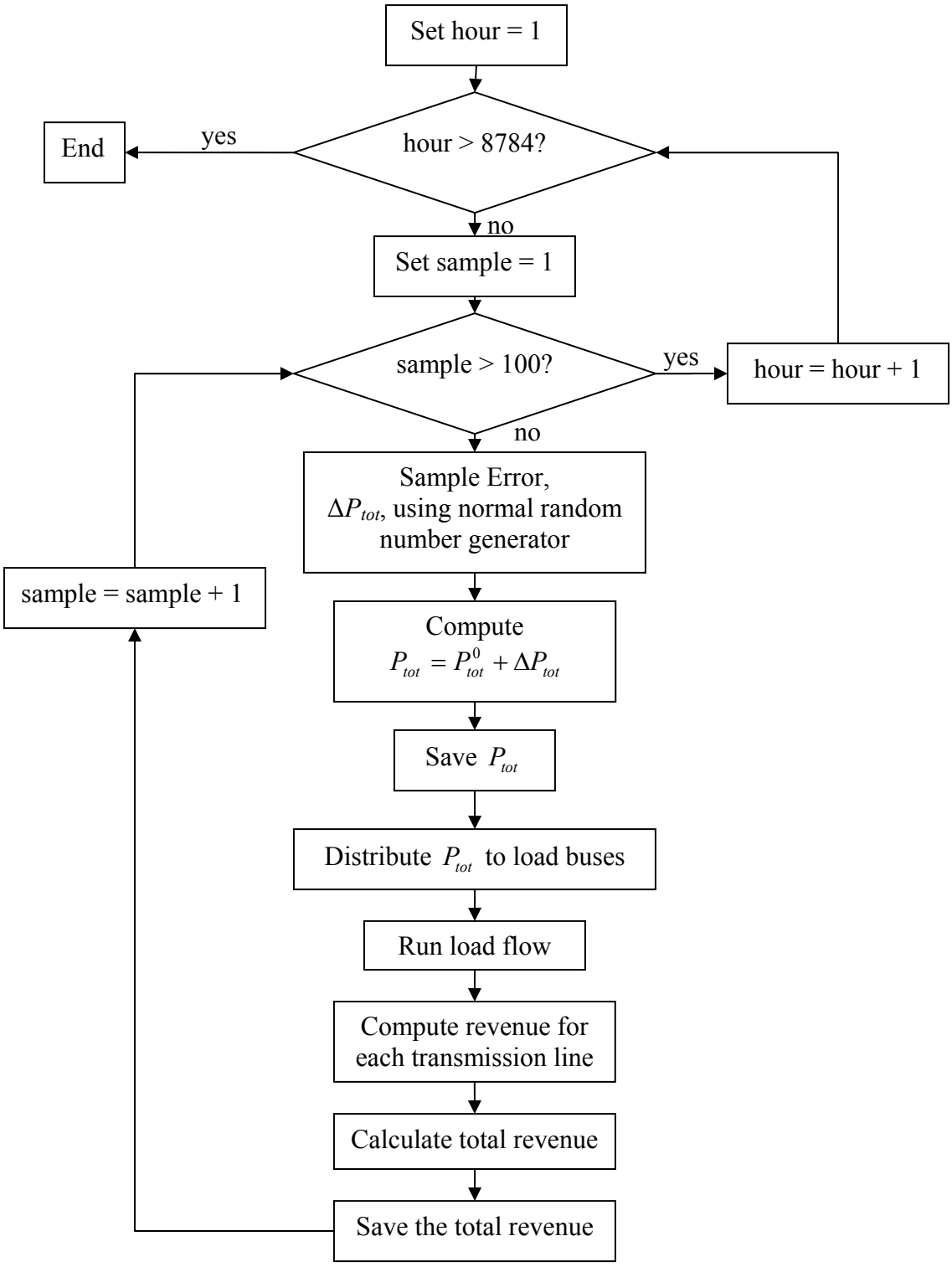

Figure 3.3 Flowchart for the algorithm for the Monte Carlo simulations

3.3 Monte Carlo Simulation Results

Applying the algorithm in Figure 3.3, the Monte Carlo simulations were performed on the IEEE 14-bus test system using the base case parameters described in Chapter 2. The simulations were performed for 100 samples of each 8784 hourly increment resulting in 878 400 power flow solutions. The resulting mean total system load, mean total system revenue, and standard deviation of the total revenue of the 100 samples for the hours specified in Table 2.4 are listed in Table 3.1.

A histogram of each hour may also be plotted using the 100 samples obtained in the simulation. The histogram also reflects the standard deviation and statistical mean of the 100 samples. Figure 3.4 illustrates the typical bell-curve of the normal distribution in the system revenue for hour 329 (1700 = 5pm on January 14). In the figure, the mean value of the distribution appears to be near the $502.80 listed in Table 3.1. The standard deviation of σ = $14.16 is also evident in Figure 3.4. It is often assumed that the mean plus or minus 3 standard deviations will include all samples.

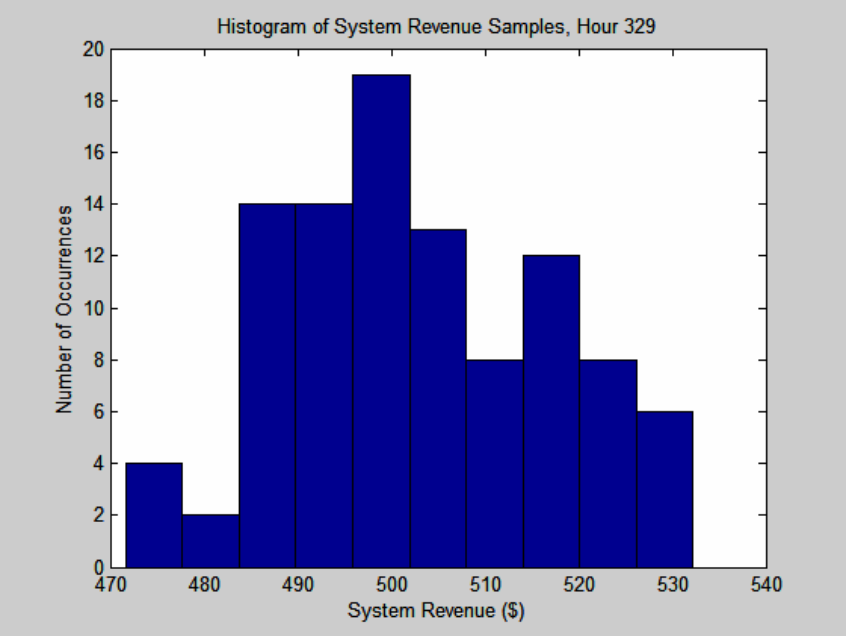

Figure 3.4 Histogram displaying the distribution of the system revenue for 100 samples

Table 3.1 Statistical Results by Hour from the Monte Carlo Solutions for January 14, 2004

Time	Date	Simulated Mean System Load (MW)	Simulated Mean System Revenue ($)	Simulated Standard Deviation $\sigma_{revenue}$ ($)
100	1/14/04	305	390.66	12.49
200	1/14/04	298	382.23	11.28
300	1/14/04	295	378.27	12.82
400	1/14/04	299	383.13	12.29
500	1/14/04	308	394.60	13.23
600	1/14/04	333	427.99	14.47
700	1/14/04	371	478.56	14.23
800	1/14/04	395	510.09	16.94
900	1/14/04	391	505.21	14.03
1000	1/14/04	388	501.30	13.83
1100	1/14/04	385	497.15	13.93
1200	1/14/04	380	490.09	12.79
1300	1/14/04	383	494.68	13.83
1400	1/14/04	379	488.98	15.66
1500	1/14/04	376	484.86	15.24
1600	1/14/04	376	484.97	14.77
1700	1/14/04	389	502.80	14.16
1800	1/14/04	416	537.99	17.39
1900	1/14/04	420	543.86	16.76
2000	1/14/04	415	536.59	19.71
2100	1/14/04	408	527.99	14.94
2200	1/14/04	388	500.62	15.19
2300	1/14/04	360	464.40	13.47
2400	1/14/04	333	427.75	14.41

4. Analytical Solution

This chapter presents results that use linear power flow methods to analytically predict the same results as obtained using the exhaustive Monte Carlo solutions. The linear approximations presented in this investigation are derived using the relationships in the DC power flow. These approximations are used in calculating the power transfer distribution factors (PTDF). The PTDFs are defined as the relative change in the power flow on a particular line from bus *i* to bus *j* due to a change in injection, ΔP_k, and corresponding withdrawal at the system swing or slack bus as shown in Figure 4.1. Using the PTDFs, the change in flow on each transmission line in the system may be calculated for the change in injection at one or more buses using superposition. This calculated change in flow on the transmission line causes a change in the amount of revenue generated. Using the methods described in this chapter, by using PTDFs, the calculation of the change in revenue ultimately leads to the evaluation of the distribution of the revenue for that hour.

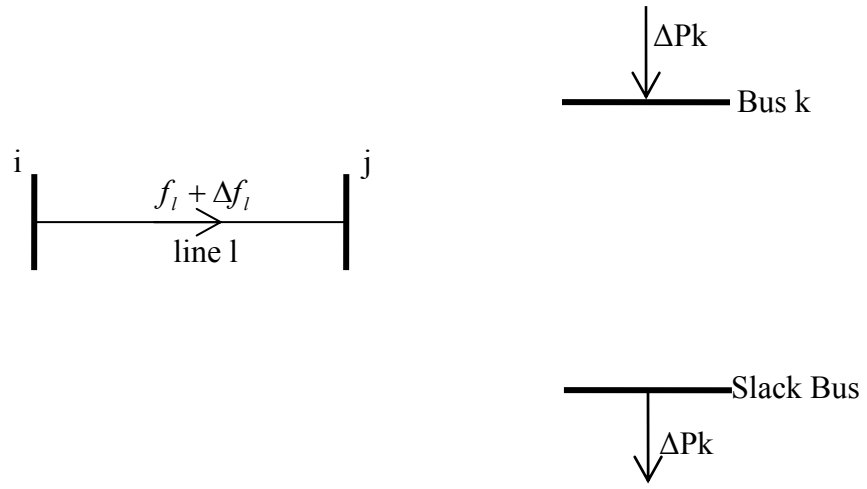

Figure 4.1 Illustration of the change of the flow on the line from bus i to bus j due to a change in injection at load bus k.

4.1 Calculation of Susceptance Matrix Using DC Power Flow

To begin the derivation of the distribution factors, the derivation of the DC power flow must be addressed. To discuss the basis for the DC power flow, the formulation of the Newton power flow equations must be discussed. Consider a power system with *N* buses. Each bus *i* may be characterized by the net power injections, $P_{net\,i}$ and $Q_{net\,i}$, and the voltage phasor $\overline{E_i} = V_i e^{j\theta_i}$ At each bus, the variables are represented with the relationship in Equation (4.1).

$$\begin{bmatrix} \overline{I_1} \\ . \\ . \\ . \\ \overline{I_N} \end{bmatrix} = \begin{bmatrix} \overline{Y_{11}} & . & . & . & \overline{Y_{1N}} \\ . & . & & & . \\ . & & . & & . \\ . & & & . & . \\ \overline{Y_{N1}} & . & . & . & \overline{Y_{NN}} \end{bmatrix} \begin{bmatrix} \overline{E_1} \\ . \\ . \\ . \\ \overline{E_N} \end{bmatrix} \tag{4.1}$$

The $\underline{\overline{I}}$ vector contains the current injection phasors, where $\overline{I_j}$ is the current into bus *j*. The $\underline{\overline{E}}$ vector is the voltage phasor measured with respect to the ground node, where $\overline{\boldsymbol{E}_j}$ represents the voltage at bus *j* with respect to ground. The bus admittance matrix referenced to the ground bus is represented by the **Y** matrix in Equation (4.1). The bus admittance matrix $\underline{\overline{Y}} = \left[\overline{Y_{ij}}\right]$ may be calculated using Equation (4.2).

$$\underline{\overline{Y}} = \underline{G} + j\underline{B} \tag{4.2}$$

The bus conductance matrix in Equation (4.2) is defined as $\underline{G} = \left[G_{ij}\right]$, and the bus susceptance matrix is defined as $\underline{B} = \left[B_{ij}\right]$. The diagonal elements $\overline{Y_{ii}}$ of the bus admittance matrix are the algebraic sums of all of the complex admittances of the lines of the incident bus *i*.The off-diagonal elements $\overline{Y_{ij}}$ of the bus admittance matrix are the negative sums of the lines connecting buses *i* and *j*. The $\overline{Y_{ij}}$ component of the matrix will be nonzero if and only if buses *i* and *j* are connected by a transmission line or transformer. The system can be modeled using the assumption that the transmission lines may be represented by the π-equivalent model as shown in Figure 4.2.

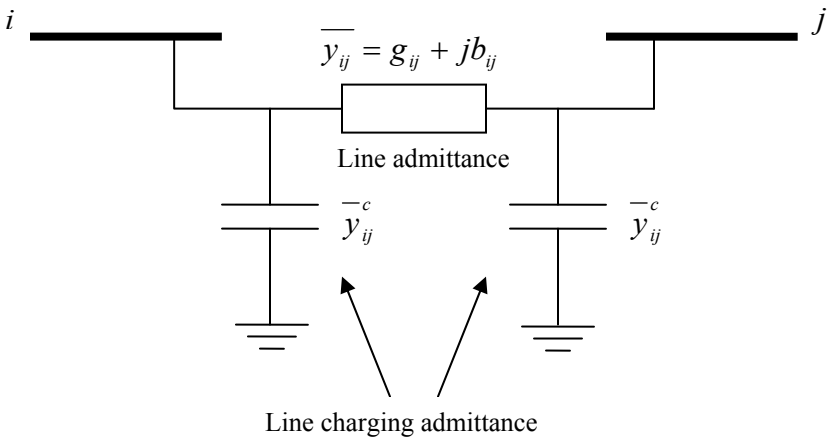

Figure 4.2 Representation of the π-equivalent transmission line model

With this model, the off-diagonal bus admittance matrix elements are determined given Equation (4.3).

$$\overline{Y_{ij}} = -\overline{y_{ij}} = -g_{ij} - jb_{ij} \tag{4.3}$$

Thus, from Equation (4.2), the conductance is $G_{ij} = -g_{ij}$, and the susceptance is $B_{ij} = -b_{ij}$. With the line impedance written as $\bar{z} = r + jx$, the admittance term $\bar{y}_{ij}$ in Equation (4.3) may also be written as a function of the impedance, ultimately creating a relationship between the resistance *r* and the reactance *x* by Equation (4.4).

$$\bar{y}_{ij} = \frac{1}{\bar{z}_{ij}} = \frac{1}{r_{ij} + jx_{ij}} = \frac{r_{ij}}{\left(r_{ij}^2 + x_{ij}^2\right)} - j\frac{x_{ij}}{\left(r_{ij}^2 + x_{ij}^2\right)} \tag{4.4}$$

Using the real and imaginary expressions in Equation (4.4), the conductance G_{ij} and susceptance B_{ij} values are defined in Equations (4.5) and (4.6), respectively.

$$G_{ij} = -g_{ij} = \frac{-r_{ij}}{\left(r_{ij}^2 + x_{ij}^2\right)} \tag{4.5}$$

$$B_{ij} = -b_{ij} = \frac{x_{ij}}{\left(r_{ij}^2 + x_{ij}^2\right)} \tag{4.6}$$

To form the basic power flow equations, bus 1 in the *N*-bus system is chosen as the slack bus in which both the voltage *V* and angle θ are known and constant. The power flow equations have the form $\underline{\boldsymbol{g}}(\underline{\boldsymbol{x}}) = \underline{\mathbf{0}}$, where $\underline{\boldsymbol{x}}$ is called the system state containing the bus angles θ and bus voltages *V* of all of the buses excluding the system slack bus. The power flow equations are solved by Equations (4.7) and (4.8) for the buses of the system not including the system slack bus.

$$g_i^p = G_{ii}V_i^2 + V_i \sum_{\substack{k=buses\\ connected\\ to\\ i}} V_k\left[G_{ik}\cos\left(\theta_i - \theta_k\right) - B_{ik}\sin\left(\theta_i - \theta_k\right)\right] - P_{net_i} = 0 \tag{4.7}$$

$$g_i^q = B_{ii}V_i^2 + V_i \sum_{\substack{k=buses\\ connected\\ to\\ i}} V_k\left[G_{ik}\sin\left(\theta_i - \theta_k\right) + B_{ik}\cos\left(\theta_i - \theta_k\right)\right] - Q_{net_i} = 0 \tag{4.8}$$

The Newton power flow scheme is an iterative method obtained by the Taylor series expansion about a point. Using the Newton power flow scheme, a Jacobian matrix is defined as the gradient of the power flow equations $\nabla_{\underline{x}}\underline{\boldsymbol{g}}$. The structure of the Jacobian matrix appears as shown in Equation (4.9).

$$\underline{\boldsymbol{J}}(\underline{\boldsymbol{x}}) = \frac{\partial \underline{\boldsymbol{g}}}{\partial \underline{\boldsymbol{x}}} = \begin{bmatrix} \dfrac{\partial \underline{\boldsymbol{g}}^{\boldsymbol{p}}}{\partial \underline{\boldsymbol{\theta}}} & \dfrac{\partial \underline{\boldsymbol{g}}^{\boldsymbol{p}}}{\partial \underline{\boldsymbol{V}}} \\ \dfrac{\partial \underline{\boldsymbol{g}}^{\boldsymbol{q}}}{\partial \underline{\boldsymbol{\theta}}} & \dfrac{\partial \underline{\boldsymbol{g}}^{\boldsymbol{q}}}{\partial \underline{\boldsymbol{V}}} \end{bmatrix} \tag{4.9}$$

The equations used in the Newton power flow scheme are simplified to form the decoupled power flow method by applying the following assumptions according to the terms in the Jacobian matrix:

1. $\frac{\partial P_i}{\partial |V_k|} \cong 0$ as a result of neglecting all interactions between P_i and $|V_k|$.
2. $\frac{\partial Q_i}{\partial \theta_k} \cong 0$, as a result of neglecting all interactions between Q_i and θ_k.
3. $\cos(\theta_i - \theta_j) \cong 1$, due to the usually small value of $(\theta_i - \theta_j)$.
4. $G_{ik} \sin(\theta_i - \theta_k) << B_{ik}$.
5. $Q_i << B_{ii} |V_i|^2$

The first two assumptions illustrate the power system property that real power is more sensitive to perturbations in the voltage angle as opposed to perturbations in the voltage magnitude. Thus, the reactive power is more sensitive to changes in the voltage magnitude than changes in the voltage angle. Using the assumptions listed above, the Jacobian equations and power flow equations may be written as Equations (4.10) and (4.11) and Equations (4.12) and (4.13), respectively.

$$\frac{\partial P_i}{\partial \theta_k} = -|V_i||V_k|B_{ik} \tag{4.10}$$

$$\frac{\partial Q_i}{\left(\frac{\partial |V_k|}{|V_k|}\right)} = -|V_i||V_k|B_{ik} \tag{4.11}$$

$$\Delta P_i = \left(\frac{\partial P_i}{\partial \theta_k}\right)\Delta\theta_k \tag{4.12}$$

$$\Delta Q_i = \left[\frac{\partial Q_i}{\left(\frac{\partial |V_k|}{|V_k|}\right)}\right]\frac{\Delta |V_k|}{|V_k|} \tag{4.13}$$

By substituting Equation (4.10) into Equation (4.12) and Equation (4.11) into Equation (4.13), the following relationships may be derived in Equation (4.14) and Equation (4.15):

$$\Delta P_i = -|V_i||V_k|B_{ik}\Delta\theta_k \tag{4.14}$$

$$\Delta Q_i = -|V_i||V_k|B_{ik}\frac{\Delta |V_k|}{|V_k|} \tag{4.15}$$

Dividing Equations (4.14) and (4.15) by $|V_i|$ and assuming that $|V_k| \cong 1$, further simplification can be made to derive Equations (4.16) and (4.17).

$$\frac{\Delta P_i}{|V_i|} = -B_{ik}\Delta\theta_k \tag{4.16}$$

$$\frac{\Delta Q_i}{|V_i|} = -B_{ik}\Delta|V_k| \tag{4.17}$$

As a result, the matrix equations for an *N*-bus system may be determined using Equations (4.16) and (4.17) as shown in equations (4.18) and (4.19), respectively.

$$\begin{bmatrix} \frac{\Delta P_1}{|V_1|} \\ . \\ . \\ . \\ \frac{\Delta P_N}{|V_N|} \end{bmatrix} = \begin{bmatrix} -B_{11} & . & . & . & -B_{1N} \\ . & . & & & . \\ . & & . & & . \\ . & & & . & . \\ -B_{N1} & . & . & . & -B_{NN} \end{bmatrix} \begin{bmatrix} \Delta\theta_1 \\ . \\ . \\ . \\ \Delta\theta_N \end{bmatrix} \tag{4.18}$$

$$\begin{bmatrix} \frac{\Delta Q_1}{|V_1|} \\ . \\ . \\ . \\ \frac{\Delta Q_N}{|V_N|} \end{bmatrix} = \begin{bmatrix} -B_{11} & . & . & . & -B_{1N} \\ . & . & & & . \\ . & & . & & . \\ . & & & . & . \\ -B_{N1} & . & . & . & -B_{NN} \end{bmatrix} \begin{bmatrix} \Delta|V_1| \\ . \\ . \\ . \\ \Delta|V_N| \end{bmatrix} \tag{4.19}$$

Further simplification to the $\Delta P - \Delta\theta$ relationship is made using three more assumptions. First, all shunt reactances to ground are ignored. Second, all shunts to ground from autotransformers are ignored. Lastly, the line resistance can be neglected due to the value of the line resistance being much smaller than the line reactance, $r_{ik} << x_{ik}$. This last assumption simplifies the calculation of $-B_{ik}$ in Equation (4.6) to Equation (4.20).

$$-B_{ik} = \frac{-1}{x_{ik}} \tag{4.20}$$

The $\Delta Q - \Delta|V|$ relationship is simplified by eliminating the effects from all phase shift transformers. The simplifications to both relationships create two different **B** matrices as assigned in Equations (4.18) and (4.19). The **B'** matrix is the new simplified **B** matrix in Equation (4.16) for the $\Delta P - \Delta\theta$ relationship by ignoring the shunt susceptances. The off-diagonal elements B'_{ik} are calculated using Equation (4.20) as shown in Equation (4.21). The diagonal elements B'_{ii} are then calculated using Equation (4.22).

$$B_{ik}^{'} = -B_{ik} = \frac{-1}{x_{ik}} \tag{4.21}$$

$$B_{ii}^{'} = \sum_{k=1}^{N} \frac{1}{x_{ik}} \tag{4.22}$$

The **B**" matrix is the new simplified **B** matrix in Equation (4.19) for the $\Delta Q - \Delta|V|$ relationship. The off-diagonal elements $B_{ik}^{"}$ are calculated using Equation (4.6) as shown in Equation (4.23). The diagonal elements $B_{ii}^{'}$ are then calculated using Equation (4.24).

$$B_{ik}^{"} = B_{ik} = -\frac{x_{ik}}{\left(r_{ik}^2 + x_{ik}^2\right)} \tag{4.23}$$

$$B_{ii}^{"} = \sum_{k=1}^{N} - B_{ik} \tag{4.24}$$

The **B**' and **B**" matrices remain constant and only need to be calculated once, which is one of the advantages of the decoupled power flow. The DC power flow is derived from the decoupled power flow formulation by omitting the $\Delta Q - \Delta|V|$ relationship and by setting all $|V_i| = 1.0\,p.u.$ As a result, Equation (4.18) becomes Equation (4.25), which produces the DC power flow equation.

$$\mathbf{\Delta P = B^{'} \Delta \theta} \tag{4.25}$$

Equation (4.25) implies that the DC power flow only calculates the MW flows on transmission lines and transformers without giving any information of MVar flows. For this investigation, the information provided by the DC power flow is sufficient. For example, the **B**' matrix for the IEEE 14-bus test system is calculated according to the line data given in Table 2.1 and Equations (4.21) and (4.22). Because the test system slack bus is assumed to be bus 1, the first row of the **B**' matrix refers to bus 2 of the system. Equation (4.23) shows the calculation of the off-diagonal element $B_{12}^{'}$ relating to the transmission line connecting buses 2 and 3. Equation (4.24) displays the calculation of the diagonal element $B_{11}^{'}$, which is the sum of the admittances of the lines connecting bus 2 to buses 1, 3, 4, and 5.

$$B_{12}^{'} = \frac{-1}{0.19797 \text{ p.u.}} = -5.0513 \text{ p.u.} \tag{4.23}$$

$$B_{11}^{'} = \frac{1}{0.05917 \text{ p.u.}} + \frac{1}{0.19797 \text{ p.u.}} + \frac{1}{0.17632 \text{ p.u.}} + \frac{1}{0.17388 \text{ p.u.}} = 33.374 \text{ p.u.} \tag{4.24}$$

Thus, the complete **B**' matrix for the IEEE 14-bus test system is shown in Equation (4.25).

$$\mathbf{B}' = \begin{bmatrix} 33.374 & -5.0513 & -5.6715 & -5.7511 & 0 & 0 & 0 & 0 & 0 & 0 & 0 & 0 & 0 \\ -5.0513 & 10.898 & -5.8469 & 0 & 0 & 0 & 0 & 0 & 0 & 0 & 0 & 0 & 0 \\ -5.6715 & -5.8469 & 41.846 & -23.747 & 0 & -4.7819 & 0 & -1.798 & 0 & 0 & 0 & 0 & 0 \\ -5.7511 & 0 & -23.747 & 37.95 & -3.9679 & 0 & 0 & 0 & 0 & 0 & 0 & 0 & 0 \\ 0 & 0 & 0 & -3.9679 & 20.581 & 0 & 0 & 0 & 0 & -5.0277 & -3.9092 & -7.6764 & 0 \\ 0 & 0 & -4.7819 & 0 & 0 & 19.549 & -5.677 & -9.0901 & 0 & 0 & 0 & 0 & 0 \\ 0 & 0 & 0 & 0 & 0 & -5.677 & 5.677 & 0 & 0 & 0 & 0 & 0 & 0 \\ 0 & 0 & -1.798 & 0 & 0 & -9.0901 & 0 & 26.421 & -11.834 & 0 & 0 & 0 & -3.6985 \\ 0 & 0 & 0 & 0 & 0 & 0 & 0 & -11.834 & 17.041 & -5.2064 & 0 & 0 & 0 \\ 0 & 0 & 0 & 0 & -5.0277 & 0 & 0 & 0 & -5.2064 & 10.234 & 0 & 0 & 0 \\ 0 & 0 & 0 & 0 & -3.9092 & 0 & 0 & 0 & 0 & 0 & 8.9122 & -5.003 & 0 \\ 0 & 0 & 0 & 0 & -7.6764 & 0 & 0 & 0 & 0 & 0 & -5.003 & 15.553 & -2.8734 \\ 0 & 0 & 0 & 0 & 0 & 0 & 0 & -3.6985 & 0 & 0 & 0 & -2.8734 & 6.5719 \end{bmatrix} \tag{4.25}$$

Ultimately, by Equation (4.25), the power flowing on each line *l* connecting buses *i* and *j* can then be calculated according to Equation (4.26).

$$f_l = P_{ij} = \frac{1}{x_{ij}}\left(\theta_i - \theta_j\right) \tag{4.26}$$

4.2 Calculation of Distribution Factors

The distribution factors use the standard matrices calculated in the DC power flow equations in the previous section. Given the linearity of the DC power flow model, the changes due to any set of system conditions can be calculated. For this particular investigation, the load, or power withdrawn from the bus, is changed at all load buses. Thus, a relationship between the resulting change in the bus voltage angles $\Delta\theta$ and the change in the bus power injections ΔP is desired. Manipulating Equation (4.25) to calculate the change in bus voltage angles given a known change in the bus power injections results in Equation (4.27), and thus the relationship between the **X** matrix and the $\mathbf{B}'$ matrix is defined in Equation (4.28).

$$\mathbf{\Delta\theta = X\Delta P} \tag{4.27}$$

$$\mathbf{X} = (\mathbf{B}')^{-1}|_{\text{incremented with a row and column of zeros at the swing bus}}$$

$$\underline{\boldsymbol{X}} = \left[\begin{array}{c|ccc} 0 & 0 & . \quad . & 0_N \\ \hline 0 & & & \\ . & & & \\ . & & \underline{\boldsymbol{B}}'^{-1} & \\ . & & & \\ 0_N & & & \end{array}\right] \tag{4.28}$$

The power on the swing bus is equal to the sum of the injections of the remaining buses in the system. Therefore, in Equation (4.27), it can also be assumed that the change in power on the swing bus is the sum of the perturbations in the injections on the remaining buses. Thus, the **X** matrix in Equation (4.28) includes an entry of zeros in the row and column of the system swing bus. For the IEEE 14-bus test system used in this investigation with Bus 1 as the slack bus, **X** matrix for this system is shown in Equation (4.29) and is calculated from Equation (4.28) and the $\mathbf{B}'$ matrix in Equation (4.25).

X=

0	0	0	0	0	0	0	0	0	0	0	0	0	0
0	0.049586	0.044173	0.039496	0.036127	0.037272	0.038892	0.038892	0.038574	0.038343	0.037817	0.037375	0.037456	0.038085
0	0.044173	0.1495	0.069463	0.056531	0.060929	0.067144	0.067144	0.065925	0.065037	0.063019	0.061324	0.061632	0.064048
0	0.039496	0.069463	0.095352	0.07416	0.081366	0.091552	0.091552	0.089553	0.088098	0.084791	0.082013	0.082519	0.086477
0	0.036127	0.056531	0.07416	0.086862	0.082542	0.076437	0.076437	0.077635	0.078507	0.080489	0.082154	0.081851	0.079479
0	0.037272	0.060929	0.081366	0.082542	0.24846	0.12676	0.12676	0.15064	0.16803	0.20754	0.24073	0.23469	0.18739
0	0.038892	0.067144	0.091552	0.076437	0.12676	0.22418	0.22418	0.18394	0.17378	0.15068	0.13128	0.13481	0.16246
0	0.038892	0.067144	0.091552	0.076437	0.12676	0.22418	0.40033	0.18394	0.17378	0.15068	0.13128	0.13481	0.16246
0	0.038574	0.065925	0.089553	0.077635	0.15064	0.18394	0.18394	0.23359	0.21885	0.18534	0.1572	0.16232	0.20243
0	0.038343	0.065037	0.088098	0.078507	0.16803	0.17378	0.17378	0.21885	0.2793	0.22463	0.17204	0.17518	0.19976
0	0.037817	0.063019	0.084791	0.080489	0.20754	0.15068	0.15068	0.18534	0.22463	0.31395	0.20579	0.20442	0.19368
0	0.037375	0.061324	0.082013	0.082154	0.24073	0.13128	0.13128	0.1572	0.17204	0.20579	0.37377	0.27784	0.20995
0	0.037456	0.061632	0.082519	0.081851	0.23469	0.13481	0.13481	0.16232	0.17518	0.20442	0.27784	0.31155	0.22757
0	0.038085	0.064048	0.086477	0.079479	0.18739	0.16246	0.16246	0.20243	0.19976	0.19368	0.20995	0.22757	0.36558

(4.29)

Sensitivity factors can be calculated for a change in power at bus *i*, which is compensated by an opposite change in power at the swing bus. The PTDF ρ_{lk} for each line *l* connecting bus *i* to bus *j* with respect to a change in injection at bus *k* may be calculated by applying Equations (4.26) and (4.27) using Equation (4.30).

$$\rho_{l,k} = \frac{df_l}{dP_k} = \frac{d}{dP_k}\left[\frac{1}{x_l}\left(\theta_i - \theta_j\right)\right] = \frac{1}{x_l}\left(\frac{d\theta_i}{dP_k} - \frac{d\theta_j}{dP_k}\right) = \frac{X_{ik} - X_{jk}}{x_l} \tag{4.30}$$

In Equation (4.30), x_l represents the line reactance of line *l* connecting buses *i* and *j*, and the values X_{ik} and X_{jk} are the respective elements of the **X** matrix defined in Equation (4.28). The distribution factors $\rho_{l,k}$ are computed for each load bus for the test system using Equation (4.30) and are listed in Table 4.1.

Because this experiment is concerned with the error or change in load at the load buses, ΔP_k will be negative, the opposite of an injection at bus *k*. With *m* load buses in the system, the resulting change in the flow of real power on line *l* connecting buses *i* and *j* is calculated as ΔP_l using the sensitivity factor from Equation (4.30) as shown in Equation (4.31).

$$\Delta f_l = \sum_{k=1}^{m} \rho_{lk} \Delta P_k \tag{4.31}$$

A test of the sensitivity factors defined in Equation (4.30) was then conducted using Equation (4.31). The load at one load bus was increased by 20% of the base case load value with all other loads remaining the same as the respective base case values. Power flows were performed to compute the real power flow on all of the lines. The change in the load is calculated as the difference between the newly calculated flow on the line and the base case value of the flow on the line. This simulated change in the flow on the line was compared to the calculated change in the flow on the line using Equation (4.31) and the sensitivity factors listed in Table 4.1.

Table 4.1 Distribution Factors for Load Buses for the IEEE 14-Bus Test System

Line *l*	Bus *i*	Bus *j*	$\rho_{l,2}$	$\rho_{l,3}$	$\rho_{l,4}$	$\rho_{l,5}$	$\rho_{l,6}$	$\rho_{l,9}$	$\rho_{l,10}$	$\rho_{l,11}$	$\rho_{1,12}$	$\rho_{1,13}$	$\rho_{1,14}$
1	1	2	-0.83803	-0.74654	-0.66751	-0.61056	-0.62992	-0.65192	-0.648	-0.6391	-0.6317	-0.633	-0.6437
2	1	5	-0.16197	-0.25346	-0.33249	-0.38944	-0.37008	-0.34808	-0.352	-0.3609	-0.3683	-0.367	-0.3563
3	2	3	0.027343	-0.53203	-0.15137	-0.10307	-0.11949	-0.13815	-0.1348	-0.1273	-0.121	-0.1221	-0.1311
4	2	4	0.057224	-0.14343	-0.31678	-0.2157	-0.25008	-0.28913	-0.2822	-0.2664	-0.2532	-0.2556	-0.2745
5	2	5	0.077406	-0.071076	-0.19935	-0.29178	-0.26035	-0.22464	-0.231	-0.2454	-0.2575	-0.2553	-0.2381
6	3	4	0.027343	0.46797	-0.15137	-0.10307	-0.11949	-0.13815	-0.1348	-0.1273	-0.121	-0.1221	-0.1311
7	4	5	0.080021	0.30709	0.50325	-0.30164	-0.02793	0.28302	0.22776	0.10215	-0.0034	0.01584	0.16621
8	4	7	0.0028891	0.011087	0.018169	-0.01089	-0.21708	-0.45134	-0.4097	-0.3151	-0.2356	-0.2501	-0.3633
9	4	9	0.0016577	0.0063616	0.010425	-0.006249	-0.12456	-0.25897	-0.2351	-0.1808	-0.1352	-0.1435	-0.2085
10	5	6	-0.0045468	-0.017449	-0.028595	0.017139	-0.65836	-0.28969	-0.3552	-0.5041	-0.6292	-0.6065	-0.4282
11	6	11	-0.002738	-0.010507	-0.017219	0.010321	0.20573	-0.17445	-0.2846	-0.535	0.17569	0.15221	-0.0316
12	6	12	-0.0004021	-0.001543	-0.002529	0.0015158	0.030216	-0.025622	-0.0157	0.00686	-0.5201	-0.1687	-0.0882
13	6	13	-0.0014067	-0.005398	-0.008847	0.0053024	0.1057	-0.089625	-0.0549	0.02399	-0.2849	-0.59	-0.3084
14	7	8	7.88E-17	1.58E-16	7.88E-17	7.88E-17	0	0	0	0	0	0	0
15	7	9	0.0028891	0.011087	0.018169	-0.01089	-0.21708	-0.45134	-0.4097	-0.3151	-0.2356	-0.2501	-0.3633
16	9	10	0.002738	0.010507	0.017219	-0.010321	-0.20573	0.17445	-0.7154	-0.465	-0.1757	-0.1522	0.03162
17	9	14	0.0018088	0.0069414	0.011376	-0.006818	-0.13591	0.11525	0.07061	-0.0308	-0.1951	-0.2413	-0.6034
18	10	11	0.002738	0.010507	0.017219	-0.010321	-0.20573	0.17445	0.2846	-0.465	-0.1757	-0.1522	0.03162
19	12	13	-0.0004021	-0.001543	-0.002529	0.0015158	0.030216	-0.025622	-0.0157	0.00686	0.47994	-0.1687	-0.0882
20	13	14	-0.0018088	-0.006941	-0.011376	0.0068183	0.13591	-0.11525	-0.0706	0.03085	0.19509	0.24132	-0.3966

32

For example, an increase of 4.34 MW of load at bus 2 yields a value of $\Delta P_2 = -4.34$ MW. Table 4.1 is used to find the distribution factors for each of the lines with respect to bus 2, which is the third column in Table 4.1. The value for ΔP_2 and the corresponding distribution factors are used to calculate the change in the line flow for all of the lines using Equation (4.31). The resulting values are displayed in Table 4.2 along with the actual change in line flows obtained from the power flows.

Table 4.2. Analysis of Distribution Factors with Change in Bus 2 Load

Perturbation at Bus 2 ΔP_2 (MW)	Power Flow Δf_l (MW)	Calculated Δf_l (Equation 4.2.4) (MW)	% Error (%)
-4.34	3.83	3.637	5.04
-4.34	0.75	0.7029	6.27
-4.34	-0.122	-0.1187	2.73
-4.34	-0.256	-0.2484	2.99
-4.34	-0.345	-0.3359	2.63
-4.34	0.118	0.1187	0.57
-4.34	-0.343	-0.3473	1.25
-4.34	-0.014	-0.01254	10.44
-4.34	-0.008	-0.007194	10.07
-4.34	0.023	0.01973	14.20
-4.34	0.0139	0.01188	14.51
-4.34	0.0018	0.001745	3.04
-4.34	0.007	0.006105	12.78
-4.34	-0.000036	0.00	0.00
-4.34	-0.014	-0.01254	10.44
-4.34	-0.0137	-0.01188	13.26
-4.34	-0.0086	-0.007850	8.72
-4.34	-0.0137	-0.01188	13.26
-4.34	0.0017	0.001745	2.66
-4.34	0.0087	0.00785	9.77

In the same process as that used for Table 4.2, a single load was changed for each power flow to calculate the error in the distribution factors with respect to the change in load for each load bus. Table 4.3 displays the amount of error that was found for each distribution factor using this method. For example, there was a 0.57% error in the calculation of the change in the power

Table 4.3 Percent Error of the Change in Line Flows Using Distribution Factors for Load Buses for the IEEE 14-Bus Test System

Line l	**%Error** ΔP_2 $\rho_{l,2}$	**%Error** ΔP_3 $\rho_{l,3}$	**%Error** ΔP_4 $\rho_{l,4}$	**%Error** ΔP_5 $\rho_{l,5}$	**%Error** ΔP_6 $\rho_{l,6}$	**%Error** ΔP_9 $\rho_{l,9}$	**%Error** ΔP_{10} $\rho_{l,10}$	**%Error** ΔP_{11} $\rho_{l,11}$	**%Error** ΔP_{12} $\rho_{1,12}$	**%Error** ΔP_{13} $\rho_{1,13}$	**%Error** ΔP_{14} $\rho_{l,14}$
1	5.04	13.07	10.50	9.01	8.97	10.76	10.96	10.52	10.39	10.98	12.81
2	6.27	12.25	9.10	7.22	7.48	8.11	8.57	8.14	9.03	9.18	10.62
3	2.73	10.08	8.93	7.84	7.38	10.72	10.77	9.07	8.90	9.66	12.38
4	2.99	2.59	4.19	3.85	2.75	4.27	4.70	4.37	4.38	4.69	6.53
5	2.63	1.60	4.33	2.74	3.77	4.03	4.64	4.56	5.37	5.44	6.90
6	0.57	0.37	5.60	5.05	4.07	7.48	7.71	6.20	5.40	6.33	9.33
7	1.25	1.86	0.52	2.66	51.87	1.63	3.53	23.28	90.25	52.75	7.68
8	10.44	15.77	20.69	18.23	10.51	0.30	0.47	3.06	8.05	5.66	0.30
9	10.07	16.77	23.34	35.69	10.72	0.92	0.99	3.73	8.50	6.14	0.37
10	14.20	17.40	22.34	18.41	4.11	2.05	3.56	4.36	5.92	5.68	6.72
11	14.51	18.24	22.75	14.51	7.45	3.10	2.83	2.35	4.40	8.84	27.18
12	3.04	5.30	22.26	92.00	31.42	10.59	2.01	100.02	10.79	5.27	3.48
13	12.78	18.64	25.16	15.14	8.11	3.68	9.32	39.94	11.74	5.46	6.88
14	0.00	0.00	0.00	0.00	0.00	0.00	0.00	0.00	0.00	0.00	0.00
15	10.44	15.77	19.21	18.23	10.51	0.0035	0.33	3.06	8.05	5.66	0.39
16	13.26	17.07	21.01	15.35	8.74	1.32	0.10	1.53	5.74	10.06	25.62
17	8.72	14.36	21.59	29.55	13.98	1.64	4.79	49.95	10.60	3.41	1.85
18	13.26	17.28	21.50	14.51	8.51	1.84	1.60	1.31	5.48	9.85	25.98
19	2.66	3.73	19.68	92.00	32.71	12.73	3.88	100.02	12.32	7.16	5.30
20	9.77	14.08	21.93	31.19	14.45	1.46	4.65	49.95	11.06	4.07	2.53

flow on line 6 due to a 20% increase in the load at bus 2 using the PTDF, $\rho_{6,2}$, and power flow calculations. The percent error values in Table 4.3 range from 0.37% to 100%. The percent error in the calculation of the power flow on the lines increases when the actual power flow on the line decreases by as small as 0.1 MW. As a result, the PTDFs provide reasonably accurate results when the real power flow on the line is large.

4.3 Calculation of the Hourly Revenue

To calculate the distribution of the hourly revenue due to uncertainty in the load forecast, three values are necessary: the transmission tariff, the length of the transmission line, and the megawatt flow on each transmission line. The first two values are constant, but the flow on the transmission lines must be constantly calculated. The amount of error due to the uncertainty in the load forecast can be represented in terms of a change in the injection at the load buses. Therefore, the sensitivity factors discussed in the previous subsection can be applied to calculate the change in the flow on each transmission line in the system. The analytical method first addresses the uncertainty in the load forecast by defining a random variable $\Delta\upsilon$, which represents the deviation or error from the forecasted load for the hour. As in the Monte Carlo simulations, $\Delta\upsilon$ is sampled from a normal distribution with a mean $\mu = 0$ and a specified standard deviation σ_υ. As a result, Equation (4.32) displays the amount of error, or change in injection in the power at each load bus *k*.

$$\Delta P_k = \alpha_k \Delta\upsilon P_{tot}^0 \tag{4.32}$$

The variable P_{tot}^0 is defined as the total system load forecasted for the hour. The variable α_k represents the percentage of the total system load at each load bus *k*. Table 4.4 displays the values of α_k for each of the load buses in the IEEE 14-bus test system using the base case values of the system defined in Chapter 2 with a base case system load of 259 MW.

Table 4.4 Percentage of System Load at Each Load Bus

Load Bus *k*	**Base Case Bus Load (MW)**	**Base Case System Load (MW)**	**α_k**
2	21.7	259	0.083784
3	94.2	259	0.36371
4	47.8	259	0.18456
5	7.6	259	0.029344
6	11.2	259	0.043243
9	29.5	259	0.1139
10	9.0	259	0.034749
11	3.5	259	0.013514
12	6.1	259	0.023552
13	13.5	259	0.052124
14	14.9	259	0.057529

Substitution of Equation (4.32) into Equation (4.31) yields Equation (4.33).

$$\Delta f_l = \sum_{k=1}^{m} \rho_{lk} \alpha_k \Delta \upsilon P_{tot}^0 \tag{4.33}$$

In Equation (4.33), the topology of the network remains the same and the distribution of the system load among the load buses is constant for this investigation. As a result, the terms ρ_{ik} and α_k only need to be calculated once. Thus, these two terms can be set equivalent to a constant c_l with the relationship shown in Equation (4.34).

$$c_l = \sum_{k=1}^{m} \rho_{lk} \alpha_k \tag{4.34}$$

Using Equation (4.33), the flow on each transmission line as a result of the error in the load forecast is derived in Equation (4.35), where f_l^0 is the flow on line l resulting from the base case forecasted load for the hour.

$$f_l = f_l^0 + \Delta f_l = f_l^0 + \sum_{k=1}^{m} \rho_{lk} \alpha_k \Delta \upsilon P_{tot}^0 \tag{4.35}$$

As stated in Chapter 2, the revenue generated from the transmission tariffs I_l is directly related by Equation (2.5) to the transmission tariff t, the transmission line lengths l_l, and the megawatt flows on the transmission lines P_l. The transmission tariff remains constant, and the transmission line lengths do not change. Therefore, Equation (2.5) can be simplified by assigning a constant for the value of the transmission tariff and the line lengths in Equation (4.36).

$$d_l = t l_l \tag{4.36}$$

Substituting Equations (4.35) and (4.36) into Equation (2.5), an expression for the total system revenue I generated for the hour is derived in Equation (4.37).

$$I = \sum_{\substack{l \\ total \\ lines}} \left[\left(f_l^0 + \Delta f_l \right) d_l \right] = \sum_{\substack{l \\ total \\ lines}} \left\{ \left[f_l^0 + \left(\sum_{k=1}^{m} \rho_{lk} \alpha_k \right) \Delta \upsilon P_{tot}^0 \right] d_l \right\} \tag{4.37}$$

Equation (4.37) can be written in terms of the total base case system revenue for the hour I^0 using the relationship in Equation (2.5) as shown in Equation (4.38).

$$I = \sum_{\substack{l \\ total \\ lines}} \left\{ P_l^0 d_l + \left[\left(\sum_{k=1}^{m} \rho_{lk} \alpha_k \right) \Delta \upsilon P_{tot}^0 \right] d_l \right\} = I^0 + \sum_{\substack{l \\ total \\ lines}} \left\{ \left[\left(\sum_{k=1}^{m} \rho_{lk} \alpha_k \right) \Delta \upsilon P_{tot}^0 \right] d_l \right\} \tag{4.38}$$

The constants in Equation (4.38) can be grouped into one large constant A as defined in Equation (4.39) using the definitions from Equations (4.34) and (4.36).

$$A = \sum_{\substack{l \\ total \\ lines}} \left[\left(\sum_{k=1}^{m} \rho_{lk} \alpha_k \right) d_l \right] \tag{4.39}$$

As a result, Equation (4.39) can be substituted into Equation (4.38) to calculate the total change in system revenue for the hour ΔI in Equation (4.40).

$$\Delta I = I - I^0 = A P_{tot}^0 \Delta \upsilon \tag{4.40}$$

The equations listed above are applied to the test system. Table 4.5 lists the constants for the system calculated using Equations (4.34), (4.36), and (4.39) and the line parameters listed in Chapter 2.

Table 4.5 IEEE 14-Bus Test System Analytical Constants

Line Number	Bus *i*	Bus *j*	Line Length (miles)	$\Sigma\rho_l$	c_l	d_l ($/MW)	A_l ($)
1	1	2	4.024	-6.4707	0.70039	0.16	0.11
2	1	5	15.170	-3.6600	0.29961	0.61	0.18
3	2	3	13.465	-1.6531	0.26624	0.54	0.14
4	2	4	11.992	-2.4897	0.20439	0.48	0.10
5	2	5	11.826	-2.1971	0.14598	0.47	0.07
6	3	4	11.632	-0.6531	-0.097465	0.47	-0.05
7	4	5	2.864	1.3524	-0.25305	0.11	-0.03
8	4	7	0	-2.2209	0.11147	0	0
9	4	9	0	-1.2743	0.063958	0	0
10	5	6	0	-3.5047	0.16319	0	0
11	6	11	54.112	-0.5122	0.024766	2.16	0.05
12	6	12	69.595	-0.7841	0.029194	2.78	0.08
13	6	13	35.441	-1.2085	0.065984	1.42	0.09
14	7	8	47.923	-7.8785e-16	1.2231e-16	1.92	0
15	7	9	29.929	-2.2209	0.11147	1.20	0.13
16	9	10	22.989	-1.4905	0.023497	0.92	0.02
17	9	14	73.559	-1.0074	0.038026	2.94	0.11
18	10	11	52.254	-0.4878	-0.011252	2.09	-0.02
19	12	13	54.379	0.2159	0.0056418	2.18	0.01
20	13	14	94.681	0.00743	0.019503	3.79	0.07
TOTAL							1.09

4.4 Distribution of System Revenue

Equation (4.40) creates an important relationship between the random variate $\Delta\upsilon$ and system revenue for the hour. Because the random variable is sampled from a normal distribution with a zero mean and a known standard deviation, $\Delta\upsilon \sim N(0, \sigma_\upsilon)$, Equation (4.40) indicates that the change in the system revenue, ΔI, also has a normal distribution with some known mean and a variance, $\Delta I \sim N(0, \sigma_{revenue})$. The following mathematical properties can be used in the derivation of the standard deviation of the system revenue in Equations (4.41) and (4.42) where D is a scalar, Y is a known distribution, $E[Y]$ is the expected value, or mean, of the distribution of Y, and $VAR[Y]$ is the variance, or the standard deviation squared, of the distribution of Y.

$$\mu = E[DY] = DE[Y] \tag{4.41}$$

$$\sigma^2 = VAR[DY] = D^2 VAR[Y] \tag{4.42}$$

With the relationship in Equation (4.40) and the statistical properties in Equations (4.41) and (4.42), the mean and standard deviation of the change in revenue can be derived using Equations (4.43) and (4.44), respectively.

$$\mu_{revenue} = E\left[AP_{tot}^0 \Delta\upsilon\right] = AP_{tot}^0 E[\Delta\upsilon] = AP_{tot}^0 \mu_\upsilon = 0 \tag{4.43}$$

$$\sigma_{revenue} = \sqrt{\sigma_{revenue}^2} = \sqrt{VAR\left[AP_{tot}^0 \Delta\upsilon\right]} = \sqrt{\left(AP_{tot}^0\right)^2 VAR[\Delta\upsilon]} = \sqrt{\left(AP_{tot}^0\right)^2 \sigma_\upsilon^2} = AP_{tot}^0 \sigma_\upsilon \tag{4.44}$$

Equation (4.44) indicates that the standard deviation of the total system revenue for each hour will vary depending directly on the total forecasted system load. The standard deviation is calculated according to Equation (3.2).

4.5 Analytical Method Results

The analytical methods discussed above were then used to calculate the distributions of the system revenue for each hour on January 14, 2004 as shown in Table 4.6. The mean of the system revenue was scaled to match the base case system revenue value.

Table 4.6 Calculated Distributions from the Analytical Method for January 14, 2004

Time	Date	Base Case Load, P_{tot}^{0} (MW)	Base Case Revenue, I^{0} ($)	Standard Deviation $\sigma_{revenue}$ ($)
100	1/14/04	305	390.96	9.96
200	1/14/04	299	382.95	9.76
300	1/14/04	298	381.11	9.72
400	1/14/04	300	384.06	9.79
500	1/14/04	307	393.56	10.03
600	1/14/04	332	426.22	10.83
700	1/14/04	371	479.04	12.13
800	1/14/04	395	510.85	12.91
900	1/14/04	392	506.51	12.81
1000	1/14/04	389	501.86	12.69
1100	1/14/04	385	496.49	12.56
1200	1/14/04	381	491.41	12.43
1300	1/14/04	380	490.73	12.42
1400	1/14/04	379	488.53	12.36
1500	1/14/04	375	483.91	12.25
1600	1/14/04	376	484.78	12.27
1700	1/14/04	391	504.46	12.76
1800	1/14/04	416	538.33	13.59
1900	1/14/04	421	544.99	13.75
2000	1/14/04	416	538.02	13.58
2100	1/14/04	408	527.33	13.32
2200	1/14/04	389	502.73	12.71
2300	1/14/04	362	466.21	11.81
2400	1/14/04	305	430.47	10.93

The probability density function (pdf) of a normal distribution is given in Equation (4.46).

$$F(x) = \frac{1}{\sqrt{2\pi}\sigma} e^{\left[\frac{-(x-\mu)^2}{2\sigma^2}\right]} \tag{4.46}$$

The mean and standard deviation of the normal distribution are represented by μ and σ, respectively. Using the values for the base case revenue and standard deviation calculated in Table 4.6, a probability density function can be drawn according to the relationship in Equation (4.46). The representation of the distribution of the system revenue for hour 329 (1700 hours on January 14, 2004) is shown in Figure 4.3. The figure displays the typical bell-curve of the probability density function of the normal distribution.

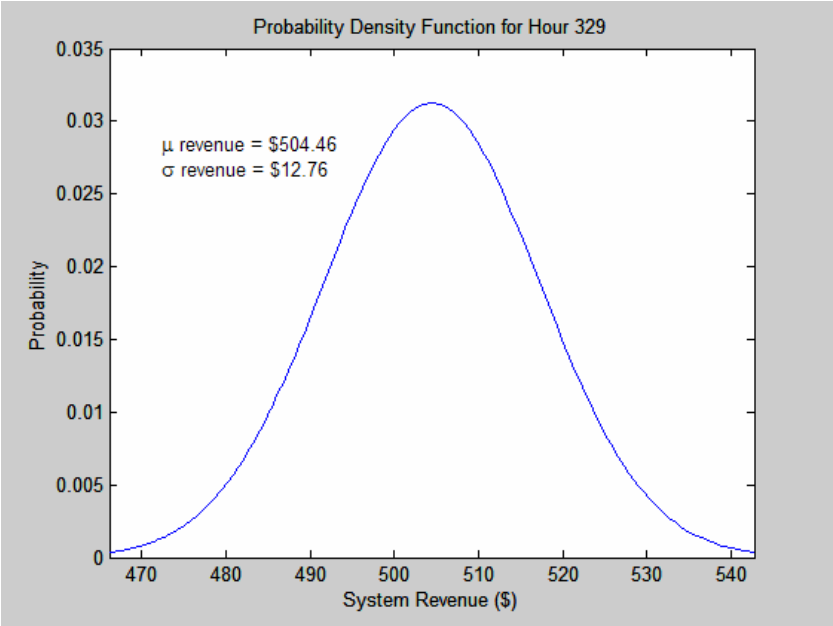

Figure 4.3 Normal distribution of the system revenue using the analytical calculated standard deviation

5. Comparison of Solutions

The two methods, Monte Carlo simulations and the Analytical Method, presented in Chapters 3 and 4 can be compared based on their results presented in the previous chapters. Both methods provide results for the distribution of the system revenue. Table 5.1 lists the results from both methods for January 14, 2004.

Table 5.1 Comparison of Monte Carlo and Analytical Methods for January 14, 2004

Hour	Time	Date	Mean Total Revenue ($)	Base Case Total Revenue I^0 ($)	Error in Total Revenue (%)	Simulated Standard Deviation $\sigma_{revenue}$ ($)	Analytical Standard Deviation $\sigma_{revenue}$ ($)	Error in Standard Deviation (%)
313	100	1/14/2004	390.66	390.96	0.08	12.49	9.96	20.24
314	200	1/14/2004	382.23	382.95	0.19	11.28	9.76	13.44
315	300	1/14/2004	378.27	381.11	0.75	12.82	9.72	24.19
316	400	1/14/2004	383.13	384.06	0.24	12.29	9.79	20.33
317	500	1/14/2004	394.60	393.56	0.26	13.23	10.03	24.21
318	600	1/14/2004	427.99	426.22	0.41	14.47	10.83	25.17
319	700	1/14/2004	478.56	479.04	0.10	14.23	12.13	14.77
320	800	1/14/2004	510.09	510.85	0.15	16.94	12.91	23.77
321	900	1/14/2004	505.21	506.51	0.26	14.03	12.81	8.73
322	1000	1/14/2004	501.30	501.86	0.11	13.83	12.69	8.21
323	1100	1/14/2004	497.15	496.49	0.13	13.93	12.56	9.83
324	1200	1/14/2004	490.09	491.41	0.27	12.79	12.43	2.78
325	1300	1/14/2004	494.68	490.73	0.80	13.83	12.42	10.21
326	1400	1/14/2004	488.98	488.53	0.09	15.66	12.36	21.05
327	1500	1/14/2004	484.86	483.91	0.20	15.24	12.25	19.63
328	1600	1/14/2004	484.97	484.78	0.04	14.77	12.27	16.93
329	1700	1/14/2004	502.80	504.46	0.33	14.16	12.76	9.92
330	1800	1/14/2004	537.99	538.33	0.06	17.39	13.59	21.86
331	1900	1/14/2004	543.86	544.99	0.21	16.76	13.75	17.95
332	2000	1/14/2004	536.59	538.02	0.27	19.71	13.58	31.10
333	2100	1/14/2004	527.99	527.33	0.13	14.94	13.32	10.85
334	2200	1/14/2004	500.62	502.73	0.42	15.19	12.71	16.31
335	2300	1/14/2004	464.40	466.21	0.39	13.47	11.81	12.33
336	2400	1/14/2004	427.75	430.47	0.64	14.41	10.93	24.14

Table 5.1 displays the percent difference in both the mean and standard errors from the results using the Monte Carlo simulations and the analytical method. The percentage of error from the base case system revenue values from Chapter 2 is calculated for the mean value of revenue obtained from the 100 samples in the Monte Carlo simulations for all hours. The percentage of error was less than 1%. However, the percentage of error in the standard deviation calculated using the Monte Carlo simulation results and the analytical method for each hour was more significant with a range of 1.28% to 30.96%. This range of differences in the standard error could be due to the calculation of the PTDFs. As shown in Table 4.3, error is inherent in the calculation of the PTDFs. This error propagates through the analytical calculations to contribute to the overall difference in the percent difference between the two values.

Another source of error in the calculation of the standard deviation could be due to the fact that the power losses in the transmission lines were not accounted for in the analytical method, whereas the losses were considered in the power flows computed in the Monte Carlo simulations. Therefore, the revenues obtained from the simulations would possibly be smaller than the mean value for the revenue generated using the analytical method.

Finally, some of the values obtained using the Monte Carlo simulations may be different from those obtained using the analytical methods because the random number generator also possesses some percentage of error in the 100 random samples generated, as discussed in Chapter 3. More Monte Carlo simulations would have to be performed with different numbers of samples for each hour to test the accuracy and the optimal number of samples for the hour.

6. Line Outages

6.1 Monte Carlo Simulation

This chapter reports on the extension of the previous work to include the effect of line outages on transmission revenues together with the uncertainty in the load. A Monte Carlo method was performed to develop a data set that could be used to quantify the impact of topology on transmission revenues. The outages of the transmission lines were simulated by opening the transmission lines one at a time and analyzing the effects for each hour of uncertain load as indicated in the flowchart of Figure 6.1.

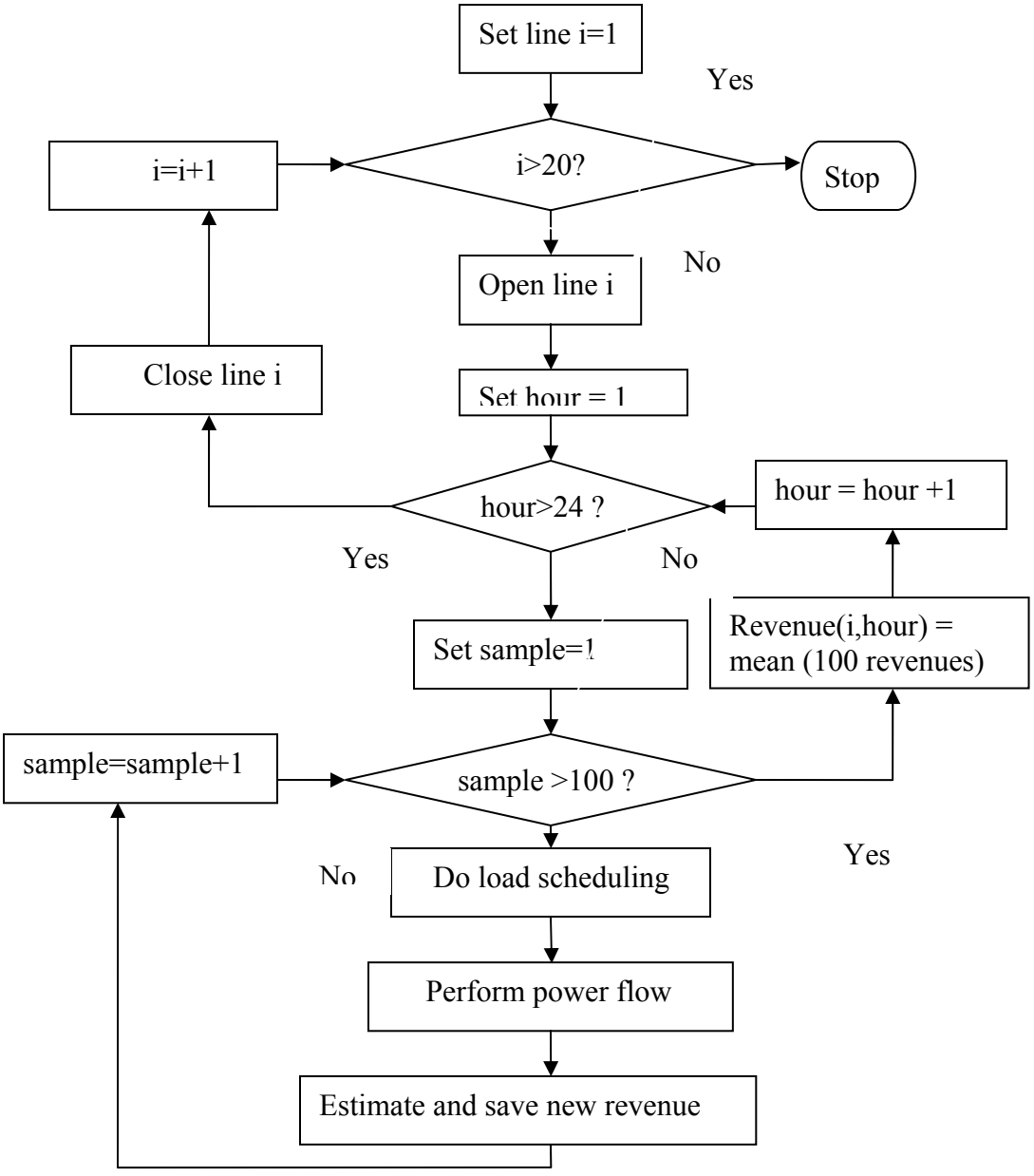

Figure 6.1 Flow chart of the Monte Carlo simulation

As in the earlier chapters, Monte Carlo simulations were performed on the IEEE 14-bus test system for each hour of January 14, 2004. Table 6.1 shows the sample mean results of the Monte Carlo simulation. In the experiment presented here, a sample size of 100 was used. The standard deviation of the revenues for the case of 100 samples was also computed and tabulated in Table 6.2. The values that are blank were from a case were at least one of the100 random load-flow solutions did not converge.

Table 6.1 is read as follows: the second row of the table corresponds to the hourly revenue for the IEEE 14-bus system for hours 1 through 24 when line 1 connecting bus 1 and bus 2 is out. The second column of the table corresponds to the hourly revenue earned between 12:00 a.m. and 1:00 a.m. when lines 1 through 20 are opened and closed systematically, with one line open at a time. The last row gives the mean value (simple average) of the revenues for the corresponding hour.

Table 6.1 Expected Revenues Computed Using 100 Samples Per Hour.

	Hr1	2	3	4	5	6	7	8	9	10	11	12	13	14	15	16	17	18	19	20	21	22	23	24
Ln1																								
2	377	370	368	371	380	411	463					476	475	472	468	469							450	415
3	447	437	435	439	450	490																		496
4	396	388	386	389	398	431	484	517	512	508	502	497	496	494	489	490	510	545	552	544	534	508	471	435
5	379	372	370	373	382	413	464	495	491	486	481	476	475	473	469	469	489	521	528	521	511	487	451	417
6	376	368	366	369	378	410	460	491	487	483	477	472	472	470	465	466	485	517	524	517	507	483	448	414
7	433	424	422	425	436	474	534	570	565	560	553	548	547	544	539	540	562	601	609	601	588	560	519	479
8	407	398	397	400	410	444	498	532	527	522	517	511	511	508	503	504	525	561	568	561	549	523	485	449
9	426	417	415	419	429	464	522	556	552	547	541	535	535	532	527	528	550	587	594	586	575	548	508	469
10	601	589	586	591	605	657																	723	664
11	394	386	384	387	397	430	484	517	512	508	502	497	496	494	489	490	510	544	551	544	533	508	471	434
12	390	382	380	383	393	425	478	510	505	501	496	490	490	487	483	484	503	537	544	537	526	502	465	430
13	446	437	435	438	449	486	547	584	579	573	567	561	560	558	552	553	576	616	624	616	603	574	532	491
14	394	386	384	387	397	429	481	513	509	504	499	494	493	491	486	487	507	541	548	541	530	505	468	433
15	413	404	402	405	415	450	505	540	535	530	524	519	518	516	511	512	533	570	577	569	558	531	492	454
16	401	393	391	394	404	437	490	523	518	514	508	503	502	500	495	496	516	551	558	551	540	515	477	441
17	407	399	397	400	410	444	500	534	529	524	518	513	512	510	505	506	527	563	571	563	552	525	486	448
18	383	376	374	377	386	418	471	502	498	493	488	483	482	480	476	476	496	529	536	529	518	494	458	422
19	384	376	375	377	387	419	471	502	498	493	488	483	482	480	476	476	496	529	536	529	518	494	458	423
20	385	377	376	378	388	420	473	505	501	496	491	486	485	483	478	479	498	532	539	532	521	497	460	425
Mean	416	408	406	409	419	455	513	547	543	538	532	526	526	523	518	519	540	579	586	578	566	539	498	459

Table 6.2 Standard Deviation of Revenues Computed Using 100 Samples Per Hour

	Hr#1	2	3	4	5	6	7	8	9	10	11	12	13	14	15	16	17	18	19	20	21	22	23	24
Line#1																								
2	12	12	12	12	12	14	16					15	15	16	16	16							15	14
3	15	15	15	15	16	18																		18
4	13	13	13	13	13	14	16	17	17	17	16	16	16	16	16	16	17	18	18	18	18	17	15	14
5	12	12	12	12	12	13	15	16	16	16	16	16	16	15	15	15	16	17	17	17	17	16	15	14
6	12	12	12	12	13	14	15	16	16	16	16	15	15	15	15	15	16	17	17	17	17	16	15	14
7	15	14	14	14	15	16	18	19	19	19	18	18	18	18	18	18	19	20	21	20	20	19	17	16
8	14	13	13	13	14	15	16	18	18	17	17	17	17	17	16	16	17	19	19	19	18	17	16	15
9	14	14	14	14	14	15	17	18	18	18	18	18	17	17	17	17	18	19	20	19	19	18	17	15
10	20	19	19	20	20	23																	26	23
11	13	13	13	13	13	14	16	17	17	17	16	16	16	16	16	16	17	18	18	18	17	17	16	15
12	13	13	12	13	13	14	16	17	17	16	16	16	16	16	16	16	16	18	18	18	17	16	15	14
13	15	14	14	14	15	16	18	19	19	19	19	19	19	18	18	18	19	21	21	21	20	19	18	16
14	13	13	12	13	13	14	16	17	17	16	16	16	16	16	16	16	17	18	18	18	17	16	15	14
15	13	13	13	13	14	15	17	18	18	18	17	17	17	17	17	17	18	20	20	20	19	18	16	15
16	13	13	13	13	13	14	16	17	17	17	17	16	16	16	16	16	17	18	18	18	18	17	16	14
17	13	13	13	13	13	15	17	18	18	18	17	17	17	17	17	17	18	19	20	19	19	18	16	15
18	13	12	12	12	13	14	15	16	16	16	16	16	16	16	16	16	16	17	18	17	17	16	15	14
19	13	12	12	12	13	14	15	16	16	16	16	16	16	16	16	16	16	17	18	17	17	16	15	14
20	13	12	12	12	13	14	16	17	16	16	16	16	16	16	16	16	16	18	18	18	17	16	15	14

A histogram for revenue samples obtained for hour 9 when line 20 is out is shown in Figure 6.2. The 100 revenues have a mean of 501 and a standard deviation of 16.

Transmission revenues were also computed for the base case loading with the transmission lines opened. This was in order to see how close the Monte Carlo simulation results were with the actual revenue that would have been obtained with lines opened, one at a time. No random samples of load were used. These results are shown in Table 6.3.

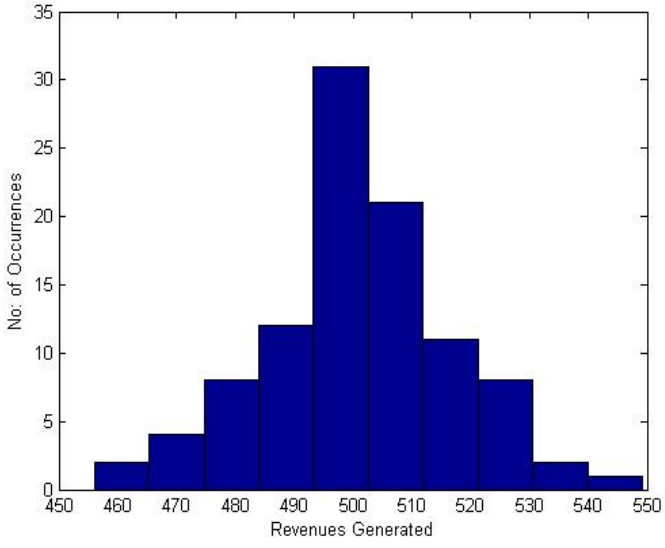

Figure 6.2 Histogram of the 100 revenues obtained for hour 9 when line 20 is open.

Table 6.3 Revenue Computed for Base Case Loading

	Hr#1	2	3	4	5	6	7	8	9	10	11	12	13	14	15	16	17	18	19	20	21	22	23	24
Ln1																								
2	377	369	368	371	380	411	462					475	474	472	467	468							450	415
3	447	437	435	439	450	490																		495
4	396	388	386	389	398	431	484	517	512	508	502	497	496	494	489	490	510	545	552	544	533	508	471	435
5	379	372	370	373	382	413	464	495	490	486	481	476	475	473	469	469	489	521	528	521	511	487	451	417
6	376	368	366	369	378	410	460	491	487	482	477	472	472	469	465	466	485	517	524	517	507	483	448	414
7	433	424	422	425	436	475	533	569	565	559	553	547	546	544	539	540	562	601	609	601	588	560	519	479
8	407	398	396	400	410	444	498	532	527	522	517	511	510	508	503	504	525	561	568	561	549	523	485	449
9	426	417	415	418	429	464	522	556	552	547	541	535	534	532	527	528	549	586	594	586	575	548	508	469
10	601	589	586	591	605	656																	723	664
11	394	386	384	387	397	430	484	516	512	508	502	497	496	494	489	490	510	544	551	544	533	508	471	434
12	390	382	380	383	393	425	478	510	505	501	495	490	490	487	483	484	503	537	544	537	526	502	465	430
13	446	437	434	438	449	486	547	583	578	573	567	561	560	558	552	553	576	616	624	615	603	574	532	491
14	394	386	384	387	397	429	481	513	509	504	499	494	493	491	486	487	507	541	548	541	530	505	468	433
15	413	404	402	406	415	449	505	539	535	530	524	519	518	515	511	511	533	569	577	569	557	531	492	454
16	401	393	391	394	404	437	490	523	518	514	508	503	502	500	495	496	516	551	558	551	540	515	477	441
17	407	399	397	400	410	444	500	534	529	524	518	513	512	510	505	506	527	563	570	563	551	525	486	448
18	383	376	374	377	386	418	471	502	498	493	488	483	482	480	476	476	496	529	536	529	518	494	458	422
19	384	376	375	377	387	419	471	502	498	493	488	483	482	480	476	476	496	529	536	529	518	494	458	423
20	385	377	376	378	388	420	473	505	500	496	491	486	485	483	478	479	498	532	539	531	521	497	460	424
Mean	416	408	406	409	419	455	513	547	543	538	532	526	525	523	518	519	540	578	585	577	565	539	498	460

Comparing Tables 6.1 and 6.3, it can be seen that the revenues obtained closely match, thus confirming that the mean value of revenue variation computed from the hundred samples of normal distribution of load is near zero.

From these raw solution sets, statistical information such as the expected revenue from the system given that one line is outaged can be computed. This would require knowledge of the probability of each line outage. Since this number would normally be quite small, the impact of this uncertainty on the revenue would also be quite small. However, there is a considerable variation in revenue depending on the network topology. This indicates that the analysis could be used to evaluate the benefits of adding new lines.

6.2 Analytical Method

This section presents an analytical method to approximate the same solution that was obtained from the exhaustive Monte Carlo solution. The analytical method utilizes the well-known concept of a Line Outage Distribution Factor (LODF) [16].

Once the LODFs are computed and the base case megawatt flows are given, it is possible to compute the change in megawatt flows on other lines due to the outage of a particular line. With the knowledge of the new megawatt flowing over the lines, the revenues for any hour can be computed using the expression, hourly revenue = 0.04*linelength'*new LineMW. While the analytical method always provides a solution for line outage cases, the cases where the Monte Carlo solutions failed to converge have been left blank here to avoid comparison.

Table 6.4 Expected Revenues Computed Analytically.

	Hr#1	2	3	4	5	6	7	8	9	10	11	12	13	14	15	16	17	18	19	20	21	22	23	24
Line#1																								
2	378	371	369	372	381	413	464					476	476	474	469	470							452	417
3	439	430	428	431	442	479																		483
4	395	387	385	388	398	431	484	517	512	508	502	497	496	494	489	490	510	545	551	544	534	508	471	435
5	380	372	370	373	382	414	466	497	492	488	483	478	477	475	470	471	490	523	530	523	513	489	453	418
6	377	369	367	370	379	411	461	492	488	483	478	473	473	470	466	467	486	518	525	518	508	484	449	415
7	426	417	415	418	428	464	522	557	552	547	541	536	535	532	527	528	550	587	594	586	575	548	508	469
8	409	401	399	402	412	446	502	535	530	526	520	515	514	511	507	508	528	563	570	563	552	526	488	451
9	427	418	416	419	430	465	522	557	552	547	541	536	535	533	528	529	550	587	594	587	575	548	508	470
10	596	584	581	585	600	649																	709	655
11	395	387	385	388	397	430	484	516	511	507	501	496	495	493	489	489	509	544	550	543	533	508	471	435
12	390	382	380	383	393	425	478	510	506	501	496	491	490	488	483	484	504	538	544	537	527	502	465	430
13	443	434	432	436	446	483	543	580	575	569	563	557	557	554	549	550	572	611	619	611	599	570	528	488
14	391	383	381	384	394	426	479	511	507	502	497	491	491	489	484	485	504	538	545	538	527	503	466	431
15	409	401	399	402	412	446	502	535	530	526	520	515	514	511	507	508	528	563	570	563	552	526	488	451
16	401	393	391	394	403	437	491	523	519	514	509	504	503	501	496	497	517	552	558	551	540	515	478	441
17	407	398	396	399	409	443	497	531	526	522	516	510	510	507	503	503	524	560	567	559	548	522	484	447
18	384	376	374	377	386	418	470	501	497	493	487	482	482	479	475	476	495	528	535	528	518	493	457	422
19	384	376	375	377	387	419	471	502	498	493	488	483	482	480	476	476	496	529	536	529	518	494	458	423
20	385	377	375	378	387	420	472	503	499	494	489	484	483	481	477	477	497	530	537	530	519	495	459	424
Mean	414	406	404	407	417	452	508	542	537	533	527	521	521	518	513	514	535	572	579	571	560	533	494	456

The following mathematical properties can be used in the derivation of the standard deviation of the system revenue [20]. If D is a scalar and Y has a known

distribution, $E[Y]$ is the expected value or mean of the distribution of Y, and $VAR[Y]$ is the variance or the standard deviation squared of the distribution of Y, then

$$\mu = E[DY] = DE[Y] \text{ and } \sigma^2 = VAR[DY] = D^2 VAR[Y] \quad (6.1)$$

Thus, if the 100 load samples of the Monte Carlo solution had a standard deviation of 3% of the base case load then the revenues will have a standard deviation of 0.03 times the revenues of the base case load. Thus, for hour 3 when line 2 is out, the revenue generated is \$369 with a standard deviation of 0.03*369 = 11.07. The standard deviations computed analytically in this manner are given in Table 6.5.

Table 6.5 Standard Deviations Computed Analytically.

	Hr#1	2	3	4	5	6	7	8	9	10	11	12	13	14	15	16	17	18	19	20	21	22	23	24
Line#1																								
2	11	11	11	11	11	12	14					14	14	14	14	14							14	13
3	13	13	13	13	13	14																		14
4	12	12	12	12	12	13	15	15	15	15	15	15	15	15	15	15	15	16	17	16	16	15	14	13
5	11	11	11	11	11	12	14	15	15	15	14	14	14	14	14	14	15	16	16	16	15	15	14	13
6	11	11	11	11	11	12	14	15	15	15	14	14	14	14	14	14	15	16	16	16	15	15	13	12
7	13	13	12	13	13	14	16	17	17	16	16	16	16	16	16	16	16	18	18	18	17	16	15	14
8	12	12	12	12	12	13	15	16	16	16	16	15	15	15	15	15	16	17	17	17	17	16	15	14
9	13	13	12	13	13	14	16	17	17	16	16	16	16	16	16	16	17	18	18	18	17	16	15	14
10	18	18	17	18	18	19																	21	20
11	12	12	12	12	12	13	15	15	15	15	15	15	15	15	15	15	15	16	17	16	16	15	14	13
12	12	11	11	12	12	13	14	15	15	15	15	15	15	15	14	15	15	16	16	16	16	15	14	13
13	13	13	13	13	13	14	16	17	17	17	17	17	17	17	16	16	17	18	19	18	18	17	16	15
14	12	11	11	12	12	13	14	15	15	15	15	15	15	15	15	15	15	16	16	16	16	15	14	13
15	12	12	12	12	12	13	15	16	16	16	16	15	15	15	15	15	16	17	17	17	17	16	15	14
16	12	12	12	12	12	13	15	16	16	15	15	15	15	15	15	15	16	17	17	17	16	15	14	13
17	12	12	12	12	12	13	15	16	16	16	15	15	15	15	15	15	16	17	17	17	16	16	15	13
18	12	11	11	11	12	13	14	15	15	15	15	14	14	14	14	14	15	16	16	16	16	15	14	13
19	12	11	11	11	12	13	14	15	15	15	15	14	14	14	14	14	15	16	16	16	16	15	14	13
20	12	11	11	11	12	13	14	15	15	15	15	15	14	14	14	14	15	16	16	16	16	15	14	13

6.3 Comparison of the Results

Comparing the results of Tables 6.1 and 6.4, we see that the analytical method gives a very good approximation of the expected revenues obtained using the Monte Carlo method. To illustrate this fact, a normal distribution of the Monte Carlo simulation result and analytical result is shown in Figure 6.3 for the case for hour 9 when line 20 is out. A histogram of the hundred revenues obtained for the 100 samples of the Monte Carlo simulation is plotted. The Monte Carlo simulation gave mean revenue of $501 with a standard deviation of 16. The analytical method estimated mean revenue of $499 with a standard deviation of 15.

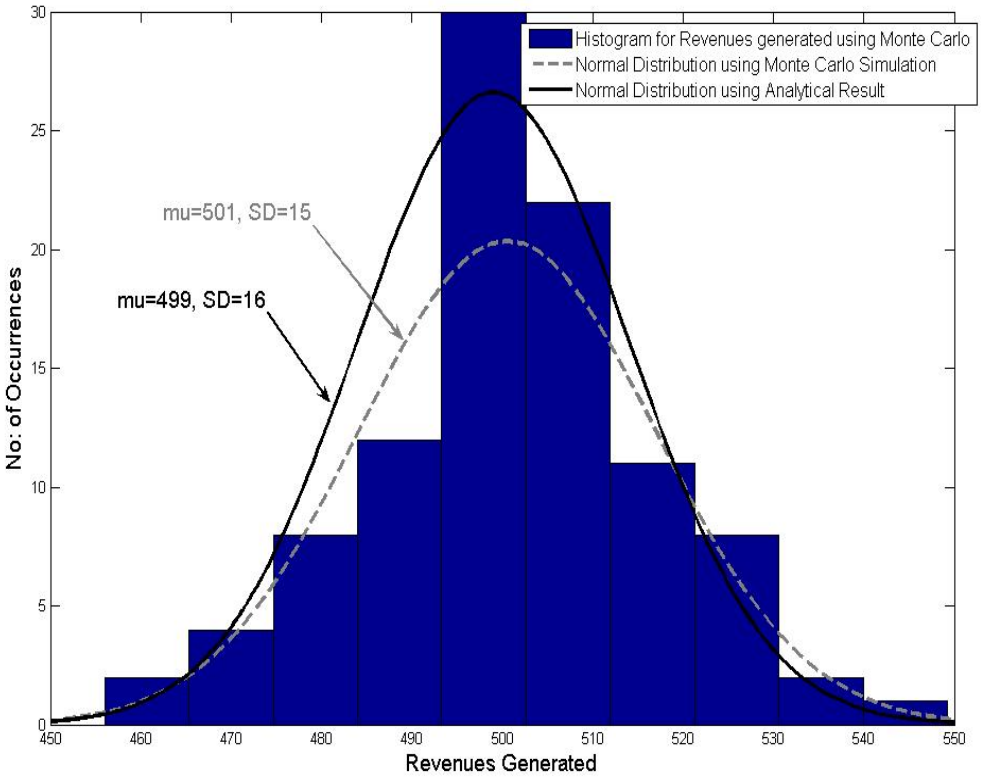

Figure 6.3 Normal distribution curve for Monte Carlo and analytical revenues for hour 9 with line 20 open.

The percentage error in the revenue computed analytically can be found as (analytical revenue-Monte Carlo revenue)*100/Monte Carlo revenue and is given in Table 6.6. The blank figures correspond to cases that would not solve in the Monte Carlo results.

Table 6.6 Percentage Error in Revenues.

	Hr1	2	3	4	5	6	7	8	9	10	11	12	13	14	15	16	17	18	19	20	21	22	23	24
Ln1																								
2	0.3	0.3	0.3	0.3	0.3	0.4	0.3					0.3	0.3	0.3	0.3	0.3							0.4	0.5
3	-1.9	-1.8	-1.8	-1.8	-1.9	-2.4																		-2.5
4	-0.2	-0.2	-0.2	-0.2	-0.2	-0.1	0.0	0.0	0.0	0.0	0.0	0.0	0.0	0.0	0.0	0.0	0.0	0.0	-0.1	0.0	0.0	0.0	0.0	0.0
5	0.1	0.1	0.0	0.1	0.1	0.3	0.4	0.4	0.4	0.4	0.4	0.4	0.4	0.4	0.4	0.4	0.4	0.4	0.4	0.4	0.4	0.4	0.4	0.3
6	0.2	0.2	0.2	0.2	0.2	0.2	0.2	0.2	0.2	0.2	0.2	0.2	0.2	0.2	0.2	0.2	0.2	0.2	0.2	0.2	0.2	0.2	0.2	0.2
7	-1.8	-1.7	-1.7	-1.7	-1.8	-2.1	-2.1	-2.3	-2.2	-2.2	-2.2	-2.2	-2.2	-2.1	-2.1	-2.1	-2.2	-2.4	-2.4	-2.4	-2.3	-2.2	-2.1	-2.1
8	0.6	0.6	0.6	0.6	0.6	0.5	0.6	0.6	0.6	0.6	0.6	0.6	0.6	0.6	0.6	0.6	0.6	0.4	0.4	0.4	0.5	0.6	0.6	0.5
9	0.2	0.2	0.2	0.2	0.2	0.2																	0.1	0.2
10	-0.9	-0.9	-0.9	-0.9	-1.0	-1.2	-2.1	-1.7	-1.7	-1.8	-1.9	-2.0	-2.0	-2.1	-2.1	-2.1	-1.7	-1.1	-0.9	-1.1	-1.3	-1.8	-2.0	-1.3
11	0.2	0.2	0.2	0.2	0.2	0.1	-0.1	-0.1	-0.1	-0.1	-0.1	-0.1	-0.1	-0.1	-0.1	-0.1	-0.1	-0.1	-0.1	-0.1	-0.1	-0.1	-0.1	0.1
12	0.1	0.0	0.0	0.0	0.0	0.0	0.1	0.1	0.1	0.1	0.1	0.1	0.1	0.1	0.1	0.1	0.1	0.1	0.1	0.1	0.1	0.1	0.1	0.0
13	-0.5	-0.5	-0.5	-0.5	-0.5	-0.6	-0.6	-0.7	-0.7	-0.6	-0.6	-0.6	-0.6	-0.6	-0.6	-0.6	-0.7	-0.8	-0.8	-0.8	-0.7	-0.7	-0.6	-0.6
14	-0.8	-0.8	-0.8	-0.8	-0.8	-0.6	-0.5	-0.5	-0.5	-0.5	-0.5	-0.5	-0.5	-0.5	-0.5	-0.5	-0.5	-0.5	-0.5	-0.5	-0.5	-0.5	-0.5	-0.5
15	-0.8	-0.8	-0.9	-0.9	-0.8	-0.7	-0.8	-0.9	-0.9	-0.8	-0.8	-0.8	-0.8	-0.8	-0.8	-0.8	-0.9	-1.1	-1.2	-1.1	-1.0	-0.9	-0.7	-0.7
16	-0.1	-0.1	-0.1	-0.1	-0.1	0.0	0.1	0.1	0.1	0.1	0.1	0.1	0.1	0.1	0.1	0.1	0.1	0.1	0.1	0.1	0.1	0.1	0.1	0.0
17	-0.1	-0.1	-0.2	-0.1	-0.1	-0.3	-0.5	-0.6	-0.5	-0.5	-0.5	-0.5	-0.5	-0.5	-0.5	-0.5	-0.5	-0.7	-0.7	-0.6	-0.6	-0.5	-0.4	-0.3
18	0.1	0.1	0.1	0.1	0.1	0.0	-0.1	-0.1	-0.1	-0.1	-0.1	-0.1	-0.1	-0.1	-0.1	-0.1	-0.1	-0.1	-0.2	-0.1	-0.1	-0.1	-0.1	0.0
19	0.0	0.0	0.0	0.0	0.0	0.0	0.0	0.0	0.0	0.0	0.0	0.0	0.0	0.0	0.0	0.0	0.0	0.0	0.0	0.0	0.0	0.0	0.0	0.0
20	-0.1	-0.1	-0.1	-0.1	-0.1	-0.1	-0.3	-0.3	-0.3	-0.3	-0.3	-0.3	-0.3	-0.3	-0.3	-0.3	-0.3	-0.4	-0.4	-0.4	-0.3	-0.3	-0.3	-0.2

The percentage error in the standard deviation (SD) computed analytically is (analytical SD-Monte Carlo SD)*100/Monte Carlo SD and is shown in Table 6.7.

Tables 6.6 and 6.7 display the percentage error in the mean and standard deviation among the results of the Monte Carlo simulations and the analytical method. The percentage of error for the mean revenue for the methods varies between the range of 0-2.4%. The percentage of error in the standard deviation calculated using the Monte Carlo simulation results and the analytical method for each hour was in the range of 0 to 20%.

Table 6.7 Percentage error in standard deviation.

	Hr#1	2	3	4	5	6	7	8	9	10	11	12	13	14	15	16	17	18	19	20	21	22	23	24
Line#1																								
2	-8	-8	-8	-8	-8	-8	-11					-8	-8	-9	-10	-10							-10	-9
3	-14	-14	-13	-14	-15	-20																		-21
4	-9	-9	-9	-9	-9	-8	-8	-9	-9	-9	-9	-9	-9	-9	-8	-8	-9	-10	-10	-10	-10	-9	-8	-8
5	-8	-8	-9	-8	-8	-7	-8	-8	-8	-8	-8	-8	-8	-8	-8	-8	-8	-8	-8	-8	-8	-8	-8	-7
6	-9	-9	-9	-9	-9	-9	-7	-8	-8	-8	-8	-8	-8	-8	-8	-8	-8	-8	-9	-8	-8	-8	-7	-9
7	-14	-13	-13	-13	-14	-13	-11	-13	-12	-12	-12	-12	-12	-11	-11	-11	-12	-14	-14	-14	-13	-12	-10	-12
8	-10	-9	-9	-9	-10	-9	-7	-10	-10	-9	-9	-8	-8	-8	-8	-8	-9	-11	-11	-11	-10	-9	-6	-8
9	-8	-8	-8	-8	-8	-9	-8	-9	-8	-8	-8	-8	-8	-8	-8	-8	-8	-9	-9	-9	-9	-8	-8	-9
10	-10	-10	-10	-10	-11	-14																	-17	-15
11	-9	-8	-8	-8	-9	-11	-9	-8	-8	-8	-8	-8	-8	-8	-9	-9	-8	-9	-9	-9	-8	-8	-10	-11
12	-9	-9	-9	-9	-9	-9	-8	-8	-8	-8	-8	-8	-8	-8	-8	-8	-8	-9	-9	-9	-8	-8	-8	-9
13	-9	-9	-9	-9	-9	-10	-10	-11	-11	-10	-10	-10	-10	-10	-10	-10	-10	-12	-12	-12	-12	-10	-10	-10
14	-8	-8	-8	-8	-8	-8	-8	-9	-9	-8	-8	-8	-8	-8	-8	-8	-9	-9	-9	-9	-9	-8	-8	-8
15	-9	-9	-9	-9	-9	-9	-10	-11	-11	-11	-10	-10	-10	-10	-10	-10	-11	-14	-15	-14	-12	-11	-10	-9
16	-8	-8	-8	-8	-8	-7	-8	-8	-8	-8	-8	-8	-8	-8	-8	-8	-8	-8	-9	-8	-8	-8	-8	-7
17	-8	-8	-8	-8	-8	-10	-10	-11	-11	-11	-11	-11	-11	-11	-11	-11	-11	-12	-13	-12	-12	-11	-10	-10
18	-9	-9	-9	-9	-9	-10	-8	-8	-8	-8	-8	-8	-8	-8	-8	-8	-8	-9	-9	-9	-9	-8	-9	-10
19	-9	-9	-9	-9	-9	-9	-8	-8	-8	-8	-8	-8	-8	-8	-8	-8	-8	-9	-9	-9	-8	-8	-8	-9
20	-9	-9	-9	-9	-9	-11	-9	-9	-9	-9	-9	-9	-9	-9	-9	-9	-9	-10	-10	-10	-9	-9	-9	-11

The Monte Carlo method and the analytical methods have some elegance in their own way. The choice of a method for a particular application is dependent on many other details specific to the application. The advantages of the Monte Carlo sampling approach are: conceptual simplicity, i.e., each sampled scenario can be seen as a possible "history" of system operation; and flexibility, i.e., it is easy to incorporate complex modeling features. One limitation of the Monte Carlo method is related to the computational effort, which increases significantly with the required accuracy of the estimates. Analytical models have several attractive features: they are reasonably accurate, computationally efficient and, perhaps most important, they provide the planner with insight on the relationships between input variables and final results. Their major limitations are related to the simplifying assumptions which may be required for analytical tractability. The extension of analytical models to incorporate additional features often leads to infeasible computational requirements.

7. Conclusions and Recommendations

The primary goal of this portion of the project was to evaluate and compare the Monte Carlo method and the analytical method for incorporating uncertainty in load forecasts, and to investigate the impact of line outages on transmission revenues. The theoretical basis for both the Monte Carlo method and the analytical method were explored and documented with an illustration on the IEEE 14-bus test system. The expected value and variance of the transmission revenue were computed for the case with all lines in service and for the cases where one line was outaged. The results indicate that the analytical method provides very good approximations of the exhaustive Monte Carlo method. This was observed both in the incorporation of load uncertainty and in the investigation of the impact of line outages.

The analysis did not incorporate any probability of line outages, or consideration of "length of outage". The analysis did include the computation of the "mean" revenue by simply computing the average expected revenue considering all individual line outage cases. This was the expected value of the revenue given that one line was outaged. The expected value of revenue considering uncertainty in both load forecast and topology would be equal to a weighted sum of the expected revenue values computed here with the corresponding probabilities of individual line outages plus the probability of all lines in service.

References

[1] S. M. Helyer, et al., "Resource and transmission adequacy recommendations," June 2004, http://www.nerc.com.

[2] R. Billinton et al., "Reliability issues in today's electric power utility environment," *IEEE Transactions on Power Systems*, vol. 12, pp. 1708-1714, Nov. 1997.

[3] H. M. Merrill, et al., "Evaluation of transmission tariff methods in restructured power markets," in *IEEE Power Engineering Society General Meeting*, 2003, vol. 2, pp. 819-824.

[4] M. Ivey, et al., "Consortium for electric reliability technology solutions grid of the future white paper on accommodating uncertainty in planning and operations," prepared for the Transmission Reliability Program Office of Power Technologies Assistant Secretary for Energy Efficiency and Renewable Energy U.S. Department of Energy. Contract No. DE-AC04-94AL85000, Dec. 1999.

[5] V. Neimane, "Distribution network planning based on statistical load modeling applying genetic algorithms and Monte-Carlo simulations," paper accepted for presentation at IEEE Porto Power Tech Conference, Porto, Portugal, 2001.

[6] M. Emmerton and D. Somatilake, "Probabilistic transmission planning comparative options & demonstration," Parsons Brinckerhoff Associates. Report No. 150251, Aug. 2004.

[7] C. T. Su, et al., "Production costing and reliability evaluation for composite systems with outages and uncertainties," *Electric Power Systems Research*, vol. 10, pp. 215-222, Apr. 1986.

[8] J. Endrenyi et al., "Bulk power system reliability concepts and applications," *IEEE Transactions on Power Systems*, vol. 3, pp. 109-116, Feb. 1988.

[9] L. Wenyuan and R. Billinton, "Effect of load bus uncertainty and correlation in composite system adequacy evaluation," *IEEE Transactions on Power Systems*, vol. 6, pp. 1522-1529, Nov. 1991.

[10] M. A. Pai, *Computer Techniques in Power System Analysis*. New Delhi: Tata McGraw Hill, 1979.

[11] O. I. Elgerd, *Electric Energy Systems Theory: An Introduction*. New York: McGraw-Hill, 1971.

[12] PJM Interconnection, "Overview," 2005, http://www.pjm.com/about/overview.html.

[13] PJM Interconnection, "Hourly Load Data," 2005, http://www.pjm.com/markets/jsp/loadhryr.jsp.

[14] C. Moler, "Normal behavior: Ziggurat algorithm generates normally distributed random numbers," *Matlab News & Notes*, Spring 2001, http://www.mathworks.com/company/newsletters/news_notes/clevescorner/spring01_cleve.html.

[15] J. M. Hammersly and D. C. Handscomb, *Monte Carlo Methods*. London: Chapman and Hall, Ltd., 1964.

[16] A. J. Wood and B. F. Wollenberg, *Power Generation, Operation, and Control*. New York: John Wiley & Sons, 1996.

[17] C. E. Winn, et al., "Reliability concepts in bulk power electric system," North American Electric Reliability Council, Feb. 1985.
[18] R. Billinton, R. J. Ringlee, and A. J. Wood, *Power- Systems Reliability Calculations*. Cambridge, MA: MIT Press, 1973, pp 1-2.
[19] R. C. Kuether, et al., "Electricity transfers and reliability," North American Electric Reliability Council, Oct. 1989.
[20] B. A. Westendorf, "Stochastic transmission revenues," M.S thesis, University of Illinois at Urbana-Champaign, 2005.
[21] B. Borkowska, "Probabilistic load flow," *IEEE Transactions on Power Apparatus and Systems*, vol. PAS-93, pp. 752–759, Apr. 1974.
[22] M. V. F. Pereira, M. E. P. Maceira, G. C. Oliveira, and L. M. V. G. Pinto, "Combining analytical models and Monte-Carlo techniques in probabilistic power system analysis," *IEEE Transactions on Power Systems*, vol. 7, no. 1, pp. 265-272, February 1992.